General Disclaimer

One or more of the Following Statements may affect this Document

- This document has been reproduced from the best copy furnished by the organizational source. It is being released in the interest of making available as much information as possible.

- This document may contain data, which exceeds the sheet parameters. It was furnished in this condition by the organizational source and is the best copy available.

- This document may contain tone-on-tone or color graphs, charts and/or pictures, which have been reproduced in black and white.

- This document is paginated as submitted by the original source.

- Portions of this document are not fully legible due to the historical nature of some of the material. However, it is the best reproduction available from the original submission.

LEGIBILITY NOTICE

A major purpose of the Technical Information Center is to provide the broadest dissemination possible of information contained in DOE's Research and Development Reports to business, industry, the academic community, and federal, state and local governments.

Although a small portion of this report is not reproducible, it is being made available to expedite the availability of information on the research discussed herein.

ANL/EES-TM-214

Experimental Gas-Fired Pulse-Combustion Studies

C. A. Blomquist

ANL/EES-TM--214

DE83 009753

prepared for
Jet Propulsion Laboratory

ARGONNE NATIONAL LABORATORY
Energy and Environmental Systems Division

operated for
U. S. DEPARTMENT OF ENERGY
under Contract W-31-109-Eng-38

ARGONNE NATIONAL LABORATORY
9700 South Cass Avenue
Argonne, Illinois 60439

ANL/EES-TM--214

DE83 009753

ANL/EES-TM-214

EXPERIMENTAL GAS-FIRED PULSE-COMBUSTION STUDIES

by

C.A. Blomquist

Energy and Environmental Systems Division

September 1982

work sponsored by

JET PROPULSION LABORATORY
4800 Oak Grove Drive
Pasadena, California 91109

CONTENTS

SUMMARY..... xiii

ACKNOWLEDGMENTS..... xxii

ABSTRACT..... 1

1 INTRODUCTION..... 1

1.1 Operating Principles of Pulse Combustion Burners..... 3
1.2 Types of Pulse Combustion Burners..... 5
1.3 Fuels for Pulse Combustion Burners..... 11
1.3.1 Coal-Fired Pulse Combustion Burners..... 15
1.3.2 Gas-Fired Pulse Combustion Burners..... 19
1.4 Scope of ANL Experimental Program..... 19

2 EXPERIMENTAL EQUIPMENT..... 21

2.1 Burner Assembly..... 21
2.1.1 Gas Valve..... 21
2.1.2 Air Valve..... 29
2.1.3 Corebustor and Tailpipe Aspirator..... 29
2.1.4 Burner Safety Circuit..... 33
2.2 Mufflers..... 36
2.3 Cooling System..... 37
2.4 Instrumentation..... 43
2.5 Data-Acquisition System..... 47
2.6 Exhaust-Decoupling Chamber..... 47
2.7 Air Supply..... 48
2.8 Gas Supply..... 48

3 EXPERIMENTAL PROCEDURE..... 50

3.1 Procedure for Startup, Operation, and Shutdown..... 50
3.2 Visual Studies..... 52
3.3 Burner Tests..... 52
3.4 Operating Problems..... 54
3.5 Exhaust-Gas Analyses..... 56

4 FUNDAMENTAL FREQUENCY..... 61

4.1 Measured Frequency..... 67
4.2 Comparison of Theory with Experimental Results..... 69

5 OPERATING PRESSURE..... 77

5.1 Results from Previous Experiments..... 77
5.2 Results from ANL Pulse Combustion Experiment..... 82

6 HEAT TRANSFER..... 90

6.1 Convective Heat Transfer..... 90

CONTENTS (Cont'd)

6.1.1 Free Convection..... 90
6.1.2 Forced Convection..... 91
6.1.3 Mixed Convection..... 101
6.2 Radiative Heat Transfer..... 105
6.3 Heat Transfer with Pulsating Flow..... 107
6.4 Heat-Transfer Measurements..... 117
6.5 Gas-Temperature Measurements..... 121
6.6 Heat-Transfer Predictions..... 128

7 ACOUSTICS..... 134

7.1 Results from Previous Experiments..... 134
7.2 Noise Measurements in ANL Experiments..... 137

8 INLET DECOUPLING CHAMBER..... 142

9 CONCLUSIONS AND RECOMMENDATIONS FOR FUTURE STUDIES..... 151

9.1 Conclusions..... 151
9.2 Recommendations for Future Studies..... 151

APPENDIX A: DRAWINGS..... 155

APPENDIX B: SELECTED EXPERIMENTAL DATA..... 161

APPENDIX C: FORTRAN PROGRAM FOR ANALYSIS OF HEAT-TRANSFER DATA..... 177

APPENDIX D: EXPERIMENTAL DATA ON HEAT TRANSFER AND EXHAUST-GAS TEMPERATURES..... 191

APPENDIX E: REVIEW OF STUDIES OF GAS-FIRED PULSE COMBUSTION..... 239
E.1 Work of Francis, Hoggarth, and Reay..... 241
E.2 Work of Griffiths, Thompson, and Weber..... 245
E.3 Work of Hanby..... 249
E.4 Work of Katsnel'son, Marone, and Tarakanovskii..... 250
E.5 Work of Griffiths and Weber..... 251
E.6 Work of Reay..... 255
E.7 Further Work of Hanby..... 257
E.8 Work of Briffa..... 258
E.9 Work of Reader..... 260
E.10 Work at Ray W. Herrick Laboratories..... 262
E.11 Remarks..... 267

APPENDIX F: APPLICATIONS OF PULSE COMBUSTION..... 269
F.1 Propulsion..... 271
F.2 Steam Raising..... 271
F.3 Water Heating..... 271
F.4 Air Heating..... 273
F.5 Constant-Volume Pressure-Rise Combustion for Gas Turbines..... 274
F.6 Portable Heaters..... 274

CONTENTS (Cont'd)

F.7 Drying and Conveying..... 275
F.8 Fogging..... 276
F.9 Ice and Snow Melting..... 276
F.10 Other Uses of Pulse Combustion..... 277
F.11 Remarks..... 279

REFERENCES..... 281

FIGURES

S.1 Ratio of Heat Transfer per Cooling Channel for Pulsating and Steady-Flow Operation of Burner at Approximately 99,000 Btu/h Heat Input..... xix

1.1 Schematic Diagram of a Pulse Combustion Burner/Heater..... 6

1.2 Types of Flapper Valves..... 8

1.3 Aerodynamic Valve..... 9

1.4 Pulse Pot..... 9

1.5 Improved Pulse Pot..... 10

1.6 Reynst Combustion Pot..... 10

1.7 Original Form of Schmidt Pulse Combustion Chamber..... 11

1.8 Gas-Fired Helmholtz Burner..... 12

2.1 Schematic Diagram of ANL Pulse Combustion Burner System..... 22

2.2 View of ANL Pulse Combustion Facility..... 23

2.3 ANL Pulse Combustion Burner..... 24

2.4 Air-Inlet-Tee Assembly..... 25

2.5 Pulse Combustion Burner Assembly..... 26

2.6 Gas-Valve Assembly..... 27

2.7 Component Parts of Gas Valve..... 28

2.8 Air-Valve Assembly..... 30

2.9 Air-Valve Plate..... 31

2.10 Air-Valve Components..... 32

FIGURES (Cont'd)

2.11 Flow Characteristics for Air Flapper Valve..... 33

2.12 Effect of Valve Lift on Air-Flow Rate..... 34

2.13 Tailpipe Aspirator..... 35

2.14 Schematic Diagram of a Low-Pass Noise Filter..... 36

2.15 Air-Intake Muffler..... 38

2.16 Exhaust-Gas Muffler..... 39

2.17 Schematic of Parallel-Flow Water Cooling of the Pulse Combustion Burner..... 41

2.18 Schematic of Series-Flow Water Cooling of the Pulse Combustion Burner..... 42

2.19 Combustion-Chamber Cooling Channel..... 43

2.20 Combustion-Chamber Head and Cooling Channel..... 44

2.21 Tailpipe Cooling Channels..... 45

2.22 Data-Acquisition System..... 47

3.1 Sketch Based on Visual Observations of Operating Burner..... 53

4.1 Compressible-Flow Model Prediction of the Fundamental Frequency of a Pulse Combustor..... 67

4.2 Molecular Weight of Flue Gas for Methane Combustion..... 70

4.3 Flue-Gas Molar-Specific Heat as a Function of the Air-Fuel Equivalence Ratio for Methane Combustion..... 71

4.4 Flue-Gas Acoustic Velocity for Stoichiometric Methane Combustion... 72

4.5 Constant-Pressure Adiabatic Flame Temperature for Methane Combustion..... 75

5.1 Pressure-Fluctuation Distribution Along Tailpipe..... 80

5.2 Distribution of Fundamental Pulsation Amplitude..... 81

5.3 Pressure-Pulsation Waveforms at the Gas-Distributor Head for a 95,460 Btu/h Heat Input with An 11.9 Air-Fuel Ratio..... 83

5.4 Mean Value of the Peak Positive-Pressure Amplitude as a Function of the Burner Heat-Input Rate..... 88

FIGURES (Cont'd)

6.1 Variation of the Mean Nusselt Number for Laminar-Flow Convective Heat Transfer in the Combined Thermal and Hydrodynamic Entry Region of a Tube With Constant Surface Temperature..... 93

6.2 Local Nusselt Numbers for the Turbulent-Flow Convective Heat Transfer to Air in the Entry Region of a Constant-Surface-Temperature Tube with an Abrupt Entrance..... 98

6.3 Factors F_1 and F_2 to be Used in Eq. 6.27..... 103

6.4 Ratio of Pulsating to Steady-State Heat-Transfer Coefficient as a Function of a Dimensionless Pulsation Velocity..... 115

6.5 Error in Unshielded Thermocouple Temperature for Various Heat-Input Rates to the Burner..... 124

6.6 Exhaust-Gas Emissivity for Radiative Heat Transfer to the Thermocouples..... 126

6.7 Error in Unshielded Thermocouple Temperature When Radiative Heat Transfer for the Gas Is Considered..... 127

7.1 Typical Noise-Spectrum Data..... 139

7.2 Near-Field Overall Noise Level vs. Heat-Input Rate..... 141

8.1 Pressure Pulse in Air-Inlet Tee for a Zero-Volume Decoupling Chamber..... 143

8.2 Pressure Pulse in Air-Inlet Tee for a 566-in.^{3} Decoupling-Chamber Volume..... 144

8.3 Pressure Pulse in Air-Inlet Tee for a 944-in.^{3} Decoupling-Chamber Volume..... 145

8.4 Pressure Pulse in Air-Inlet Tee for a 1510-in.^{3} Decoupling-Chamber Volume..... 146

8.5 Pressure Pulse in Air-Inlet Tee for a 2264-in.^{3} Decoupling-Chamber Volume..... 147

8.6 Air-Inlet-Tee Pressure Pulses for the Burner with an Inlet Decoupling Chamber, a 151,814 Btu/h Heat-Input Rate, a 9.8 Air/Fuel Ratio and a 75-Hz Frequency..... 149

8.7 Air-Inlet-Tee Pressure Pulses for the Burner with an Inlet Decoupling Chamber, a 49,160 Btu/h Heat-Input Rate, a 10.1 Air/Fuel Ratio, and a 70-Hz Frequency..... 150

D.1 Heat Transfer along Burner for a 32,887 Btu/h Heat Input and a 13.2 Air/Fuel Ratio..... 194

FIGURES (Cont'd)

D.2 Heat Transfer along Burner for a 50,245 Btu/h Heat Input and a 9.9 Air/Fuel Ratio 195

D.3 Heat Transfer along Burner for a 54,194 Btu/h Heat Input and a 12.5 Air/Fuel Ratio..... 196

D.4 Heat Transfer along Burner for a 58,655 Btu/h Heat Input and a 10.1 Air/Fuel Ratio..... 197

D.5 Heat Transfer along Burner for a 95,458 Btu/h Heat Input and an 11.89 Air/Fuel Ratio..... 198

D.6 Heat Transfer aLong Burner for a 32,887 Btu/h Heat Input and a 13.2 Air/Fuel Ratio..... 199

D.7 Heat Transfer along Burner for a 96,782 Btu/h Heat Input and a 10.3 Air/Fuel Ratio..... 200

D.8 Heat Transfer along Burner for a 99,577 Btu/h Heat Input and a 10.1 Air/Fuel Ratio..... 201

D.9 Heat Transfer along Burner for a 100,215 Btu/h Heat Input and a 9.9 Air/Fuel Ratio..... 202

D.10 Heat Transfer along Burner for a 100,941 Btu/h Heat Input and a 10.1 Air/Fuel Ratio..... 203

D.11 Heat Transfer along Burner for a 101,713 Btu/h Heat Input and a 9.9 Air/Fuel Ratio..... 204

D.12 Heat Transfer along Burner for a 103,576 Btu/h Heat Input and a 10.1 Air/Fuel Ratio..... 205

D.13 Heat Transfer along Burner for a 194,371 Btu/h Heat Input and a 9.38 Air/Fuel Ratio..... 206

D.14 Heat Transfer along Burner for a 98,013 Btu/h Heat Input and a 9.96 Air/Fuel Ratio..... 207

D.15 Heat Transfer along Burner without Flapper Valves for a 53,589 Btu/h Heat Input and a 12.5 Air/Fuel Ratio..... 208

D.16 Heat Transfer along Burner without Flapper Valves for a 102,645 Btu/h Heat Input and an 11.39 Air/Fuel Ratio..... 209

D.17 Heat Transfer along Burner with a Tailpipe Aspirator for a 50,418 Btu/h Heat Input and a 10.0 Air/Fuel Ratio..... 210

D.18 Heat Transfer along Burner with a Tailpipe Aspirator for a 98,620 Btu/h Heat Input and a 9.6 Air/Fuel Ratio..... 211

FIGURES (Cont'd)

D.19 Heat Transfer along Burner with an Inlet Muffler for a 53,116 Btu/h Heat Input and an 11.0 Air/Fuel Ratio..... 212

D.20 Heat Transfer along Burner with an Inlet Muffler for a 103,728 Btu/h Heat Input and a 10.1 Air/Fuel Ratio..... 213

D.21 Heat Transfer along Burner with an Inlet Muffler for a 101,532 Btu/h Heat Input and a 10.1 Air/Fuel Ratio..... 214

D.22 Heat Transfer along Burner with an Exhaust Muffler for a 53,429 Btu/h Heat Input and an 11.5 Air/Fuel Ratio..... 215

D.23 Heat Transfer along Burner with Inlet and Exhaust Mufflers for a 50,227 Btu/h Heat Input and a 9.4 Air/Fuel Ratio..... 216

D.24 Heat Transfer along Burner with Inlet and Exhaust Mufflers for a 100,580 Btu/h Heat Input and an 8.9 Air/Fuel Ratio..... 217

D.25 Heat Transfer along Burner with a 1-in.-Diameter, 48-in.-long Corebustor for a 49,867 Btu/h Heat Input and a 9.9 Air/Fuel Ratio..... 218

D.26 Heat Transfer along Burner with a 1-in.-Diameter, 48-in.-long Corebustor for a 50,341 Btu/h Heat Input and a 9.8 Air/Fuel Ratio..... 219

D.27 Heat Transfer along Burner with a 1-in.-Diameter, 48-in.-long Corebustor for a 50,882 Btu/h Heat Input and a 10.1 Air/Fuel Ratio..... 220

D.28 Heat Transfer along Burner with a 1-in.-Diameter, 48-in.-long Corebustor for a 99,996 Btu/h Heat Input and a 9.7 Air/Fuel Ratio..... 221

D.29 Heat Transfer along Burner with a 1-in.-Diameter, 48-in.-long Corebustor for a 101,248 Btu/h Heat Input and a 10.1 Air/Fuel Ratio..... 222

D.30 Heat Transfer along Burner with a 1-in.-Diameter, 36-in.-long Corebustor for a 50,042 Btu/h Heat Input and a 10.1 Air/Fuel Ratio..... 223

D.31 Heat Transfer along Burner with a 1-in.-Diameter, 36-in.-long Corebustor for a 97,009 Btu/h Heat Input and a 10.1 Air/Fuel Ratio..... 224

D.32 Heat Transfer along Burner with a 1-in.-Diameter, 36-in.-long Corebustor for a 100,533 Btu/h Heat Input and a 9.8 Air/Fuel Ratio..... 225

FIGURES (Cont'd)

D.33 Heat Transfer along Burner with an Air-Decoupling Chamber for a 100,794 Btu/h Heat Input and a 10.5 Air/Fuel Ratio..... 226

D.34 Measured Exhaust-Gas Temperature for the Burner Operating at Approximately 100,000 Btu/h..... 227

D.35 Measured Exhaust-Gas Temperature for the Burner Operating with a High Air-Fuel Equivalence Ratio..... 228

D.36 Effect of Air-Fuel Equivalence Ratio on the Measured Exhaust-Gas Temperature..... 229

D.37 Measured Exhaust-Gas Temperature for the Burner Operating with an Equivalence Ratio of 1.05..... 230

D.38 Effect of Heat Input to the Burner on the Measured Exhaust-Gas Temperature..... 231

D.39 Measured Exhaust-Gas Temperature for the Burner without Flapper Valves..... 232

D.40 Measured Exhaust-Gas Temperature for the Burner with a Tailpipe Aspirator..... 233

D.41 Measured Exhaust-Gas Temperature for the Burner with an Inlet Muffler or Air-Decoupling Chamber..... 234

D.42 Measured Exhaust-Gas Temperature for the Burner with Inlet and Exhaust Mufflers..... 235

D.43 Measured Exhaust-Gas Temperature for the Burner with a 48-in.-long Corebustor..... 236

D.44 Measured Exhaust-Gas Temperature for the Burner with a 36-in.-long Corebustor..... 237

E.1 Pulse Combustors Used by Francis, Hoggarth, and Reay..... 242

E.2 Pulse Combustion Device Using Separate Air- and Gas-Flapper Valves..... 246

E.3 Pulse Combustion Device Using a Single Flapper Valve..... 247

E.4 Pulse Combustion Burner Studied by American Gas Association..... 252

E.5 Schematic Diagram of Ray W. Herrick Laboratories Experimental Pulse Combustor..... 263

TABLES

1.1 Studies of Gas-Fired Pulse Combustion..... 20

2.1 Composition of Natural Gas Used in ANL Tests..... 49

3.1 Burner Tests..... 55

3.2 Composition of Tailpipe Exhaust Gas for a Heat-Input Rate of 100,000 Btu/h..... 57

3.3 Exhaust-Gas CO_2 Content..... 58

3.4 Composition of Tailpipe Exhaust Gas for Two Different Heat-Input Rates and Air/Fuel Ratios..... 59

3.5 Flue-Gas CO and CO_2 Content..... 60

4.1 Comparison of Measured and Predicted Helmholtz-Burner Frequencies with Changes in the Combustion-Chamber and Tailpipe Length..... 65

4.2 Measured Fundamental Frequency of ANL Experimental Pulse Combustor..... 68

4.3 Flue-Gas Acoustic Velocity and Corresponding Temperature for the Experimental Burner..... 73

4.4 Estimated Adiabatic Flame and Exhaust Gas Temperatures..... 74

5.1 Mean Values of the Positive and Negative Peak Pressure Amplitude... 86

6.1 Correlations for Turbulent-Flow Convective Heat Transfer in a Circular Tube..... 97

6.2 Burner Heat-Transfer Data..... 118

6.3 Combustion-Chamber Heat-Transfer Data..... 130

6.4 Tailpipe Heat-Transfer Data..... 130

6.5 Steady-State Heat-Transfer Coefficients Predicted for the Combustion Chamber..... 132

6.6 Steady-State Heat-Transfer Coefficients Predicted for the Tailpipe..... 133

7.1 Combustor Sound-Pressure Level, Pressure, and Acoustic Efficiency..... 137

7.2 Measured Noise Level of Experimental Pulse Combustor..... 138

8.1 Performance Data for Three Inlet Configurations..... 148

SUMMARY

S.1 INTRODUCTION

Combustion driven by self-sustained oscillations is known as "pulse combustion." Pulse combustors have been built in a variety of sizes and shapes and fired with oil, gas, and coal. There are three basic forms of this type of combustor: the Helmholtz resonator, the Schmidt tube, and the Reynst-Topf device (or "pulse pot"). A compilation of the collected work of F.H. Reynst* describes his patents and other significant investigations of pulse combustion.

The development and acceptance of pulse combustion systems has been hindered historically by their high noise levels, the complex underlying theory of their operation, and the close-coupled character of their components (as well as by the past abundance of cheap fuels). Unlike conventional combustion systems, pulse combustion devices are strongly coupled; small changes in configuration have significant effects on performance. Because operating functions are so interrelated, the various components must be developed together rather than separately. Thus, designs have evolved more by trial and error and from empirical correlations than from the application of basic principles.

In recent times dwindling reserves, instability of supplies, and rising prices of fossil fuels have spurred the development of more efficient combustion systems for heating. Pulse combustion, with its positive venting, high combustion intensity, minimal standby losses, and potential for superior heat transfer, is now an attractive heating technology. But the disadvantages of pulse combustion, together with the lack of design information, remain to be overcome.

To address these problems and advance the technological base of pulse combustion, an experimental program was initiated at Argonne National Laboratory (ANL) in June of 1978 under the sponsorship of the U.S. Energy Research and Development Administration (later the U.S. Department of Energy). Equipment fabrication, assembly, and checkout (and the solving of early operating problems) precluded data acquisition until late 1979. Because of Department of Energy budget cuts, the ANL program was unexpectedly terminated in January of 1981, before the program goals could be achieved. The present report records what was accomplished during the program's life and summarizes others' experimental findings about pulse combustion.

---

*_Pulsating Combustion: The Collected Works of F.H. Reynst_, M.W. Thring, ed., Pergamon Press, New York, N.Y. (1961).

S.2 EQUIPMENT

The ANL experimental pulse combustion burner was of the Helmholtz type, designed for a nominal heat-input rate of 150,000 Btu/h. The combustion chamber and tailpipe were fabricated of carbon steel. The air and gas valves were of the mechanical flapper type. A spark igniter was mounted in the combustion chamber above the gas-distributor head. There were 11 cooling channels on the combustion chamber and 43 on the tailpipe; the flow through each channel was measured in a sequential stepping arrangement with three turbine flowmeters.

A small blower supplied air for starting and purging the system. While operating, the pulse combustor drew air through the blower housing, a one-inch pipe, a turbine flowmeter, the side branch of a four-inch pipe tee, and then through the flapper valves into the combustion chamber. Natural gas was supplied through a pressure regulator, a turbine flowmeter, a small decoupling chamber, and then through the flapper valves into a gas-delivery tube running into the gas-distributor head. The gas was 94.5-96.6% methane.

A minicomputer with 64k RAM memory was used for recording data, for controlling a Fluke data logger, and for operating the solenoids that switched the water through the flowmeters. An oscilloscope was used to record the pressure signals and determine the burner operating frequency (utilizing a tunable bandpass filter).

S.3 PROCEDURE

The burner was operated under varying conditions by adjustment of the air/fuel ratio. Some problems encountered during operation were:

- Deterioration of igniter wires, which apparently extended too far into the combustion chamber.
- Water leakage into the combustion chamber through the instrument penetrations into the chamber and tailpipe.
- Failure of the gas and air flowmeter bearings and the rotor shaft on two of the water flowmeters.
- Scaling of the cooling-channel passages because of improper water treatment.
- Cooling-channel seal failure because of insufficient water flow.

This cooling-channel scaling and seal failure required that the cooling channels be removed from the burner. The difficulty in assembling the

individual cooling channels prevented us from making the intended variations in tailpipe diameter and length.

The burner was stably operated in its standard form between heat inputs as low as 32,890 Btu/h and as high as 194,370 Btu/h. The low heat-input rate required a volumetric air/fuel ratio of 13.2, while the high firing rate was slightly substoichiometric (9.4 air/fuel ratio). At a heat input of about 100,000 Btu/h, stable operation was obtained for air/fuel ratios as low as 7.9 and as high as 11.9. Tests were conducted using an inlet muffler, an exhaust muffler, and both together. With both mufflers in place, the burner could not be started, because the blower could not supply a sufficient quantity of air. (Starting was accomplished by using pressurized air; after starting, the burner operated stably without the pressurized air.)

To compare pulsating operation with nonpulsating (steady flow), we removed the flapper valves from the burner. The resulting flame was oxygen-starved and unstable, and when the blower was switched on to increase air flow the flame was extinguished. Removal of the blower, air-supply pipe, and flange improved operations slightly. Stable operation was finally achieved by using pressurized air and a needle valve to control the flow rate, with above-stoichiometric air/fuel ratios.

In order to obtain a tailpipe-geometry change, tests were conducted with a one-inch-diameter solid rod (a "corebustor") centered inside the tailpipe and extending either the entire length of the tailpipe or only the last 36 in. In addition, two tests were run using a tailpipe aspirator -- a copper-tube reducer with its small end butted onto the end of the tailpipe.

With the burner operating at approximately 100,000 Btu/h, a mass-spectrometer analysis of the exhaust gas showed a carbon monoxide content of about 1% on a dry-volume basis, even with 21.6% excess air. A 1% measurement represented the lower limit of accuracy of the measurement technique, so an infrared analyzer was used to measure the CO content of the exhaust gas independently. With this instrument, CO values of 0.45% and 0.36% were obtained for a heat input of approximately 100,000 Btu/h and air/fuel ratios of 9.9 and 10.1, respectively. For similar air/fuel ratios but with a heat input of only about 50,000 Btu/h, the CO content of the exhaust gas was 1.3-2.3% on a dry-volume basis. These high CO values could result from incomplete mixing of the fuel and air or from insufficient residence time in the combustion chamber. Data on the heat transfer from the experimental burner's combustion chamber are not adequate to determine the cause of the high quantities of CO.

S.4 OPERATING PRESSURE

Pressures were measured in the combustion chamber (gas-inlet tube) and at several locations along the tailpipe. The observed pressure-pulsation signals were complex waveforms produced by the compounding of the fundamental frequency with its higher harmonics. To obtain the pulsation waveform at the

fundamental and harmonic frequencies, the pressure-transducer signal was routed through a tunable filter (3% frequency bandwidth) before being displayed on the oscilloscope. An added complexity encountered was the apparent time variation of the pressure amplitude.

Agreement between the experimental data and predictions of the distribution of the normalized pressure-fluctuation amplitude along the tailpipe (based on a linearized compressible-flow model) appeared reasonable. The shape of the pressure distribution suggested by the data varied less strongly -- relative to the theoretical curve -- in the central part of the tailpipe and more strongly near the exit. One source of the discrepancy may be the large gas-temperature gradient along the tailpipe.

The addition of either an inlet muffler or an exhaust muffler did not affect the combustion-chamber pressure, but the use of both mufflers resulted in a slight pressure reduction. The installation of the corebustor in the tailpipe caused the combustion-chamber pressure to increase. The addition of the aspirator to the end of the tailpipe had much the same effect on the positive peak pressure as did the corebustor, but the negative pressure component was even further increased with the aspirator (especially for the higher heat-input rate).

S.5 BURNER FUNDAMENTAL FREQUENCY

By considering a frictionless, compressible-flow model for the tailpipe and representing the combustion chamber as a volume in which uniform, isentropic compression and expansion takes place, the following equation may be obtained for the fundamental frequency of the burner*:

$$\left(\frac{2\pi fL}{c}\right) \tan\left(\frac{2\pi fL}{c}\right) = \frac{V_p}{V_c} \qquad (S.1)$$

where:

c = acoustic velocity, ft/s

f = fundamental frequency, Hz

L = tailpipe length, ft

*Ahrens, F.W., and G.T. Kartsounes, *Pulse Combustion Technology for Heating Applications: Quarterly Progress Report, April-June 1978*, Argonne National Laboratory Report ANL/EES-TM-12 (July 1978).

V_c = combustion-chamber internal volume, $in.^3$

V_p = tailpipe internal volume, $in.^3$

The fundamental frequency of a Helmholtz resonator (without end correction) is given by:

$$f = \frac{c}{2\pi L}\sqrt{\frac{V_p}{V_c}} \tag{S.2}$$

The effect of the corebustor is to reduce V_p. The exhaust muffler is similar to a double-cavity resonator; because the neck-to-cavity volume ratio is small, the muffler should have only a slight effect on the fundamental frequency of the burner.

The acoustic velocity of an ideal gas can be obtained from:

$$c = \sqrt{\frac{g_c \kappa RT}{M}} \tag{S.3}$$

where:

g_c = 32.2 $lb_m ft/lb_f s^2$

M = molecular weight of gas, $lb_m/(lb\text{-}mole)°R$

R = gas constant = 1545 $ft\text{-}lb_f/(lb\text{-}mole)°R$

T = gas temperature, °R

κ = gas specific-heat ratio = C_p/C_v

C_p = gas specific heat at constant pressure, $Btu/(lb\text{-}mole)°R$

C_v = gas specific heat at constant volume, $Btu/(lb\text{-}mole)°R$

For an ideal gas, $C_v = C_p - 1.987$. If it is assumed that the flue gas is composed of the products of stoichiometric combustion of methane, then M = 27.62 $lb_m/lb\text{-}mole°R$. Then Eq. S.3 reduces to the following expression:

$$c = \sqrt{\frac{1801\ C_p\ T}{(C_p - 1.987)}} \tag{S.4}$$

The molecular weight of the flue gas would not be significantly different for slightly nonstoichiometric conditions. The molar specific heat of the

exhaust-gas components is temperature-dependent, but equations are available for the prediction of the instantaneous specific heat as a function of temperature.

The exhaust-gas temperature at the tailpipe inlet was obtained from the adiabatic flame temperature minus the temperature difference due to removal of heat from the combustion chamber. Because the actual gas temperature in combustion is less than the adiabatic flame temperature, the estimated temperatures in the tailpipe are too high. From the data, one cannot determine readily which equation (Eq. S.1 or Eq. S.2) and which temperature should be used to predict the burner's fundamental frequency. But the fundamental frequency of the burner with the corebustor can be predicted from the frequency data for the standard burner (if the speed of sound is assumed to be equal in the two configurations). The frequency prediction is coupled to the speed of sound. Using Eq. S.1 and assuming a sound speed of 2000 ft/s, the predicted frequencies for the burner-with-corebustor are 65.2 Hz (68 Hz measured) and 55 Hz (54 Hz measured) for heat inputs of approximately 100,000 Btu/h and 50,000 Btu/h, respectively. Using Eq. S.2, the predicted frequency of the burner-with-corebustor is 61.6 Hz (68 Hz measured) for the higher heat input and 52.9 Hz (54 Hz measured) for the lower heat input. It appears that the burner's fundamental frequency is better described by Eq. S.1.

The use of both the inlet and exhaust mufflers reduced the operating frequency by about 2 Hz; the use of either muffler alone had no effect on operating frequency. With a tailpipe aspirator installed, the frequency was increased by 1.5 Hz for a heat input of 50,420 Btu/h but decreased by 0.8 Hz for the higher heat input.

S.6 ACOUSTICS

Beyond the use of an inlet or an exhaust muffler, no attempt was made to attenuate the noise from the burner. To achieve simplicity, low cost, and minimal back pressure, a low-pass noise filter was designed and fabricated. The inlet and exhaust mufflers were of like configuration. When used alone, they were effective in reducing the inlet and exhaust noise but not the structural noise; however, the two-muffler combination reduced the noise level to that of the burner operating without flapper valves.

With the corebustor installed, the measured noise level was essentially the same as that for the standard burner. For the ≈100,000 Btu/h heat-input test with the tailpipe aspirator, the noise level was about 5 dB higher than that obtained with the standard burner configuration; there was no increase in noise level when the burner was operated at the ≈50,000 Btu/h heat-input rate. High noise levels measured for the 32,890 Btu/h heat-input experiment were attributed to the high air/fuel ratio.

S.7 HEAT TRANSFER

The rate of heat transfer from each burner cooling channel was calculated from the mass flow of water through the channel and its temperature rise. In most cases the heat rate in the combustion chamber reached a maximum a few inches above the gas-supply-tube head and then decreased as the exhaust gas funneled toward the tailpipe entrance. The entrance effect at the tailpipe resulted in increased heat transfer for this region. A quasi-oscillatory pattern of increasing and decreasing heat-transfer rate along the burner was observed in all the experiments. A "phasing effect" was also observed. (For similar burner conditions, the rise and fall in heat rate for the same cooling channel could be 180° out of phase.)

Figure S.1 provides additional information about the heat-transfer behavior observed for pulsating and steady-flow burner operation. Heat

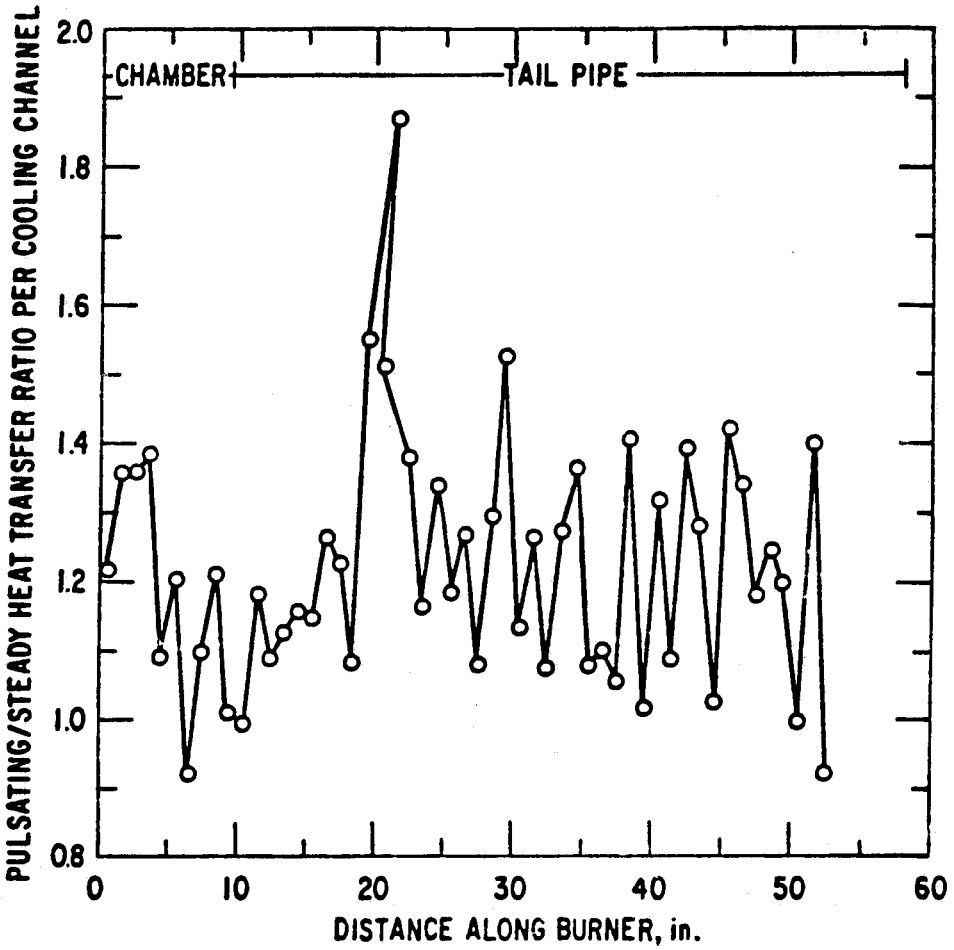

Fig. S.1 Ratio of Heat Transfer per Cooling Channel for Pulsating and Steady-Flow Operation of Burner at Approximately 99,000 Btu/h Heat Input

transfer in the combustion chamber was enhanced by about 20% by pulsations at a heat input of ≈100,000 Btu/h (compared with about 25% at a heat input of ≈54,000 Btu/h). In the tailpipe, heat transfer was enhanced by about 23% and 35% for the higher and lower heat inputs, respectively. the lower heat-transfer enhancement at the higher firing rate may result partly from the higher heat input for the nonpulsating case. In addition, the maximal pressure amplitude in the combustion chamber for the pulsating burner was lower than the pressures obtained for similar heat inputs. In any case, pulse combustion does enhance heat transfer, albeit not by as much as might have been expected.

Some observations about the heat-transfer data for various burner conditions follows:

- As the heat input to the burner increased, the percentage of heat removed from the burner decreased.
- The percentage of heat removed in the combustion chamber decreased as the heat input increased.
- The use of a corebustor increased heat removal from the burner.
- There was no significant difference in heat removal between the standard burner and the burner with both an inlet and an exhaust muffler installed.
- The burner heat transfer was slightly enhanced by the addition of a tailpipe aspirator.

The use of a corebustor increased burner heat transfer, but most of this increase occurred in the combustion chamber rather than in the tailpipe. Conventional radiative and convective heat-transfer mechanisms cannot explain the failure of the corebustor to enhance the tailpipe's heat transfer; the solution must be sought in the effects of pulsating flow on heat transfer. (The corebustor may be suppressing pulsating effects in one of the directional modes to a greater extent than would be anticipated by its 17% reduction of the operating frequency.)

S.8 CONCLUSIONS

The ANL experiments have demonstrated the enhanced heat-transfer capability of the Helmholtz-type pulse combustion burner. Reliable operation was achieved for a range of heat inputs, air/fuel ratios, and geometrical configurations. Problems still remain: high carbon monoxide content of the exhaust gas, structurally emitted noise, lack of tailpipe heat-transfer enhancement by the corebustor, and the difficulty of finding the appropriate gas temperature

for prediction of the acoustic velocity. These and other difficulties (such as those occasioned by the strongly coupled nature of pulse combustors) will require more systematic research efforts than any undertaken thus far.

ACKNOWLEDGMENTS

Funding for this report was provided by the Jet Propulsion Laboratory under NASA Defense Purchase Request No. WO-8723. The experimental work was sponsored by the U.S. Department of Energy, Assistant Secretary for Fossil Energy, Office of Fossil Energy, under Contract No. W-31-109-Eng-38 with the Combustion Division of the Pittsburgh Energy Technology Center.

I wish to express my appreciation to J.M. Clinch of Argonne National Laboratory for his technical and administrative assistance and to H.H. Chiu of the University of Illinois, Chicago campus, for his technical assistance.

A special thanks is extended to L.S. Benson, B.C. O'Meara, and B.A. Salbego for the excellent job they did in transforming my handwritten material into its present form. I would also like to thank R.B. Walker for her assistance in typing and assembling this report.

EXPERIMENTAL GAS-FIRED PULSE COMBUSTION STUDIES

by

C.A. Blomquist

ABSTRACT

This report describes experimental studies conducted at Argonne National Laboratory on a gas-fired, water-cooled, Helmholtz-type pulse combustion burner. In addition to the experimental work, the report presents information on the evolution of pulse combustion, the types of pulse combustion burners and their applications, and the types of fuels used. Also included is a survey of other pertinent studies of gas-fired pulse combustion.

The burner used in the Argonne research effort was equipped with adjustable air and gas flapper valves and was operated stably over a heat-input range of 30,000-200,000 Btu/h. The burner's overall heat transfer in the pulsating mode was 22-31% higher than when the unit was operated in a steady mode. Important phenomena discussed in this report include (1) effects on performance produced by inserting a "corebustor" to change tailpipe diameter, (2) effects observed following addition of an air-inlet decoupling chamber to the unit, and (3) occurrence of carbon monoxide in the exhaust gas.

1 INTRODUCTION

Combustion-driven oscillations have been observed in almost every type of combustion system since they were first reported by Byron Higgins in the late 1700s. These oscillations produce generally undesirable effects, such as excessive noise and vibration; the latter can destroy combustion equipment and other facilities. Hence, efforts have been focused on the elimination of these oscillations.

The beneficial use of combustion-driven oscillations has been intriguing to both researchers and designers of combustion equipment. In this context, combustion with self-sustained oscillations is known as "pulsating combustion" or (as it is called in this document) "pulse combustion." The associated burners are referred to as "pulse combustion burners."

In the early part of this century, several patents were issued for pulse combustion burners (see Ref. 1). Patents on combustors in which the

explosions were not in resonance with the natural frequency of the gas column were issued to Gobbe in 1900 (German No. 118917), to Riedel in 1920 (Swiss No. 94396), and to Paget in 1925 (German No. 441337). None of these combustors was used, because the equipment to control the gas cycle was too complicated and because inertia and the throttling loss resulting from the presence of valves, flaps, etc. made the frequency of the gas cycle too low. Combustors based on the dynamic gas cycle (a gas column oscillating at its natural frequency and using its inertia to fill and empty a chamber fitted with flapper valves) were built and patented in France: the Esnault-Pelterie in 1906 (No. 373141), the Karavodine in 1906 (No. 374124), the Armengand in 1907 (No. 376176), and the Marconnet in 1910 (No. 412478). These units are described in Chapter 10 of Ref. 1.

Combustion systems with oscillating gas columns were produced in the early 1900s but drifted into oblivion because they couldn't be used to power aircraft or to generate gas pressure for turbines. There was also a lack of interest in using such systems as heat generators or firing systems for steam boilers. Without knowledge of Marconnet's patent, Paul Schmidt considered (from 1928 to 1930) how an aircraft could be propelled by means of the rearward thrust of an exploding mixture. Schmidt considered the possibility of improving efficiency by projecting a large quantity of air pistonwise into the combustible mixture in a tube open at one end and then detonating the mixture by means of a shockwave. This process would then be repeated periodically. When Schmidt tried to patent this process in 1938, the German Patent Office informed him of Marconnet's patent of 1930; however, Schmidt was issued a patent (No. 523655) on the air-flow pattern. His combustor is known as the "Schmidt tube" (or the "Argus-Schmidt tube," because of the work done by G. Diedrich at the Argus Engine Co. in the production of the pulse-jet propulsion engine for the V-1 flying robot bomb during the later years of World War II).

Reynst's combustor differs from the Schmidt-type oscillatory combustor in that the former has no valves, and the hole connecting it to the resonance tube is always open and serves as both the inlet and exit. Reynst obtained a Swiss patent (No. 196312) in 1938 on this device; however, the phenomenon of the so-called "pulse pot" was documented before Jan Van Hewven, notary at Haarlem, The Netherlands, on May 5, 1933.

Following World War II, there was considerable interest in the pulse jet. The National Advisory Council on Aeronautics (NACA) conducted studies and experiments ("Project Squid") from 1944 to 1953. With the advent of V-2 type rocket propulsion and atomic power, and given the low flight thermal efficiency (approximately 10%) of the pulse jet, interest in this combustion system declined. Investigations of the applications of pulse combustion technology for gas turbines, water heating, and steam raising were sparsely conducted in the late 1950s and in the 1960s. The Lucas-Rotax Pulsamatic®* residential hot-water boiler was marketed in Canada for several years. The

*Pulsamatic® was a tradename used by Lucas-Rotax Ltd., Toronto, Ontario, Canada, for its pulse combustion units.

abundance and low cost of fossil fuels, plus the lack of technical information on pulse combustion systems and their high noise levels, have limited their acceptance by the commercial and industrial market.

In 1971, the First International Symposium on Pulsating Combustion was held at the University of Sheffield, England, on September 20-23. The objectives of the Symposium were to provide a forum for discussion on the applications of pulse combustion, to appraise the success of previous and current work, and to consider the prospects for usage of pulse combustion in the future. There were 42 registered participants and 18 presented papers, one of which (by Putnam[2]) provided a summary of previous studies. The history of the pulse jet from 1906-1966 has been presented by Reader.[3] Dwindling reserves, instability of supplies, and rising prices of fossil fuels have sparked the development of combustion heating systems with higher efficiencies, so pulse combustion burners have generated a renewed interest.

On November 29-30, 1979, a symposium on Pulse Combustion Technology for Heating Applications was held at Argonne National Laboratory (ANL), Argonne, Illinois. The purpose of the Symposium was to exchange technical information and ideas on pulse combustion and to aid manufacturers in acquiring useful background information. There were 107 registered participants, and 15 papers were presented. One of these papers (by Putnam[4]) was principally a survey of Russian investigations. Recently (March 2-3, 1982), a symposium on pulse combustion applications was held in Atlanta, Georgia, where 18 papers were presented. It appears that interest in the utilization of pulse combustion is increasing.

1.1 OPERATING PRINCIPLES OF PULSE COMBUSTION BURNERS

For simplicity, consider a pulse combustion burner to consist of a combustion chamber that has an opening on one end and air and fuel inlet valves on the other end. Initial startup of the combustor is achieved by supplying fuel and air through the inlet valves and then igniting the mixture with a spark. The air is supplied by a small blower or from a pressurized source. After ignition, the pressure and temperature in the combustion chamber rise rapidly, causing the inlet valves to close and preventing fresh fuel and air from entering. The combustion products are accelerated and forced out the open end of the combustor by the positive-pressure wave. The inertia of the exiting gas creates a partial vacuum in the combustion chamber and allows the inlet valves to open and admit a fresh charge of air and fuel; flow reversal of the exhaust gas also occurs. The new air/fuel mixture is self-ignited to complete the cycle. The precise mechanism of this re-ignition is not completely understood; it occurs by the re-entry of the hot exhaust gas, by the presence of residual heat in the combustion chamber, by shock-waves, or by a combination of these phenomena. Once this cycle is sustained, the starting air blower or spark igniter is not used. The system as a whole now behaves as a self-powered resonator with an operating frequency determined

by the system geometry. This sustained cyclic operation, with positive and negative pressures produced in an oscillatory fashion, is the basis for the name "pulse combustion."

Pulse combustion burners appear to have a number of potential advantages over contemporary burners. A pulse combustion burner is relatively simple in construction and is self-powered (i.e., it regulates its own supply of combustion air and fuel, ignites it, and vents the combustion products through a relatively small conduit without the need of external devices or power). The mean combustion-chamber pressure during stable operation is greater than atmospheric pressure. Thus, the burned gases are forcibly vented, without the assistance of a blower or natural draft from a chimney. Some of the other attractive technical features of pulse combustion burners for potentially economical fuel-saving applications include: minimal standby heat loss, no standing pilot, low air/fuel ratio due to excellent mixing, no limitation on exhaust temperature (as is imposed by natural venting considerations), and excellent heat-exchange characteristics resulting from fluctuating flow (compact design). For a given steady-state efficiency target, the pulse combustion system may have the highest seasonal efficiency, and thus the lowest fuel consumption, of the available heating options.

Among the disadvantages of pulse combustion are high noise levels and the potential for destructive vibrations or premature failure of equipment from erosion. The noise level of a pulse combustor can be intolerable; such terms as "screaming combustion" have been applied to these devices. The noise from one of Reynst's experimental pulse-pot burners was said to have been audible up to six miles away.[5] However, it is possible to reduce the noise to acceptable levels with mufflers, sound-absorbing materials, and out-of-phase operation of multiple burners.

Because of the oscillatory nature of the pulse combustion process, vibrations are inherently present, but not much information is available. Sommers[6] reported considerable vibration of the boiler crown when the unit was tested with a pulse combustion burner firing coal dust. Tests conducted by Babkin[7] on an oil-fired pulse combustion burner installed in the boiler of a steelworks power station revealed that the walls, tubes, and casing of the boiler did not vibrate significantly, but mortar disappeared from the joints in the arches over the furnace chambers. Hence, the potential for vibration damage exists, but either (1) damage has gone unreported, (2) damage has seemed inconsequential in the equipment tested, or (3) the duration of testing has been insufficient to produce damage.

The operating behavior of a heating system based on pulse combustion is strongly affected by the burner components. For example, the magnitude and frequency of the pressure fluctuations within the combustion chamber and the inlet and exhaust lines have major effects on the (potentially high) noise level of the system. At the same time, these fluctuations influence the high instantaneous velocities within the heat-exchange regions of the system. These velocities have an important bearing on the heat-transfer effectiveness,

and hence on the required size and cost, of the appliance. Also, the fuel-input rate is fundamentally related to the design of the valving and to the pressure pulsations in the combustion chamber. Because of the many interactions of the design parameters, the various components for a pulse combustion burner must be developed in unison rather than separately. Consequently, designs have evolved from trial and error and from empirical correlations, rather than from application of basic principles.

In addition to component coupling, the complex underlying theory of operation of pulse combustion burners (along with the existence of cheap and abundant fuels) has hindered these burners' development. The pulse combustion process is intermittent and involves both chemical reactions and nonsteady flow of a compressible fluid. The thermodynamic cycle of the process is complex and incompletely understood. In addition, the mechanism coupling the gas-dynamic oscillations with the combustion process is obscure. Theoretical studies are largely lacking.

1.2 TYPES OF PULSE COMBUSTION BURNERS

There are many different types of pulse combustion burners. A simplified system (shown schematically in Fig. 1.1) might consist of the following:

- A fuel-supply system,
- An air-supply system,
- A combustion chamber with inlet valves for air and fuel,
- A tailpipe (resonance or exhaust tube),
- An exhaust decoupling chamber, and
- A secondary heat-exchanger section, in which the fluid motion is steady.

Also important in a real system (but not shown in Fig. 1.1) are an ignition starter, inlet and exhaust mufflers, and an inlet-decoupling chamber.

The exhaust-decoupling chamber decouples the pulsations in the combustion chamber and tailpipe from the downstream components and piping. Similarly, an inlet-decoupling chamber would isolate the air- or gas-supply system from the combustion-chamber pulsations.

Air and gaseous fuels enter the combustion chamber through mechanical (flapper), aerodynamic, or rotary valves. Liquid fuels may be injected directly into the combustion chamber, carburetted into the air stream, atomized by the entering air, or prevaporized. Solid fuels can be supplied continuously or carried in by the entering air.

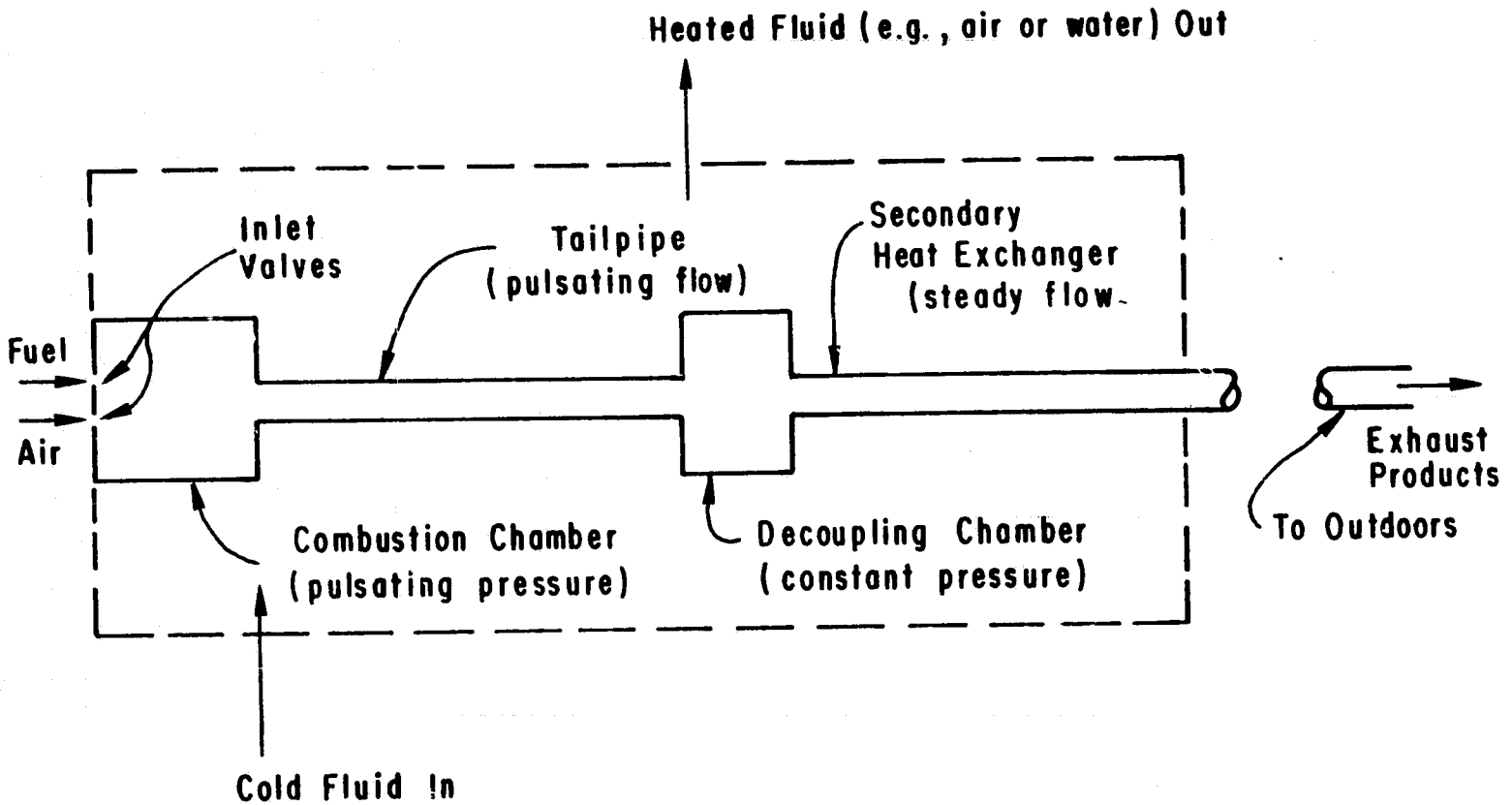

Fig. 1.1 Schematic Diagram of a Pulse Combustion Burner/Heater

The types of flapper valves are shown in Fig. 1.2. Reed valves (Fig. 1.2a) consist of a series of holes covered by strips of a thin elastic material, clamped along one edge and free to bend under the action of the pressure difference across the valve. Early valves of this type used spring steel, which had a short operating life and failed because of material fatigue. Coating the spring steel enhanced the operating life of these valves. Several studies found that lightly seated valves gave longer operating life. Valve failure apparently was resulting from impact fatigue and flame leakage through the seats. Consequently, the ring-type flapper valve (Fig. 1.2b) was developed. It consists of a soft material to seal the inlet holes and a backing ring to support the soft material and protect it from flame impingement. These valves can be adjusted for a wide flow range by varying the "lift" (the space between the flapper and the inlet holes).

Aerodynamic valves can range from simple drilled holes to orifices, nozzles, or other shaped sections of varying complexity, such as the cup-shaped valve of Bertin[8] shown in Fig. 1.3. Aerodynamic valves have no moving parts, can operate at high temperature, and are resistant to erosion from particles in the inlet air. However, these valves permit a backflow of combustion products into the inlet streams, which may be undesirable for a gas heater. This backflow can be used to aspirate air to furnish extra combustion air for cooling dilution or to produce an optimal flow velocity and extra thrust. There are no clearly defined design procedures for these valves, but there should be a high ratio of forward to reverse flow; the pressure loss in the forward direction should be low. From an economic standpoint, too, the valve should not be too complex.

Rotary valves, which utilize a motor-driven disk to interrupt the air supply to the burner, require a synchronous motor to drive the valve at a speed tuned to the burner frequency. Babkin[7] found that a rotary valve is sufficiently reliable and showed experimentally that the conditions for pulsating combustion are not determined by regular interruptions of the air stream. The frequency of interruptions should coincide within ±1% with the instantaneous resonant frequency of the combustion chamber; otherwise, the ability to self-aspirate deteriorates rapidly, and beating and flame-out can occur. Rotary valves are not widely used in pulse combustion burners; such valves detract from the self-powered operation of these burners.

Pulse combustion burners have been built in a variety of shapes, but there are three basic types: (1) the pulse pot ("Reynst-Topf Pot" or "Reynst Combustion Pot"), (2) the Schmidt tube, and (3) the Helmholtz combustor. The Rijke tube, another type of pulse combustor, is not discussed in this report.

In its simplest form, the pulse pot (Fig. 1.4) is a closed container with an opening in the top. A pool of liquid at the bottom of the pot is ignited, and oscillating combustion occurs. The flame is contained inside the pot. In rapid succession, gas is ejected and air is sucked in through the opening in the top. Reynst devoted most of his working life to the development of this combustion device. It was discovered that the addition of a

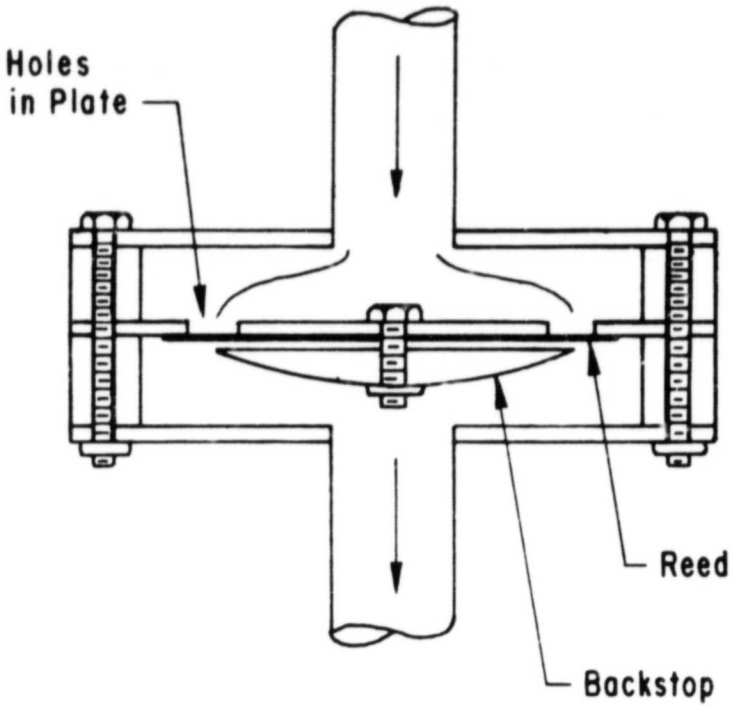

(a) Reed-Type Flapper Valve

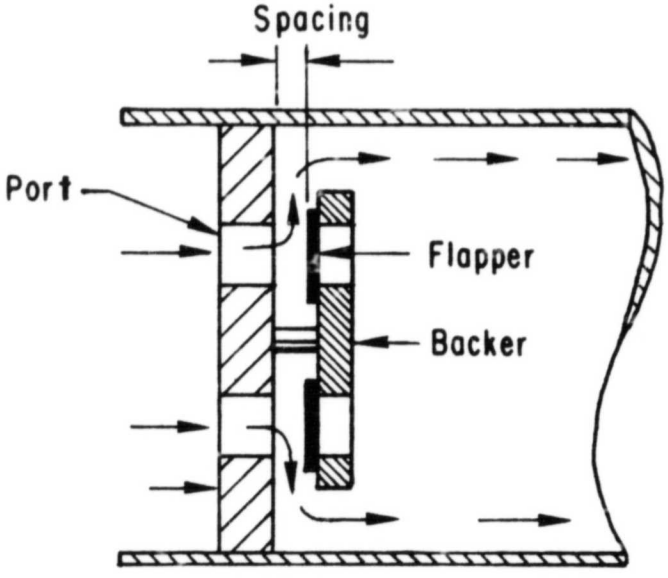

(b) Ring-Type Flapper Valve

Fig. 1.2 Types of Flapper Valves

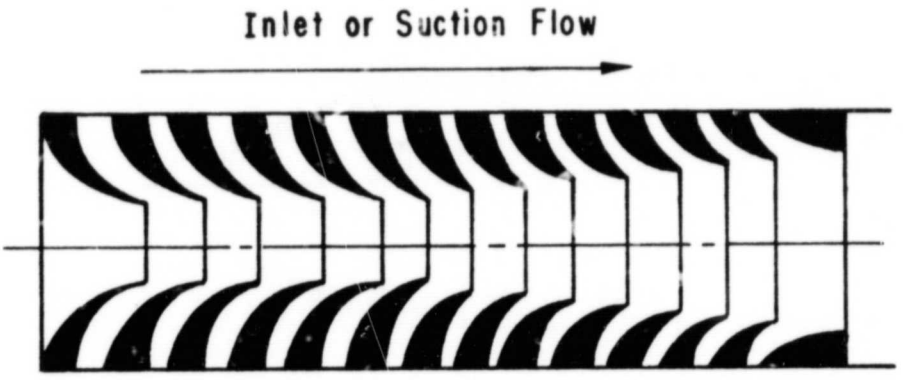

Fig. 1.3 Aerodynamic Valve (Source: Ref. 8)

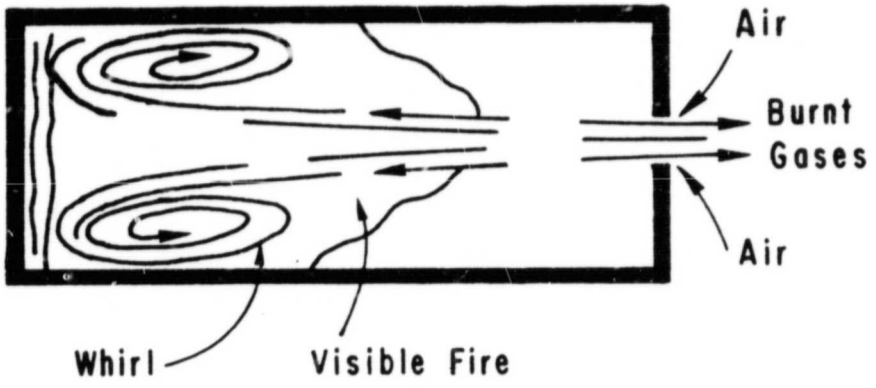

Fig. 1.4 Pulse Pot

vortex ring or venturi tube between the opening and the bottom of the combustion chamber resulted in an improved pot (Fig. 1.5). The venturi tube forces the inflow further towards the bottom of the chamber and creates a stable vortex system, which aids recharging and ignites the next pulse as it comes in. The introduction of a diffuser or resonance tube to carry the exhaust gas away permits tuning of the burner, so that the sonic frequency of the pot coincides with the combustion frequency. Hence, the Reynst Combustion Pot shown in Fig. 1.6 evolved. It consists of a blind-ended combustion chamber and an associated diffuser, with a total length of one meter. The air and fuel are admitted through an annular gap between the two components. The gas column oscillates in a quarter wave, like the gas column in an organ pipe, with a frequency of 200 Hz. The pressure amplitude in the bottom of the pot is +10.3 and -7.4 psi, and the shape of the pressure curve is approximately sinusoidal. A heat release of about 4,500,000 Btu/hr-ft^3 was obtained. The noise produced could be heard about six miles away and sounded like a steamship's fog horn. This noise problem probably prevented the utilization of this combustor, in spite of its simplicity and high combustion intensity.

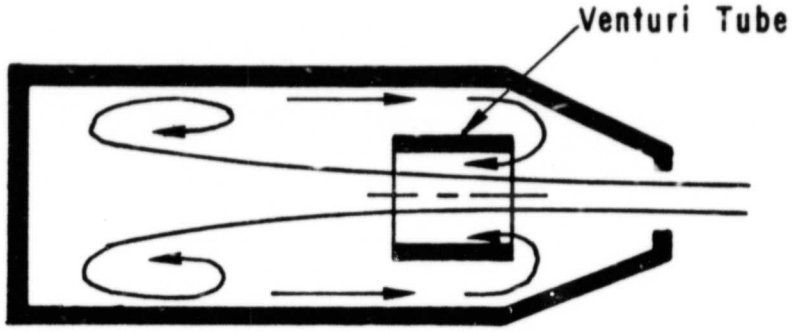

Fig. 1.5 Improved Pulse Pot

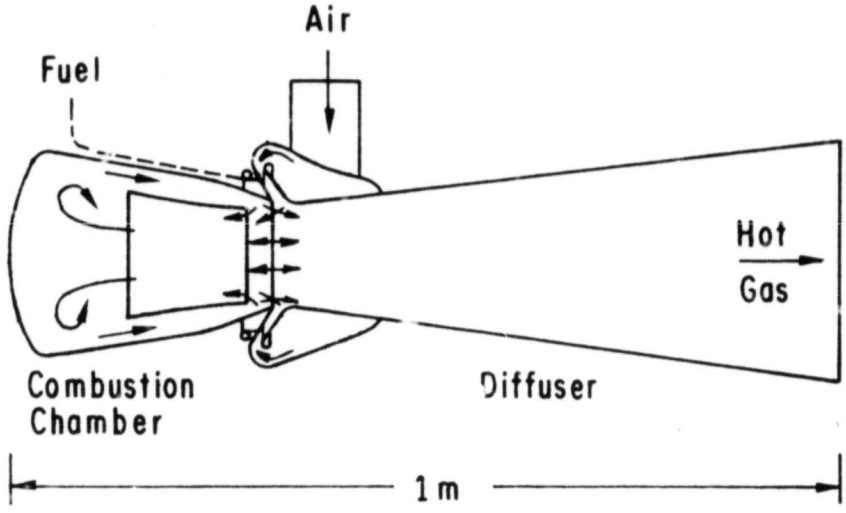

Fig. 1.6 Reynst Combustion Pot

The Schmidt tube (Fig. 1.7) is a cylindrical or slightly conical tube, closed at one end by flapper valves at the site of fuel injection and open at the opposite end. The original combustor design was modified by the Argus Engine Co. for production of the pulse-jet engine for the V-1 flying bomb. The original Schmidt tube had no bulges or other increases in diameter or turbulence creators. The tube operates in a constant-volume mode and oscillates like an organ pipe on a quarter wave length. Ignition is extremely fast, and a high pressure rise is obtained. Opinions vary as to how the fuel/air mixture flows into the tube without ignition and then suddenly ignites throughout. In Chapter 23 of Ref. 1, Reynst postulated that the fuel/air mixture in a Schmidt tube is ignited by burning particles in a boundary layer at the inner surface of the tube. As soon as the laminar in-flow becomes turbulent, these particles move from the wall to the tube's centerline at a relatively high speed. Ignition is retarded by the entering laminar flow, which repels the residual exhaust gases and pushes the burning particles out

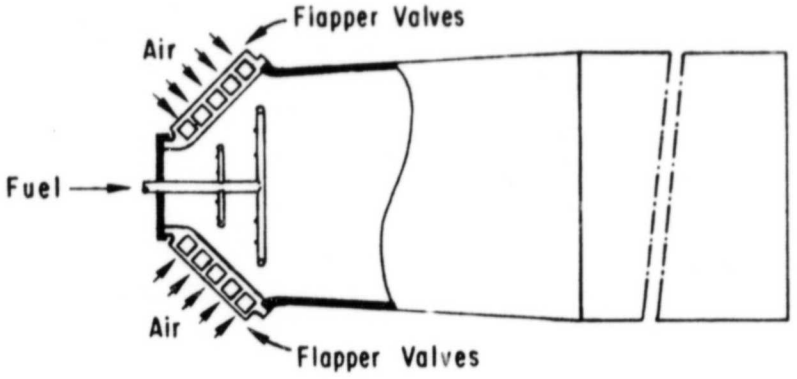

Fig. 1.7 Original Form of Schmidt Pulse Combustion Chamber

to the tube walls. As long as laminar flow remains dominant, the particles cannot move inward.

The constant-volume mode of the Schmidt tube is excellent for thrust production in aircraft propulsion, but the step-like pressure rise and the wide variation in exhaust-gas flow velocity are highly undesirable for utilization of the gas's kinetic energy. Thus, despite its very high efficiency, the Schmidt tube has not yet found any other application than as a reaction-power pack or heater. The Schmidt tube also has the disadvantage of a stagnant flow at the moment of explosion (during the instant the flapper valves are closed).

The Helmholtz combustor (Fig. 1.8) is similar to the Schmidt tube, but the resonance tube of the former has a smaller diameter. This produces an acoustic system that operates like a Helmholtz resonator (an acoustic enclosure with a small opening, which causes it to resonate at a frequency dependent on its geometry). Most tests and applications of pulse combustion burners in the last 20 years have utilized Helmholtz-type burners.

Additional details on types and components of pulse combustion burners can be found in Ref. 4.

1.3 FUELS FOR PULSE COMBUSTION BURNERS

Fuels burned in pulse combustion burners have included solids, liquids, and gases. Liquid fuels were utilized in early pulse combustion studies and tests. Karavodine's 1909 combustor, a bulged vessel and pipe with a check valve at one end, was fired with benzene. In the Haarlem document of 1933 [Appendix 1 of Ref. 1], Reynst mentions the use of a methylated spirit (alcohol) as fuel for the described combustion phenomenon. Reynst[1] also used the jam-pot experiment with an alcohol fuel to demonstrate the principle of the pulsating-pot combustion chamber.

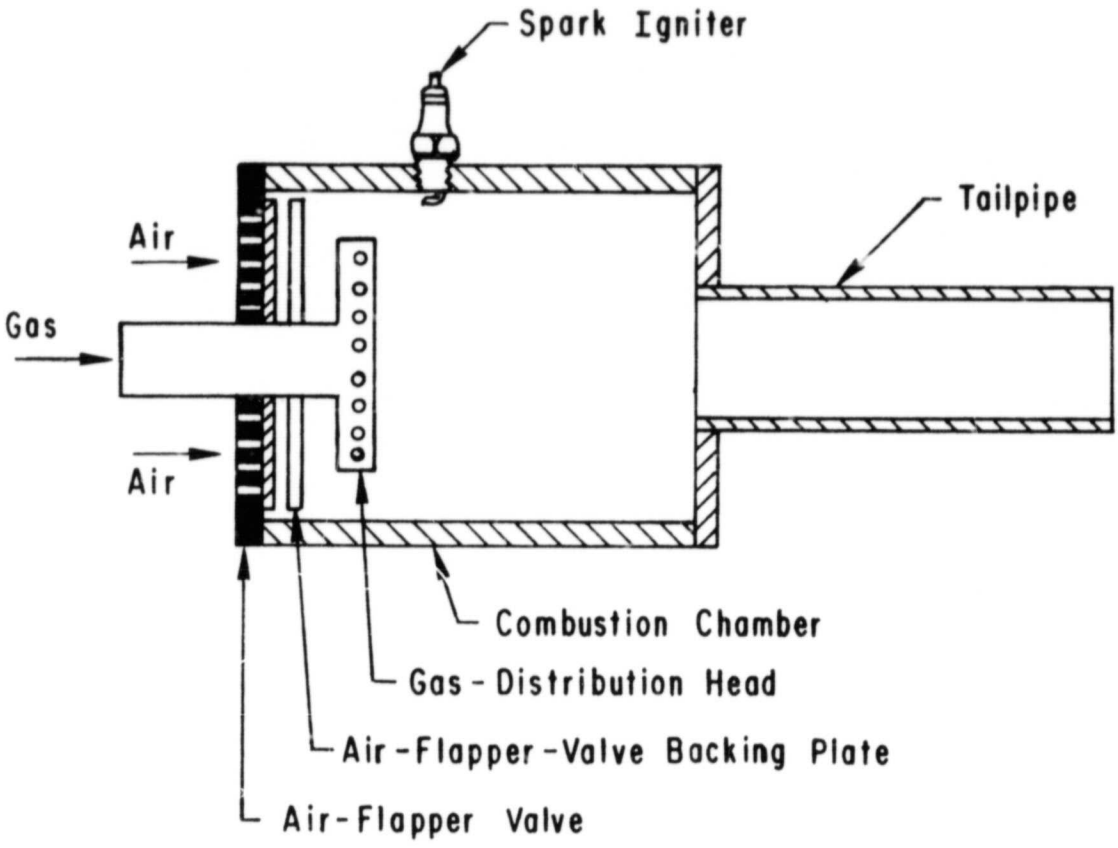

Fig. 1.8 Gas-Fired Helmholtz Burner

Schmidt used gasoline in his pulse combustion studies and as the fuel for the V-1 flying bomb. Gasoline was used also by Sommers[6] in a Helmholtz-type burner fitted with a free ball valve instead of one with flapper valves. A pulsation intensity of one standard atmosphere (1 atm) was obtained in the combustor, which consisted of a pear-shaped combustion chamber approximately 400 mm long and a 1.25-m long tailpipe. With intensive water cooling of the entire combustor wall, the unit would operate only at approximately stoichiometric combustion. Without cooling or insulation, and with pre-heated air and fuel, the air/fuel ratio could be varied widely. Successive explosions could not be maintained when the peak temperature in the main combustion zone was below 1200°C. The Soundrive Engine Co.[9] also burned gasoline in some pulse combustion tests. Huber[10] developed a gasoline-fired pulse combustion air heater for buses and other vehicles. Persechino[11] tested several variations of single and double pulse combustors for ice-melting applications. These units were fired with either gasoline or diesel fuel, vaporized by the heat of the combustion chamber.

Fuel oil was utilized in the testing and development of the Escopette (Blunderbuss) and Ecrevisse (Crayfish) pulse jets by SNECMA[8,12-15] from the mid 1940s through the 1960s. Heavy-duty stove oils were fired in pulse combustion tests by the Soundrive Engine Co.[9]

Lockwood[16] reports that the development of special fuel nozzles in the Hiller Propulsion Research Laboratory was the key to successful operation of miniature valveless pulse jets with a variety of fuels, including several grades of gasoline, jet-propulsion (JP) fuels, diesel fuel, gaseous propane, and even methane (city gas) at low pressures.

Babkin[7] burned liquid fuels, from kerosene to heavy oil (including nigrol) and liquid anthracene tar but excluded ordinary fuel oil. Tests were conducted at liquid-flow rates of 33.1-198.5 lb/h, pressure amplitudes of 2.2-7.3 psi, and frequencies of 30-120 Hz. Eight types of valves were investigated. The tests showed that pulse combustion burners were relatively insensitive to the properties of the fuels burned. Equivalent combustion quality, area heat load, and pressure amplitude were obtained with liquid fuels, from kerosene to nigrol; however, conditions deteriorated when anthracene tar was used. In a number of tests, the small pressure amplitudes, the occurrence of ozone, and the high degree of gas ionization suggested that radicals play an important part in the fuel's dissociation and ignition.

Babkin also found that self-aspiration, pulsation amplitudes, and the extent of gasification of liquid fuels increased when the fuel was preheated prior to ignition. When the fuel was injected directly into the combustion chamber, only light fuels (kerosene and solar oil) could be burned. The combustion of heavy oils resulted in smoking, loss of output, and attenuation of pulsations. These conditions were improved by the introduction of an extra chamber and a section of heat-exchanger duct between the mechanical valve and the combustion chamber. This arrangement, which promoted alternating movement of the gases and heating of the oil in the duct, resulted in the characteristic increase in combustion intensity. With heated heavy oils, the thermal condition of the combustion chamber walls (e.g., cooled or insulated) is unimportant. However, use of heavy fuels also requires that the pulse combustion burner have aerodynamic valves.

The greatest combustion chamber loadings and pressure amplitudes were obtained with primary-air equivalence ratios of 0.8-0.9. Under these conditions, a distinctive feature of pulse combustion was the gasification of the carbon in the fuel. With self-aspirating or a little supercharging of pulse combustors, the gases in the pulse tube moved back and forth so that the discharge of each successive portion of the combustion products was accompanied by the formation and collapse of a strong toroidal vortex. This periodic vortex enabled the gases to mix vigorously with secondary air and burn rapidly at volume heat releases of more than one million Btu/h-ft^3.

In 1960, tests were conducted with a double counter-phase pulse combustor installed in a 10 ton/hr steelworks power-station boiler. Low-sulfur fuel oil (grade 40-60) was fired at a total rate of 1654 lb/h. Combustion took place without smoke, and the furnace volume contained completely transparent gases. The pulsation frequency was 68 Hz, and the total pressure amplitude was 4.4 psi. The apparent surface heat release of the chamber throat was 17 x 10^6 Btu/h-ft^2, and the volume heat release was 1.8 x 10^6

Btu/hr-ft^3. A great deal of noise developed, which imposed a strain on the station staff. The walls, tubes, and casing of the boiler did not vibrate seriously; however, mortar disappeared from the joints in the arches over the combustion chambers.

Based on these tests, a dual unit was built at the Taganroy boiler works in 1963 and installed under a medium-pressure boiler (70 ton/h steam capacity) at the Ufimsk Heat and Power Station No. 1. Hot gas from the combustion chambers was discharged into an unused slag hopper (about 706 ft^3 in volume), which acted as a secondary combustion chamber. The combustion chamber was charged by a mixture of hot and cold air (VM-50 fan). Secondary air entered radially at the end of each pulse tube. Acoustic de-excitation was achieved by blind-branch pieces adjusted to be slightly above the chamber's working frequency.

High-sulfur fuel oil (grade 100) was fired at a rate of 9261 lb/h. The combustion chambers pulsated stably in counter-phase with a frequency of 31 Hz. The total amplitude of pressure oscillations was 2.2 psi. The area heat release was 17.6 x 10^6 Btu/hr-ft^2 at the pulse-tube throat and 10.4 x 10^6 Btu/h-ft^2 at the exit. A total volume heat load of 0.7 x 10^6 Btu/h-ft^3 was achieved. Noise in the boiler room was equivalent to that from the VM-50 fan.

According to V.I. Hanby and T.D. Brown,[17] the pulse combustion burner that fired heavy fuel oil (described by Babkin[7]) had two disadvantages: (1) It was necessary to preheat (crack) the oil to sustain pulse combustion; and (2) combustion took place in two stages, leading to a reduction in the pressure amplitude of oscillation upon which the advantages of the device depend. Two-stage combustion also leads to difficulties in arranging for the combustor to aspirate its own air supply. Hence, a combustor was designed for a throughput of 1.02 x 10^6 Btu/h with a theoretical operating frequency of 80 Hz. The combustor is of the Helmholtz type, with a 1.64-ft long expanding-conical-section combustion chamber that is cast in a refractory. A 15-mm diameter disc-shaped flameholder is situated at the inlet to the chamber. An oil atomizer is located at the disc center and is surrounded by four propane jets (0.12-in. diameter) for starting. The tailpipe, a 4.92-ft long expanding conical section formed from stainless steel, is intended to assist the self-aspiration action of the combustor and is air-cooled. There were no flapper or aerodynamic air valves. Pressurized air was supplied through a choked orifice into a 1.97-in. diameter pipe and then into the 3.94-in. diameter combustion-chamber inlet. The compressed-air supply was necessary to ensure accurate air-flow measurements. A 950-s (dynamic viscosity) fuel oil was supplied from a heated tank at an atomizing pressure of 362 psi. The maximum heat release was 1.23 x 10^6 Btu/hr, at which the pressure amplitude was ±7.5 psi. The operating frequency was 82 Hz, and the maximum combustion intensity was 2.6 x 10^6 Btu/h-ft^3. Stable-pulsation operation could be achieved with a turndown ratio of 4:1. The combustor discharged the exhaust gases into a simple brick furnace, which had a number of openings to the laboratory. Sound levels of 86-88 dBA were measured in the laboratory.

1.3.1 Coal-Fired Pulse Combustion Burners

The rate of combustion of pulverized coal is limited by the rate at which individual coal fragments are scrubbed by the combustion air to bring fresh oxygen to their surfaces and to remove the products of combustion from their surfaces. If the gaseous medium can be given a velocity relative to the fragment, the oxygen supply to the fragment's surface will be increased, the combustion rate accelerated, and the combustion intensity increased. Ultrasonic and sonic waves have been tried, but a large amount of power is required to produce an appreciable increase in the combustion rate. The high-amplitude acoustic field produced by pulse combustion has been proposed to produce the gas-particle velocity differences.

In Chapter 12 of Ref. 1, Reynst states that pulverized coal was used to fuel the pulse-jet engine of the V-1 buzz bomb at the end of the war when Germany's gasoline supply ran out. Also in Ref. 1 (Chapters 3 and 4), Reynst discusses pulse combustion of pulverized coal. Reynst spent a great amount of time and energy initiating and partially developing his ideas, but he was not able to bring these ideas completely into practical use during his lifetime.

In 1951, a short account of the pulse combustion tests conducted by the Soundrive Engine Co. was published.[9] With pulverized coal, combustion intensities of 5×10^6 Btu/ft^3 were obtained and heat-transfer coefficients were doubled. The open-ended burner could be heard over a mile away. Soundrive burners operated at close to 100 Hz, were 2-ft long, and were between 2 and 5 in. in diameter. Combustion efficiency was close to 100%, and residence time was 1/12 that of a conventional burner. It was also stated that small burners with a 200-Hz resonant frequency require coal particles to be less than 100 mesh in size.

In Germany, Sommers[6] conducted tests with small pulse combustors up to 3.9 in. in diameter at the Ruhrgas test plant in Herten. The intent of these tests was the use of the high combustion intensity of pulse combustion for the gasification of pulverized coal into producer gas (using air) or into synthesis gas (using oxygen and steam). After these small-scale tests were completed, a pulse combustor was installed on a boiler with a combustion capacity of one to two tons of coal per hour at the Shamrock 1/2 Pit of the Hibernia Mining Co. Data on four tests, conducted between September 1954 and April 1955, are given. One test was with synthesis residual gas, two with screened coal dust, and one with pulverized coal. Each test lasted about one day.

Either coal dust or pulverized coal was fed from a hopper and pneumatically metered into the downward-pointing conical combustion chamber of the pulse combustor. Air from a fan was preheated to 392-752°F and entered the combustor through an aerodynamic valve. Secondary air could be added at the exit of the resonance tube where it joined the slag chamber. The exhaust gas entered the slag chamber from the resonance tube tangentially to give good slag removal and then flowed into the oblique tube boiler. The resonance tube had a 15.75-in. diameter and a volume of 22.6 ft^3. The total length of the

combustion chamber and resonance tube was 14.76 ft. The pulsation frequency of 30-40 Hz corresponded to quarter-wave organ-pipe operation. Oscillation intensity up to 0.15 psi was measured with gas firing. Pressure measurements were not obtained for coal combustion, because slag plugged the sampling pipes too rapidly. The resonance tube and slag chamber were cooled by the tubes of a Lamont system. A grate in the form of three vertical rows of pipes was provided at the end of the slag chamber. The old boiler was a tilted-tube nest with two steam superheaters arranged between them. It was necessary to heat up the combustion chamber, resonance tube, and slag chamber with gaseous fuel before beginning coal-dust combustion.

The coal dust had a 12% ash content, a heating value of 12,380 Btu/lb, and a particle size 38% greater than 90 μm. Heat input to the combustor was 57.1 x 10^6 Btu/h. Combustion intensity was 2.02 x 10^6 Btu/h-ft^3 in the resonance tube and 2.58 x 10^6 Btu/h-ft^3 in the combined resonance tube and slag collector. About 20% of the total heat transfer was in the resonance tube, with a heat flux of 1.44 x 10^5 Btu/h-ft^2, and 32% in the slag chamber, with a heat flux of 55,300 Btu/h-ft^2. Burnout reached 90%, of which 80% occurred in the pulse combustor. Slag flowed as a colorless liquid from the edge of the resonance tube through the slag chamber into the sump. The gas oscillation leaving the resonance tube was damped relatively quickly in the flue flow path, but despite this rapid damping the crown of the boiler and other components vibrated considerably.

The pulverized coal had an ash content of 21%, a heating value of 11,040 Btu/lb, and a particle size of 18% greater than 90 μm. Heat input to the combustor was 35.7 x 10^6 Btu/h. Combustion intensity was 1.24 x 10^6 Btu/h-ft^3 in the resonance tube and 1.92 x 10^5 Btu/h-ft^3 in the combined resonance tube and slag chamber. About 22% of the total heat transfer occurred in the resonance tube, with a heat flux of 92,190 Btu/h-ft^2, and 34% in the slag chamber, with a heat flux of 36,880 Btu/h-ft^2. Burnout reached 88%, of which 74% was in the pulse combustor.

Sommers concluded that improvements could be made in the combustor and that it was not possible to determine if it could be incorporated into the design of future steam generators or gas producers.

In 1967, V.I. Hanby and D.J. Brown[18] in England conducted studies with a pulse combustor capable of firing 50 lb/h of pulverized coal. The coal, a highly volatile Elsecar Silkstone, was ground to 99.9% < 204 μm and 88.6% < 64 μm. The heating value (on a dry, ash-free basis) was 14,780 Btu/lb. The combustor was a conical chamber 12-in. long and expanding from 3- to 9-in. diameter; its volume was 0.5 ft^3. A 3-in. diameter, 5-ft long tailpipe was attached to the large diameter of the combustion chamber. Primary air was supplied by a 100,000 ft^3/h fan at 0.94 psi pressure to a flapper valve. Pulverized coal was delivered by a Mono powder-pump and injected through two 3/8 in. diameter, tangential jets located below the air valve. The combustor was attached to a brick furnace, which acted as a thermal load.

Stable pulse combustion was obtained without the addition of town gas. The stability of the flame varied with the fuel/air ratio. Under stoichiometric conditions the flame was not very stable; minor fluctuations caused by blockages in the coal-supply line caused flame extinguishment. As the air supply decreased the flame became more stable and the noise level increased considerably. The maximum air-flow rate was just sufficient to give a stoichiometric mixture at a minimum feasible coal-flow rate of 20 lb/h.

The operating frequency of the combustor was 75 Hz, and a pressure amplitude of ±0.72 psi was obtained with town gas, and ±1.81 psi with pulverized coal. Almost complete (95%) combustion was obtained in a time of 0.08 seconds, which corresponds to a combustion intensity of 0.8×10^6 Btu/h-ft^3. The brick furnace acted as an effective sound dampener, so the noise level was 80 dB at a distance of 6 ft from the furnace (an increase of 9 dB over the background).

The combustor was not in use long enough for information to be obtained on component life or for corrosion or slagging properties to be investigated. Sufficient heat transfer to the combustion tube walls was available to reduce the gas temperature below the ash fusion temperature so that no slag was formed in the combustor.

In the Soviet Union in 1969, Severyanin[19] conducted tests with three pulse combustors fired with pulverized Chelyabinsk brown coal. The coal -- which contains 28-33% ash, 8-10% water, and 40-42% volatiles and has a heating value of 7610 Btu/lb -- was ground so that 60-62% was <88 mesh and 27-30% was <200 mesh. All the combustors were started on liquid fuel (petroleum, turbine or transformer oil) and then switched to pulverized coal after being heated up.

The initial pulse combustor was made from refractory material and had a 19.66-in. long pear-shaped combustion chamber with a maximum diameter of 11.81 in. The resonance tube diameter was 3.94 in., and its length was 118.11 in. Coal was supplied to an air injector with a double-flight screw-type feeder and then to the burner via a 1.58-in. diameter flexible tube. Secondary air entered the combustion chamber through an annular aperture.

The burner operated at a frequency of 40-50 Hz, and pressure amplitudes of 0.20-0.44 psi were obtained. Maximum fuel consumption was 10.2 lb/h. A long period of pulse combustion was not achieved. Pulsations were observed until enough heat had accumulated in the lining (from liquid-fuel combustion) to displace the core of the flame along the resonance tube; when the luminous flame region left the combustion chamber, pulse combustion ceased. Attempts to increase the stability of pulsations by increasing the primary-air temperature, recirculating flue gas, varying the burner position and configuration, and improving the aerodynamics of the combustion chamber (setting up a strong swirl, vortices, and return gas flows) were unsuccessful.

A coaxial combustor having a 10.63-in. diameter combustion chamber that tapered down to a 3.94 in. diameter resonance tube was tested next. The length of the combustion chamber and resonance tube was not given. Pulverized coal was fed to the combustion chamber through a 1.58-in. diameter tube centered in the resonance tube. Combustion took place at the bottom of a reflector in the combustion chamber. Unheated secondary air entered the combustion chamber from four tangential openings above the reflector. For this combustor, the pulverized fuel heated up stably, the flame was held in the combustion chamber, and pulsating conditions existed in the whole range of loads.

The third burner tested was described as having a dipolar chamber with extremely good acoustical properties. The chamber diameter was 8.27 in., and the one containing the burner was 57.87-in. long. The other chamber, through which the resonance tube (2.99-in. diameter, 185-in. long) passed, was 65.75-in. long. Both chambers were equipped with a secondary air line. Surrounding the resonance tube was the air/pulverized-fuel mixture inlet line. The annular gap was 0.197-0.315 in. The two chambers were connected by a region (center of dipole) of maximum acoustic displacement in the first harmonic of the standing wave. The fuel-air mixture was preheated by the exhaust gases and then subjected to intense acoustical action in the center of the dipole. The fuel, which ignited stably and burned in the dipole, continued to burn in the resonance tube. The combustor had a 50-60 Hz operating frequency and pressure amplitudes of 0.46-0.91 psi. The firing rate was 6.6-8.3 lb/h, the overall excess air factor was 0.7-1.1, and the combustion intensity obtained was 0.94-1.33 x 10^6 Btu/h-ft^3. It was noted that the pressure amplitude increased when the excess air was decreased, and when the excess-air factor was <0.7, combustion was explosive. When the air supply was approximately 50% higher than stoichiometric, combustion had a distinctly turbulent, rather than pulsating, nature.

Ellman, Belter, and Dockter[20] operated a large (24,000,000 Btu/h) pulse jet on a mixture of lignite and residual oil (3% by weight). Combustion intensities of 500,000 Btu/h-ft^3 were obtained from a Helmholtz-type combustor with an overall length of 35 ft and a main-tube length of 30 ft. Powdered lignite, a waste product of the lignite-mining operation, was dropped into a vertical stainless-steel standpipe that projected into the center of a refractory-lined combustion chamber. The high-amplitude pulsations were found to facilitate ash discharge; the molten ash formed a pool in the bottom of the combustion chamber and was ejected as it flowed into the tailpipe section. The noise, produced at the low operating frequency of 15 Hz, was less irritating than the sound from an 8-ft long, 70-Hz pulse jet. At 5 ft from the engine, the sound level was 120 dB; at 40 ft, it was 100 dB. However, the noise was reported to be audible at a distance of 20 miles.

Notably absent from recorded testing of solid-fuel-fired pulse combustors is the use of wood or wood waste as a fuel.

1.3.2 Gas-fired Pulse Combustion Burners

Pulse combustors have been fired with natural gas, town gas, methane, propane, hydrogen, acetylene, and butane. Natural gas is gas that occurs naturally in underground reservoirs or in solution with crude-oil deposits. Its composition varies with the source but is principally methane, with the remaining constituents being ethane, propane, and other paraffinic hydrocarbons, along with small amounts of hydrogen sulfide, carbon dioxide, nitrogen, and (in some deposits) helium. Town gas is manufactured from coal and is used in Great Britain for heating and illumination. The gas contains about 50% hydrogen and 10% carbon monoxide by volume, the remainder being methane and other gases. Its heating value is about half that of natural gas. Pertinent studies of gas-fired pulse combustion are listed in Table 1.1. Additional details are presented in Appendix E of this report.

1.4 SCOPE OF ANL EXPERIMENTAL PROGRAM

Dwindling reserves, instability of supplies, and rising prices of fossil fuels have sparked the development of combustion heating systems with higher efficiencies. Pulse combustion, with its positive venting, high combustion intensity, minimal standby losses, and potential for increased heat transfer, is an attractive heating technology, provided that its disadvantages and the lack of design information can be overcome. In order to address these problems, an experimental program was initiated at Argonne National Laboratory in June of 1978, under the sponsorship of the U.S. Energy Research and Development Administration (later the U.S. Department of Energy).

The purpose of this program was to develop and expand the technology base for fossil-fuel-fired pulse combustion heating systems so that it could be readily used by manufacturers of such equipment. In order to accomplish this goal, several phases of investigation were required. One phase was to define the influence of burner design parameters on the perf rmance and efficiency of pulse combustion equipment. Initial studies would utilize gaseous fuels, with solid and liquid fuels to be employed later (especially synthetic fuels from coal or oil shale). A second phase was to be the identification of noise sources and their suppression. As part of this activity, the formation of pollutants and the operational safety of pulse combustion systems were to be investigated. A third phase was to evaluate the potential of pulse combustion technology relative to other technologies, in order to determine its best applications and overall impact. This phase was also to provide for the development and dissemination of design guidelines and procedures so that reasonable tradeoffs between performance, noise, and cost could be made.

As part of the ANL program, an experimental Helmholtz-type pulse combustor was designed, fabricated, and assembled, along with ancillary equipment. These activities, equipment checkout, preliminary testing, and operational problems precluded any significant data acquisition until late 1979. Due to budget cuts by the U.S. Department of Energy, the ANL program was unexpectedly terminated in January 1981, before the program goals could be achieved.

Table 1.1 Studies of Gas-Fired Pulse Combustion

Fuel	Investigators	Reference Number
Natural gas	Griffiths, Thompson, and Weber	21
	Kitchen	22
	Griffiths and Weber	23
	Kunsagi	24
	Vogt, Yen, Schoenhals, and Soedel	25
	Vogt	26
	Dhar, Soedel, and Schoenhals	27
	Vogt, Yen, Schoenhals, and Soedel	28
	Dhar, Soedel, and Schoenhals	29
	Dhar, Huang, Lee, Soedel, and Schoenhals	30
Town gas	Francis, Hoggarth, and Reay	31
	Hanby and Brown	18
	Reay	32
Methane	Reader	3
	Briffa and Romaine	33
	Katsnel'son, Marone, and Tarakanovskii	34
Propane	Muller	35
	Beale, Clarke, and Everson	36
	Ringer, Lane, and Slawinski	37
	Belter	38
	Kentfield	39, 40
	Hanby	41, 42
	Hanby and Brown	43
Acetylene	Katsnel'son, Marone, and Tarakanovskii	34
Hydrogen	Katsnel'son, Marone, and Tarakanovskii	34
Butane	--	9

2 EXPERIMENTAL EQUIPMENT

The ANL experimental pulse combustion burner system is shown schematically in Fig. 2.1 and photographically in Fig. 2.2. Details of the ANL system are presented in the following sections.

2.1 BURNER ASSEMBLY

The burner was a gas-fired and water-cooled one of the Helmholtz type. Its design was based on information supplied by Griffiths and Weber[23] for a nominal heat-input rate of 150,000 Btu/h. The design incorporated some experimental flexibility by providing adjustable air and gas valves and adjustable tailpipe length. Individual cooling channels surrounded the combustion chamber and tailpipe to make local heat-transfer data obtainable. Initially, a quartz window was planned for the combustion chamber so that the flame and air valve could be observed visually and photographically. However, the curved quartz windows cracked, and a solid-wall combustion chamber had to be used.

The burner, shown schematically in Fig. 2.3, consisted of an air-inlet tee, a combustion chamber, a tailpipe, water-cooling channels, a gas-distribution head, and the air and gas flapper valves. The combustion chamber was a carbon-steel cylinder with a 4-in. inside diameter (ID), a 4.5-in. outside diameter (OD), and a length of 9 3/8 in. above the center line of the gas-distributor head. The chamber contained a spark igniter positioned just above the gas-distributor head. The tailpipe, a carbon-steel tube with 1.75-in. ID, 1 15/16-in. OD, and a length of 48 3/8-in., was screwed into the 3/8-in. thick head of the combustion chamber. The gas-distributor head was 3.5-in. in OD and had 16 1/8 in. diameter holes equally spaced around the circumference. The air-inlet tee was a 4-in., schedule 40, stainless-steel, butt-welding tee that had been modified. The tee branch had a short pipe stub and a slip-on flange. The run of the tee was modified to support the air- and gas-valve assemblies. A picture of the air-inlet tee with the valve assemblies and gas-distributor head is shown in Fig. 2.4. The burner was mounted on a Unistrut Corp. frame in a vertical position, with the combustion chamber below the tailpipe. A picture of the burner assembly is shown in Fig. 2.5; detailed drawings are included in Appendix A.

2.1.1 Gas Valve

The gas valve was a variable-lift flapper valve with the flapper seating over 10 holes, each 1/8-in. in diameter. The adjustable-lift range (distance between the valve seat and the flapper, when open) was from 0 to about 1/2 in. A picture of the assembled gas valve is shown in Fig. 2.6, and its component parts are shown in Fig. 2.7. The flapper was a ring of Midwest

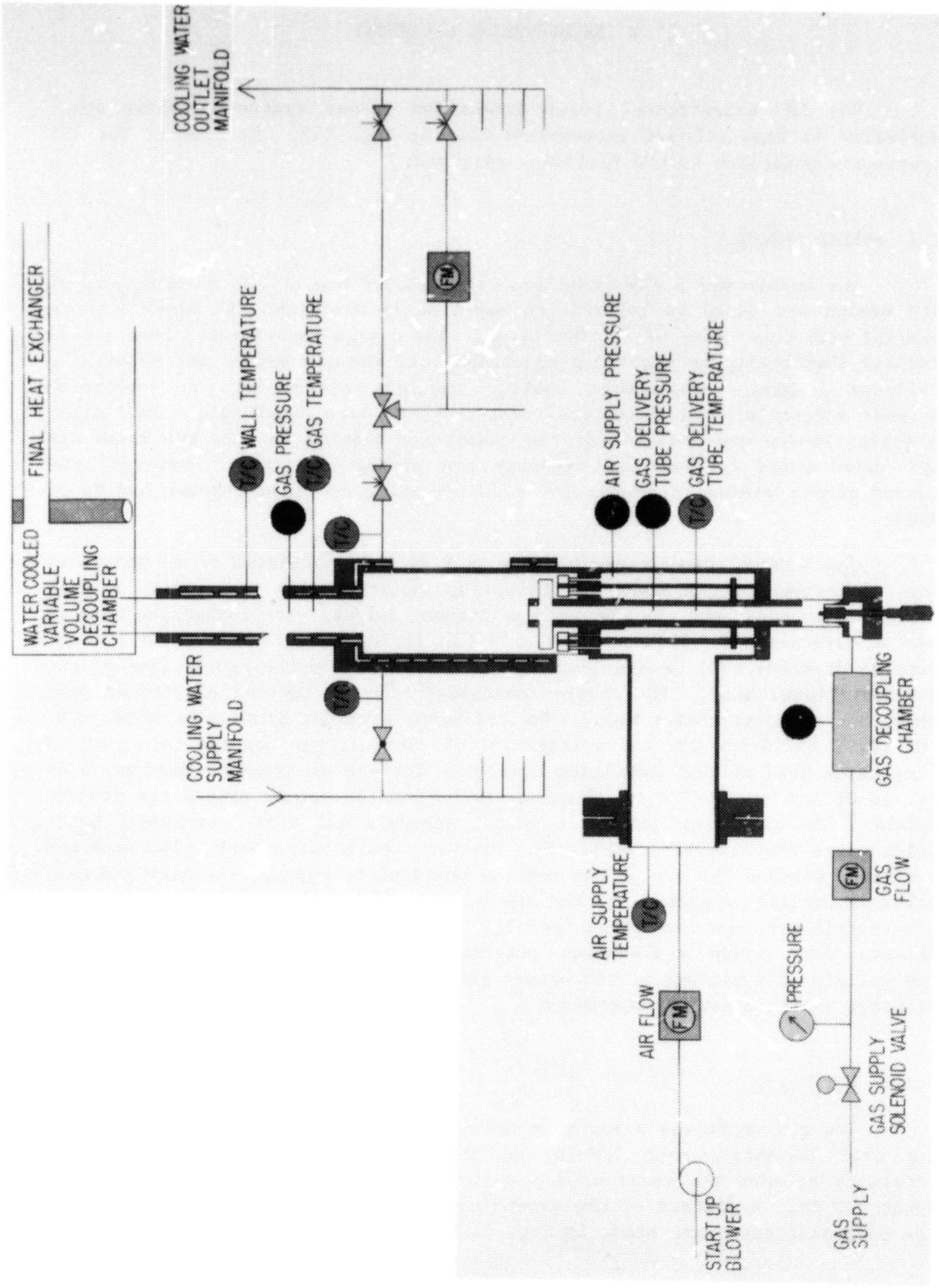

Fig. 2.1 Schematic Diagram of ANL Pulse Combustion Burner System

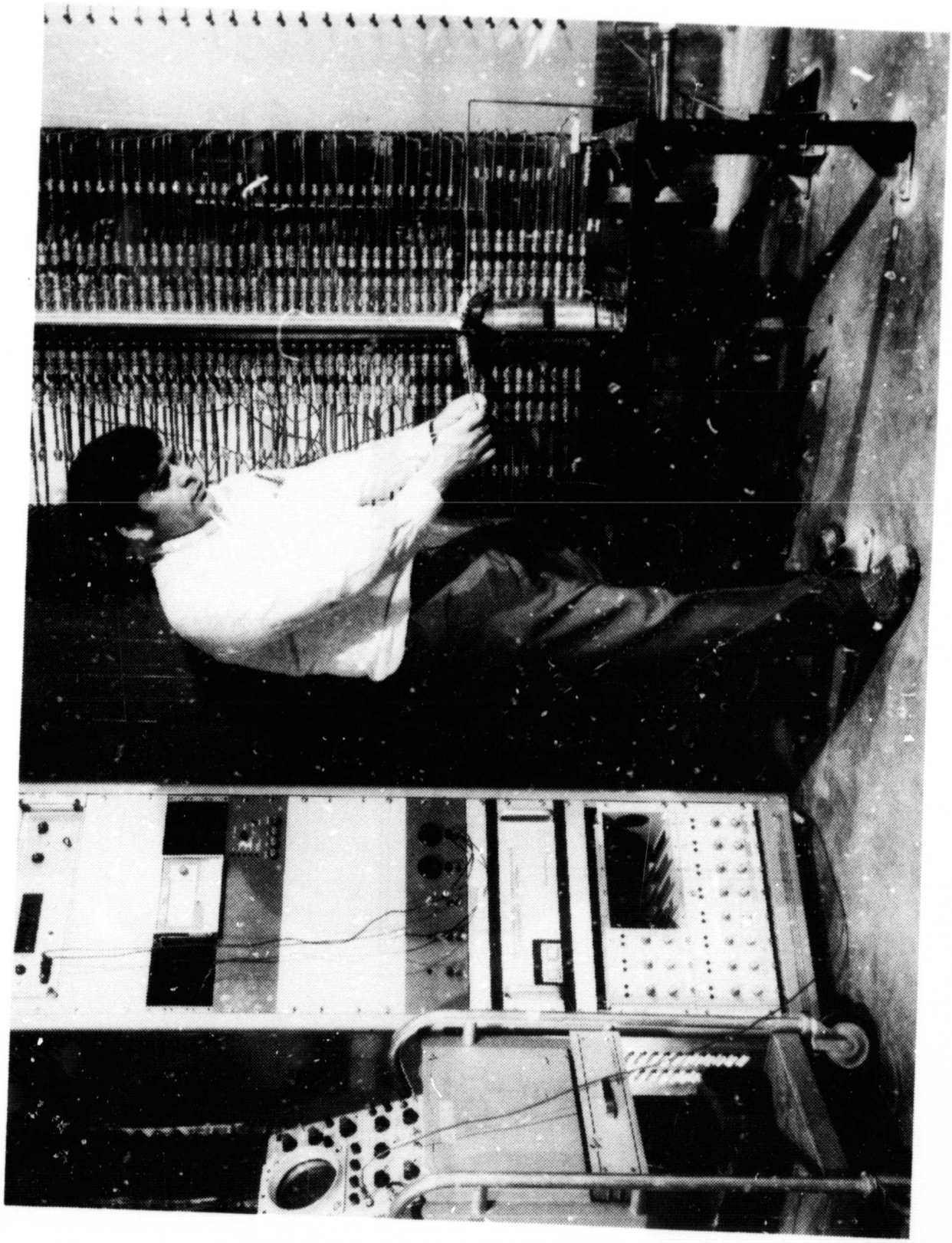

Fig. 2.2 View of ANL Pulse Combustion Facility

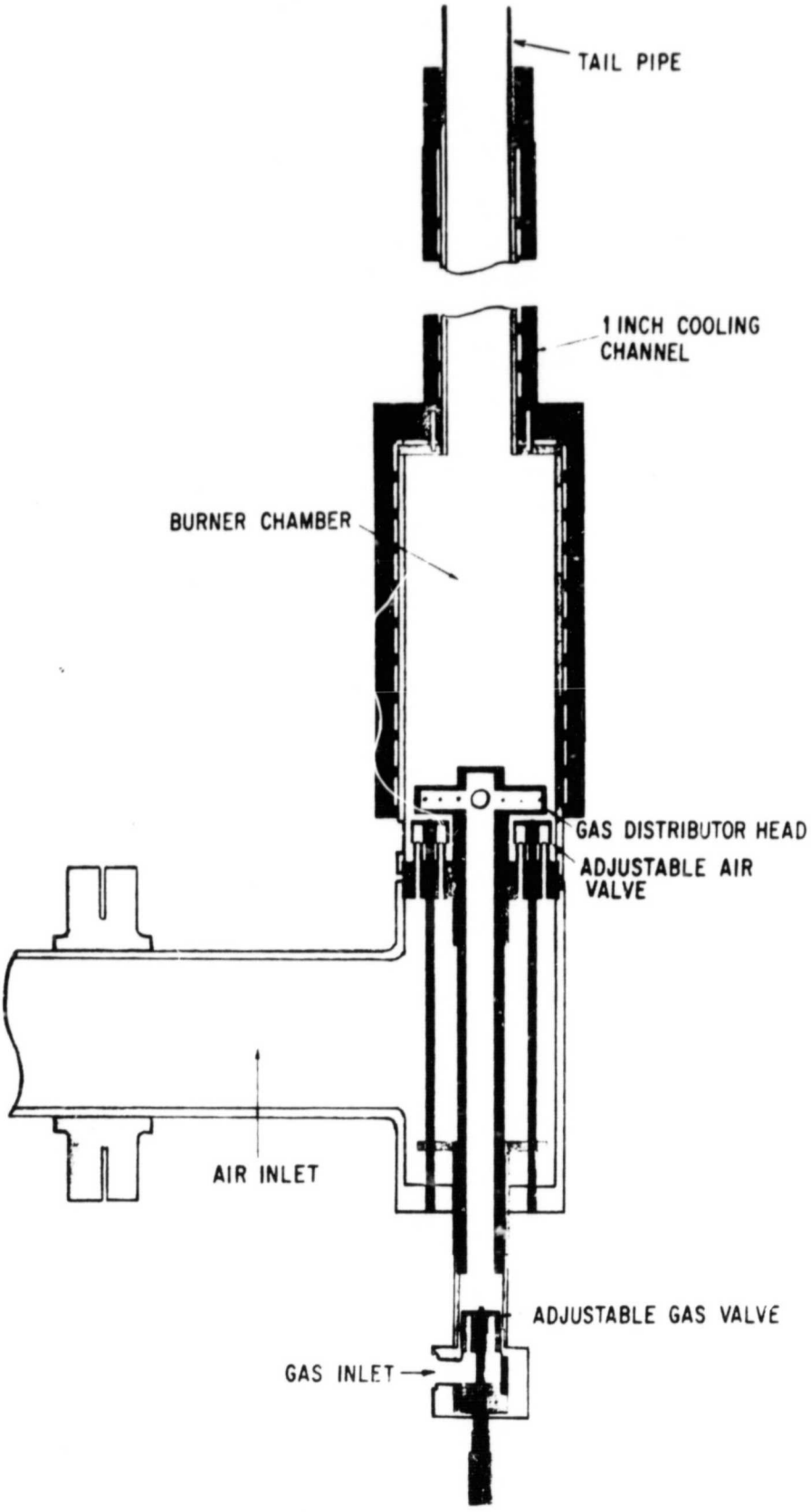

Fig. 2.3 ANL Pulse Combustion Burner

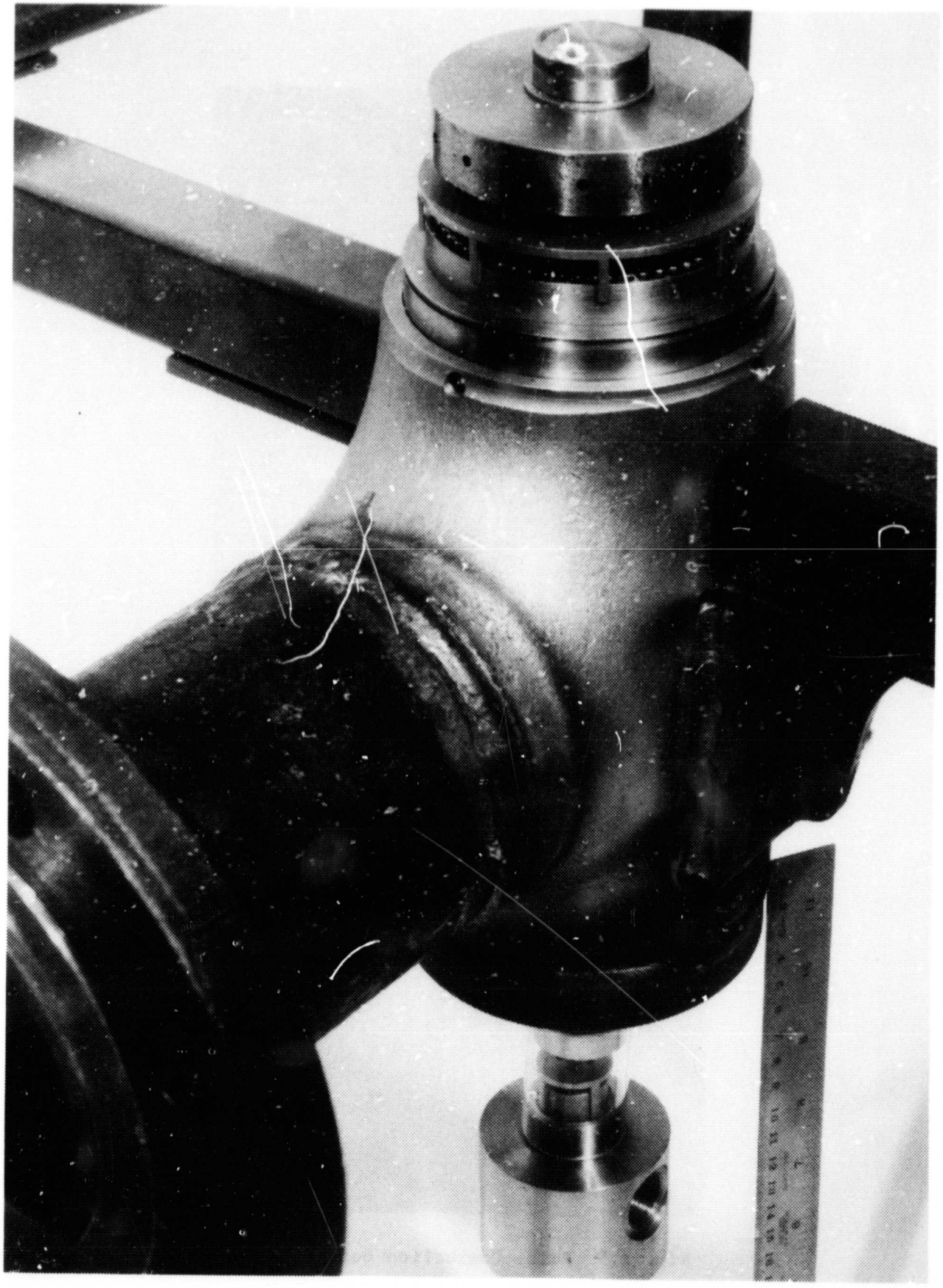

Fig. 2.4 Air-Inlet-Tee Assembly

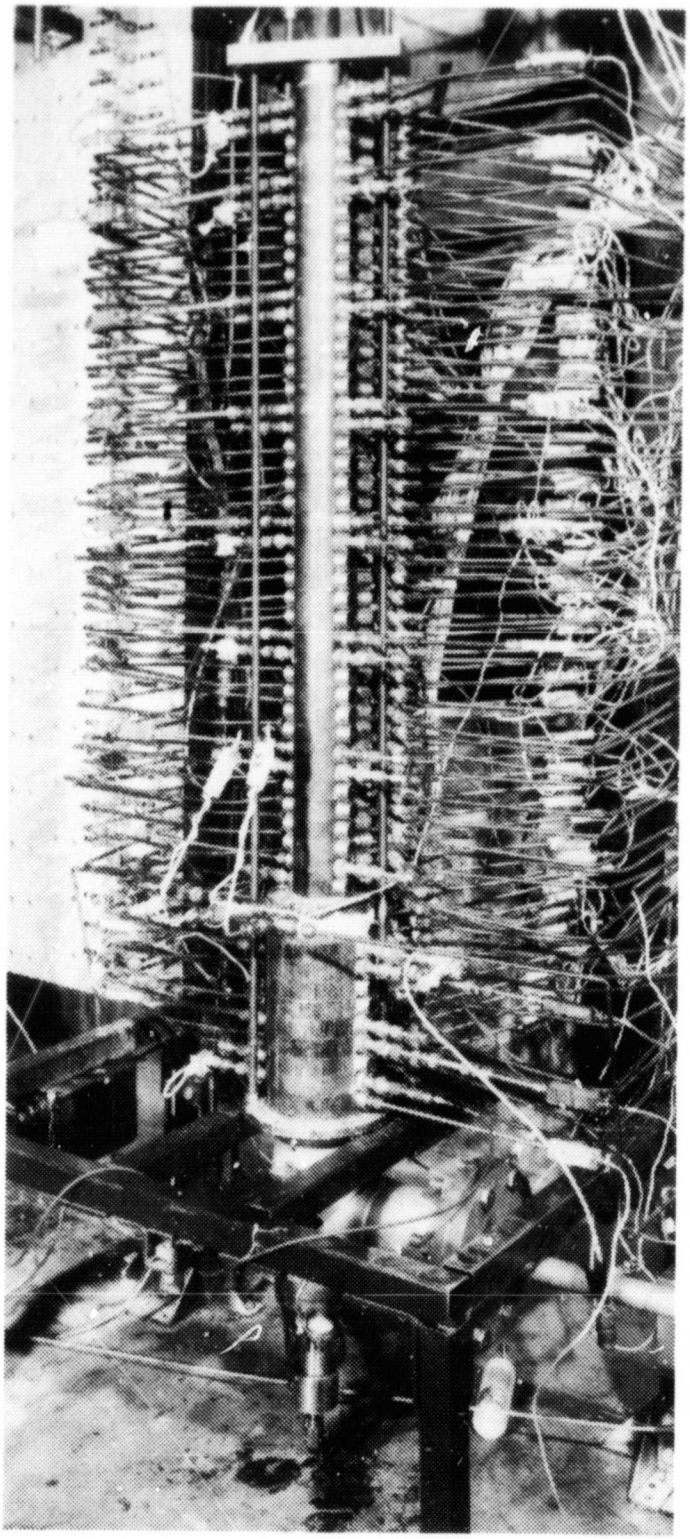

Fig. 2.5 Pulse Combustion Burner Assembly

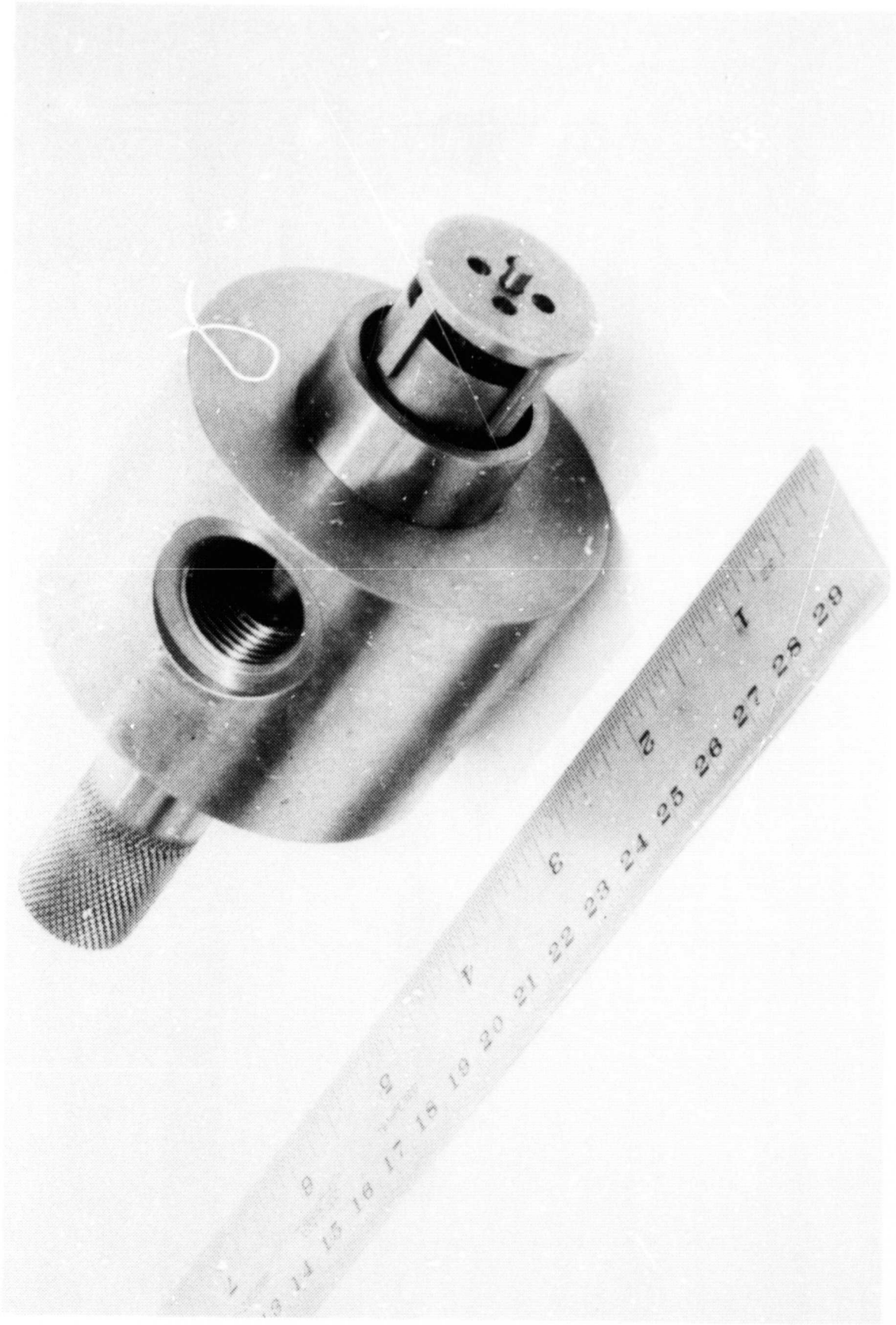

Fig. 2.6 Gas-Valve Assembly

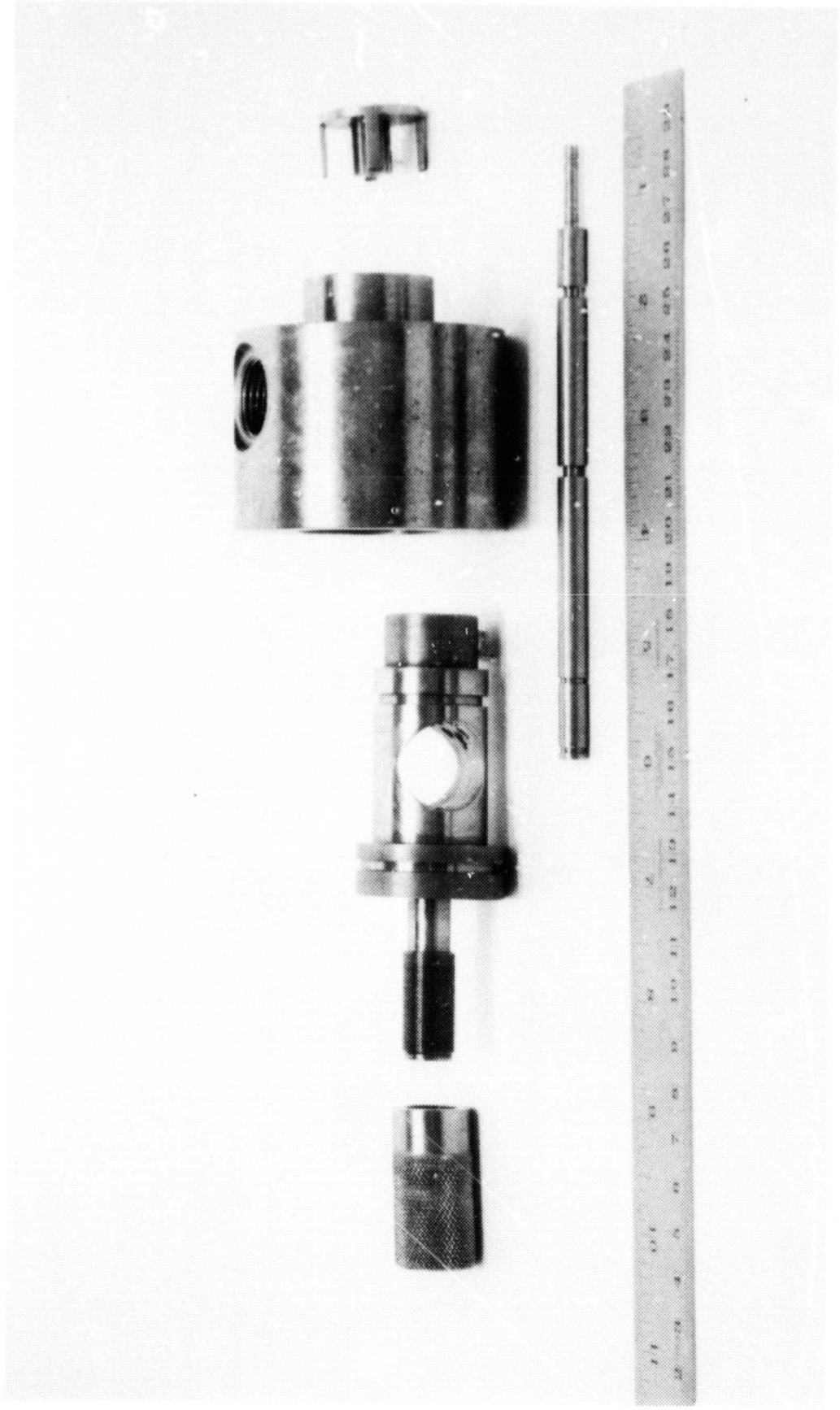

Fig. 2.7 Component Parts of Gas Valve

Belting Industries, Inc., No. 02010 Teflon®-coated* fiberglass having a nominal thickness of 0.010 in.

2.1.2 Air Valve

The air valve was a variable-lift flapper valve with two concentric sets of flappers. The inner flapper was 2 3/8-in. OD, 1 7/8-in. ID, and seated over 36 holes, 1/8-in. diameter. The outer flapper was 3 5/8-in. OD, 3 1/8-in. ID, and seated over 60 holes, 1/8-in. diameter. A picture of the assembled air valve is shown in Fig. 2.8; the air-valve plate is shown in Fig. 2.9, and the remaining components are shown in Fig. 2.10.

Prior to final burner assembly in the laboratory, some steady-flow tests of the air flapper valve were performed. The objectives were to verify the valve design and to establish the flow characteristics over a range of flapper lifts. The valve was mounted in the combustion chamber, which was maintained below atmospheric pressure by means of a blower. At each desired flapper lift, the air-volume flow rate was measured as a function of pressure difference across the valve, which was varied by changing the combustion-chamber pressure. The results are presented in Fig 2.11. In the limit of small lift and low flow rate (thus, low Reynolds number), the flow was linearly proportional to pressure drop at constant lift. This would be expected for a laminar flow with negligible inertial effects. Over the range of lift and flow predominating in the operating burner, however, the flow at constant lift was proportional to the square root of pressure drop. This also is expected behavior.

The variation of air-flow rate with lift (i.e., with valve flow area) at constant pressure difference is shown in Fig 2.12. Although there is some uncertainty in the smaller lift values, the relationship is quite linear, implying that the valve-discharge coefficient was essentially constant.

2.1.3 Corebustor and Tailpipe Aspirator

In order to obtain a tailpipe-geometry change, a 1-in.-diameter solid rod was centered inside the tailpipe for its entire length or, in some tests, only for the last 36 in. This rod is referred to as a "corebustor."

While visiting ANL for pulse-combustion discussions, John Kitchen demonstrated that a simple copper-tube reducer with the small end butted onto the end of the tailpipe could increase the pressure amplitude in the combustion chamber. Therefore, this fitting (called a "tailpipe aspirator") was utilized for some tests (see Fig. 2.13).

---

*Teflon® is a registered tradename of E.I. duPont de Nemours & Co., Inc., Wilmington, Del.

Fig. 2.8 Air-Valve Assembly

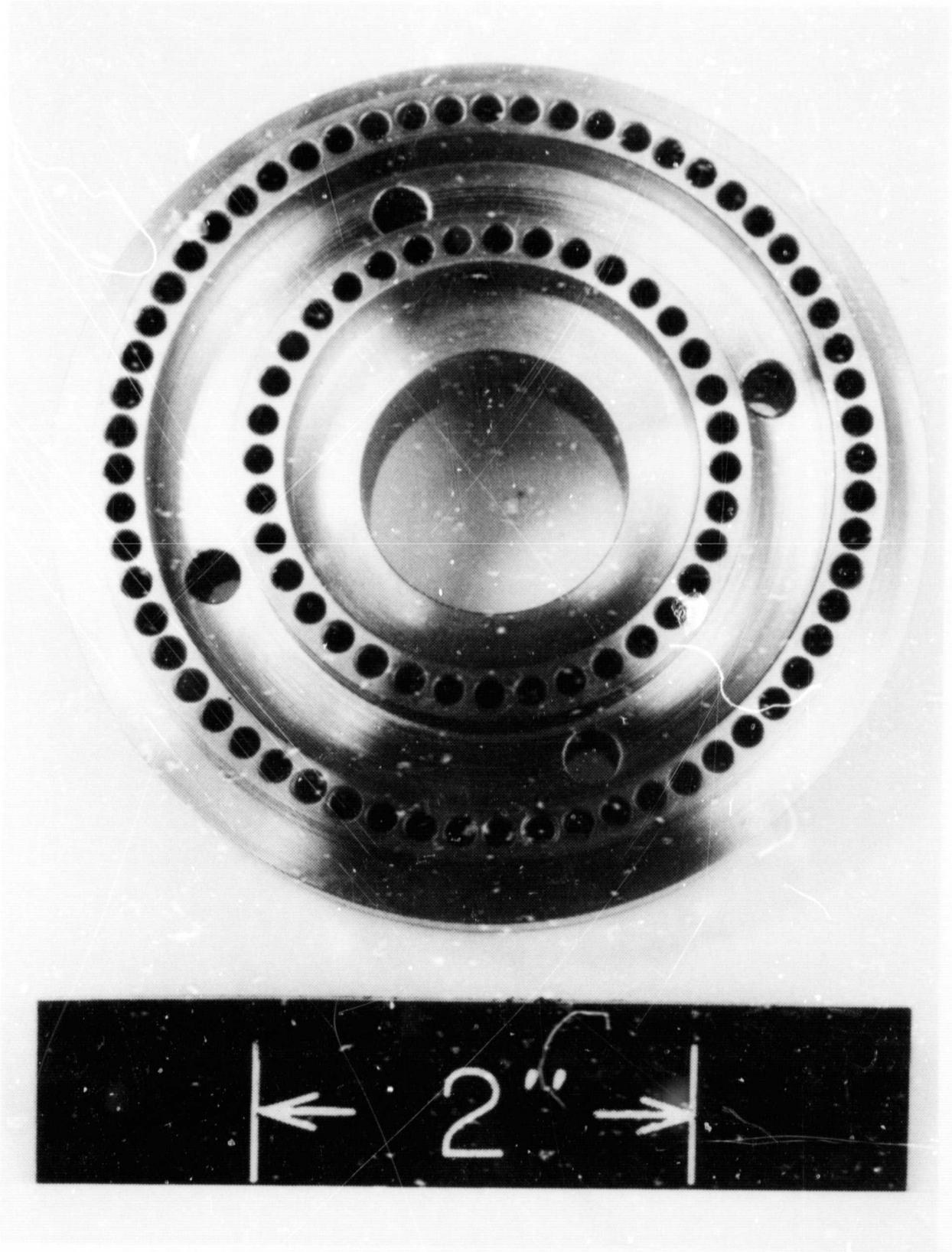

Fig. 2.9 Air-Valve Plate

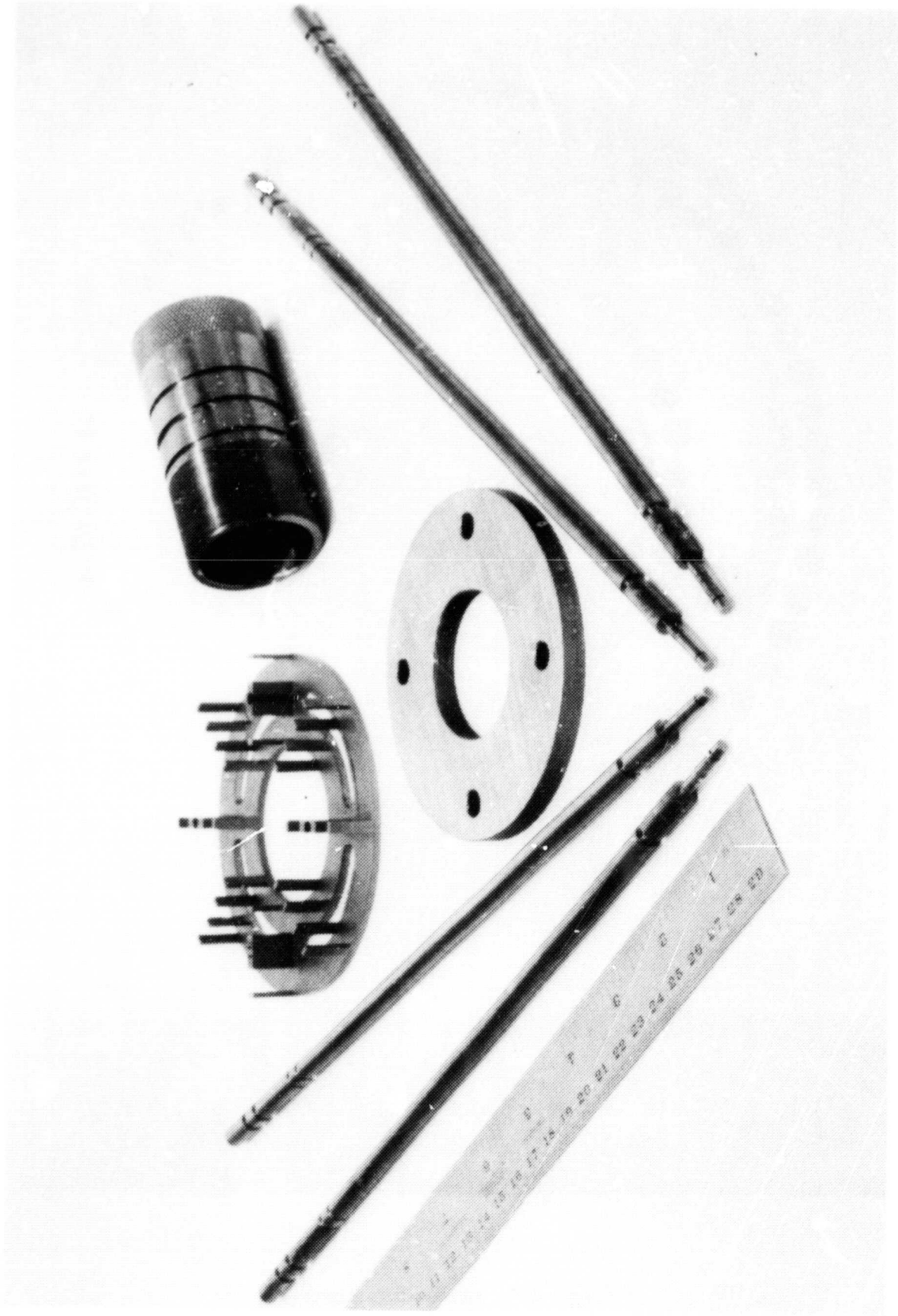

Fig. 2.10 Air-Valve Components

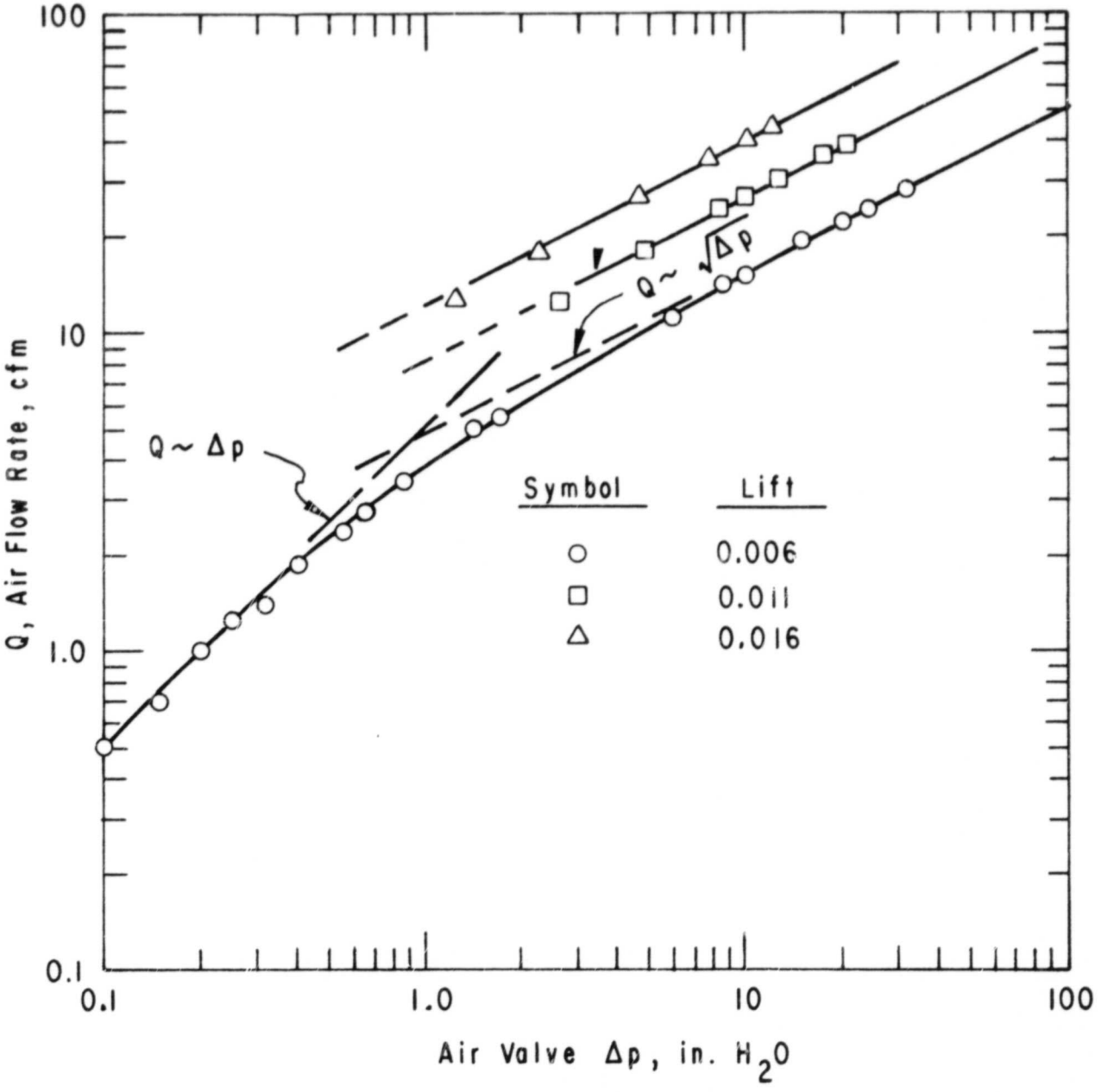

Fig. 2.11 Flow Characteristics for Air Flapper Valve

2.1.4 Burner Safety Circuit

In operating the burner, a safety circuit was incorporated for automatic shutdown in case ignition of the gas mixture should fail to occur. Light-emitting diodes on the front panel of the safety-circuit cabinet showed the status of components of the system. These indicators were: power-on, remote-shutdown switch, purge-fan, gas-valve, and ignition. With the remote-shutdown switch open (off), the burner would not run, because power was off to the logic system that controlled the gas valve and igniter. If the remote-shutdown switch was open, its front panel indicator was lighted. When any of

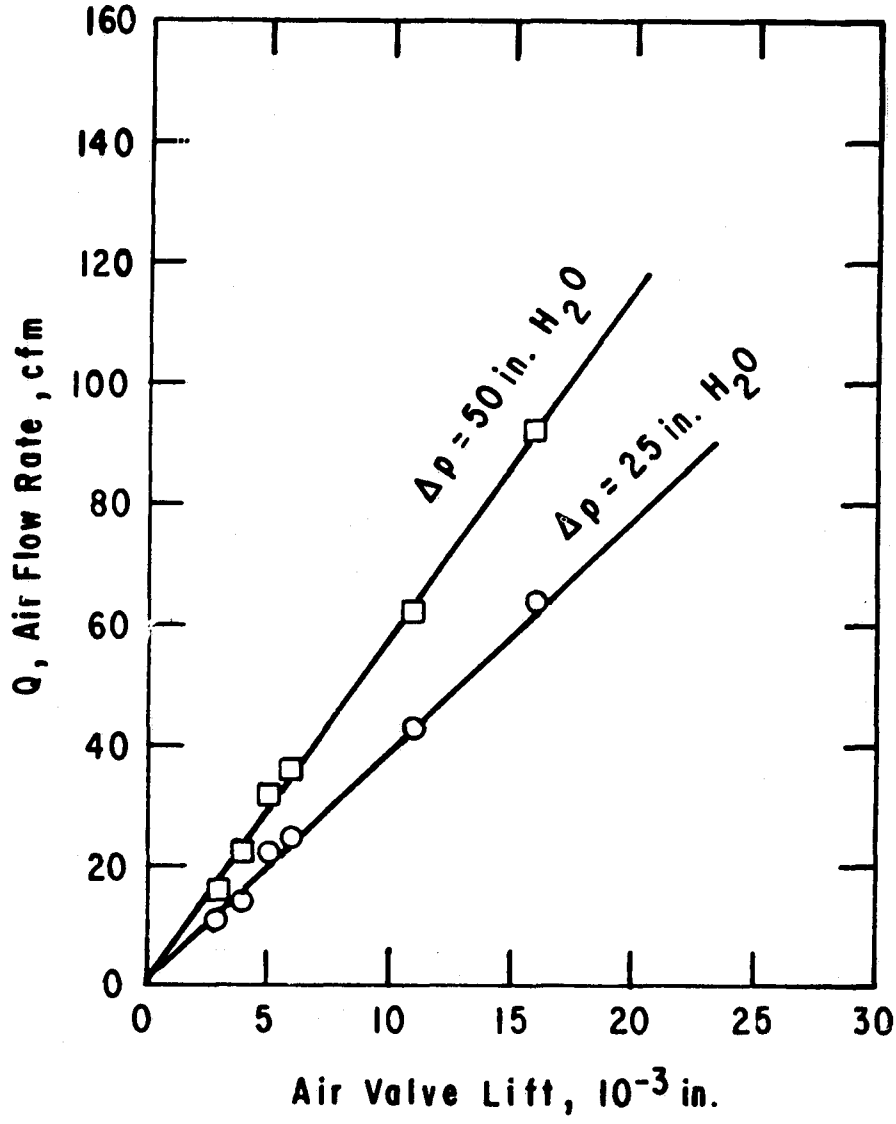

Fig. 2.12 Effect of Valve Lift on Air-Flow Rate

the last three indicators was lighted, the component it represented was activated.

There were two switches on the front panel. The start switch started a timing sequence for start-up. The mode-selector switch had three positions. The "Off" position grounded the input to the logic circuit. In the "Manual" position, the air-supply fan ran, forcing air through the burner. The "Auto" position allowed the system to be started up. The front panel also had four indicator-type fuse holders. The fuses were: logic, fan, gas valve, and igniter. A glowing indicator would mean a blown fuse and possible defect in that portion of the burner safety system.

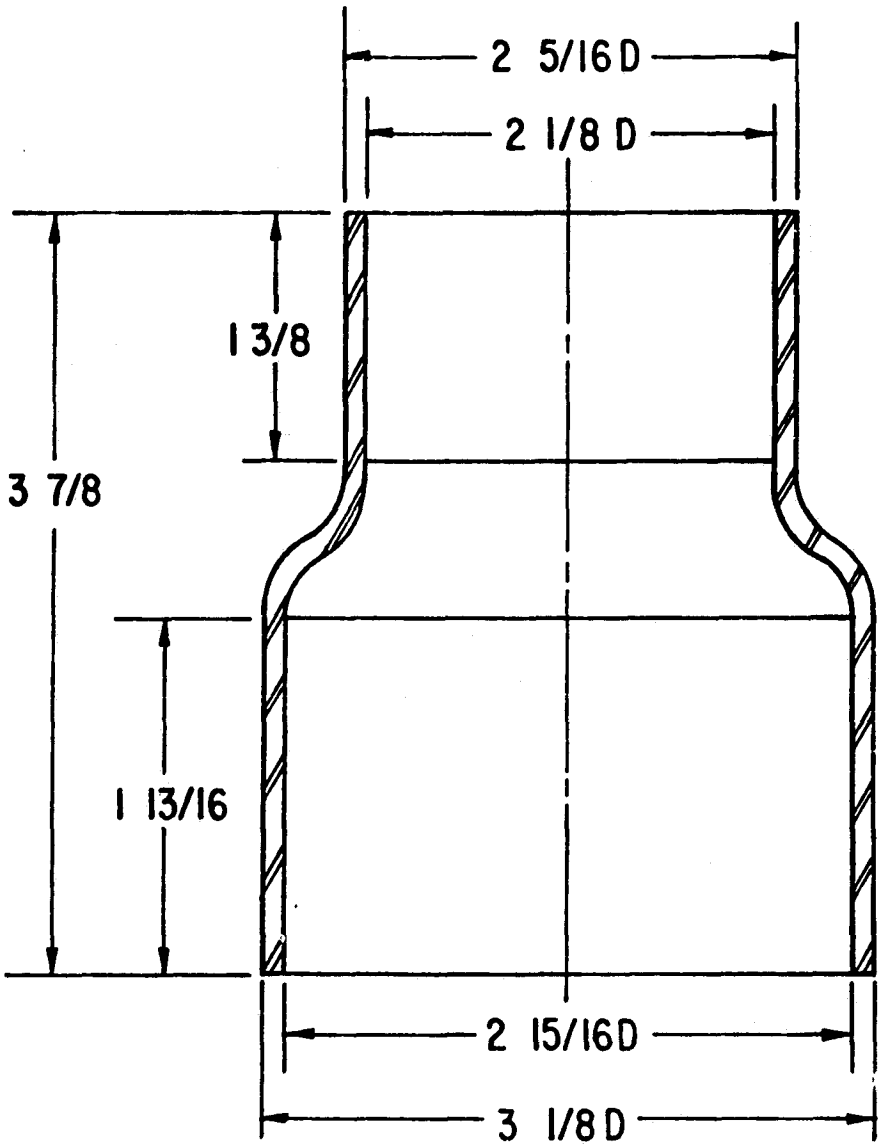

Fig. 2.13 Tailpipe Aspirator (all measurements are in inches)

To start the burner, the power indicator had to be lighted. The four fuse indicators and the remote-shutdown indicator would be off. When the mode-selector switch was in the "Auto" position, the purge fan and fan indicator came on. When the switch was depressed, the timing sequence began. Approximately 10 s after the start button was pushed (purge time), the gas valve opened and the igniter turned on. The valve and igniter remained in this state for about 10 s. At the end of that time, if ignition had not been detected by a thermocouple (later by a pressure wave) in the combustion chamber, the gas valve shut and the igniter turned off. The purge fan remained on to clear the chamber. If ignition was detected, the igniter and

purge fan shut off and the gas valve remained open. Extinguishing of the flame during operation would be detected by the flame thermocouple, and its temperature controller would signal the safety circuit; the gas valve would close and the purge fan would start. Placing the mode-selector switch in the "Off" position also shut the gas valve.

2.2 MUFFLERS

A wide variety of commercial mufflers that could be installed in the exhaust and air-intake lines to the burner system was available for noise suppression. However, it was felt that a fundamental approach should be taken to investigate the effect of design and size of mufflers on noise control.

From the viewpoint of simplicity of low-cost muffler design and minimum back-pressure requirements, it was decided to size a low-pass noise filter (reactive muffler) based on a procedure outlined in Refs. 44 and 45. This device filters out most of the noise above a certain cut-off frequency that is less than the fundamental pulsation (firing) frequency of the burner. As an engineering approximation, the muffler is considered as an expansion volume with a neck, which represents an exit tailpipe (see Fig. 2.14). This combination can mathematically be interpreted as a one-degree-of-freedom Helmholtz resonator. The fundamental Helmholtz angular frequency ω_{n2} of the filter is:

$$\omega_{n2} = c\sqrt{\frac{A_2}{LV}} \tag{2.1}$$

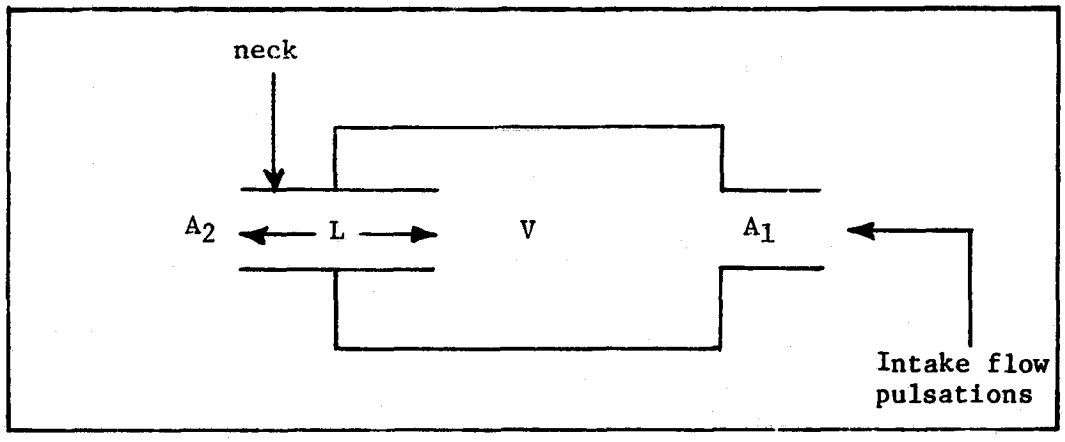

V = expansion volume

ω_{n1} = pulsation angular frequency of combustor

A_1 = entrance tailpipe area

A_2 = exit tailpipe area (neck)

L = length of exit tailpipe (neck)

Fig. 2.14 Schematic Diagram of a Low-Pass Noise Filter

where c = sound velocity at exhaust temperature, and the other variables are defined in the figure.

According to Ref. 8, for effective filtering it is necessary that:

$$\omega_{n2} << \frac{\omega_{n1}}{\sqrt{2}} \tag{2.2}$$

where ω_{n1} = pulsation angular frequency of combustor.

In addition, the intake tailpipe area A_1 should be at least equal to the area of the exit tailpipe A_2 (neck), so that the mean flow is not restricted.

For the ANL burner system, the frequency of oscillation was given by:

$$f_{n1} = \frac{\omega_{n1}}{2\pi} \approx 75 \text{ Hz} \tag{2.3}$$

Assuming that $\omega_{n2} = 0.48\ \omega_{n1}$, Eq. 2.1 can be solved to obtain the expansion volume:

$$V = \frac{A_2}{L}\left(\frac{c}{226.195}\right)^2 \tag{2.4}$$

Since the muffler must connect to the inlet-air or exhaust-gas piping, assume that $A_2 = A_1$. Hence, Eq. 2.4 can be solved by assuming values for L. The dimensions of the exhaust and intake mufflers were sized according to the diameter. To match the acoustic impedance, an equivalent volume V was attached to the Helmholtz volume to provide a combination muffler.

The intake and exhaust mufflers shown in Figs. 2.15 and 2.16 were fabricated and tested on-line to determine their noise-reduction effectiveness (insertion loss) as a function of the air and gas flow into the pulse combustion burner system.

2.3 COOLING SYSTEM

Treated cooling water from a storage tank was circulated (35 gal/min maximum) by a centrifugal pump to a header that supplied water to the 54 cooling channels on the burner. The water-flow rate to each channel was set manually with a flow-control valve. As the water left a cooling channel, it passed through a three-way solenoid valve that was computer-controlled to route the water either to a flowmeter or to the return header and back to the storage tank (or to a 10-ton evaporative-type cooling tower and then to the storage tank). A temperature sensor at the pump outlet controlled a valve that diverted the return flow to either the storage tank or the cooling tower. The cooling tower was outside the laboratory and elevated above the storage tank so that the water from the tower drained directly into the storage tank. To compensate for evaporative losses, de-ionized water from an elevated makeup tank flowed into the storage tank under the control of a float valve in the

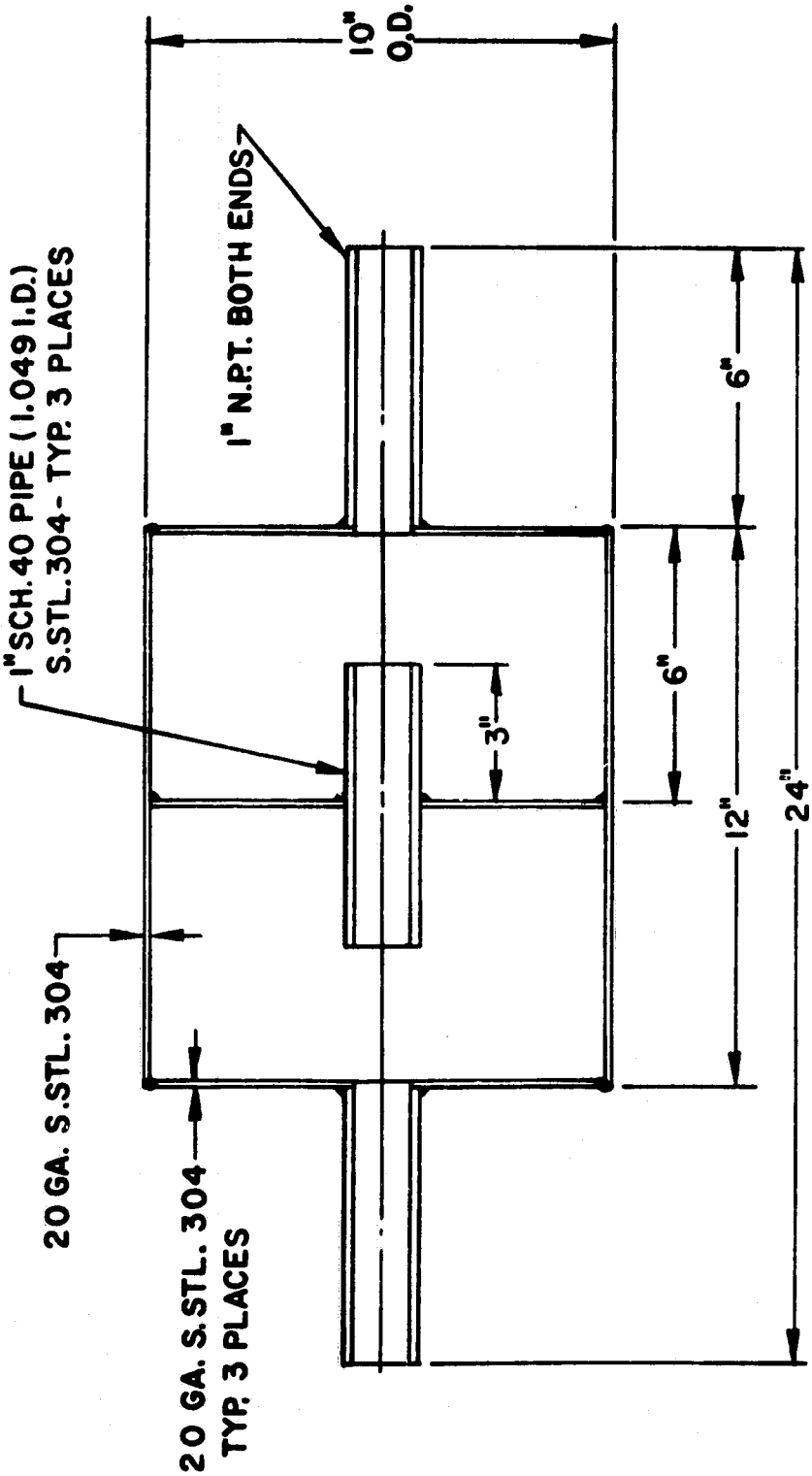

Fig. 2.15 Air-Intake Muffler

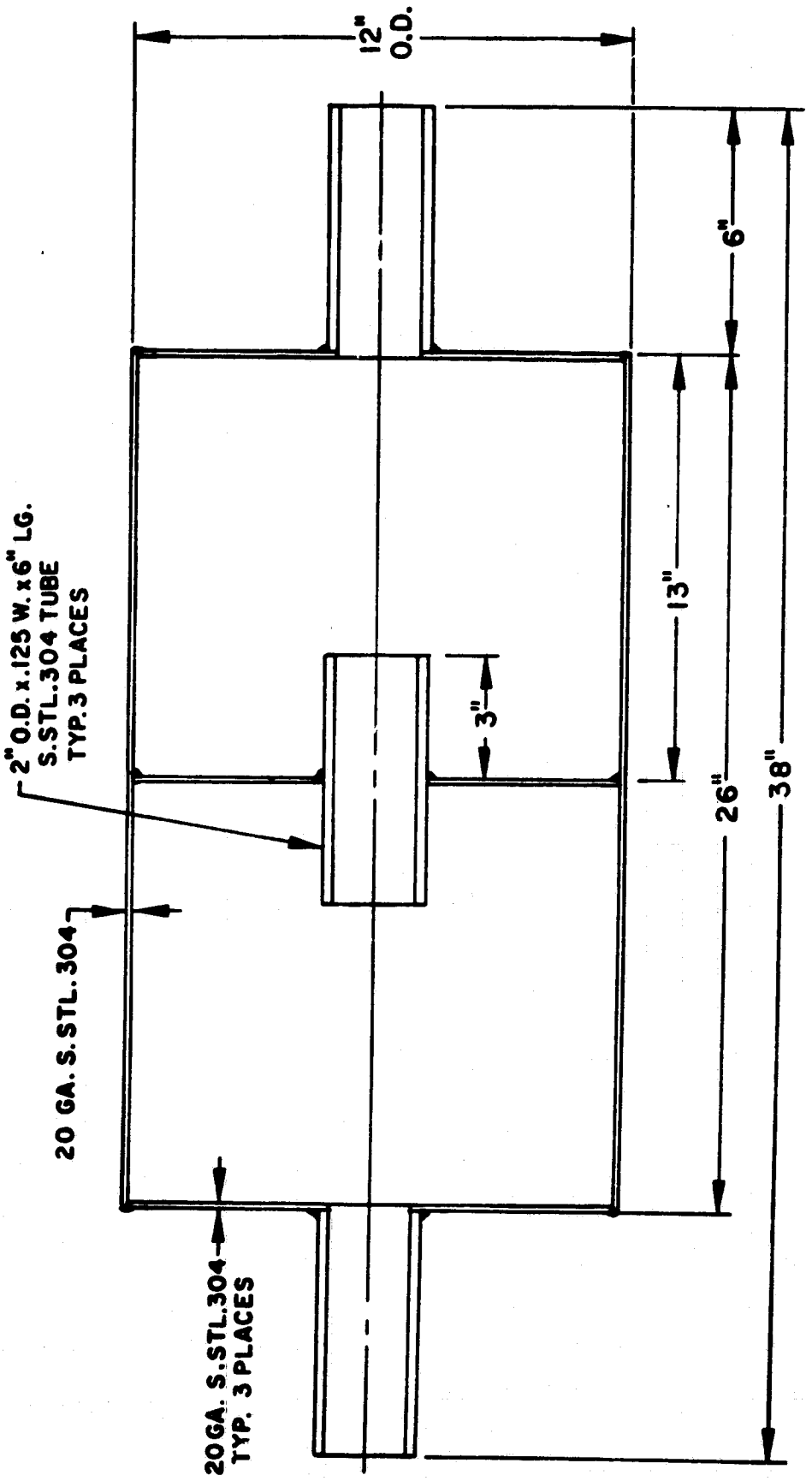

Fig. 2.16 Exhaust-Gas Muffler

latter tank. De-ionized water for the makeup tank was obtained from the domestic cold-water supply by passing it through ion-exchange cartridges.

A schematic of the normal flow arrangement for the burner is shown in Fig. 2.17. For the sake of clarity, not all the coolant inlet and exit lines are shown. In this parallel-flow arrangement, water at a constant initial temperature continuously enters each cooling channel from the common supply header. The flow rate through each channel is measured in groups of three (e.g., channels 1, 20, and 40; 2, 21, and 41) by the turbine flowmeters designated "A," "B," and "C" in Fig. 2.17. (The dotted line in the figure indicates the flow diverted to the meter.) A computer-controlled switching arrangement diverts the coolant flow and/or exit flow through the meters. When flowmeter "B" failed, the burner was repiped into a series-flow arrangement (shown in Fig. 2.18) while awaiting its repair to reduce the time needed for flow measurements. The first 18 cooling channels, covering the combustion chamber and tailpipe-entrance regions of the burner, were series-plumbed into groups of three (e.g., 1, 7, 13; 2, 8, 14) and utilized flowmeter "A". The remaining 36 cooling channels were also series-plumbed in groups of six (e.g., 19, 25, 31, 37, 43, 49; 20, 26, 32, 38, 44, 50; etc.) and utilized flowmeter "C". This arrangement required only six switchings of the flow path to measure the coolant flow through all 54 channels, in contrast to the 19 switchings required for parallel flow. One disadvantage of this arrangement was that burner operation was limited to approximately a 100,000 Btu/h heat input because the low flow range of flowmeter "C" did not allow sufficient coolant flow for heat removal at the higher heat-input rates.

Cooling channels 1-11 were used to remove heat from the combustion chamber, and channels 12-54 were used on the tailpipe. The last 5-in. of the tailpipe was uncooled. Channels 1-10 were identical 1-in. thick disks with a water passage approximately 0.828-in. high and 0.131-in. wide. A typical combustion-chamber cooling channel is shown in Fig. 2.19. The rectangular strips were dividers that separated the water inlet and outlet. Cooling water flowed circumferentially around the chamber.

The combustion-chamber head, which contained cooling channel No. 11, is shown in Fig. 2.20(a). The cooling channel (No. 54) shown in Fig. 2.20(b) was used to cool the tailpipe entrance and also contained the water inlet and outlet connections for channel No. 11.

A typical tailpipe cooling channel is shown in Fig. 2.21. This channel was also 1-in. thick, with a water passage 0.856-in. high and 0.086-in. wide (radial gap). As with the combustion-chamber channel, the water entrance and exits were adjacent and were separated by a rectangular strip. The water also flowed circumferentially around the tailpipe.

Sealing between the individual cooling channels was accomplished using O-rings. The channels were held in place by threaded rods between support plates.

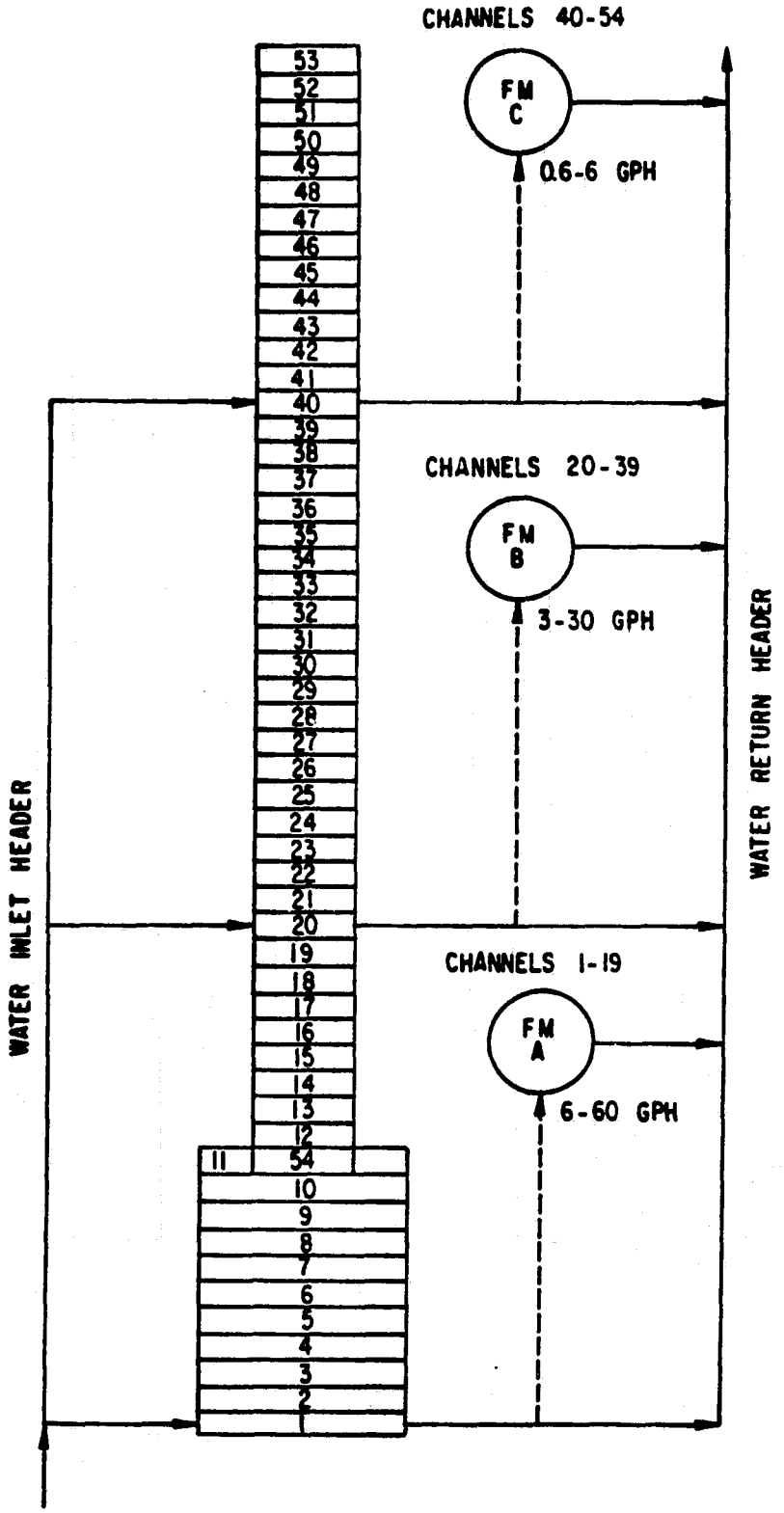

Fig. 2.17 Schematic of Parallel-Flow Water Cooling of the Pulse Combustion Burner

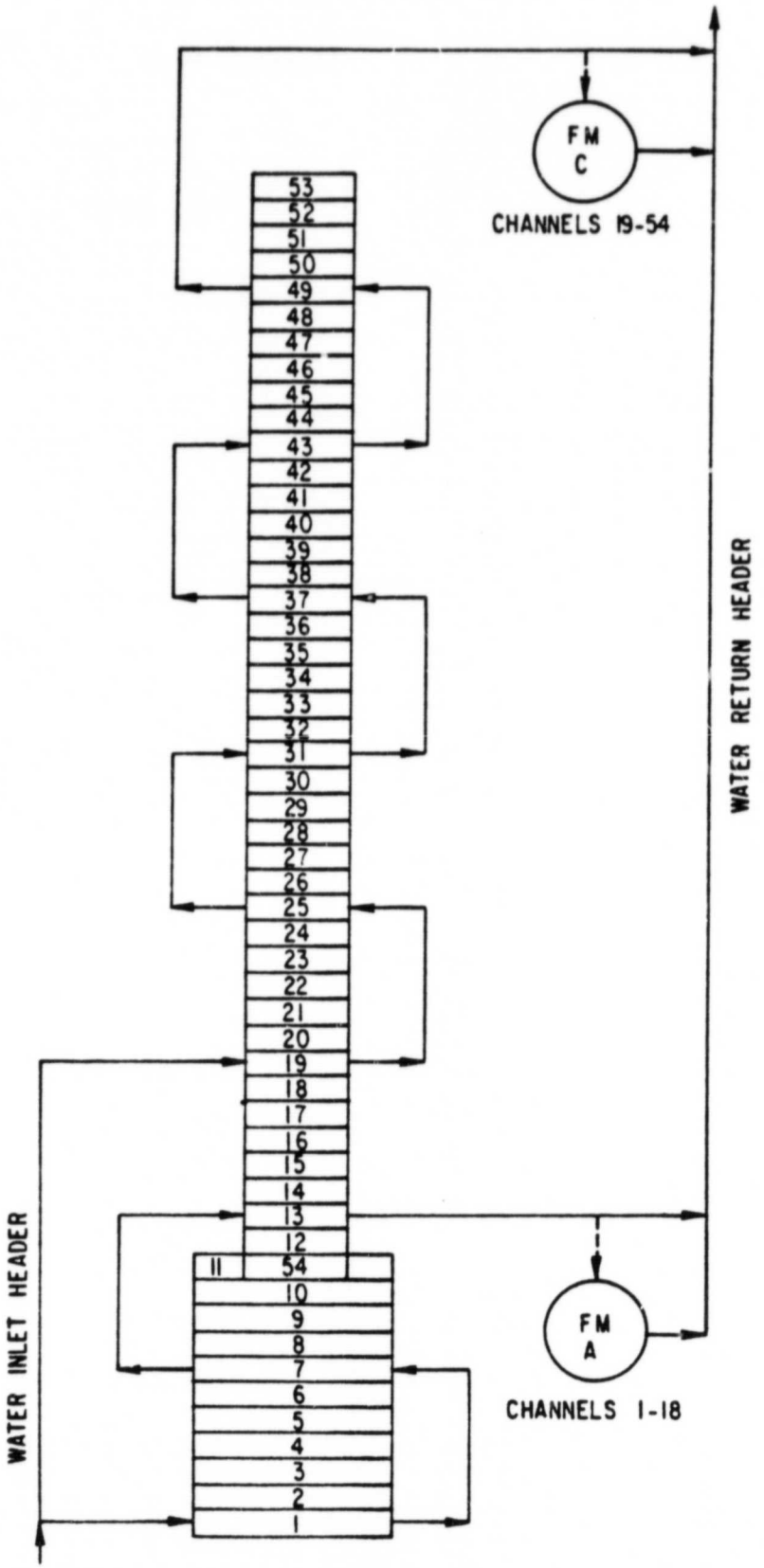

Fig. 2.18 Schematic of Series-Flow Water Cooling of the Pulse Combustion Burner

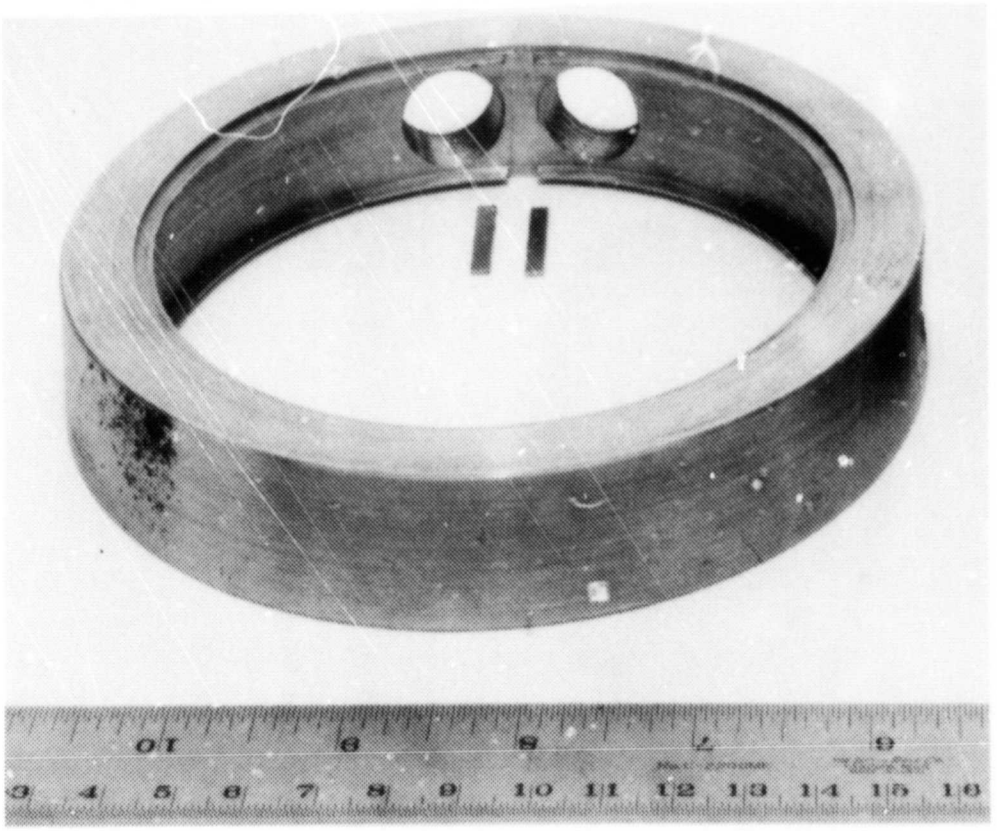

Fig. 2.19 Combustion-Chamber Cooling Channel

2.4 INSTRUMENTATION

Instrumentation consisted of thermocouples for temperature measurements, turbine flowmeters, pressure transducers, a sound-level meter, a CO monitor, and a CO_2 monitor.

Type T (copper-constantan) thermocouples (1/4-in. diameter sheath, grounded junction, 0.040-in. wire diameter) were used for measuring the temperature of the air, gas, burner wall, and cooling water. There was an inlet and outlet water-temperature measurement for each of the 54 cooling channels. The wall temperature of the burner was measured at channels 4, 8, 25, 31, 37, 43, 49 and 53. The combustion-products temperature was measured with type K (Chromel-Alumel®*) thermocouples (1/4-in. diameter sheath, grounded junction, 0.040-in wire diameter) through inserts in cooling channels 1, 4, 8, 13, 19, 25, 31, 37, 43, 49 and 53. The thermocouple sheath was threaded with a 1/4-28-NF thread and then screwed into the tapped hole in the wall of the tailpipe or combustion chamber. Teflon® tape was used to seal the threads to prevent water from leaking into the burner. A bare-wire type K thermocouple (through cooling channel number 2), with its tip at the approximate center of the burner, was used to provide the permissive logic

*Chromel-Alumel® is a registered tradename of the Hoskins Manufacturing Co., Detroit, Mich.

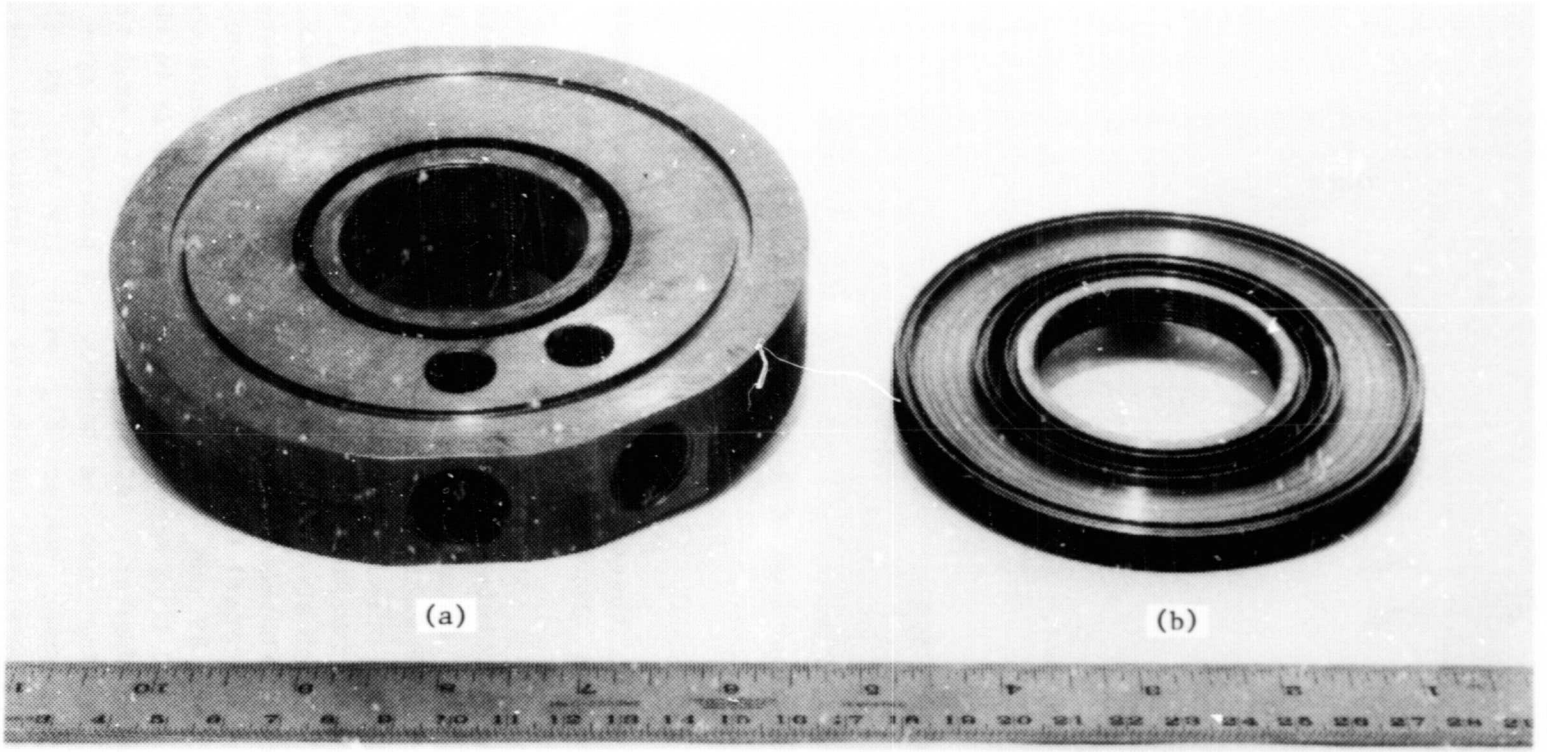

Fig. 2.20 Combustion-Chamber Head and Cooling Channel

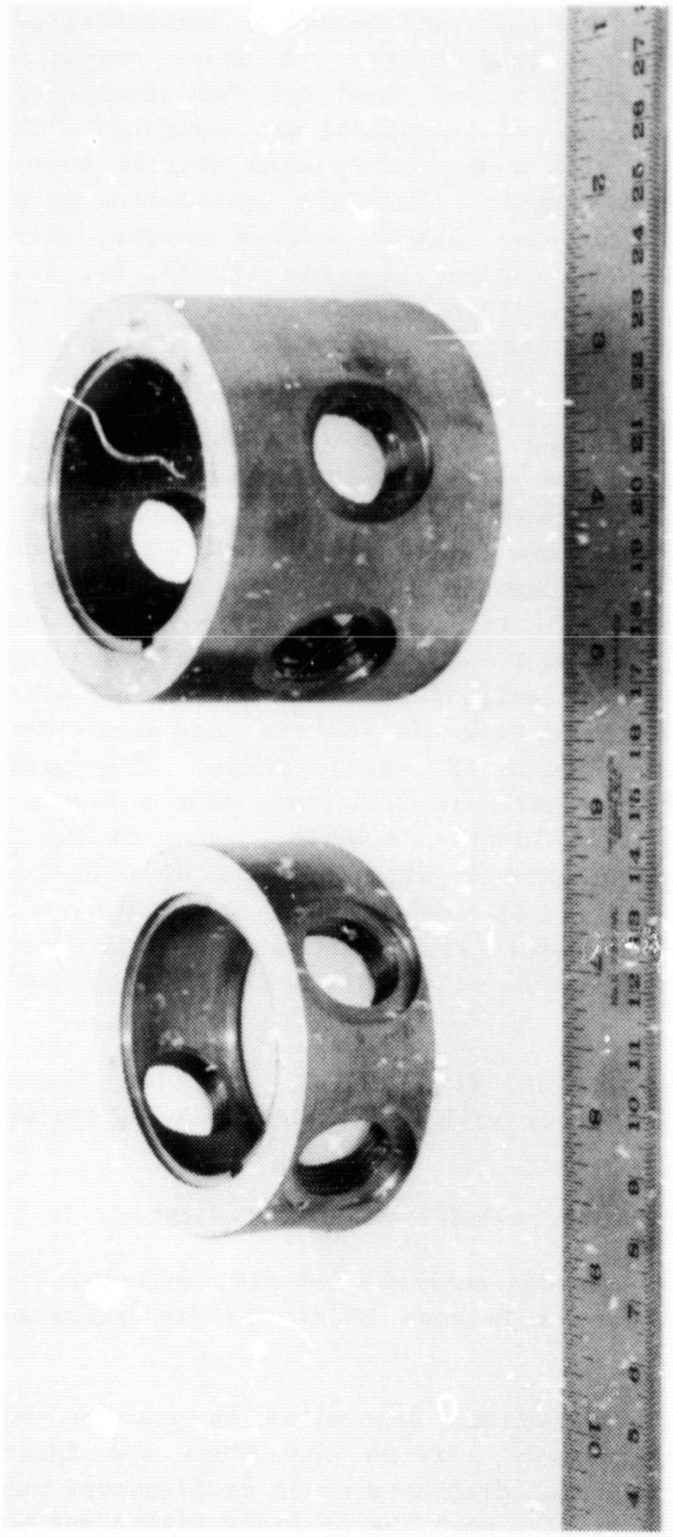

Fig. 2.21 Tailpipe Cooling Channels

signal for the burner safety system. The thermocouple was connected to a Honeywell Temperature Controller Model R7161B.

Pressures were measured with National Semiconductor backward-gage pressure transducers, Model LX1701GB, ±5 psig range. A Kepco voltage-regulated power supply, Model No. 25C-32-1.5, was used for the transducer excitation voltage. The output signal from the transducer was monitored with a Tektronix Type 515A oscilliscope or with a Hewlett-Packard digital voltmeter, Model 3440A with a Model 3444A plug-in. Pressure transducers were initially installed in the following locations: gas-decoupling chamber, air-inlet tee, and combustion chamber (through cooling channels 12, 18, 24, 30, 36, 42, 48, and 52). The high failure rate of these transducers and lack of funds for their replacement prohibited making pressure measurements at all locations.

All flow measurements were obtained using Flow Technology, Inc., turbine flowmeters. The air flowmeter was a model FT-16N50-GB, ball-bearing, 1-in. female NPT ("national pipe-thread") standard-line turbine flowmeter with a range of 5-50 actual ft^3/min. The meter was factory-calibrated with air on an air-velocity test stand. The gas flowmeter was also a ball-bearing, standard line flowmeter, Model FT-8N5-GB. It had 1/2-in. female NPT end fittings and a range of 0.5-5 actual ft^3/min and utilized a range-extending amplifier, Model LFA-300-A. The meter was calibrated with a Bell Prover with air as the calibration fluid. The three water flowmeters were Omniflo®* meters with jewel bearings and 1/2-in. female NPT end fittings. They were calibrated with water on a ballistic-flow calibration stand. With reference to Fig. 2.17, flowmeter "A" was a Model FTM-N10-LJS with a range of 0.1-1 gal/min; flowmeter "B" was a Model FTM-N5-LJS with a range of 0.05-0.5 gal/min; and flowmeter "C" was a Model FTM-NL-LJS with a range of 0.01-0.1 gal/min. The output signal from the flowmeters was amplified and supplied to a microcomputer, where the pulses were counted for a specified time period and then converted into a flow reading.

Sound-level measurements were obtained with a Bruel and Kjaer Model 2218 precision integrating sound-level meter with a tunable bandpass filter and level recorder.

Valve lift was measured with a Starrett Model 196 dial indicator.

The CO_2 content of the exhaust gas was measured for some tests with a Dwyer Model 1101 CO_2 indicator and with a Beckman Model 865 CO_2 infrared analyzer.

The resonant frequency of the system was determined by passing the signal from the chamber pressure transducer through the Bruel and Kjaer tunable bandpass filter. The signal was then displayed on an oscilloscope and the frequency read directly off the tuner dial when the pressure signal was at a maximum.

---

*Omniflow® is a registered tradename of Flow Technology, Inc., Phoenix, Ariz.

2.5 DATA-ACQUISITION SYSTEM

The data-acquisition system, shown schematically in Fig. 2.22, basically consisted of a computer-controlled data logger. The data logger was a Fluke Model 2242B, a data processor that can be expanded by the use of optional plug-in modules. This capability could provide considerable flexibility in formulating a user-designed data-acquisition system capable of handling up to 1000 channels of analog data. The ANL system had 180 data channels.

The microcomputer was a Digital Micro Systems machine with 64K bits of dynamic random-access memory (RAM) and two Shugart dual, double density, 500-kilobyte capacity, floppy-disk drives for mass storage. Computer operation was controlled by a Lear-Seglar ADM-3A video display terminal. A Lear-Seglar parallel-input, 1200-baud line printer was used for hard-copy output. The data logger was controlled by software programs written in assembler language. Other software included Fortran, Basic, Pascal, and CP/M. Programs were developed for the switching of the solenoid valves in the cooling-water system and for storing and manipulating temperature and flow data.

2.6 EXHAUST-DECOUPLING CHAMBER

A variable-volume exhaust decoupling chamber was fabricated from a 84-in. long section of 16-in. OD pipe with a 1/4-in. thick wall. One end of the pipe was closed by a welded plate and the other was fitted with a piston that used a bicycle inner tube for its seal. The outside surface of the decoupling chamber was wrapped spirally with 3/8-in. OD copper tubing soldered to the surface of the chamber. Cooling water could be circulated through the tubing to cool the chamber. Exhaust from the pulse combustion burner entered the decoupling chamber through a hole in the chamber wall near the closed end. The gases left the chamber through a secondary heat exchanger attached to the movable piston. The secondary heat exchanger was an 88-in. long section of 3-in. OD x 2 3/4-in. ID tubing and had 3/8-in. OD copper tubing wrapped spirally and soldered on its outer surface. Cooling water also could be circulated

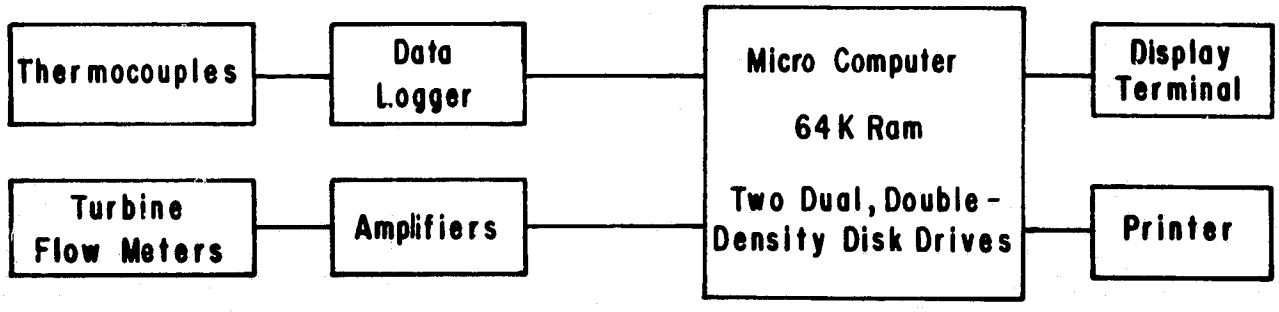

Fig. 2.22 Data-Acquisition System

through this tubing to cool the heat exchanger. The decoupling chamber and secondary heat exchanger were mounted from the ceiling of the laboratory above and slightly to the left of the burner tailpipe. The decoupling chamber and secondary heat exchangers were never used.

2.7 AIR SUPPLY

Room-temperature air was utilized for combustion. A small "squirrel-cage" blower supplied air for starting and purging, but during normal operation, air was aspirated by the burner. Air entered through the blower housing, flowed through about 4 ft of 1-in. pipe and a turbine flowmeter, and entered the side branch of the air-inlet tee. Inside the tee, the air made a 90° turn to flow between the gas-distributor tube and the body of the tee and then entered the combustion chamber through the 96 holes in the air-flapper valve.

2.8 GAS SUPPLY

Natural gas from the Gulf Coast was supplied by Northern Illinois Gas Co.; the supplier furnished an account of its composition. A mass spectrometer analysis of the natural gas was also performed, and the results are compared with the supplier's analysis in Table 2.1. The stoichiometric air/fuel ratio for this gas mixture is 9.68, and its calculated higher heating value is 1026 Btu/ft^3. If the "higher hydrocarbons" measured in the mass-spectrometer analysis are considered to be propane (C_3H_8), the calculated stoichiometric air/fuel ratio is 9.62, and the higher heating value is 1005 Btu/ft^3.

Pure methane (CH_4) has a higher heating value of 1012 Btu/ft^3 and a stoichiometric air/fuel ratio of 9.53 for perfect combustion.

Gas was supplied from the main distribution system at 15 psi, flowed through a solenoid valve operated by the burner safety circuit, and was then regulated to a pressure of 3-6 in. H_2O. After passing through the regulator, the gas flowed through a turbine flowmeter and then into a small decoupling chamber. This chamber was fabricated from 3.125-in OD x 2.945-in. ID copper water tubing with soldered caps on each end. A 1/2-in. female NPT in each cap provided the gas inlet and outlet for the chamber. The overall chamber length was 11 1/4-in., and its internal volume was approximately 75 in^3. From the decoupling chamber, the gas entered the side of the gas-valve body, made a 90° turn, and discharged through the 10 holes in the flapper valve into the gas-delivery tube. The gas flowed up the delivery tube and entered the combustion chamber radially through the 18 holes in the gas-distributor head.

Table 2.1 Composition of Natural Gas Used in ANL Tests

Component	Composition (% by volume)	
	Supplier's Analysis[a]	Mass-Spectrometer Analysis
CH_4	96.65	94.5
C_2H_6	1.60	2.6
C_3H_8	0.37	
(i)C_4H_{10}[c]	0.09	
(n)C_4H_{10}[c]	0.09	
(i)C_5H_{12}	0.03	0.8[b]
(n)C_5H_{12}	0.02	
$C_6H_{14}^+$	0.10	
N_2	0.48	0.6
CO_2	0.57	0.6
H_2O	-[d]	0.9
	100.0	100.0

[a]Furnished by Northern Illinois Gas Co.

[b]Total abundance of all "higher hydrocarbons."

[c]Note that "i" signifies "iso-" and "n" signifies "normal."

[d]No water content was given in supplier's analysis.

3 EXPERIMENTAL PROCEDURE

This section provides information on startup and shutdown procedures, visual studies, tests conducted, and operating problems associated with the ANL experimental pulse combustion unit.

3.1 PROCEDURE FOR STARTUP, OPERATION, AND SHUTDOWN

Prior to igniting the burner, a number of system checks were performed. Initially the cooling-water system was shut down between runs, but fouling and plugging of narrow passages in the system occurred. These problems, along with failure of the O-ring seals resulting from inadvertent operation of the burner without cooling water, led to a policy of continually circulating water through the system.

As the checkout procedure continued, the block valve between the storage tank and the makeup tank was opened. The water level in the makeup tank was kept at half full; if it was not at this level, the block valves between the domestic cold-water supply and the ion-exchange cartridges were opened. If a cartridge was spent (as indicated by its color change) the water supply was shut off and the cartridge replaced. When the makeup-tank water level became stationary at the desired level, the water flow to the ion-exchange cartridges was shut off. If the cooling-water system was off, the pump was started. The water flow to each burner cooling channel was adjusted to ensure that the flow was within the range of the appropriate flowmeter.

Other pretest checkout activities included the following:

- Verification that the system instrumentation was functioning properly. If a cooling-channel thermocouple was faulty, the cooling system was shut down and the thermocouple replaced. If a gas-temperature thermocouple or pressure transducer was faulty, it generally was not replaced because of the difficulty in sealing the penetration and a lack of replacement instrumentation. If a flowmeter was faulty, then the run was terminated.

- Warming up and checking the calibration of the CO and CO_2 monitors.

- Installation of the sound recording meter.

- Ensuring that sufficient film was available for taking pictures of the pressure wave form as displayed on the oscilloscope.

- Positioning the exhaust duct over the tailpipe exit.

- Loading the data-acquisition program in the computer and verifying its operation. The computer was left on at all times, but the printer was turned on and off as required.

A safety circuit that controlled the burner operation had to be energized before startup could be achieved. With the burner off and the safety circuit in operation, the purge blower continued to supply air to the combustion chamber. The remote-shutdown switch was set in the permissive run position. The burner was ignited by pushing the start (igniter) button on the safety-circuit panel. In approximately five seconds, the safety circuit would energize the gas-supply valve and a 10,000-V ignition transformer, which supplied power to the igniter in the combustion chamber. Ignition was detected by sensing the pressure wave in the combustion chamber. If this wave was not detected within about ten seconds, the gas valve was closed and the igniter was switched off. After a suitable purging period, the starting procedure was repeated. If the burner again failed to start, adjustments were made to the air- or gas-valve lift. Valve settings from the last burner operation should have sufficed for startup. If they did not, then the gas-valve lift was to be between 0.003 and 0.008 in. and the air-valve lift between 0.012 and 0.020 in. Only small changes in the gas-valve settings were to be made, but a number of adjustments with the air valve were tried. When sustained ignition was obtained, the safety circuit would switch off the purge blower and igniter.

After sustained ignition was achieved, the air- and gas-valve settings were adjusted to obtain the desired heat-input rate and air-fuel ratio. When the burner was operating stably, the automatic data-acquisition program in the computer started. This program automatically took a series of data sets (usually six) and then switched the solenoid valves so that a different set of cooling-channel water flows was measured by the flowmeters. During the test run, sound-level measurements, exhaust gas CO and CO_2 measurements, and pressure measurements were taken. Occasionally a sample of the exhaust gas was collected for laboratory analysis.

After all pertinent data had been taken, the air and gas valves could be readjusted for another run or the burner could be shut down. Shutdown was accomplished by placing the mode switch on the safety circuit panel in the "Manual" or "Off" position or by using the remote-shutdown switch located next to the computer. The switches shut off the gas flow to the burner. After the burner cooled, the water flow to the cooling tower was routed to the supply tank. All other recording instruments and the ventilation blower were turned off. For a prolonged shutdown period, the cooling water system and the makeup-water system would be shut down.

3.2 VISUAL STUDIES

Quartz windows were initially planned for the combustion chamber, but their breakage on installation prevented them from being used to observe the combustion process inside the chamber. Therefore, a transparent pulse combustor was constructed with a Pyrex®* combustion chamber and a fused-quartz tailpipe. The chamber and tailpipe were coupled with a stainless-steel flange. The inside dimensions of the glass burner were the same as those of the metallic burner; the valve assembly could be interchanged between them. Thus, apart from variations due to differences in heat loss characteristics, both units should have exhibited similar pressure and flow pulsation behavior when operating at the same fuel- and air-input rates.

An unsuccessful attempt was made to take high-speed movies of the transparent burner in operation. However, direct visual observation provided a qualitative understanding reflected in the sketch in Fig. 3.1. The flame zone (natural-gas heat-input rate of 100,000 Btu/h, with a 10:1 air/fuel ratio) appeared to begin very close to the ports in the gas-distributor head, indicating a rapid mixing of the fuel and air in that region. The variation in flame brightness just above the gas-distributor head suggested the presence of a recirculation zone in that region. The most intense combustion appeared to occur in a region located about 40% of the chamber height above the gas-distributor head. This observation was supported by the occurrence of softening and slight bulging of the Pyrex® in a 1-in. band, at that height, after several minutes of operation. Finally, the visual observations suggest that virtually the entire combustion chamber was filled with gases that were at relatively high (but non-uniform) temperature.

Following these preliminary observations, another burner (made entirely of fused quartz) was constructed. However, this burner was never utilized, because the program was terminated.

3.3 BURNER TESTS

Initial attempts at starting the burner resulted in erratic pulsations and failure to sustain ignition. This problem was solved by adjustments to the air and gas valves. Afterward, the burner was operated under varied conditions by adjusting the air/fuel ratio. A number of preliminary tests were conducted, for which detailed data are not available, during the installation and checkout phase of the burner.

The burner was stably operated in its standard form from a heat input as low as 32,890 Btu/h to a maximum of 194,370 Btu/h. The low heat-input rate required a volumetric air/fuel ratio of 13.2, whereas the high firing rate was slightly substoichiometric with an air/fuel ratio of 9.4. The stoichiometric air/fuel ratio for methane is 9.5. At a heat input of about 100,000 Btu/h,

---

*Pyrex® is a registered tradename of the Corning Glass Works, Corning, N.Y.

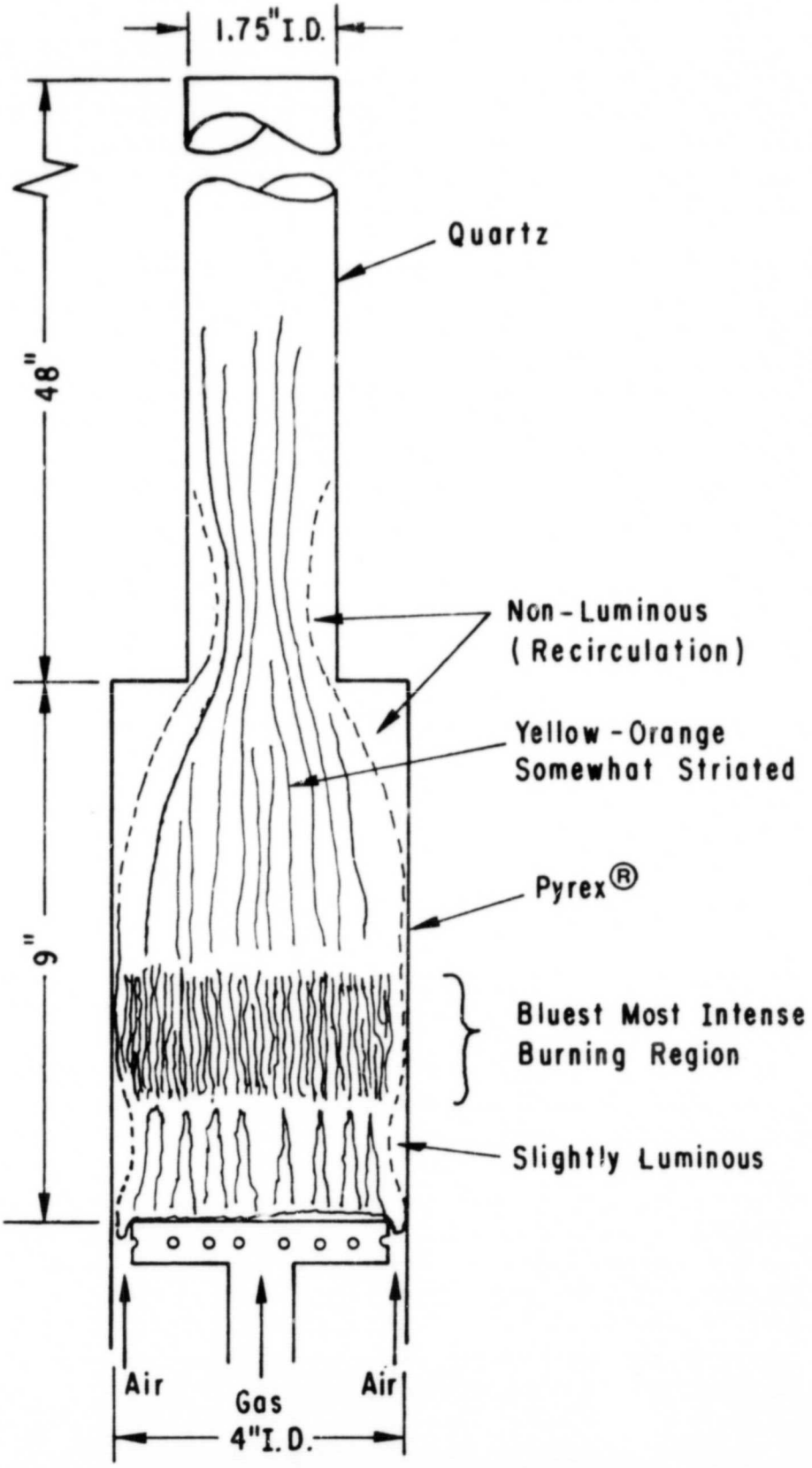

Fig. 3.1 Sketch Based on Visual Observations of Operating Burner

stable operation was obtained for ratios as low as 7.9 and as high as 11.9. Tests were conducted using an inlet muffler, an exhaust muffler, and both together. With both the inlet and exhaust mufflers in place the burner could not be started, because the blower could not supply a sufficient quantity of air. Starting was accomplished by using pressurized air. After starting, the burner operated stably without the pressurized air.

To compare pulsating with non-pulsating operation, the flapper valves were removed from the burner. Attempts to obtain sustained ignition were unsuccessful. The flame was oxygen-starved and unstable, and when the blower was switched on to increase air flow, the flame was extinguished. Removal of the blower, air-supply pipe, and flange improved operations slightly. Stable burner operation was finally achieved by using pressurized air and a needle valve to control the flow rate. Stable operation was obtained with above-stoichiometric air/fuel ratios: the lower the heat input, the higher the air/fuel ratio had to be.

In order to obtain a tailpipe-geometry change, tests were conducted with the 1-in. diameter "corebustor" extending the entire length of the tailpipe or only the last 36 inches of the tailpipe. Two sets of tests were also run using an aspirator (Fig. 2.13) on the outlet of the tailpipe.

The heat-input rate, air/fuel ratio, and burner configuration for tests conducted are given in Table 3.1.

3.4 OPERATION PROBLEMS

Some problems encountered during operation were:

- Deterioration of igniter wires, which apparently extended too far into the combustion chamber. A single wire shielded by a quartz tube with the wire's tip almost flush with the combustion-chamber wall solved the problem. Ignition was achieved by electrical sparks from the wire to the combustion-chamber wall.

- Water leakage into the combustion chamber through the instrument penetrations into the chamber and tailpipe. This leakage damaged several pressure transducers and caused sticking of the flapper valves.

- Failure of the gas and air flowmeter bearings and the rotor shaft on two of the water flowmeters.

- Scaling of the cooling-channel passages because of improper water treatment. After treatment, some plugging of cooling-water passages was produced by undissolved chemicals.

Table 3.1 Burner Tests

Heat Input (Btu/h)	Air/Fuel Ratio	Burner Configuration
32,887	13.21	Standard Burner
50,245	9.89	Standard Burner
54,194	12.48	Standard Burner
58,655	10.08	Standard Burner
95,458	11.89	Standard Burner
96,782	10.34	Standard Burner
97,464	7.90	Standard Burner
99,577	10.05	Standard Burner
100,215	9.89	Standard Burner
100,941	10.13	Standard Burner
101,713	9.87	Standard Burner
103,576	10.12	Standard Burner
194,371	9.38	Standard Burner
98,013	9.96	Insulated Standard Burner
53,589	12.50	No Flapper Valves
102,645	11.39	No Flapper Valves
50,418	10.02	Tailpipe Aspirator
98,620	9.60	Tailpipe Aspirator
53,116	11.03	Inlet Muffler
101,532	10.09	Inlet Muffler
103,728	10.10	Inlet Muffler
53,429	11.50	Exhaust Muffler
50,227	9.42	Inlet and Exhaust Mufflers
100,580	8.86	Inlet and Exhaust Mufflers
48,867	9.93	48-in. long Corebustor
50,341	9.82	48-in. long Corebustor
50,882	10.13	48-in. long Corebustor
99,996	9.73	48-in. long Corebustor
101,248	10.09	48-in. long Corebustor
50,042	10.07	36-in. long Corebustor
97,009	10.11	36-in. long Corebustor
100,553	9.82	36-in. long Corebustor
100,794	10.45	Air Decoupling Chamber

- Cooling-channel seal failure because of insufficient water flow.
- Failure of thermocouples.
- Failure of the Fluke Data Logger.
- Failure of the computer and display terminal.

The seal failure and cooling-channel scaling required that the cooling channels be removed from the burner. This was a very time-consuming procedure. The burner was designed for detailed heat-transfer measurements and variation of tailpipe diameter and length, but the difficulty in assembling the individual cooling channels prevented us from making these variations in geometry.

3.5 EXHAUST-GAS ANALYSES

A sample of the exhaust gas taken at the center of the tailpipe at three axial locations with the burner operating at a heat input of approximately 100,000 Btu/h and a 10:1 air/fuel ratio was analyzed by mass spectrometry; the results are given in Table 3.2. The calculated exhaust-gas composition based on complete combustion and the natural-gas composition supplied by Northern Illinois Gas Co. (see Sec. 2.8) is also shown.

The presence of oxygen at the 46.5-in. position, which is 2.5-in. from the top of the combustion chamber, indicates that combustion was not complete at this point. The high oxygen content at the 6.5-in. position is indicative of air being drawn into the tailpipe. Since the CO measurements are at the lower limit of the analysis capability, it is not possible to determine whether these values resulted from measurement technique or from incomplete mixing or quenching.

The CO_2 content of the gas in the tailpipe was also measured with a Dwyer #1101 CO_2 indicator, with the results given in Table 3.3.

Exhaust-gas samples were taken at a distance of 28.5 in. from the tailpipe outlet for the burner operating at a heat-input rate of 95,458 Btu/h (11.89 air-fuel ratio) and at 97,464 Btu/h (7.90 air/fuel ratio). The mass-spectrometer analysis of these samples is indicated in Table 3.4.

Beckman Model 864 and 865 infrared analyzers were used to measure the CO and CO_2 content, respectively, of the exhaust gas for some of the experiments. These data are presented in Table 3.5. The exhaust-gas sample was taken at a position of 29.5 in. from the tailpipe outlet. For a stoichiometric air/fuel ratio of 9.6, the calculated amount of CO_2 in the flue gas is 11.9% on a dry-volume basis. Therefore, the values of 13, 14, and 15.5% are in error. In all cases the amount of CO is high, especially for the 50,341

Table 3.2 Composition of Tailpipe Exhaust Gas for a Heat-Input Rate of 100,000 Btu/h

	Composition (% by volume, dry basis)		
		Calculated	
Component	Measured[a]	Stoichiometric Conditions	3.3% Excess Air
CO_2	(11.5, 11.7, 10.0)	11.9	11.4
N_2	(86.3, 86.8, 85.4)	88.1	87.8
CO[b]	(1.0, 1.1, 0.8)	-	-
H_2	(0.3, 0.4, 0.6)	-	-
NO_x[c]	($\leq$0.02, <0.01, <0.01)	-	-
O_2	(0.9, <0.01, 3.2)	-	-

[a]The three numbers listed in parentheses for each component give the composition of that component (% by volume) at distances of 46.5 in., 28.5 in., and 6.5 in., respectively, from the tailpipe outlet.

[b]Best estimate (approximate lower limit of analysis capability).

[c]NO_x = oxides of nitrogen.

Btu/h case. The correspondingly low CO_2 measurement substantiates the high CO content. The amount of heat removed from the combustion chamber was less than for the other comparable cases. Therefore incomplete air-fuel mixing, instead of quenching of combustion products, appears to be the reason for the high CO content. Additional studies are needed to determine whether the high CO content results from insufficient air-fuel mixing, from quenching, or from a combination of both.

In most of the literature on gas-fired experiments with pulse combustors, exhaust-gas analyses are not given. Referring to his methane-fired, double-necked, Helmholtz-type pulse combustor, Reader[3] reported that the system operated very close to stoichiometric conditions (1.04-1.05 equivalence ratio) and that no combustibles or carbon monoxide were detected in the exhaust products. Francis, Hoggarth, and Reay[31] reported that CO was present in the exhaust gas of a Schmidt-type burner fired with town gas when the gas

rate was high and the air-inlet diameter was small. They also stated that for their Helmholtz burner, bad combustion often occurred at very low gas rates, presumably because of poor mixing of the gas and air. Griffiths, Thompson, and Weber[21] obtained complete combustion with various experimental units (Helmholtz burners) over a range of air equivalence ratios (1.08-1.12 and 1.36-1.70).

Table 3.3 Exhaust-Gas CO_2 Content

Distance from Tailpipe outlet (in.)	CO_2 (% by volume)
6.5	7.0
10.5	9.0
16.5	8.2
22.5	8.8
28.5	8.6
34.5	9.8
40.5	8.0
45.5	10.0

In the development of the "Pulsamatic®" boiler, Kitchen[46] reported that a prototype production unit failed combustion tests at the American Gas Association (AGA) because of excessive carbon monoxide in the exhaust gas. After a long series of experiments, it was determined that the incomplete combustion resulted from the rapid cooling of the combustion gases in the small bores of the heat-exchanger tubes. A slower cooling rate was required for the reassociation of the carbon monoxide with the available oxygen. Therefore, a single large tube was installed between the combustion chamber and the manifold for the small-diameter heat-exchanger tubes. Katsnel'son, Marone, and Tarakanovskii[34] used a water-cooled Helmholtz-type pulse combustor in their experimental studies with methane, hydrogen, and acetylene. Gas samples taken beyond the resonance tube showed no unburned gases for an air-equivalence ratio of 1.05.

The authors also reported that, with an axial supply of air, the maximum concentrations of CO_2 in the combustion chamber were near the walls. A large amount of oxygen was found in the center of the chamber. These findings indicate the presence of local zones of incomplete air-fuel mixing in the combustion chamber.

From the design details of other experimental pulse combustors, it appears that the ANL combustor did not have a sufficient length for the air and fuel to mix before combustion occurred.

Table 3.4 Composition of Tailpipe Exhaust Gas for Two Different Heat-Input Rates and Air/Fuel Ratios

Component	95,458 Btu/h Heat-Input Rate, 11.89 Air/Fuel Ratio (% by volume, dry basis)		97,464 Btu/h Heat-Input Rate, 7.90 Air/Fuel Ratio (% by volume, dry basis)[a]
	Measured	Calculated for 21.6% Excess Air	
H_2	<0.02	-	5.5
CH_4	<0.02	-	0.3
C_2H_2	<0.01	-	0.2
C_2H_6	<0.02	-	0.05
N_2	$\geq$84.9	86.3	79.4
CO	$\leq$0.8[b]	-	6.0
NO_x[c]	<0.01	-	<0.05
O_2	2.9	4.1	0.09
CO_2	11.4	9.6	8.5

[a]Measured only.

[b]Lower limit of analysis capability.

[c]NO_x = oxides of nitrogen.

Table 3.5 Flue-Gas CO and CO_2 Content

Heat Input (Btu/h)	Air/Fuel Ratio	Dry Volume (%) CO	Dry Volume (%) CO_2	Configuration
100,215	9.89	0.45	11.4	Standard Burner
32,887	13.21	0.24	13.0	Standard Burner
50,341	9.82	2.88	10.0	48-in. Long Corebustor
101,248	10.09	0.36	11.1	48-in. Long Corebustor
50,227	9.42	1.50	10.8	Inlet and Exhaust Mufflers
100,580	8.86	1.92	10.8	Inlet and Exhaust Mufflers
50,418	10.02	1.29	14.0	Tailpipe Aspirator
98,620	9.60	0.39	15.5	Tailpipe Aspirator

4 FUNDAMENTAL FREQUENCY

From any number of books on physics or acoustics, the resonant frequency for a tube closed at one end and open at the other (without taking end losses into account) can be predicted by:

$$f = \frac{c}{4L} \tag{4.1}$$

where:

f = fundamental frequency, Hz

c = acoustic velocity, ft/s

L = tube length, ft

Because the tube length constitutes a quarter wavelength for the fundamental mode of vibration, such a device is often referred to as a "quarter-wave tube." The fundamental frequency for a tube open at both ends is given by:

$$f = \frac{c}{2L} \tag{4.2}$$

The frequencies of the various harmonics for these tubes are given by:

$$f = \frac{nc}{2L} \tag{4.3}$$

where:

n = 1/2, 3/2, 5/2, 7/2, ... for a closed tube

n = 1, 2, 3, 4, ... for an open-ended tube

The acoustic velocity of an ideal gas can be obtained from:

$$c = \sqrt{\frac{g_c \gamma RT}{M}} = \sqrt{\frac{g_c (C_p/C_v) RT}{M}} \tag{4.4}$$

where:

g_c = 32.2 $lb_m ft/lb_f\text{-}s^2$

M = molecular weight of gas, $lb_m/(lb\text{-}mole)$

R = gas constant = 1545 $ft\text{-}lb_f/(lb\text{-}mole)°R$

T = gas temperature, °R

γ = gas specific-heat ratio = C_p/C_v

C_p = gas specific heat at constant pressure, Btu/(lb-mole)°R

C_v = gas specific heat at constant volume, Btu/(lb-mole)°R

Two problems arise when one tries to use these equations to predict the fundamental frequency of a Schmidt-type pulse combustor. First, the combustor is neither a completely open tube nor a completely closed one. Second, the appropriate gas temperature to use is unknown. A Schmidt-type burner with flapper valves might be expected to act as a quarter-wave tube, and hence Eq. 4.1 would apply. If aerodynamic valves were used, then Eq. 4.2 might be more appropriate. However, Hanby[42] found that the frequency of his aerodynamically valved pulse combustor could be predicted within 5% by using Eq. 4.1 and a root-mean-square gas temperature (Eq. 4.4). On the other hand, Francis et al.[31] derived the following equation for a Schmidt-type combustor with an aerodynamic valve and an air-inlet tube:

$$\frac{(\gamma_a)(c)D^2}{(\gamma)(c_a)D_a^2} \tan\left(\frac{2\pi\ fL_a}{c_a}\right) = -\tan\left(\frac{2\pi\ fL}{c}\right) \tag{4.5}$$

where:

c_a = acoustic velocity in the air-inlet tube, ft/s

D = combustor diameter, ft

D_a = air-inlet tube diameter, ft

L_a = length of air-inlet tube, ft

γ_a = specific-heat ratio for air

If one assumes that the air-inlet-tube length is zero, then Eq. 4.5 becomes

$$\tan\frac{2\pi\ fL}{c} = 0 \tag{4.6}$$

This equation is satisfied when

$$\frac{2\pi\ fL}{c} = n\pi \tag{4.7}$$

where:

$n = 1, 2, 3, 4, \ldots$

Equation 4.7 is identical to Eq. 4.3 for a tube with an open end. From the experimentally measured distance between pressure antinodes, Francis et al.[31] found that c = 1800 ft/s. The temperature corresponding to this acoustic velocity was not given, nor was the composition of the town gas or the exhaust gas. For air, this velocity would correspond to a temperature of 1427°F. Here we have two studies for a Schmidt-type burner equipped with aerodynamic valves, and the recommended equations for the burner frequency differ. Both experimental efforts used a 2-in. diameter combustor, but the air-inlet diameter of Hanby's combustor was not specified, while Francis et al. used a 3/4-in. diameter. Undoubtedly the size and design of the aerodynamic valve will dictate whether the combustor behaves as an open-ended or closed tube.

The fundamental frequency of a simple Helmholtz resonator, consisting of a closed volume to which is joined an open-ended neck, is derived by Putnam and Brown[47] to be:

$$f = \frac{c}{2\pi L_t}\sqrt{\frac{V_t}{V_c}} \tag{4.8}$$

where:

L_t = length of tailpipe or neck, ft

V_t = tailpipe or neck volume, ft^3

V_c = combustor or cavity volume, ft^3

The authors state that the frequency corresponds to the gas temperature in the neck. For a Helmholtz resonator with two openings, Putnam and Brown give the following relationship for the fundamental frequency:

$$f = \frac{1}{2\pi}\left[\frac{V_{t1}}{V_c}\left(\frac{c_1}{L_{t1}}\right)^2 + \frac{V_{t2}}{V_c}\left(\frac{c_2}{L_{t2}}\right)^2\right]^{1/2} \tag{4.9}$$

The subscripts 1 and 2 refer to necks 1 and 2, respectively.

For a Helmholtz combustor with an aerodynamic valve, Francis et al.[31] give the following equation for the resonant frequency:

$$f = \frac{c_a}{2\pi\sqrt{L_c(L_a + 0.85D_a)}}\frac{D_a}{D_c}\left[\frac{\gamma_c}{\gamma_a}\left(1 + \frac{2\pi f(L_a + 0.85D_a)\, D_t^2\, \rho_a}{c_t \tan\left(\frac{2\pi f L_t}{c_t}\right) D_a^2\, \rho_t}\right)\right]^{1/2} \tag{4.10}$$

where:

c_t = acoustic velocity in tailpipe, ft/s

D_c = combustion-chamber diameter, ft

D_t = tailpipe diameter, ft

L_c = combustion-chamber length, ft

γ_c = combustion-chamber gas specific-heat ratio

ρ_a = air density in air-inlet tube, lb_m/ft^3

ρ_t = gas density in tailpipe, lb_m/ft^3

When the length of the tailpipe is an odd multiple of a quarter-wavelength, the impedance of the tailpipe is very high, and Eq. 4.10 reduces to the equation for a Helmholtz resonator formed by the air-inlet pipe and the combustion-chamber volume:

$$f = \frac{c_a}{2\pi\sqrt{L_c(L_a + 0.85D_a)}} \frac{D_a}{D_c} \frac{\gamma_c}{\gamma_a} \tag{4.11}$$

The limitations on the accuracy of Eq. 4.10 are that (1) the air-inlet pipe is not fully open to the atmosphere at the valve end, and (2) for some part of the cycle the pipe contains combustion products. Also, viscous losses and acoustic-radiation losses have been ignored, and there is the usual difficulty in computing the effective sound velocity and density in the tailpipe.

Even though Eq. 4.11 was based on an idealized system in which the air-inlet tube is effectively open to the atmosphere at the valve, Francis et al.[31] applied it to a Helmholtz burner with multiple-reed flapper valves and obtained reasonable agreement with experimentally measured frequencies. For a combustor without an air-inlet tube (i.e., $L_a = 0$), the effect of the diameter of the air-inlet tube cannot be eliminated from Eq. 4.10. The effect of varying the tailpipe length also cannot be easily determined without a knowledge of the acoustic velocity and density of the exhaust gas. However, the effect of combustion-chamber length is given by the following relation:

$$\frac{f_1}{f_2} = \sqrt{\frac{L_{c2}}{L_{c1}}} \tag{4.12}$$

This ratio is also obtained from Eq. 4.8, which can be used to obtain the following expression for the effect of tailpipe length on frequency:

$$\frac{f_1}{f_2} = \sqrt{\frac{L_{t2}}{L_{t1}}} \tag{4.13}$$

In Table 4.1, predicted frequency changes based on Eqs. 4.12 and 4.13 are given along with the data from Francis et al.[31] for a Helmholtz combustor with a 3-in. diameter combustion chamber and a 3/4-in. diameter tailpipe.

From the data in Table 4.1, it can be seen that Eqs. 4.12 and 4.13 do not adequately predict the burner frequency for a change in its combustion-chamber or tailpipe length. In arriving at Eqs. 4.12 and 4.13, the assumption was made that the acoustic velocity would be constant if the firing rate was the same for each burner. Undoubtedly this assumption is incorrect, so these equations would have to include the acoustic-velocity ratio, which cannot be determined a priori.

By considering a frictionless, compressible-flow model (acoustic wave-equation approximation) for the tailpipe and representing the combustion

Table 4.1 Comparison of Measured and Predicted Helmholtz-Burner Frequencies with Changes in the Combustion-Chamber and Tailpipe Length

L_e (ft)	L_c (in.)	Frequency, Hz		Ratio of Predicted and Measured Frequencies
		Measured	Predicted	
2	8	79	-	-
	12	74	64.5	0.87
	15	69	57.7	0.84
	18	68	52.7	0.77
6	8	66	-	-
	12	63	53.9	0.86
	15	59	48.2	0.82
	18	55	44.0	0.80
10	8	55	-	-
	12	52	44.9	0.86
	15	51	40.2	0.79
	18	49	36.7	0.75
2	18	68	-	-
4	18	59	48.1	0.81
6	18	55	39.3	0.71
10	18	49	30.4	0.62

chamber as a volume in which uniform isentropic compression and expansion occurs, Ahrens and Kartsounes[48] obtained the following equation for the fundamental frequency of the burner:

$$\left(\frac{2\pi f L_t}{c}\right) \tan\left(\frac{2\pi f L_t}{c}\right) = \frac{V_t}{V_c} \tag{4.14}$$

This expression encompasses the entire range of V_t/V_c; the fundamental frequency reduces to that of a quarter-wave tube (Eq. 4.1) for $V_t/V_c \gg 1$ and to that of a Helmholtz resonator (Eq. 4.8) for $V_t/V_c \ll 1$. This predicted frequency range (from Ahrens, Clinch, and Kartsounes[49]) is shown in Fig. 4.1, along with AGA data.

From an analytical model of a pulse combustor, Ahrens, Kim, and Tam[50] derived the following equation for the frequency of a Helmholtz burner:

$$f = \frac{1}{2\pi}\left(\frac{Rg_c A_t}{MC_v L_t V_c}\right)^{1/2}\left(h_R + \frac{\Delta H}{1+r}\right)^{1/2} \tag{4.15}$$

where:

A_t = tailpipe cross-sectional area, ft^2

h_R = enthalpy of reactant mixture entering the combustion chamber, Btu/lb_m

ΔH = heat of combustion, Btu/lb_m

r = mass air/fuel ratio

For methane, Eq. 4.15 becomes

$$f = 15.95\left(\frac{A_t}{L_t V_c}\right)^{1/2}\left(127 + \frac{23{,}900}{1+r}\right)^{1/2} \tag{4.16}$$

Frequencies calculated using Eq. 4.16 were compared with AGA data, and a relatively good agreement was obtained for small values of A_t/L_tV_c (i.e., larger combustion-chamber, longer tailpipe, or smaller cross-sectional area of tailpipe). This agreement probably reflects the reduced heat loss from the burner for these conditions. However, for larger values of A_t/L_tV_c the deviations from experimental data become larger.

It can be seen that Eq. 4.15 is actually Eq. 4.8 with the acoustic velocity determined by Eq. 4.4 at the adiabatic flame temperature. As the value of A_t/L_tV_c increases, the heat loss from the burner increases and the

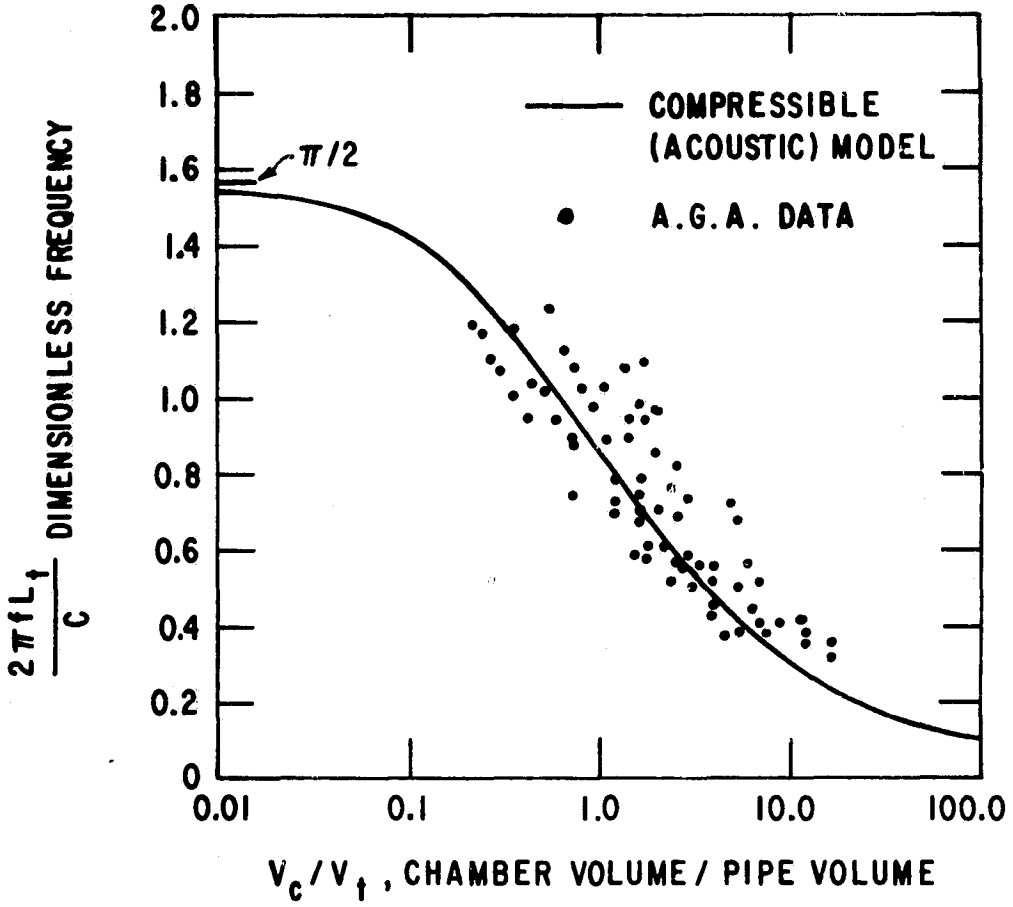

Fig. 4.1 Compressible-Flow (Acoustic) Model Prediction of the Fundamental Frequency of a Pulse Combustor

deviation of the gas temperature from the adiabatic flame temperature becomes larger. Consequently, the frequency predicted will be higher than that actually obtained.

4.1 MEASURED FREQUENCY

Experimentally measured fundamental frequencies are listed in Table 4.2. An examination of these data reveals that knowledge of the heat input to the burner and of the air/fuel ratio are not sufficient to predict the burner's fundamental frequency. For example, with a heat input of about 100,000 Btu/h and an air/fuel ratio of 10, the measured fundamental frequency was in the range of 74-76 Hz. However, a value of 70 Hz was also recorded. Decreasing the heat input resulted in a lower fundamental frequency for the same air/fuel ratio. (At a heat input of about 50,000 Btu/h and an air-fuel ratio of 10, for instance, the fundamental frequency was about 64 Hz. Increasing the burner heat input to approximately 200,000 Btu/h resulted in a

Table 4.2 Measured Fundamental Frequency of ANL Experimental Pulse Combustor

Heat Input (Btu/h)	Volumetric Air/Fuel Ratio	Frequency (Hz)	Burner Configuration
32,887	13.21	63.5	Standard Burner
50,245	9.89	64.5	Standard Burner
54,194	12.48	75.0	Standard Burner
58,655	10.08	67.0	Standard Burner
95,458	11.89	73-75	Standard Burner
96,782	10.34	74.0	Standard Burner
97,464	7.90	68.5	Standard Burner
99,577	10.05	76.0	Standard Burner
100,215	9.89	75.0	Standard Burner
100,941	10.13	73.5-74	Standard Burner
101,713	9.87	70.0	Standard Burner
103,576	10.12	75.5	Standard Burner
194,371	9.38	69-70	Standard Burner
98,013	9.96	74.0	Insulated Standard Burner
53,589	12.50	64.0	No Flapper Valves
102,645	11.39	71.0	No Flapper Valves
50,418	10.02	66.0	Tailpipe Aspirator
98,620	9.60	74.2	Tailpipe Aspirator
53,116	11.03	66.0	Inlet Muffler
103,728	10.10	75.0	Inlet Muffler
101,532	10.09	79.0	Inlet Muffler
53,429	11.50	66.0	Exhaust Muffler
50,227	9.42	62.0	Inlet and Exhaust Mufflers
100,580	8.86	72.0	Inlet and Exhaust Mufflers
49,867	9.93	54.5	48-in. Long Corebustor
50,341	9.82	54.0	48-in. Long Corebustor
50,882	10.13	54.5	48-in. Long Corebustor
99,996	9.73	68.0	48-in. Long Corebustor
101,248	10.09	68.0	48-in. Long Corebustor
50,042	10.07	55.0	36-in. Long Corebustor
97,009	10.11	68.0	36-in. Long Corebustor
100,553	9.82	64.5	36-in. Long Corebustor
100,794	10.45	76.0	Air Decoupling Chamber

fundamental frequency of 69-70 Hz. Based on the 50,000 and 100,000 Btu/h heat inputs, one might have expected an increase in the burner frequency.) The air/fuel ratio for the 200,000 Btu/h heat-input test was slightly below stoichiometric requirements. From the 100,000 Btu/h heat-input data, it appears that air-fuel equivalence rates of less than unity apparently had a greater effect on the burner frequency than did values greater than unity. The addition of a tailpipe aspirator, an inlet or an exhaust muffler, and an air decoupling chamber doesn't seem to affect the burner's fundamental frequency. However, the corebustor does affect the frequency, as would be expected for a tailpipe-volume change. The removal of the flappers from the air and gas valves did not have a significant effect on the fundamental frequency, as the inlet holes acted as aerodynamic valves.

4.2 COMPARISON OF THEORY WITH EXPERIMENTAL RESULTS

Equations 4.8 and 4.14 have been proposed for the prediction of the fundamental frequency of a Helmholtz burner, but they both contain the acoustic velocity of the exhaust gas, which is unknown. This velocity is temperature-dependent, as indicated by Eq. 4.4. If the flue gas is assumed to contain the products of methane combustion, and since $C_v = C_p - 1.987$, Eq. 4.4 can be rearranged as follows:

$$C = \sqrt{\frac{49{,}479\ C_p T}{M(C_p - 1.987)}} \tag{4.17}$$

The molecular weight of the flue gas varies slightly for equivalence ratios >1 but decreases sharply, because of the presence of hydrogen, for equivalence ratios <1, as shown in Fig. 4.2.

The molar specific heat of the exhaust gas is also temperature-dependent. Using the equations given in Ref. 51 for the specific heat of CO_2, H_2O, and N_2, the flue-gas specific heat as a function of temperature was estimated (see Fig. 4.3). Substituting these values into Eq. 4.17, one obtains the acoustic velocity of the exhaust gas as a function of equivalence ratio, shown in Fig. 4.4. Note that for up to 40% excess air, the acoustic velocity is reduced by less than 10 ft/s from the velocity for stoichiometric air/fuel ratios.

For the standard burner, V_c = 123.1 in.^{3}, V_t = 116.4 in.^{3}, and L_t = 4.03 ft. When the 48-in. long corebustor is installed, V_t = 87.8 in.^{3}. The exhaust muffler is similar to a double-cavity resonator with a cavity volume of 1445 in.^{3} and a neck volume of 14.4 in.^{3} for each section. The tailpipe aspirator has a volume of 20.6 in.^{3}. These data, the frequency data listed in Table 4.2, Eq. 4.8, and Eq. 4.14 (combined with Eq. 4.4) were used to calculate the acoustic velocity and its corresponding temperature. The results are given in Table 4.3.

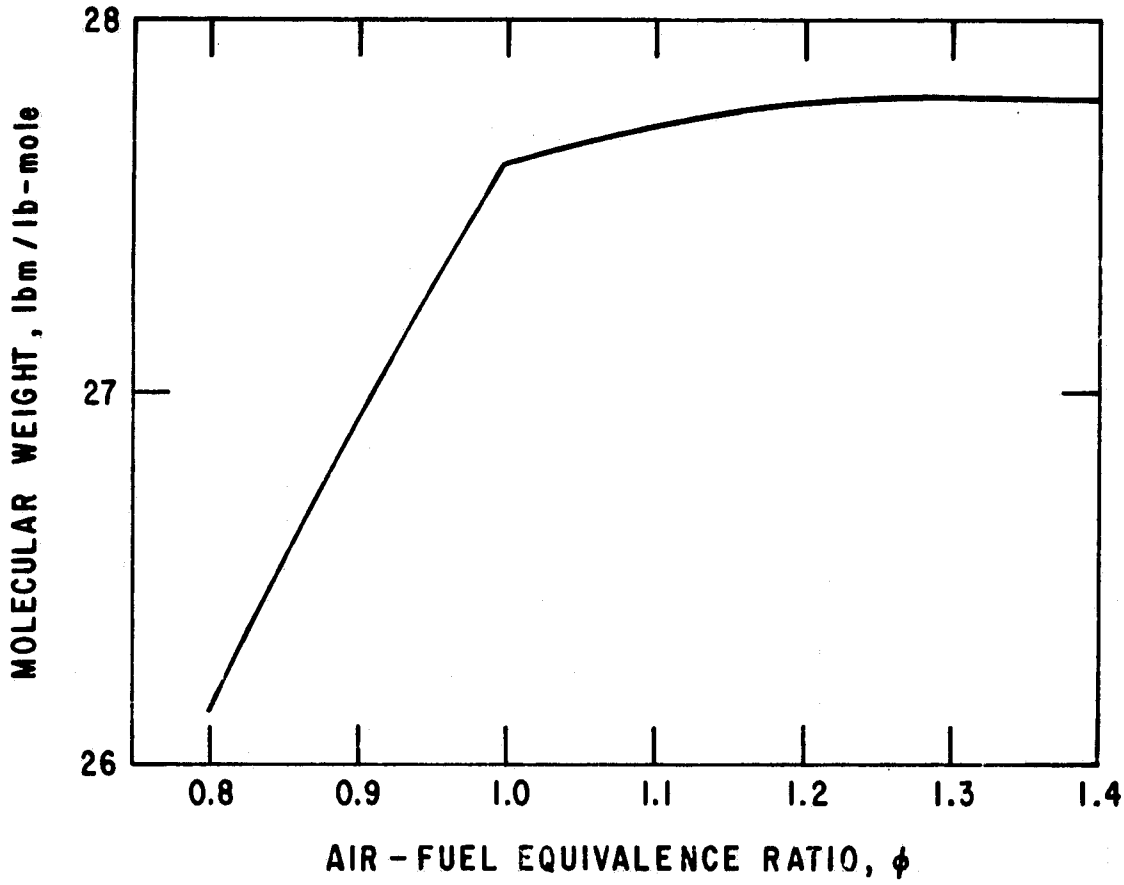

Fig. 4.2 Molecular Weight of Flue Gas for Methane Combustion

Almost the only conclusions one can derive from the data in Table 4.3 are that the exhaust-gas temperature obtained from the acoustic velocity predictions using Eq. 4.14 are about 50% higher than those obtained using Eq. 4.8, and the temperatures are indicative of those in the tailpipe.

If one uses the heat-transfer data presented in Chapter 6 and assumes that the combustion-flame temperature at the burner head is the adiabatic or theoretical flame temperature, then the exhaust-gas temperatures at the tailpipe entrance and exit can be calculated. These values, along with the arithmetic and geometric mean tailpipe temperatures, are given in Table 4.4. The adiabatic flame temperature was obtained from Edwards[52] and is indicated in Fig. 4.5. The adiabatic flame temperature is an upper limit, and different values are listed in the literature depending on the specific-heat data used in the calculations and on whether or not disassociation and equilibrium effects were accounted for. Actual flame temperatures will be less, due to heat losses, incomplete mixing, and finite reaction times. Because our experimental burner was water-cooled, it was to be expected that the actual

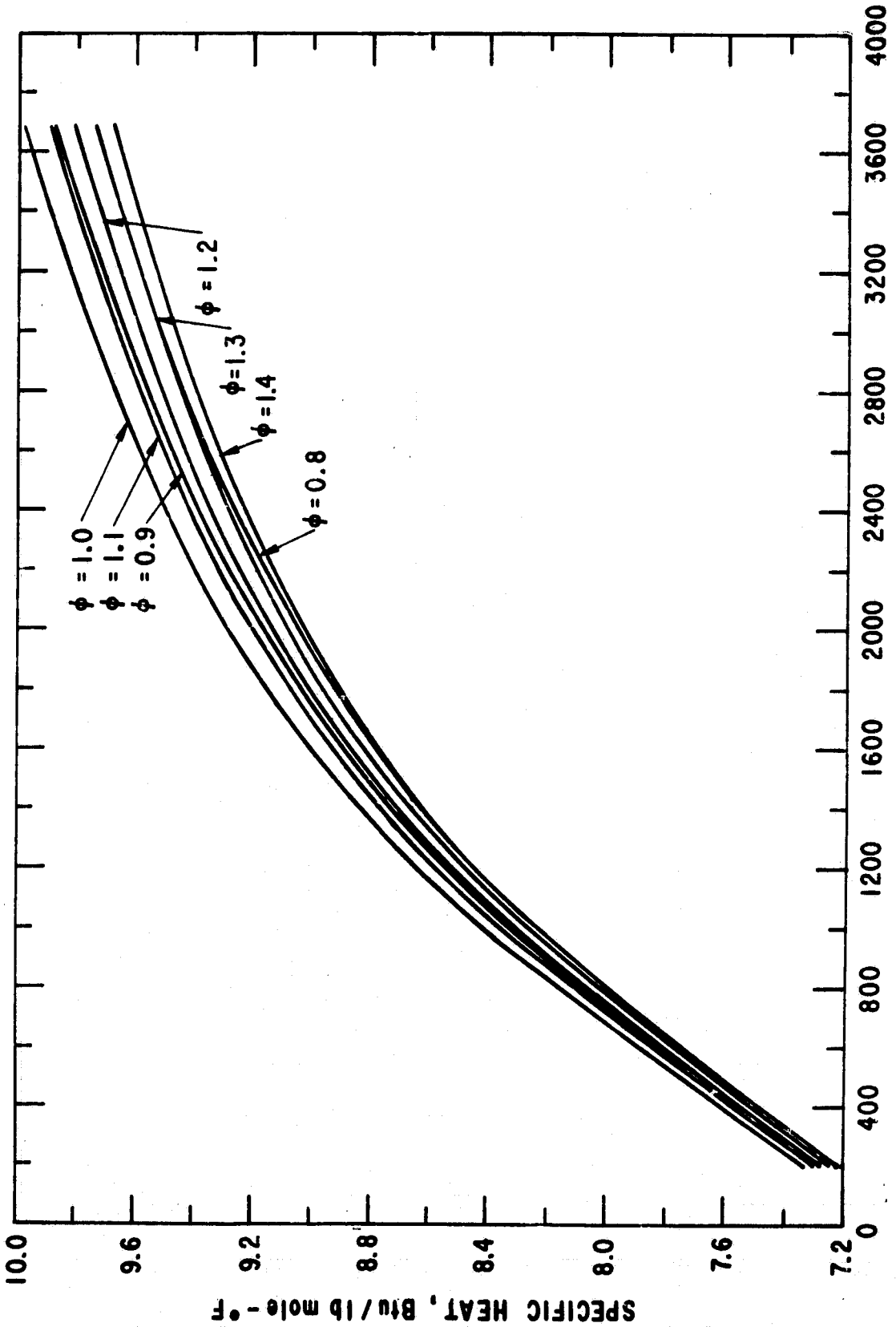

Fig. 4.3 Flue-Gas Molar-Specific Heat as a Function of the Air-Fuel Equivalence Ratio for Methane Combustion

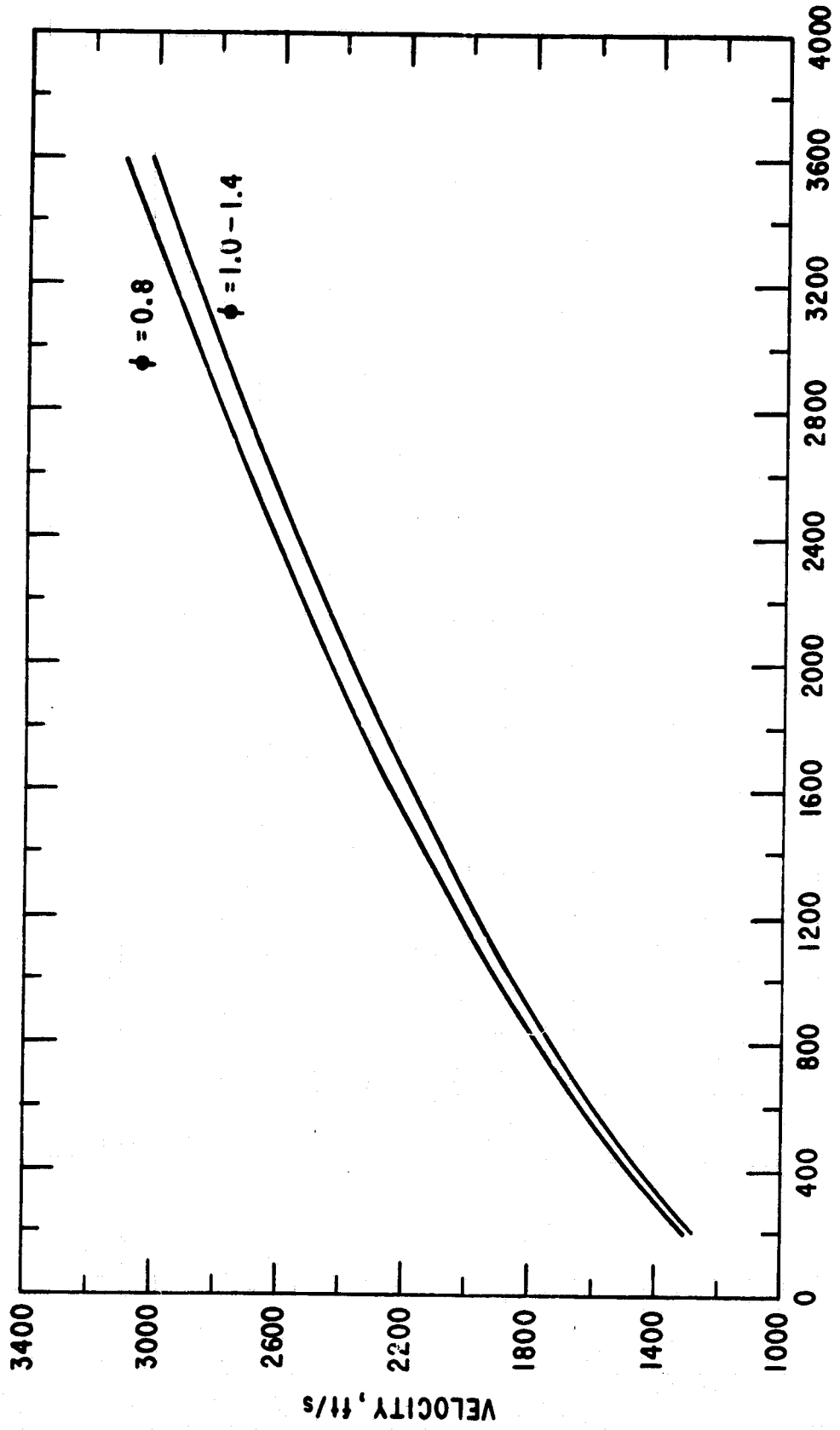

Fig. 4.4 Flue-Gas Acoustic Velocity for Stoichiometric Methane Combustion

Table 4.3 Flue-Gas Acoustic Velocity and Corresponding Temperature for the Experimental Burner

Heat Input (Btu/h)	Volumetric Air/Fuel Ratio	Measured Frequency (Hz)	Eq. 5.8, c (ft/s)	Results, t (°F)	Eq. 5.14, c (ft/s)	Results, t (°F)	Burner Configuration
32,887	13.21	63.5	1654	690	1909	1090	Standard Burner
50,245	9.89	64.5	1680	720	1939	1150	Standard Burner
54,194	12.48	75.0	1954	1160	2254	1750	Standard Burner
58,655	10.08	67.0	1745	810	2014	1280	Standard Burner
95,458	11.89	74.0	1928	1130	2224	1690	Standard Burner
96,782	10.34	74.0	1928	1130	2224	1690	Standard Burner
97,464	7.90	68.5	1784	800	2059	1360	Standard Burner
99,577	10.05	76.0	1980	1225	2284	1810	Standard Burner
100,215	9.89	75.0	1954	1180	2254	1750	Standard Burner
100,941	10.13	74.0	1928	1130	2224	1690	Standard Burner
101,713	9.87	70.0	1823	940	2104	1450	Standard Burner
103,576	10.12	75.5	1967	1210	2269	1790	Standard Burner
194,371	9.38	69.5	1810	920	2089	1420	Standard Burner
98,013	9.96	74.0	1928	1130	2224	1690	Insulated Standard Burner
53,589	12.50	64.0	1667	710	1924	1120	No Flapper Valves
102,645	11.39	71.0	1849	990	2134	1510	No Flapper Valves
50,418	10.02	66.0	1711	770	2019	1290	Tailpipe Aspirator
98,620	9.60	74.2	1924	1120	2270	1790	Tailpipe Aspirator
53,116	11.03	66.0	1719	780	1984	1230	Inlet Muffler
103,728	10.10	75.0	1954	1170	2254	1750	Inlet Muffler
101,532	10.09	79.0	2058	1360	2374	2000	Inlet Muffler
53,429	11.50	66.0	1719	780	1984	1230	Exhaust Muffler
50,227	9.42	62.0	1615	610	1863	1000	Inlet and Exhaust Mufflers
100,580	8.86	72.0	1876	1000	2164	1520	Inlet and Exhaust Mufflers
49,867	9.93	54.5	1730	800	1911	1090	48-in. Long Corebustor
50,341	9.82	54.0	1714	780	1893	1070	48-in. Long Corebustor
50,882	10.13	54.5	1730	800	1911	1090	48-in. Long Corebustor
99,996	9.73	68.0	2158	1560	2384	2040	48-in. Long Corebustor
101,248	10.09	68.0	2158	1560	2384	2040	48-in. Long Corebustor
50,042	10.07	55.0	1649	680	1842	970	36-in. Long Corebustor
97,009	10.11	68.0	2039	1330	2278	1800	36-in. Long Corebustor
100,553	9.82	64.5	1934	1140	2160	1560	36-in. Long Corebustor
100,794	10.45	76.0	1980	1225	2284	1810	Air Decoupling Chamber

Table 4.4 Estimated Adiabatic Flame and Exhaust-Gas Temperature

Heat Input (Btu/h)	Volumetric Air/Fuel Ratio	ϕ	Temperature, °F: Adiabatic Flame	Tailpipe: Inlet	Tailpipe: Exit	Tailpipe: Arithmetic Mean	Tailpipe: Geometric Mean	Burner Configuration
32,887	13.21	1.37	2950	1759	340	1050	873	Standard Burner
50,245	9.89	1.03	3565	2540	911	1726	1568	Standard Burner
54,194	12.48	1.30	3068	2114	643	1379	1225	Standard Burner
58,655	10.08	1.05	3523	2649	1093	1871	1738	Standard Burner
95,458	11.89	1.24	3170	2513	1265	1889	1805	Standard Burner
96,782	10.34	1.07	3482	2734	1292	2013	1906	Standard Burner
97,464	7.90	0.82	3355	2576	1242	1909	1813	Standard Burner
99,577	10.05	1.04	3545	2800	1291	2045	1929	Standard Burner
100,215	9.89	1.03	3565	2698	1195	1947	1826	Standard Burner
100,941	10.13	1.05	3523	2837	1461	2149	2057	Standard Burner
101,713	9.87	1.03	3565	2685	1168	1926	1803	Standard Burner
103,576	10.12	1.05	3523	2757	1188	1973	1843	Standard Burner
194,371	9.38	0.98	3610	2969	1552	2260	2167	Standard Burner
98,013	9.96	1.04	3545	2783	1277	2030	1914	Insulated Standard Burner
53,589	12.50	1.30	3068	2301	1238	1770	1705	No Flapper Valves
102,645	11.39	1.18	3275	2750	1799	2274	2233	No Flapper Valves
50,418	10.02	1.04	3545	2363	591	1477	1263	Tailpipe Aspirator
98,620	9.60	1.00	3630	2776	1048	1912	1749	Tailpipe Aspirator
53,116	11.03	1.15	3328	2140	471	1305	1096	Inlet Muffler
103,728	10.10	1.05	3523	----	----	----	----	Inlet Muffler
101,532	10.09	1.05	3523	2713	1064	1888	1739	Inlet Muffler
53,429	11.50	1.20	3240	2170	553	1361	1172	Exhaust Muffler
50,227	9.42	0.98	3610	2443	700	1571	1375	Inlet and Exhaust Mufflers
100,580	8.86	0.92	3535	2583	978	1780	1632	Inlet and Exhaust Mufflers
49,867	9.93	1.03	3565	2259	208	1234	888	48-in. Long Corebustor
50,341	9.82	1.02	3590	2399	543	1471	1234	48-in. Long Corebustor
50,882	10.13	1.05	3523	2189	242	1216	904	48-in. Long Corebustor
99,996	9.73	1.01	3610	2718	765	1742	1513	48-in. Long Corebustor
101,248	10.09	1.05	3523	2646	739	1693	1470	48-in. Long Corebustor
50,042	10.07	1.05	3523	2513	750	1632	1437	36-in. Long Corebustor
97,009	10.11	1.05	3523	2800	1106	1953	1799	36-in. Long Corebustor
100,553	9.82	1.02	3590	----	----	----	----	36-in. Long Corebustor
100,794	10.45	1.09	3440	2764	989	1877	1701	Air Decoupling Chamber

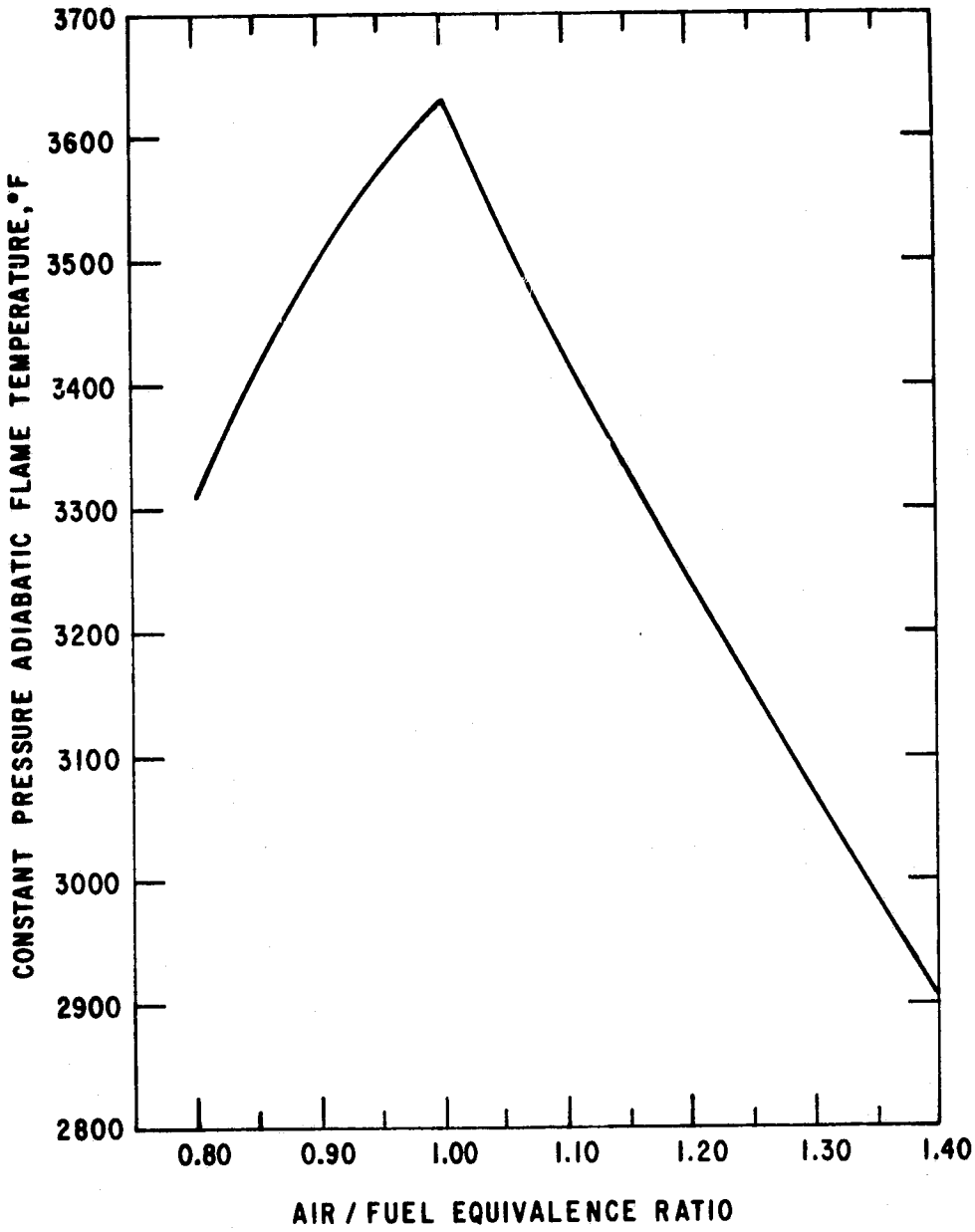

Fig. 4.5 Constant-Pressure Adiabatic Flame Temperature for Methane Combustion

flame temperature would be considerably less than the adiabatic flame temperature. However, the actual flame temperature cannot be obtained a priori, so the adiabatic flame temperature was used for the calculation of the tailpipe inlet temperature.

A comparison of the temperatures in Tables 4.3 and 4.4 does not allow a clear-cut decision as to what equation or temperature to use for determining the fundamental frequency of the experimental Helmholtz burner. The calculated temperatures listed in Table 4.4 are based on the adiabatic flame temperature, so actual temperatures will be lower. It appears that a mean temperature and Eq. 4.14 should be used for the frequency predictions. Equation 4.4 is also applicable for a Schmidt-type burner, while Eq. 4.8 would predict the burner to act as a half-wave tube.

5 OPERATING PRESSURE

5.1 RESULTS FROM PREVIOUS EXPERIMENTS

Pulse combustion has been described as constant-volume, pressure-rise combustion, and the pressure waveform was shown to be sinusoidal. For a town-gas-fired Helmholtz burner, Francis et al.[31] found that the pressure amplitude in the combustion chamber was relatively constant. They also found that the constriction between the chamber and tailpipe had little effect on the total amplitude of the fluctuating pressure, but the mean pressure fell due to the increase in mean velocity. As the gas rate was increased, the maximum positive pressure increased, while the maximum negative pressure tended to stay constant; thus, the mean pressure increased.

Katsnel'son et al.[34] found that doubling the heat release of a Helmholtz pulse combustor had little effect on the amplitude of the pressure oscillation in the combustion chamber. The pressure amplitude depended mainly on the air-fuel equivalence ratio. Two pressure peaks were obtained, one for lean mixtures and one for rich mixtures. The magnitude of the peaks depended on the fuel used.

From their studies of natural-gas-fired Helmholtz combustors, Griffiths and Weber[23] found that the combustion-chamber volume and tailpipe diameter had the greatest effect on operating pressures in a pulse combustion burner. The mean pressure in the combustion chamber increased with the gas-input rate for a constant chamber volume, but the pressure decreased as chamber volume increased. Data were also presented for the peak positive pressure in the combustion chamber as a function of the mean pressure, which is positive. For a given gas-input rate, burner operating pressures were usually higher for combustors with smaller combustion chambers and smaller tailpipe diameters.

For a propane-fired Schmidt-type burner, Hanby[42] found that the maximum pressure amplitude increased linearly with increasing heat-input rates for a constant air-fuel equivalence ratio of 1.05. The maximum pressure amplitude was also found to increase linearly with increasing equivalence ratios above 0.95 for a constant heat-input rate of 27,500 Btu/h. The higher amplitude from increasing air flow alone suggests that the kinetic energy of the flow played an important part in the combustion oscillation mechanism. Unfortunately, altering the flow rate of either air or fuel also changes the speed of flame propagation. Thus, the possibility arises that the efficiency of coupling between heat release and pressure fluctuation was responsible for the increase in maximum pressure amplitude with increasing equivalence ratio. Experimentally, the pressure amplitude was found to be strongly dependent on the fuel injector and the type of fuel used.

Briffa[33] found that for a methane-fired, single-combuster, uncoupled Helmholtz pulse combustor, the fluctuating pressure wave was modulated by a much lower frequency than the fundamental frequency. Coupling of two

combustors had no effect on the mean pressure (approximately 2.4 in. H_2O) in the burners, but the fluctuating pressure in the vicinity of their exits was elevated. Whereas the magnitude of the positive pressure was similar for both coupled and uncoupled combustors, the negative pressure in the coupled combustor was about 15.7 in. H_2O less than that in the uncoupled combustor until the exit was approached.

For a double-necked, methane-fired Helmholtz combustor, Reader[3] found that the pressure wave in the combustion chamber was sinusoidal and regular with swings of almost equal amplitude. Along the combustion-chamber length, the mean cyclic pressure was about 0.07 psi above atmospheric pressure. The ratio of the mean outlet pressure to mean inlet pressure was found to be marginally greater than unity. Along the combustion-chamber length, the maximum pressure range was 0.64 to 0.83 psi above atmospheric pressure, while the minimum pressure range was 0.30 to 0.41 psi below atmospheric pressure. However, at a location a quarter of the way along the chamber from the inlet, the maximum, minimum, and cyclic pressure swings were less than those at all other locations.

In the studies of natural-gas-fired Helmholtz pulse combustion at Purdue,[25-30] the maximum pressure on the single combustion chamber varied from 13 to 26 in. H_2O gage. The mean combustion-chamber pressure was 2 to 5 in. H_2O. At a heat-input rate of about 208,000 Btu/h with 29% excess air, the pressure amplitude in the combustion chamber was 0.75 in. H_2O for steady burning and 21 in. H_2O for pulse combustion. A computer model based on a Helmholtz-resonator approach was developed, and the predicted operational behavior of the burner was found to be strongly a function of geometry. Good agreement between calculated and measured pressure data was obtained.

From an idealized acoustic analysis for the tailpipe of a Helmholtz-type pulse combustor, Ahrens[49] obtained the following expression for the pressure fluctuation:

$$P_f = P_{max} [\cos\bar{\omega}\bar{x} - \sin\bar{\omega}\bar{x}/\tan\bar{\omega}] \cos\bar{\omega}\tau \tag{5.1}$$

where:

$$\bar{\omega} \tan\bar{\omega} = \frac{V_t}{V_c} \tag{5.2}$$

$$\bar{\omega} = \frac{2\pi f L_t}{c_t} \tag{5.3}$$

$$\bar{x} = \frac{x}{L_t} \tag{5.4}$$

$$\tau = \frac{t c_t}{L_t} \tag{5.5}$$

c_t = acoustic velocity of exhaust gas in tailpipe, ft/s

f = fundamental frequency of combustor, Hz

L_c = combustion-chamber length, ft

L_t = tailpipe length, ft

P_f = local instantaneous pressure, psi

P_{max} = maximum amplitude of pressure fluctuation, psi

t = time, s

V_c = combustion-chamber volume, ft^3

V_t = tailpipe volume, ft^3

x = distance along tailpipe from inlet, ft

In the limit as $V_t/V_c \to 0$, Eqs. 5.1 and 5.2 reduce to the following incompressible-flow solution for a classical Helmholtz resonator:

$$P = P_{max}(1-\bar{x})\cos\bar{\omega}\tau \tag{5.6}$$

$$\bar{\omega} = \sqrt{\frac{V_t}{V_c}} \tag{5.7}$$

Note that Eq. 5.7 is the same as Eq. 4.8.

Using data from early checkout runs with the burner, Ahrens[53,54] presented the normalized pressure amplitude along the tailpipe as shown in Figs. 5.1 and 5.2. Agreement between the experimental data and predictions based on the linearized compressible-flow model was reasonable. The shape of the pressure distribution suggested by the data is less strongly varying in the central part of the tailpipe and more strongly varying near the exit, relative to the theoretical curve. One possible cause of the difference may have been the large gas-temperature gradient along the tailpipe; this effect was not considered in the simplified mathematical model.

In their analysis of a pulse combustion burner, Ahrens, Kim, and Tam[50] derived the following approximation for the maximum combustion-chamber pressure:

$$P_{max} = 1.33 \frac{h_R}{\Delta H}(1+r)P_a \tag{5.8}$$

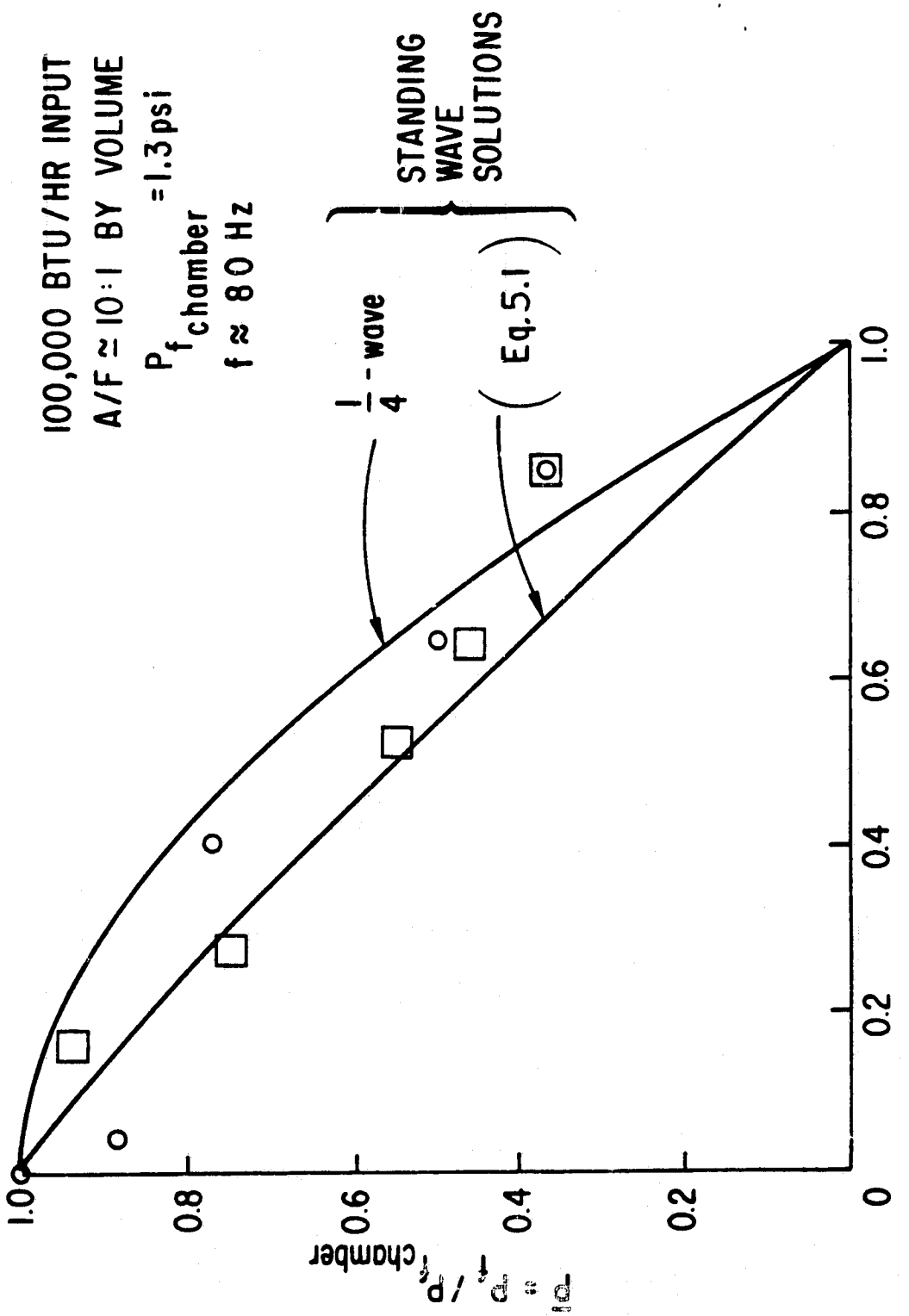

Fig. 5.1 Pressure-Fluctuation Distribution along Tailpipe

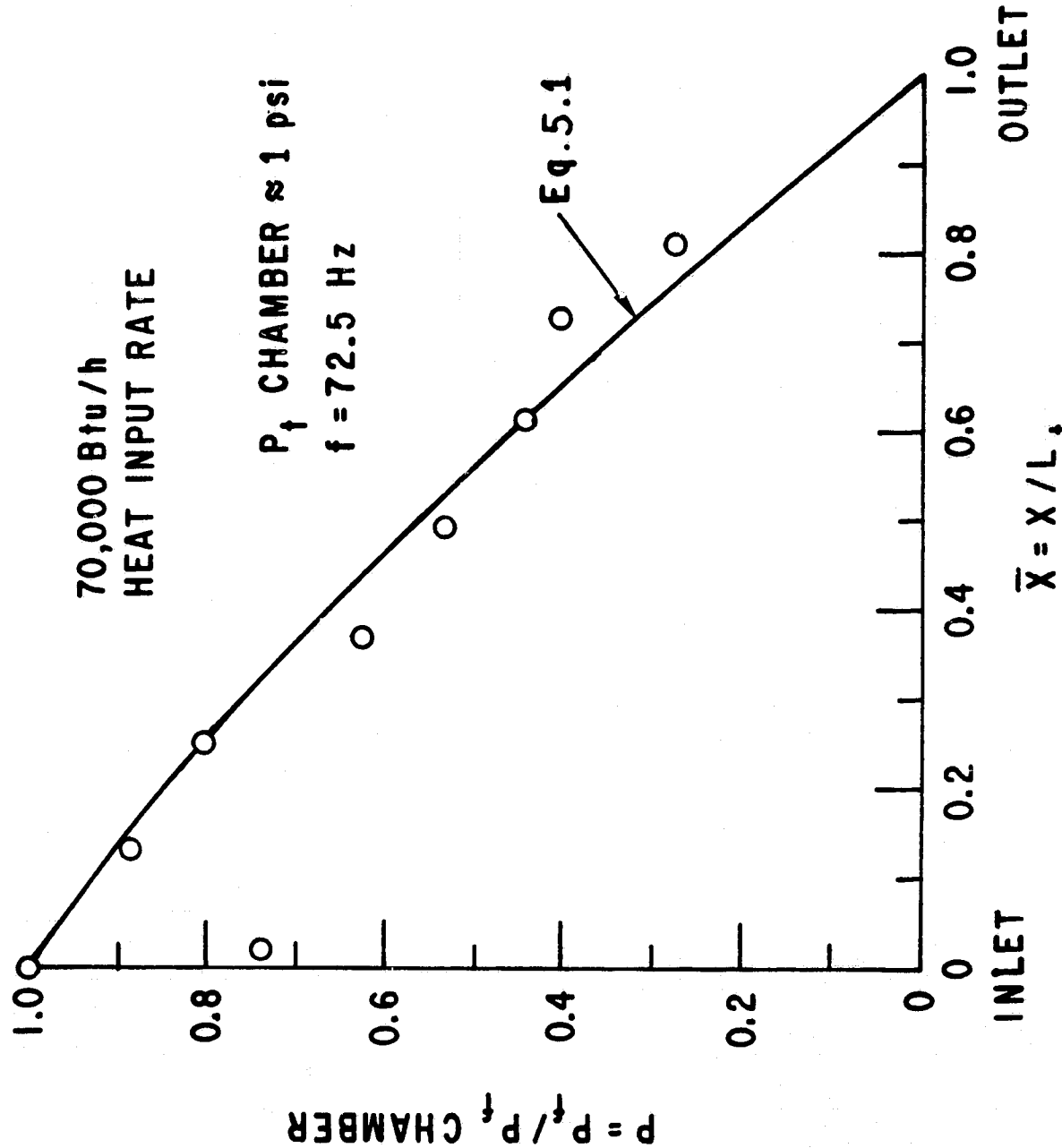

Fig. 5.2 Distribution of Fundamental Pulsation Amplitude

where:

h_R = enthalpy of air-gas mixture, Btu/lb_m

ΔH = heat of combustion, Btu/lb_m

P_a = air supply absolute pressure, psia

P_{max} = maximum combustion-chamber gage pressure, psig

r = air/fuel ratio (mass basis)

This equation predicts that the maximum combustion-chamber pressure is a linear function of the air/fuel ratio and is independent of geometric parameters. For the stoichiometric combustion of methane with atmospheric air, this equation becomes:

$$P_{max} = 0.104\ (1+r) \tag{5.9}$$

The mass- and energy-balance equations were solved numerically to obtain the maximum chamber pressure, and the results were almost linearly proportional to the air/fuel ratio. From a least-squares fit of the data, the following equation for the maximum chamber pressure was obtained:

$$P_{max} = 0.115r + 0.138 \tag{5.10}$$

5.2 RESULTS FROM ANL PULSE COMBUSTION EXPERIMENT

Instantaneous-pressure signals (5-ms display on an oscilloscope cathode-ray tube) in the combustion chamber are shown in Fig. 5.3 (a-e). Similar waveforms were obtained in the tailpipe. The observed pressure-pulsation signal is a complex waveform (Fig. 5.3a) produced by the superposition of the higher-harmonic components on the pressure signal at the fundamental frequency. To obtain the pulsation waveform at the fundamental and harmonic frequencies, the pressure-transducer signal was routed through a tunable filter (3% frequency bandwidth) prior to display on the oscilloscope. The result was the sinusoidal shape of the pressure pulsations as shown in Fig. 5.3b. At the higher harmonics (Fig. 5.3c-d) the filtered signal was not sinusoidal and the pressure amplitude varied. The effect of the higher harmonics appears to have been reinforcement of the positive pressure amplitude, so that a positive mean pressure was obtained. Another complexity was the time-varying pressure amplitude, as shown in Fig. 5.3f. This behavior, also observed by Briffa,[33] is contrary to claims for a steady pressure amplitude.

Mean values of the peak positive and negative pressure amplitudes for several locations along the burner are given in Table 5.1. The values listed,

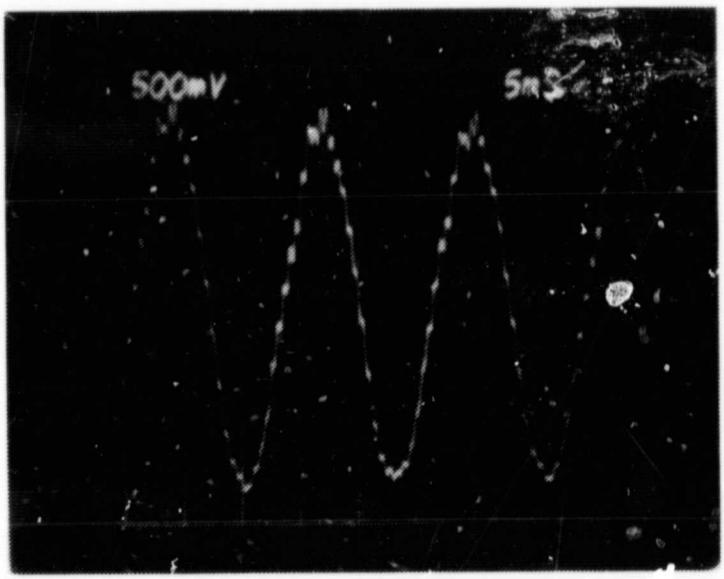

(a) Instantaneous Unfiltered Signal
(1 unit vert. = 500 mV,
1 unit horiz. = 5 ms)

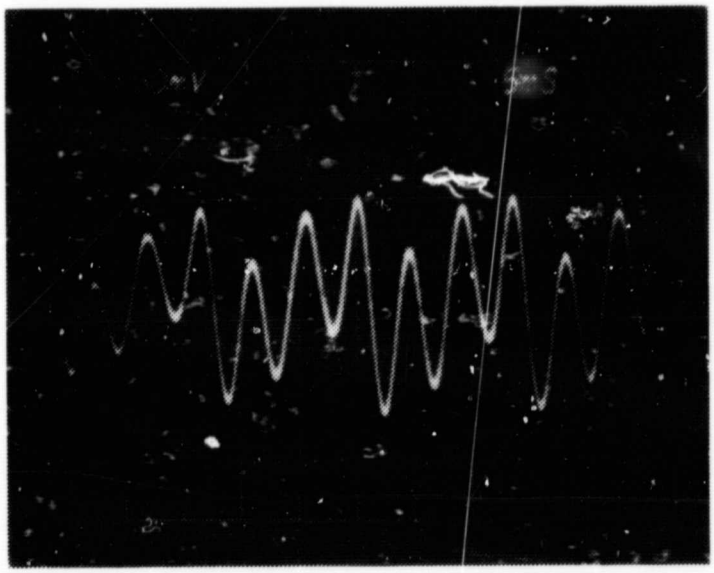

(b) Instantaneous Fundamental Frequency Signal
Using a 3% Frequency Bandwidth Filter
(1 unit vert. = 50 mV,
1 unit horiz. = 5 ms)

Fig. 5.3 Pressure-Pulsation Waveforms at the Gas-Distributor Head for a 95,460 Btu/h Heat Input with an 11.9 Air/Fuel Ratio
(1 V = 1 psig)

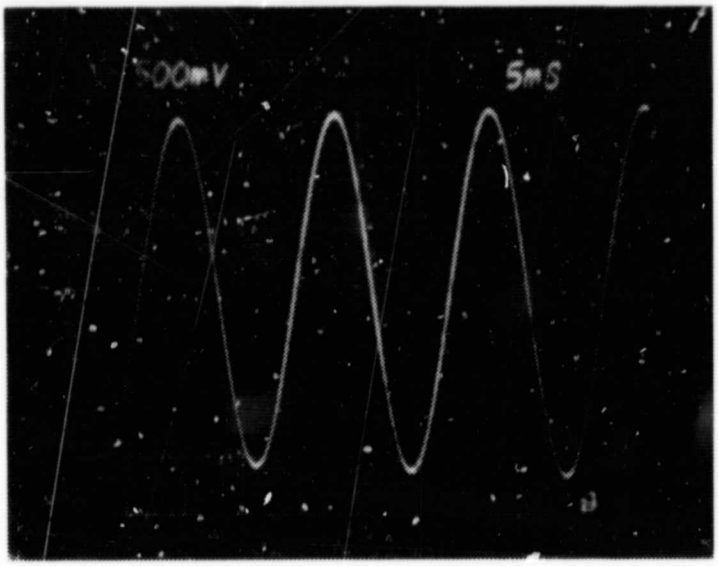

(c) Instantaneous Second Harmonic Signal
Using a 3% Frequency Bandwidth Filter
(1 unit vert. = 500 mV,
1 unit horiz. = 5 ms)

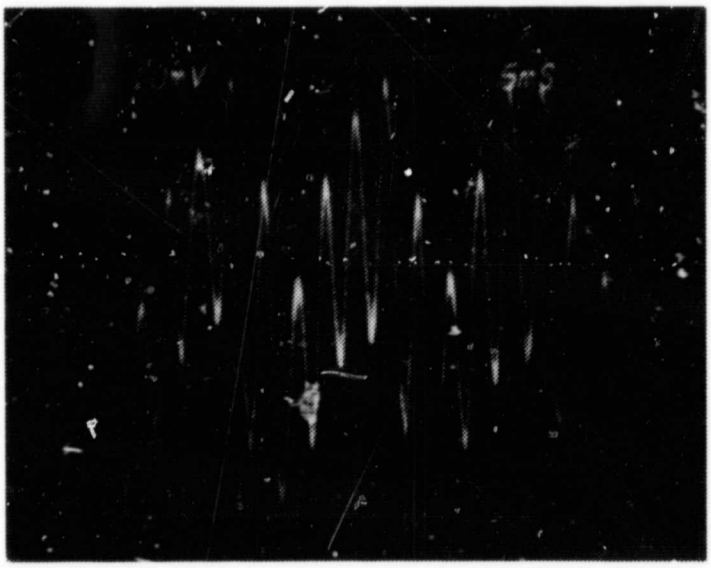

(d) Instantaneous Third Harmonic Signal Using
a 3% Frequency Bandwidth Filter
(1 unit vert. = 10 mV,
1 unit horiz. = 5ms)

Fig. 5.3 (Cont'd)

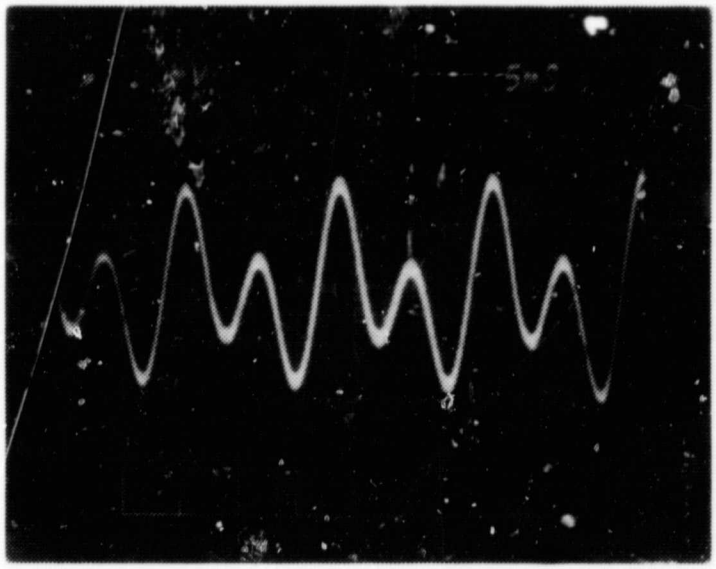

(e) Instantaneous Fifth Harmonic Signal
Using a 3% Frequency Bandwidth Filter
(1 unit vert. = 50 mV,
1 unit horiz. = 5 ms)

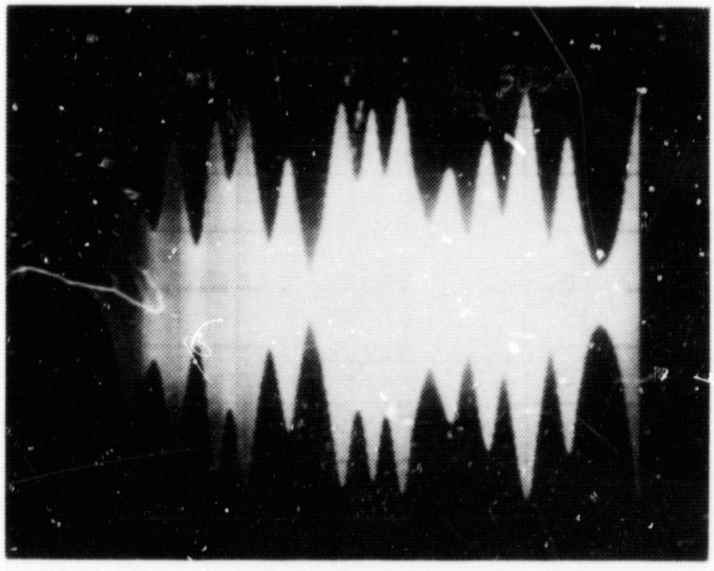

(f) 500 ms Signal Using a 3%
Frequency Bandwidth Filter
(1 unit vert. = 500 mV,
1 unit horiz. = 500 ms)

Fig. 5.3 (Cont'd)

Table 5.1 Mean Values of the Positive and Negative Peak Pressure Amplitude

Heat Input (Btu/h)	Air/Fuel Ratio	Distance Along Burner: 0.5 in. psig +	0.5 in. psig −	4.5 in. psig +	4.5 in. psig −	11.5 in. psig +	11.5 in. psig −	23.5 in. psig +	23.5 in. psig −	29.5 in. psig +	29.5 in. psig −	47.5 in. psig +	47.5 in. psig −	51.5 in. psig +	51.5 in. psig −	Burner Configuration
32,887	13.21	–	–	0.73	0.68	–	–	0.66	0.61	0.68	0.63	–	–	0.23	0.21	Standard Burner
50,245	9.89	0.7	0.7	0.75	0.75	0.65	0.7	–	–	0.90	0.90	–	–	0.23	0.22	Standard Burner
54,194	12.48	–	–	0.74	0.74	–	–	0.63	0.63	1.19	1.19	–	–	0.22	0.22	Standard Burner
58,655	10.08	1.0	1.0	–	–	–	–	0.4	0.4	0.62	0.62	0.32	0.32	0.25	0.24	Standard Burner
95,458	11.89	1.0	1.0	–	–	–	–	0.85	0.85	0.65	0.65	0.42	0.42	0.32	0.32	Standard Burner
96,782	10.34	1.4	1.4	–	–	–	–	0.46	0.46	1.4	1.2	0.31	0.3	0.23	0.23	Standard Burner
97,464	7.90	1.1	1.0	–	–	–	–	1.05	1.05	1.15	1.25	0.52	0.58	0.37	0.44	Standard Burner
99,577	10.05	–	–	0.86	0.86	–	–	–	–	0.74	0.74	–	–	0.32	0.32	Standard Burner
100,215	9.89	–	–	1.5	1.5	–	–	1.93	1.93	1.56	1.56	–	–	0.47	0.47	Standard Burner
100,941	10.13	–	–	–	–	–	–	1.3	1.25	1.15	1.05	0.65	0.62	0.45	0.42	Standard Burner
101,713	9.87	–	–	1.4	1.3	–	–	1.2	1.2	1.15	1.15	–	–	0.42	0.42	Standard Burner
103,576	10.12	1.7	1.8	1.4	1.4	1.25	1.3	–	–	2.4	2.5	–	–	0.44	0.46	Standard Burner
194,371	9.38	3.2	3.2	–	–	–	–	2.6	2.6	2.6	2.6	1.0	1.0	1.0	1.0	Standard Burner
98,013	9.96	–	–	–	–	–	–	1.3	1.2	1.4	1.1	0.75	0.65	0.8	0.5	Insulated Standard Burner
53,589	12.50	–	–	–	–	–	–	0.05	0.05	0.03	0.03	0.026	0.028	0.01	0.01	No Flapper Valves
102,645	11.39	–	–	0.12	0.18	–	–	0.09	0.13	0.05	0.08	–	–	0.01	0.018	No Flapper Valves
50,418	10.02	–	–	0.99	1.29	–	–	0.93	0.63	0.46	0.76	–	–	0.32	0.37	Tailpipe Aspirator
98,620	9.60	–	–	1.87	2.47	–	–	1.58	2.18	1.15	1.40	–	–	0.57	0.57	Tailpipe Aspirator
53,116	11.03	–	–	0.75	0.75	–	–	0.7	0.7	0.7	0.7	–	–	0.40	0.40	Inlet Muffler
103,728	10.10	–	–	1.8	1.7	–	–	1.5	1.5	1.6	1.5	–	–	0.60	0.56	Inlet Muffler
101,532	10.09	–	–	–	–	–	–	–	–	1.4	1.4	–	–	0.46	0.46	Inlet Muffler
53,429	11.50	–	–	0.69	0.69	–	–	0.58	0.58	0.83	0.83	–	–	0.26	0.26	Exhaust Muffler
50,227	9.42	–	–	0.63	0.63	–	–	0.64	0.64	0.52	0.52	–	–	0.21	0.21	Inlet and Exhaust Mufflers
100,580	8.86	–	–	1.29	1.49	–	–	0.98	1.18	1.34	1.54	–	–	0.40	0.48	Inlet and Exhaust Mufflers
49,867	9.93	–	–	0.98	0.93	–	–	0.84	0.70	0.81	0.66	–	–	0.25	0.22	48-in. Long Corebustor
50,341	9.82	–	–	0.94	0.89	–	–	0.83	0.78	0.83	0.78	–	–	0.24	0.22	48-in. Long Corebustor
50,882	10.13	–	–	1.00	0.82	–	–	0.82	0.82	0.74	0.74	–	–	0.24	0.24	48-in. Long Corebustor
99,996	9.73	–	–	1.51	1.2	–	–	1.21	0.9	1.26	1.10	–	–	0.35	0.29	48-in. Long Corebustor
101,248	10.09	–	–	1.44	1.34	–	–	1.57	1.57	1.38	1.38	–	–	0.34	0.34	48-in. Long Corebustor
50,042	10.07	0.85	0.75	0.8	0.7	0.85	0.75	–	–	0.95	0.85	–	–	0.15	0.13	36-in. Long Corebustor
97,009	10.11	1.3	1.3	0.8	0.8	–	–	–	–	0.56	0.56	–	–	0.30	0.30	36-in. Long Corebustor
100,553	9.82	1.3	1.2	1.2	1.2	1.3	1.3	–	–	2.0	1.5	–	–	0.36	0.26	36-in. Long Corebustor
100,794	10.45	–	–	0.88	0.88	–	–	–	–	1.72	1.7	–	–	0.39	0.39	Air Decoupling Chamber

obtained from photographs of the waveform displayed on the oscilloscope, are mean values of the maximum and minimum peak pressures for a 500-ms display time or from several seconds of readings from a digital voltmeter. Some general observations based on these data are:

- For the same air/fuel ratio, an increase in the heat-input rate resulted in an increase in the burner pressure.
- Unfiltered pressure amplitudes were slightly higher (1-10%) than the values obtained with filtered amplitudes.
- For the filtered signals, the positive and negative peaks were generally of equal amplitude (except when a corebustor or tailpipe aspirator was used).
- The addition of either an inlet muffler or an exhaust muffler did not affect the combustion-chamber pressure, but the use of both mufflers apparently resulted in a slight pressure reduction.
- The use of a corebustor seemed to cause the combustion-chamber pressure to increase, especially at low heat-input rates.
- The use of a tailpipe aspirator resulted in a negative pressure amplitude that was larger than the positive amplitude in the combustion chamber.

Variation of the pressure amplitude with the heat-input rate contradicts the conclusions of Katsnel'son et al.[34] and Ahrens et al.[50] that the maximum pressure amplitude is only a function of the air/fuel ratio (mass basis). For a volume-based air/fuel ratio of 10 (mass-based ratio of 18), a maximum pressure of 2.2 psig would be obtained from Eq. 5.10, which is higher than measured values for heat-input rates of up to 100,000 Btu/h. The data were not sufficient to verify Hanby's[42] conclusion that the maximum pressure amplitude varied linearly with increasing equivalence ratio above 0.95 for a constant heat-input rate. From the data in Table 5.1, it appears that the pressure amplitude increases from ϕ = 0.82 to a maximum at ϕ = 1.03 and then decreases. For methane combustion, Katsnel'son et al.[34] found pressure peaks at equivalence ratios of 0.8 and 1.5, with sharp decreases in the pressure amplitude on either side of these values.

Hanby[42] also concluded that the peak pressure varies linearly with the heat-input rate for a constant equivalence ratio. However, Katsnel'son et al.[34] concluded that doubling the heat-input rate had little effect on the magnitude of the pressure amplitude. Figure 5.4 is a plot of the standard-burner pressure data in Table 5.1 for a heat-input rate of ≈100,000 Btu/h with varying equivalence ratio. One can infer that the maximum pressure amplitude

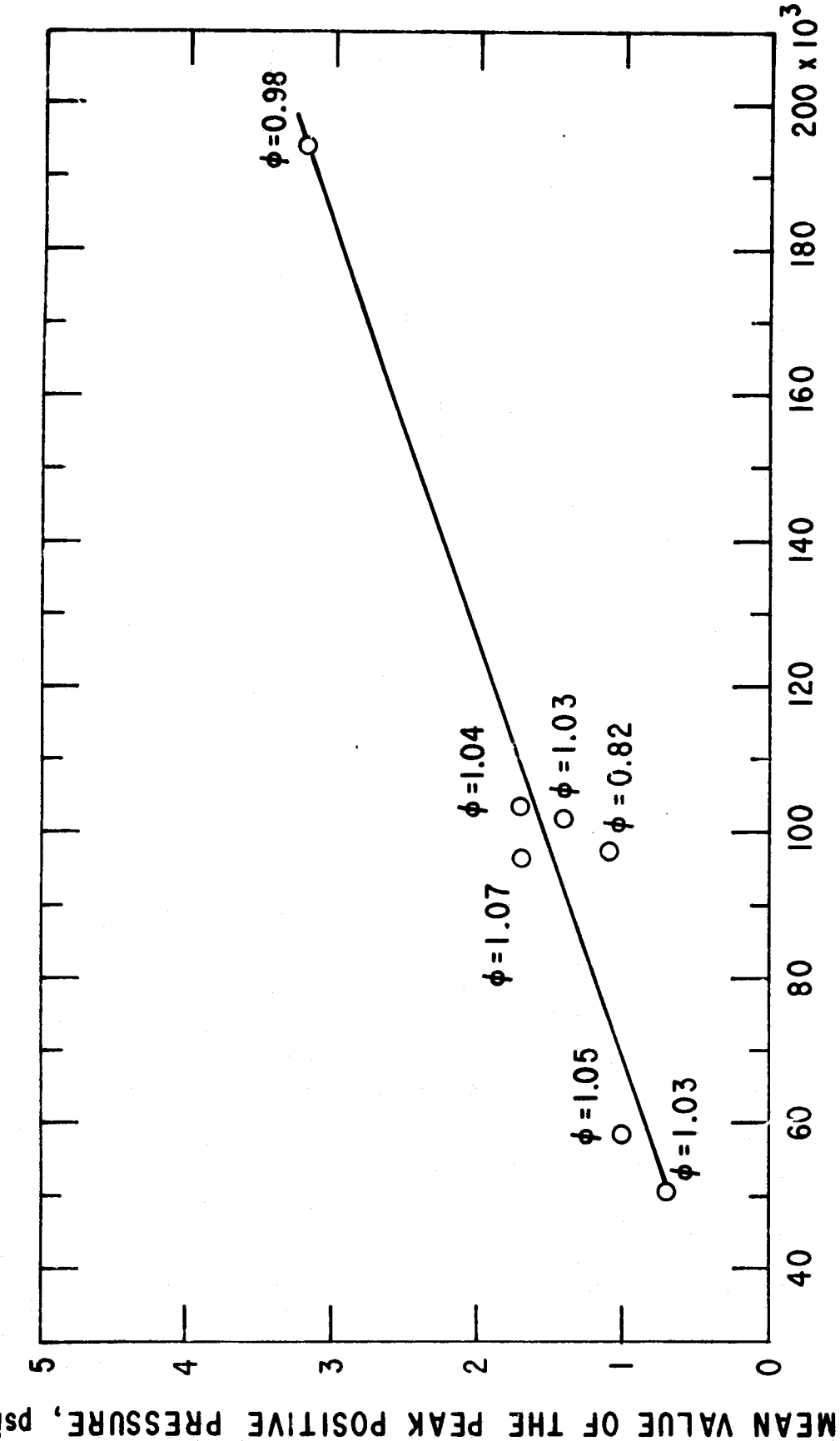

Fig. 5.4 Mean Value of the Peak Positive-Pressure Amplitude as a Function of the Burner Heat-Input Rate

is to some degree a linear function of the heat-input rate. Therefore, Katsnel'son's conclusion is incorrect. The air-fuel equivalence ratio does not appear to have a strong influence on the pressure peak.

Because this study utilized only one size burner, the effect of combustion-chamber volume on pressure (as given by Griffiths and Weber[23]) cannot be evaluated. However, the change in tailpipe volume when the core-bustor was installed appears to have had an effect on the combustion-chamber pressure. A logical expectation would be that as the volume of the combustion chamber increased, the peak pressure would decrease.

6 HEAT TRANSFER

Heat transfer to an enclosure containing a hot gas will occur by radiation and convection. Convective heat transfer occurs between a fluid and a surface, and its prediction is generally based on empirical correlations for the heat-transfer coefficient. Radiative heat transfer is a complex phenomenon, the treatment of which usually involves a number of simplifying assumptions. In most of the previous pulse combustion studies (e.g., Francis, Hoggarth, and Reay;[31] Reay;[32] Hanby;[41] and Alhaddad and Coulman[55]), the effects of radiative heat transfer have been neglected. Francis et al.[31] estimated the radiative/convective heat-transfer ratio as 0.000354, which I think is incorrectly calculated (because the wall temperature, instead of the gas temperature, was used). Reay[32] also used this ratio, and the other investigators have chosen to ignore radiation effects for the sake of convenience.

6.1 CONVECTIVE HEAT TRANSFER

Heat transfer by convection can be free, forced, or mixed.

6.1.1 Free Convection

Free convection is associated with fluid motion resulting from density differences that are caused by temperature gradients. Heat-transfer coefficients for free convection are expressed by:

$$Nu = C(Gr\ Pr)^a \tag{6.1}$$

where:

$Nu = \frac{hX}{k}$ = Nusselt number

$Gr = \frac{X^3 \rho^2 g\beta (T_g - T_w)}{\mu^2}$ = Grashof number

$Pr = \frac{Cp\mu}{k}$ = Prandtl number

a = a constant

C = a constant

Cp = constant-pressure specific heat, Btu/lb_m°F

g = acceleration of gravity = 4.17×10^8 ft^2/h

h = heat-transfer coefficient, Btu/h-ft^2-°F

k = thermal conductivity, Btu/h-ft-°F

T_g = fluid temperature, °R

T_w = wall temperature, °R

X = characteristic length, ft

β = volumetric coefficient of expansion, °R^{-1}

μ = absolute fluid viscosity, lb$_m$/ft-h

ρ = fluid density, lb$_m$/ft^3

The average Nusselt number for free convection from a vertical plate or cylinder (provided that the radius is much larger than the boundary-layer thickness) under conditions of uniform surface temperature is expressed by the following equations from McAdams:[56]

$$Nu = 0.59\,[GrPr]_f^{0.25},\quad 10^4 < GrPr < 10^9 \tag{6.2}$$

$$Nu = 0.13[GrPr]_f^{1/3},\quad 10^9 < GrPr < 10^{12} \tag{6.3}$$

In these equations the subscript "f" means that the physical properties of the gas are evaluated at the arithmetic mean of the gas and wall temperature. The characteristic length to be used in the Grashof number is the height of the plate or cylinder. Ozisik[57] lists a value of C = 0.10 instead of 0.13 for Eq. 6.3.

6.1.2 Forced Convection

Forced convection occurs from the mixing effect of a fluid in motion and its interaction with a surface. These effects are caused by external forces that are independent of temperature differences. Expressions for forced-convection heat-transfer coefficients are generally of the form:

$$Nu = C(Re)^a\,(Pr)^b \tag{6.4}$$

where:

$Re = \frac{XG}{\mu}$ = Reynolds number

b = a constant

G = fluid mass velocity, lb_m/ft^2-h

In a number of such expressions the values of a, b, and C in Eq. 6.4 are not constant. The value of C may depend on multipliers included to account for the effects of variations in physical properties and entrance-length effects, and it may also be a function of the Reynolds and Prandtl numbers. The values of a and b have also been expressed as functions of the Prandtl number. Since the flow of a fluid inside a tube is classified as laminar (Re < 2100-2500), transitional (2100-2500 < Re < 10,000) or turbulent (Re > 10,000), the forced-convection heat-transfer coefficient will depend on the flow regime. When a fluid enters a conduit, a velocity boundary layer starts to develop until it reaches the center of the tube. The region for this development is called the hydrodynamic entry length. Beyond this length is the region of fully developed velocity, where the velocity profile is invariant with tube length. If the boundary layer remains laminar until its thickness reaches the tube center, fully developed laminar flow prevails beyond that point. If the boundary layer changes into turbulent flow before it reaches the tube center, fully developed turbulent flow exists beyond the hydrodynamic entry region. The development of the thermal boundary layer can be viewed in a similar manner. The length from the tube inlet to the hypothetical location where the thermal boundary layer reaches the tube center is called the thermal entry region. Beyond this point lies the thermally developed region where the temperature profile is invariant with tube length. The temperature profile depends on the boundary condition at the tube wall. Two common boundary conditions are constant heat flux and constant surface temperature. This latter condition approximates the condition of the burner surface in this study.

6.1.2.1 Laminar Flow

For laminar flow inside a circular tube with a constant surface temperature and in the region of fully developed velocity and temperature profiles, the Nusselt number is a constant. According to Rohsenow and Hartnett[58] (pages 7-20), this constant has the value Nu = 3.656.

The classical solution of Graetz for a fully-developed (parabolic) velocity profile and a developing thermal profile in a tube with a constant surface temperature is given in many heat-transfer books, such as those by McAdams[56] and Ozisik.[57] However, the variation of the mean Nusselt number in the combined thermal and hydrodynamic entry region of a tube is of greater interest. This variation for a constant surface temperature is presented on pages 7-24 of Rohsenow and Hartnett and is shown in Fig. 6.1. The parabolic velocity profile is the classical solution of Graetz for the thermal entry region of the tube. The following formula for the mean Nusselt number in the thermal entry region for the Graetz solution was developed by Hausen and listed on page 198 of Ozisik:[57]

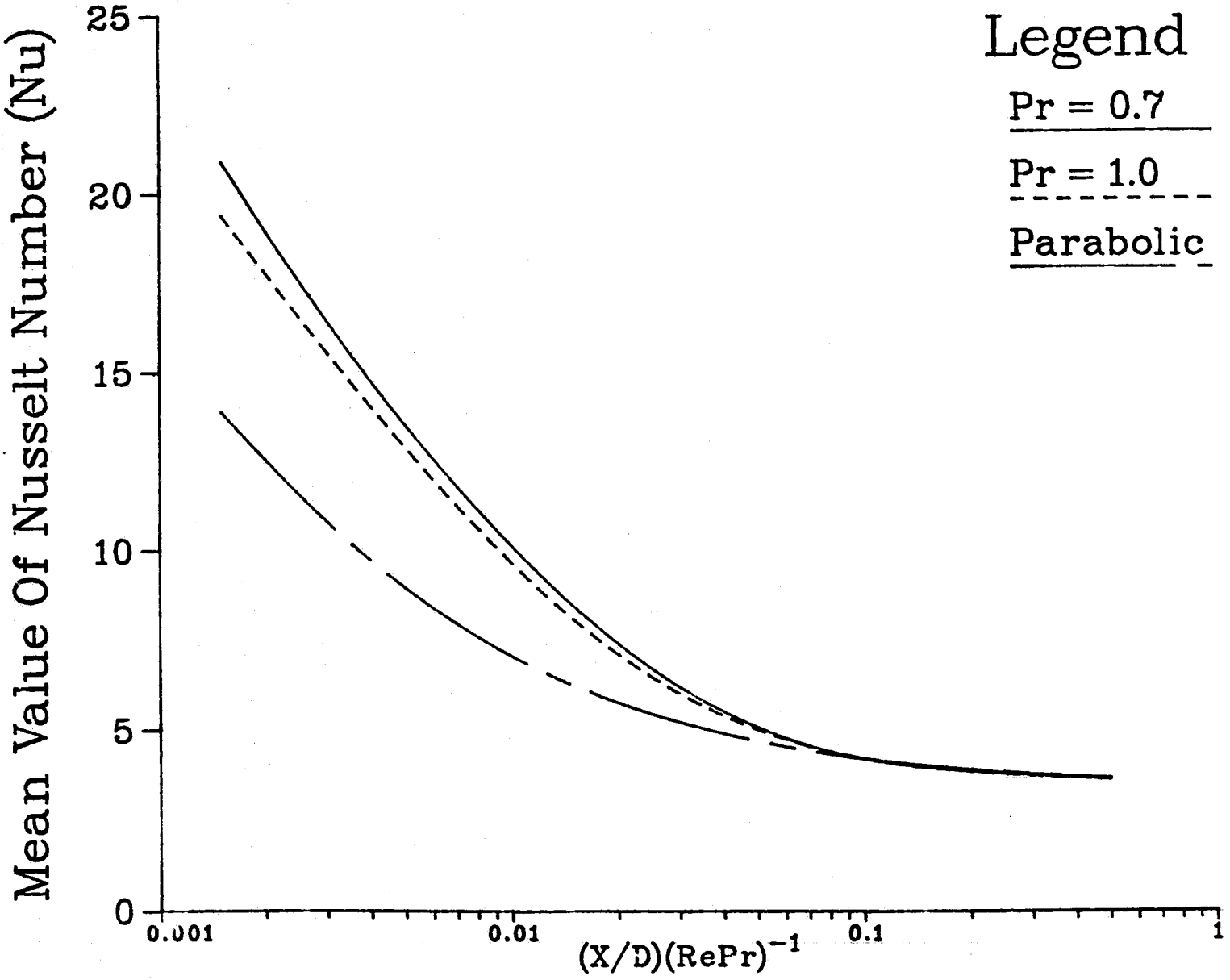

Fig. 6.1 Variation of the Mean Nusselt Number for Laminar-Flow Convective Heat Transfer in the Combined Thermal and Hydrodynamic Entry Region of a Tube with Constant Surface Temperature (Source: Ref. 58)

$$Nu = 3.66 + \frac{0.0668\ (D/X)\ RePr}{1 + 0.04\ [(D/X)\ RePr]^{2/3}} \tag{6.5}$$

where:

D = inside diameter of tube, ft

X = length of tube from entrance, ft

From Fig. 6.1 it is evident that the Nusselt numbers are higher when both the velocity and temperature profiles develop simultaneously in the entry region of a tube. The length of the entry region is approximately given by:

$$\frac{X}{D} = 0.05\ RePr \tag{6.6}$$

The heat-transfer correlations discussed were based on thermal properties that were invariant with temperature. Large temperature gradients between the bulk stream temperature and the wall temperature will cause a distortion of the velocity and temperature profiles. To account for such differences, the isothermal Nusselt number is multiplied by a "property-ratio function" (ratio of property evaluated at bulk stream temperature to that property evaluated at the wall temperature). The property ratio for liquids is a viscosity ratio, while for gases a temperature ratio is used. Hence, for gases, the mean Nusselt number is expressed by:

$$Nu = (Nu)_{cp} \left(\frac{T_b}{T_w}\right)^n \tag{6.7}$$

where the subscripts are defined as:

cp = constant properties

b = bulk stream

w = wall

The exponent n is a function of geometry and type of flow. For laminar flow of gases in tubes, Kays and Crawford[59] (page 279) list the value of n as 0.

McAdams[56] (page 237) presents the following correlation, developed by Sieder and Tate from data on heating and cooling of petroleum oils flowing at Reynolds numbers less than 2100, for a tube with uniform wall temperature:

$$Nu = 1.86 \left[(Re)(Pr)\left(\frac{D}{L}\right)\right]^{1/3} \tag{6.8}$$

This equation correlated the data with a maximum deviation of 60% for small tube diameters and temperature differences. With large tube diameters and temperature differences the maximum deviation was 250%.

In the Gas Engineer's Handbook[51] (page 2/139), it is stated that in domestic gas appliances, the gases formed by the flame initially may be turbulent, although the computed Reynolds number frequently indicates laminar flow. Thus, the prediction of the gas-side film coefficient is difficult. Inside a 4-in. diameter steel tube, and in most domestic gas appliances, combustion flow rates must be limited to laminar flows to prevent excessive tube-wall temperatures. For these conditions, it was found that the cooling-zone gas-film coefficient in a 4-in. tube, at all heat inputs greater than 10,000 Btu/h, could be correlated by the following:

$$h = (1.2 + 0.25a_x)e^{0.067w/d} \qquad (6.9)$$

where:

a_x = fraction of excess air in total air-gas mixture

d = equivalent port diameter = $(4A/\pi)^{0.5}$ (applies to both single and multiport burners; A is the port area in $in.^2$)

e = 2.718, base of natural logarithms (approximately)

w = weight of unburned gases issuing from the burner port, lb/h

The maximum observed value of the gas-film coefficient was 3.85 Btu/h-ft^2-°F, while the minimum (which was not correlated by Eq. 6.9) was 0.65 Btu/h-ft^2-°F. Because of diminishing gas turbulence, the use of Eq. 6.9 for estimating gas-film coefficients is only recommended for tubes 3-4 ft long.

Severyanin[60] reported the following equation for convective heat transfer for the laminar-flow regime (Re < 2600):

$$Nu = 0.4\ Re^{0.5}\ Pr^{0.4} \qquad (6.10)$$

The author did not list any constraints for this equation. Since it contains no length/diameter parameter, it is probably for the fully developed region. However, for fully developed velocity and thermal profiles, the Nusselt number is a constant.

6.1.2.2 Turbulent Flow

Numerous correlations are available for predicting the heat-transfer coefficient for turbulent forced convection inside circular tubes for the

fully developed region. A representative sample of these correlations and their limitations is given in Table 6.1. Some of these correlations may be for a constant-heat-flux boundary condition, but the difference between Nusselt numbers for constant heat flux and constant surface temperature is small, especially for large Reynolds numbers.

In the combined hydrodynamic and thermal entry region of a circular tube, the turbulent boundary-layer development is very strongly influenced by the shape of the tube entrance. If the tube has a nozzle or bellmouth entrance, if the tube walls are smooth, and if the free-stream turbulence level is low, a laminar boundary layer will form initially even though the Reynolds number (based on tube diameter) is much greater than the value of 2100-2500. Transition to turbulent flow will eventually occur further down the tube. Because of the initial boundary layer, the mean value of the Nusselt number actually may not be significantly higher than the value for fully developed turbulent flow. If a boundary-layer trip is provided at an appropriate point in the tube near its entrance, it is possible to obtain a turbulent boundary layer from the beginning of the tube. A separated flow occurs at the entrance, with sufficient vorticity shed into the main stream so that the heat-transfer rate is much higher than would be obtained in a developing turbulent boundary layer where turbulence originates from the surface.

Boelter, Young, and Iversen[62] measured the local Nusselt number for air flowing through a steam-heated tube with various entry configurations. The ratio of the local Nusselt number (Nu_x) to the fully developed Nusselt number (from Table 6.1) for an abrupt entrance is shown as a function of x/D in Fig. 6.2. The interesting behavior of this curve is apparently caused by the contraction and then re-expansion of the flow during the first diameter of tube length. A reasonable approximation of this curve for $x/D > 1.5$ is:

$$\frac{Nu_x}{Nu} = 0.9 + \frac{2}{(x/D)} \tag{6.19}$$

The average Nusselt number (Nu_L) over the tube length can be obtained by:

$$Nu_L = \frac{1}{L} \int_0^L Nu_x dx \tag{6.20}$$

For the curve in Fig. 6.2 and for $L/D > 20$, the average Nusselt number can be expressed by

$$\frac{Nu_L}{Nu} = 1 + \frac{6}{(L/D)} \tag{6.21}$$

Table 6.1 Correlations for Turbulent-Flow Convective Heat Transfer in a Circular Tube[a]

Name	Correlation	Limitation
Dittus-Boelter[56,57,59] (6.11)	$Nu = 0.023\ Re^{0.8}\ Pr^{b}$ $b = 0.4$ Heating $b = 0.3$ Cooling	$0.7 < Pr < 100$ $10{,}000 < Re < 120{,}000$ $L/D > 60$
Sieder-Tate[56,57] (6.12)	$Nu = 0.023\ Re^{0.8} Pr^{1/3} \left(\frac{\mu}{\mu_w}\right)^{0.14}$	$0.7 < Pr < 16700$ $10{,}000 < Re < 10^7$ $L/D > 60$
Rohsenow-Hartnett[58] (6.13)	$Nu = 0.021\ Re^{0.8}\ Pr^{0.6}$	$0.5 < Pr < 1.0$ $Re > 10{,}000$ $L/D > 60$ Constant surface temperature
Petukhov-Popov[61] (6.14)	$Nu = \frac{(\xi/8)RePr}{k_1 + k_2(\xi/8)^{1/2}(Pr^{2/3}-1)}$ $\xi = (1.82 \log_{10} Re - 1.64)^{-2}$ $k_1 = 1 + 3.4\xi$ $k_2 = 11.7 + 1.8\ Pr^{-1/3}$	$0.5 < Pr < 2000$ $10^4 < Re < 5 \times 10^6$
Sleicher-Rouse[59] (6.15)[b]	$Nu = 5 + 0.015\ Re_f^{a}\ Pr_w^{b}$ $a = 0.88 - \frac{0.24}{4 + Pr_w}$ $b = 1/3 + 0.5e^{-0.6\ Pr_w}$	$0.1 < Pr < 10^4$ $10^4 < Re < 10^6$
Petukhov-Kirillov[58,61] (6.16)	$Nu = \frac{RePr\ (\xi/2)}{12.7(\xi/2)^{1/2}\ (Pr^{2/3}-1) + 1.07}$ $\xi = [3.64 \log_{10} Re - 3.28]^{-2}$	
Severyanin[60] (6.17)	$Nu = 0.028\ Re^{0.8}\ Pr^{0.4}$	$6000 < Re < 120{,}000$
Kays-Crawford[59] (6.18)	$Nu = 0.021\ Re^{0.8}\ Pr^{0.5}$	$0.5 < Pr < 1.0$ $Re < 10^5$

[a] All properties are evaluated at the bulk fluid temperature except those with subscripts of "f" for film temperature (i.e., arithmetic mean of bulk and wall temperature) or "w" for wall temperature.

[b] Ozisik[57] (page 285) lists an equation given by Notter and Sleicher that is identical to this one except that the premultiplier 0.015 is given as 0.016.

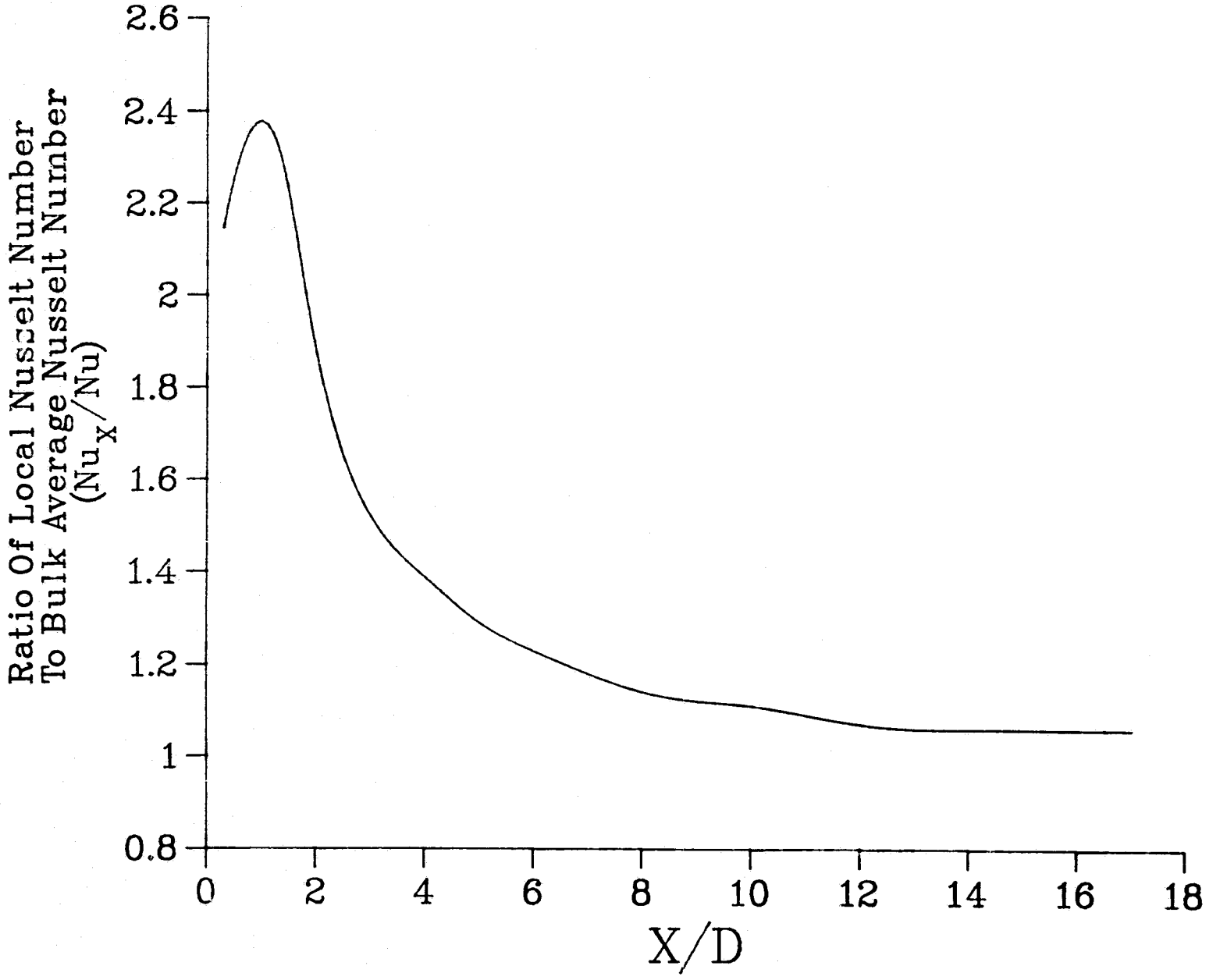

Fig. 6.2 Local Nusselt Numbers for the Turbulent-Flow Convective Heat Transfer to Air in the Entry Region of a Constant-Surface-Temperature Tube with an Abrupt Entrance (Source: Ref. 62)

For a sharp-edge entry (sudden contraction), McAdams[56] recommends the following equation:

$$\frac{Nu_L}{Nu} = 1 + (D/L)^{0.7}, \quad 1 < D/L < 68 \tag{6.22}$$

For the thermal entry region, Ozisik[57] (page 265) gives the following equation for the mean Nusselt number:

$$Nu = 0.036\ Re_f^{0.8} Pr_f^{1/3} \left(\frac{D}{L}\right)^{0.055}, \quad 10 < \frac{L}{D} < 400 \tag{6.23}$$

All of these correlations for the Nusselt number are based on constant fluid properties, so to compensate for physical-property variation with temperature, Eq. 6.7 is applicable. Ozisik[57] (page 281) recommends that for turbulent flow of a gas in a circular tube, for $x/D > 30$ and for $T_b/T_w > 1$, the value of the exponent n in Eq. 6.7 is 0. Thus, for both laminar flow and turbulent flow, no temperature correction to the mean Nusselt number is required.

6.1.2.3 Transition Flow

The transition region lies between the end of the region of laminar flow (Re < 2100 2500) and the start of the region of well-developed turbulent flow (Re > 10,000). Heat-transfer results are uncertain in this region because of when and how transition occurs.

Dalle Donne and Bowditch[63] investigated the local heat transfer and average friction coefficients for subsonic laminar, transitional, and turbulent flow of air in a tube at high temperature. Even though their results are for a constant-heat-flux boundary condition, their observations for the transition region are of interest. The authors used the following equation for the Nusselt number in both the laminar and transition regions:

$$Nu = C\ Re^a Pr^b \left(\frac{T_w}{T_b}\right)^n \left(1 + \frac{\alpha}{(L/D)}\right) \tag{6.24}$$

where:

	In the laminar region	In the turbulent region
C	0.214	0.0208
a	0.38	0.8
b	0.40	0.4
n	0	-0.558
α	34.8	6.2

From their experimental data, it was observed that the transition between turbulent and laminar flow could follow two lines: one was a prolongation of the turbulent regime into the transition region, and the other was a prolongation of the laminar regime. The laminar-transition line is less stable than the turbulent-transition one. The change between laminar and turbulent flow appears to depend on gas temperature and Reynolds number. An increase in either of these parameters may lead to a change from laminar to turbulent flow, as also may an increase in L/D. This change may be accompanied by a step in the longitudinal wall-temperature profile.

Dalle Donne and Bowditch proposed that a logical way to represent results in the transition region is to interpolate between values predicted by the laminar- and turbulent-flow equations. Two methods were employed for this correlation. The first method used Eq. 6.24 and the laminar-flow coefficients for the laminar-transition region and the turbulent-flow coefficients for the turbulent-transition region. Even though this method predicted the data for the transition region, there was no way to decide a priori whether the flow was turbulent or laminar, and considerable difference in the predicted Nusselt number was obtained. The range of Reynolds number values at which transition occurs is 3000-5000. The second method used to correlate results is to perform a linear interpolation for the coefficients of Eq. 6.24 in the range of $3000 \leq Re \leq 5000$. The interpolating was effected on CRe^a rather than on C and "a" separately, because a monotonic function could not be obtained due to the high numerical values of the Reynolds number. This method predicted the data in the transition region within +15% and -35%. Predictions using Eq. 6.24 were within ±12% for the turbulent region and ±15% for the laminar region.

McEligot, Ormand, and Perkins[64] presented the results of a semitheoretical and experimental investigation of the heat-transfer and frictional effects in air, nitrogen, and helium in steady flow in the downstream region of round tubes. They found that their data could be represented within 5% by the Dittus-Boelter correlation for heating (Eq. 6.11), with the premultiplier changed slightly (from 0.023 to 0.021) for flow at Reynolds numbers above 4000. Low-temperature-difference experiments confirmed that the equation could be used down to Re = 2500. Moderate ($T_w/T_b < 2.5$) and large-temperature-gradient ($T_w/T_b > 2.5$) heating decreases the local heat-transfer parameter $Nu_x/Pr^{0.4}$ and the local friction factor in comparison with small-temperature-difference behavior at the same Reynolds number. For moderate heating rates, the constant-property Nusselt number should be multiplied by $(T_w/T_b)^{0.5}$.

McAdams[56] states that data for the transition region are inadequate for gases even for low temperature differences. At high temperature differences, the heat transfer is complicated by the superimposed effects of natural convection and by the effect of L/D in the turbulent region. For liquids in a tube with a uniform wall temperature, $L/D > 60$, and small temperature difference, McAdams presents the following equation developed by Hausen:

$$Nu = 0.116\ [Re^{2/3}-125](Pr)^{1/3}\left(\frac{\mu}{\mu_w}\right)^{0.14} \tag{6.25}$$

Severyanin[60] presented the following correlation for the Nusselt number:

$$Nu = 0.7\ Re^{0.5}\ Pr^{0.4}\ \xi\ ,\ 2600 < Re < 6500 \tag{6.26}$$

where ξ is a correction factor ≤ 1 for impingement angles.

6.1.3 Mixed Convection

Buoyancy forces, which result from temperature differences, create fluid flows and are always present in forced-flow heat transfer. Usually they are of a smaller order of magnitude than the external forces that produce forced flow and may be neglected. Mixed convection is defined as that situation in which both free and forced convection are important. Systems in which the two sets of forces act in the same direction (e.g., a heated upward flow or a cooled downward flow) are termed "aiding" flows; those in which they act in opposition are termed "opposing" flows.

McAdams[56] (page 233) gives the following equation developed by Martinelli and Boelter[65] for laminar-flow mixed convection in vertical tubes having uniform wall temperature:

$$Nu = 1.75F_1\sqrt[3]{\frac{WC_p}{kL} \pm 0.0722\ F_2\left[\frac{D}{L}\ Gr_d\ Pr\right]^n_w} \tag{6.27}$$

where:

$n = 0.75$ or 0.84

w = mass flow rate of fluid, lb_m/h

The negative sign is used in Eq. 6.27 for opposing flows, the positive sign for aiding flows.

The Grashof number is based on diameter and initial temperature difference, which is positive for both heating and cooling. The factors F_1 and F_2 are dimensionless variables that are unique functions of a parameter Z, defined as:

$$Z = \frac{t_o - t_i}{t_2 - 0.5\ (t_o + t_i)} \tag{6.28}$$

where:

t_i = fluid inlet temperature, °F

t_o = fluid outlet temperature, °F

t_w = tube wall temperature, °F

The variables F_1 and F_2 as a function of Z are given in Fig. 6.3.

Eckert and Diaguila[66] discussed the mixed-flow convective heat transfer in circular tubes for both aiding and opposing flow. They also measured the local heat-transfer coefficients for air in a short (L/D = 5), vertical, steam-heated tube. The results of the tests revealed that the whole flow regime, as characterized by its Reynolds and Grashof numbers, could be divided into a forced-flow, a free-flow, and a mixed-flow regime. Heat-transfer coefficients in the forced-flow and free-flow regimes can be calculated with established relations; for the mixed-flow regime, coefficient values are presented in figures. Only the opposing-flow information will be discussed here.

Data on the local Nusselt number (Nu_x) for free convection were plotted against the local Grashof-Prandtl number. Superimposed on this plot were the turbulent forced-convection local Nusselt numbers for various local Reynolds numbers (Re_x). The characteristic dimension was the distance x from the lower end of the heated tube. From this plot, it was observed that the curves with constant Reynolds number tend, for large Grashof-Prandtl numbers, to converge asymptotically toward the free-convection mean-data line. This approach is more gradual than for the case of aiding flow. The limit of the pure free-convection regime is found from a line located 10% above the free-convection mean-data line into which the curves for constant Re_x are assumed to converge. This limit between free and mixed flow is expressed by:

$$Re_x = 18.15(Gr_x Pr)^{0.33} \tag{6.29}$$

The corresponding limit for pure forced flow could not be determined, because the velocity range of the investigation was not sufficient to determine the 10% limit. One problem with opposing flow is the difficulty of determining from which end of the tube the length parameter should be measured. For downward flow in a heated tube, the boundary layers start at the upper end and increase in thickness in the downward direction. Hence, the length parameter should be measured from the fluid-inlet end of the tube.

The heat-transfer coefficients found in the opposing-flow experiments were up to twice the magnitude of values calculated for pure forced-flow or free-flow convection. It might have been expected that the free- and forced-convection forces, acting in opposite directions, would tend to cancel each other partially and so reduce the heat-transfer coefficients to values less

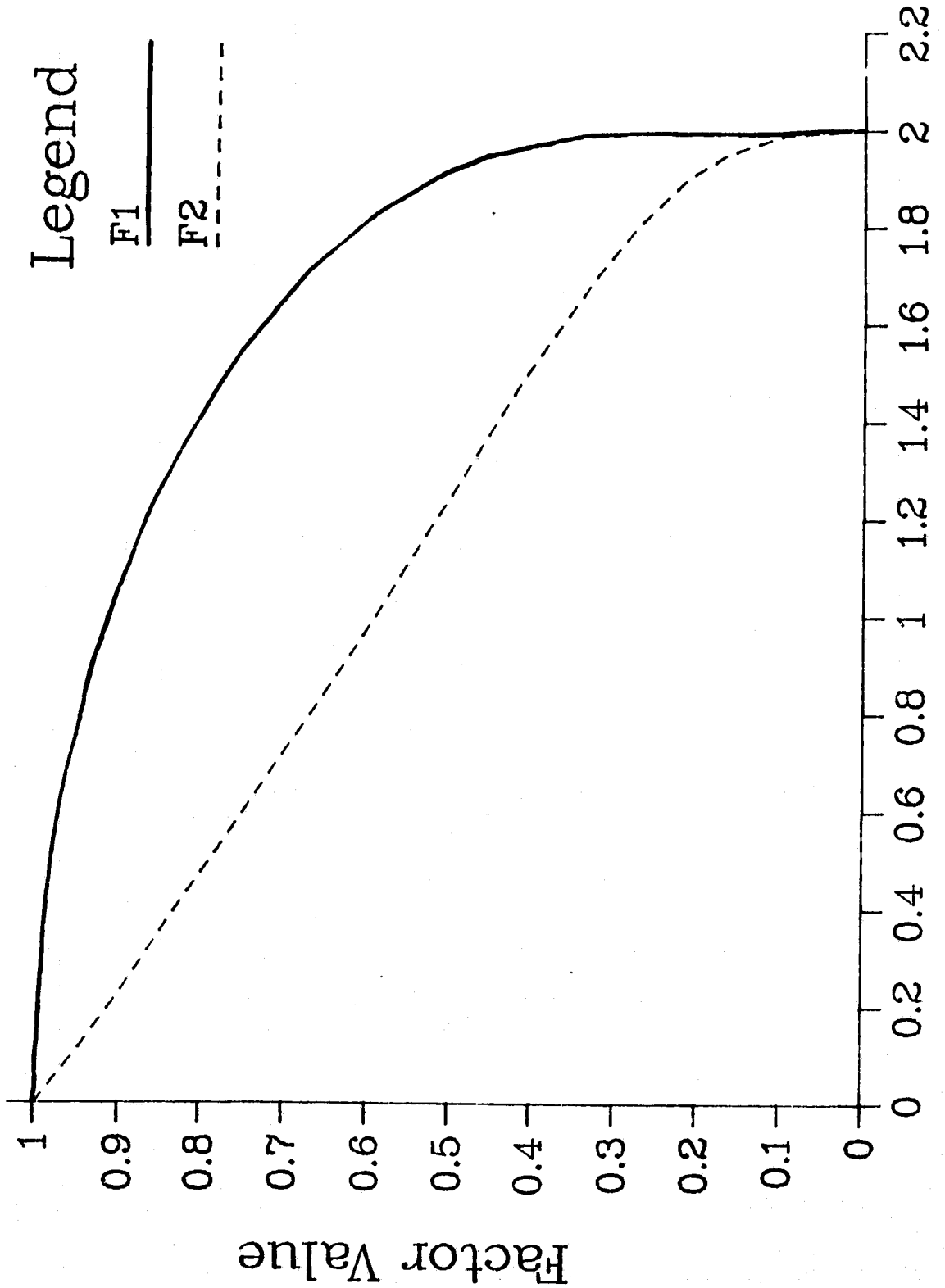

Fig. 6.3 Factors F_1 and F_2 to be Used in Eq. 6.27

than those for pure free-flow or forced-flow conditions. The large heat-transfer coefficients actually found probably resulted from an increased turbulence, which is very likely where the flow in the central core of the tube tends to move opposite to the flow in the heated boundary layers near the wall.

Eckert and Diaguila used Eq. 6.27 (with $F_1 = F_2 = 1$ and $n = 0.75$) to evaluate the limit between forced laminar flow and mixed flow. This limit, based on the stipulation that the mixed-flow Nusselt numbers exceed the forced-flow values by 10%, is expressed by:

$$Re = 0.386 \quad Gr^{3/4} \; Pr^{-1/4} \left(\frac{L}{D}\right)^{1/4} \tag{6.30}$$

In this equation both the Reynolds number and Grashof number are based on the tube diameter.

Heat-transfer experiments were conducted by Axcell and Hall[67] for turbulent downflow of air in a 26-in. long heated test section installed in a vertical 24-in. diameter pipe that was 116 ft high. The forced-flow Reynolds number varied from 20,000 to 130,000. The measured Nusselt number was normalized by the Nusselt number (Nu_o) calculated from Eq. 6.16 and then compared with the following correlation proposed by Fewster and Jackson[68] for opposing flows of water:

$$\frac{Nu}{Nu_o} = \left[1 + 4500 \; \overline{Gr} \; Re^{-21/8} \; Pr^{-1/2}\right]^{0.31} \tag{6.31}$$

where:

$$\bar{Gr} = \frac{\rho_b(\rho_b - \bar{\rho})GD^3}{\mu^2}$$

$$\bar{\rho} = \frac{1}{(T_w - T_b)} \int_{T_b}^{T_w} \rho \, dT$$

For an ideal gas, $\bar{Gr}$ and Gr are related by:

$$\frac{\bar{Gr}}{Gr} = \left(\frac{T_w}{T_w - T_b}\right)\left[1 - \frac{T_b}{(T_w - T_b)\ln(T_w/T_b)}\right] \tag{6.32}$$

Equation 6.31 reduces to the normal forced-flow convection equation for small values of $\bar{Gr} \; Re^{-21/8} \; Pr^{-1/2}$. At large values of this parameter, Nu also becomes independent of Reynolds number.

From the experimental data, it was observed that, for turbulent flows in which the forced and free components acted in opposition, heat-transfer coefficients were considerably higher than predicted for either component acting alone. This behavior is in contrast with that of non-turbulent flows, in which such a situation leads to a reduction in heat-transfer coefficient. It is believed that the increase in heat-transfer coefficients is a consequence of the changes in turbulence production caused by the modification of the shear stress distribution in the fluid by buoyancy forces. It was also observed that the experimental Nusselt number ratios exceeded those predicted with Eq. 6.31 by 20 to 25%.

6.2 RADIATIVE HEAT TRANSFER

Radiative heat transfer between bodies depends on their temperature, their surface characteristics, their shapes, their geometrical relationship, and whether the medium separating the bodies is a participating or nonparticipating medium. (A participating medium is one that may absorb, emit or scatter radiation.) Radiative heat transfer is a complicated process, and certain simplifying assumptions will be made. Surfaces will be considered to be diffuse (i.e., the absorptance or emittance characteristics of the surface will not vary with wavelength). Gases will be considered to be nonluminous (i.e., absorption or emission is by the gas mass itself and not by particles -- such as soot -- that may exist in the gas and radiate in the visible-light spectrum at high temperatures). The gas will also be gray (its emissivity and absorptivity will not vary with wavelength).

Elementary gases such as hydrogen, nitrogen, oxygen, and dry air are transparent to thermal radiation at temperatures met in most industrial applications. Complex gases such as water vapor, carbon dioxide, carbon monoxide, sulfur dioxide, ammonia, hydrogen chloride, alcohol, and hydrocarbons absorb and emit radiation significantly at certain wavelengths. Conversely, if such complex gases are heated, they radiate in the same wavelength bands. In order to treat radiation from nonluminous gas, the use of gas emissivities as presented by Hottel[69] (page 82), by Hottel and Sarofim[70] (page 225), or in Ozisik[57] (page 388) will be employed.

Emissivities for CO, CO_2, H_2O, etc. at a total pressure (P_T) of one atmosphere are presented as a function of temperature and the product P_iL, where P_i is the partial pressure (in atmospheres) of component i of a gas mixture, and L is the beam length in ft. For a gas with a total pressure greater than 1 atm, correction factors are given to adjust the emissivities obtained at 1-atm pressure. The emissivity charts are for a hemispherical gas mass of radius L, at a temperature T_g, radiating to a black surface located at the center of the base of the hemisphere; the emission of radiation from the hemispherical gas mass to a unit area at the center of the base of the hemisphere is expressed as

$$Q_r = \varepsilon_g \sigma T_g^4 \tag{6.33}$$

where:

Q_r = radiative heat transfer by gas, Btu/h

T_g = gas temperature, °R

ε_g = gas emissivity

σ = Stefan-Boltzman constant = $1714 \times 10^{12} \frac{\text{Btu}}{\text{h-ft}^2\text{°R}}$

To predict gas emissivities for shapes other than a hemisphere, an equivalent mean-path length is used in place of the beam length. Equivalent path lengths for various gas geometries are presented in the references cited.

When carbon dioxide and water vapor are present together in a gas mass, the emissivity of the mixture is somewhat less than that obtained by adding the individual emissivities for carbon dioxide and water vapor. This decrease in emissivity results from the mutual absorption of radiation. Correction factors for mutual absorption are also given.

The radiation absorbed by a gas mass from a black surface of area A and at a temperature T_s is

$$Q_r = A \alpha_g \sigma T_s^4 \tag{6.34}$$

where:

A = surface area, ft^2

T_s = surface temperature, °R

α_g = gas absorptivity evaluated at T_s

Although the gas absorptivity must equal its emissivity when $T_s = T_g$, as T_g increases above T_s, the absorptivity is affected by temperature in two ways: the molecular-absorption coefficient of the gas increases somewhat, but the number of absorbing gas molecules in a fixed path length at a fixed partial pressure decreases. To allow for these effects, α_g is equal to $(T_g/T_s)^a$ times the gas emissivity evaluated at T_s and at P_iL (T_s/T_g) instead of P_iL. The value of "a" is 0.5 (except for carbon dioxide and water vapor, which have values of "a" equal to 0.65 and 0.45, respectively). The same correction factors for pressure and mutual absorption apply.

Hence, for a gas enclosed by a black surface, the net radiative-heat exchange is given by:

$$Q_{gs} = A(\varepsilon_g T_g^4 - \alpha_g T_s^4) \tag{6.35}$$

where:

Q_{gs} = net radiative heat exchange, Btu/h

For an enclosure without black surfaces, the net radiative heat transfer is more complicated; see Ref. 70 or other similar books on radiative heat transfer.

6.3 HEAT TRANSFER WITH PULSATING FLOW

Pulsating flow and acoustic vibrations have been reported as increasing, decreasing, or having no effect on heat transfer.

West and Taylor[71] investigated the effect of partially damped pulsations from a reciprocating pump on the heat-transfer coefficients for water flowing at steady-flow Reynolds numbers of 30,000 to 85,000 inside tubes used for both heating and cooling. Water from the pump passed through a vertical cylindrical tank containing an adjustable air volume so that the degree of pulsations could be varied. The water then passed through a calming section and into a 2-in. steam-heated pipe. From the heater, the water was circulated through a 2-in. pipe that was water-cooled. A pulsation ratio was defined as the ratio of maximum air volume to minimum air volume in the cylindrical tank over the cycle of one pulsation. This also would be the ratio of the maximum to the minimum absolute pressures in the tank if the air temperatures were the same. A plot of the ratio of the heat-transfer coefficient with pulsations to that predicted for steady flow, as a function of pulsation ratio, is given. The heat-transfer-coefficient ratio increases slowly for pulsation ratios <1.1, rises more rapidly to a maximum of 1.6-1.7 at a pulsation ratio of 1.42, and then declines for higher pulsation ratios. The authors drew a smooth curve through their data, but it is obvious that the data are cyclic. One set of data shows a decrease in the coefficient ratio for a pulsation ratio of <1.1.

Morrell[72] developed an empirical method for calculating heat-transfer rates in resonating gaseous flow in a pipe, based on the following assumptions: 1) The perturbations are sufficiently similar to shocks that the one-dimensional pressure-velocity relations for normal shock waves can be used; 2) the usual Staton-number/Reynolds-number/Prandtl-number relation applies to both resonance and steady flow, provided suitable average conditions behind the shock are selected; and 3) the effect of aerodynamic heating due to the oscillations can be treated as a correction to the quasi-steady-state solution. A ratio of resonant heat transfer to steady-state heat transfer (based on the Dittus-Boelter equation for turbulent flow) was defined. Typical curves of this ratio as a function of a pressure ratio (ratio of maximum pressure behind the shock to the steady-state pressure) for several values of

Mach number and temperature ratio (ratio of maximum temperature behind the shock to the steady-state temperature) were given. From these curves, it could be seen that the heat-transfer ratio increases rapidly with pressure ratio. The temperature ratio has only a small effect on the heat-transfer ratio. Increasing Mach numbers cause a significant decrease in the heat-transfer ratio. These results appear most applicable to the conditions in a rocket engine with large-amplitude resonant burning.

The effects of acoustic vibrations on the free- and forced-convection heat transfer to air in a constant-temperature vertical tube were investigated by Jackson, Harrison, and Boteler.[73] The Nusselt number (hD/k), based on the log mean temperature difference, ranged from 17.2 to 50.6; the Graetz number (WCp/kL), based on the bulk or average air temperature, ranged from 40.2 to 1633; and the Grashof-Prandtl-D/L modulus

$$\left(\frac{gD^3\beta(t_w-t_o)\rho^2}{\mu^2}\right)\left(\frac{Cp\mu}{k}\right)\frac{D}{L}$$

based on the properties of air at the wall temperature ranged from 0.967×10^5 to 1.26×10^6, where:

C_p = constant-pressure specific heat, Btu/lb_m-°F

D = tube diameter, ft

g = gravitational acceleration, ft/h^2

h = heat-transfer coefficient, Btu/h-ft^2-°F

k = thermal conductivity, Btu/h-ft^2-°F

L = tube length, ft

t_o = entering fluid temperature, °F

t_w = wall temperature, °F

W = mass flow rate, lb_m/h

β = coefficient of volumetric expansion, $°F^{-1}$

μ = absolute or dynamic viscosity, lb_m/ft-h

ρ = density, lb_m/ft^3

The test section was a 5-ft long steam-heated vertical tube with a 3.75-in. inside diameter. Standing sound waves were imposed on the air flow by a speaker driver equipped with a 12-in. long exponential horn. The horn was

mounted in the inlet air plenum at the base of the tube. The optimal position of the driver and horn was found by raising and lowering the horn at a given frequency and power input until the position of maximum sound level was reached. The optimal position is a function of frequency, which influences the extent of acoustic coupling between the air in the experimental horn and the air in the tube. For this study, the optimal position was found for a frequency near the middle of the range studied, and the driver was left at that same position for the entire series of tests.

The complexity of the free convection, forced convection, and acoustic effects precluded a simple analysis and understanding of the heat-transfer phenomenon. However, the Nusselt number was obtained at distances along the tube for a frequency of 520 Hz, a Graetz modulus of approximately 80, a Reynolds number of about 2300, and sound levels from 108.2 to 128.9 dB. The Nusselt number was observed to decrease in the first 3 in. of the tube, increase to a maximum in the 6-12 in. range of tube length (depending on the sound level), and then decrease with increasing distance from the tube entrance. The data were compared with the following equation that the authors derived from a previous investigation of aiding-flow mixed convection:

$$Nu_{lm} = 1.128\sqrt{\left(RePr\,\frac{D}{x}\right)_b + \left[3.02\,Pr\left(GrPr\,\frac{D}{L}\right)\right]_w^{0.4}} \qquad (6.36)$$

where:

L = total length of heated section, ft

Nu_{lm} = Nusselt number based on the log mean temperature difference

x = distance from start of heated length, ft

b indicates properties are evaluated at the bulk fluid temperature.

w indicates properties are evaluated at the wall temperature.

Albeit aiding-flow mixed convection was not covered in Sec. 6.1.3, the authors found that Eq. 6.36 gave a better fit to their data than did Eq. 6.27, which predicted too low a value for the Nusselt number.

For sound-pressure levels above 118 dB, the experimental Nusselt numbers approximate that for the uniform-velocity profile without free convection. This may mean that sound, by introducing acoustic circulation, destroys the free-convection effects. The Nusselt number can be predicted by the following equation, which is valid within ±16% of the experimental data:

$$Nu = 5.7\left[\frac{e^{SPL/69.5}}{Re^{0.25} f^{0.125}}\right](Gz_x)^{1/2} \qquad (6.37)$$

where:

f = frequency, Hz

G_{zx} = Graetz number based on length "x"

SPL = sound-pressure level, dB relative to 10^{-16} W/cm^2

Below 118 dB, sound apparently has little effect on heat transfer and Eq. 6.36 may be used to determine the heat-transfer coefficient.

Lemlich and Hwu[74] have compiled a brief survey of studies not reviewed by this author, and this information will be presented here:

- Martinelli, Boelter, Weinberg, and Yakabi found little if any improvement in heat transfer to water flowing at Reynolds numbers from 1000 to 10,000 when subjected to pulsations varying from 0.22 to 4.4 Hz.

- Marchant used pulsations of 0.17, 0.42, and 1 Hz with water at Reynolds numbers of 400 to 100,000 and found some improvement in heat transfer in the laminar region but virtually no improvement at higher flow rates.

- Shirotsuka found a considerable improvement in heat tranfer to water flowing at Reynolds numbers of 3000 to 22,000 when pulsations of 1.7 to 8.3 Hz were applied.

- Linke and Hufschmidt reported considerable improvement, particularly in the laminar region, for pulsations applied to oil.

- Robinson reported some increase in heat transfer for ultrasonic vibrations of 400,000 Hz applied to flowing water.

- For air, at Reynolds numbers of 5000 to 35,000 and pulsations of 5 to 40 pulses/s, Havemann found an irregular decrease in heat transfer below a certain critical frequency, determined by the waveform, and an irregular increase above it.

- Mueller used frequencies of 0.038 and 0.025 Hz for air Reynolds numbers from 53,000 to 77,000 and obtained decreases in heat transfer. The decrease was explained in terms of the pulsations being below some critical level of disturbance and hence in the quasi-steady region.

For their experimental study, Lemlich and Hwu[74] measured the heat-transfer coefficient for air flowing in a horizontal steam-heated tube at Reynolds numbers of 560 to 5,900 with imposed resonant frequencies of 198, 256, and 322 Hz, as well as some nonresonant frequencies. The heated section was a 25-in. long copper tube with a 0.745-in. inside diameter. Vibrations were imposed by an electromagnetic driver connected to an 8-in. long tubular section. The driver was actuated through a 20-W audio amplifier by a variable sinusoidal audio-signal generator. The amplitude of vibration within the tube was characterized by measurements in the local pressures along the tube length. Resonant vibrations were found to increase the Nusselt number by as much as 51% for the laminar-flow region (Re < 2100) and by as much as 27% for the region where Re > 2100. The improvement in heat transfer peaked sharply at resonance and generally increased with both amplitude and resonant frequency. Improvement in heat transfer is believed to result from a dual mechanism of contributory disturbance, the first contribution being the vibration itself and the second its effect as a turbulence trigger. Attempts to develop a simple overall correlation proved unsuccessful; the differences between laminar and turbulent flow, as well as the complicated nature of the interaction among variables in the neighborhood of Re = 2100, are too involved. The following equations were proposed for the ratio of vibrating-mode to steady-mode Nusselt numbers, where the steady-mode Nusselt numbers were measured values that were shown to agree with those predicted by the Dittus-Boelter equation for Re > 4000:

For Re < 1500,

$$\frac{Nu_v}{Nu} = 1 + 1.3 \times 10^{-6} (P_m f)^2 \qquad (6.38)$$

For Re > 2500,

$$\frac{Nu_v}{Nu} = 1 + 0.047(P_m f^3/Re^2)^{0.8} \qquad (6.39)$$

where:

f = frequency, Hz

Nu_v = Nusselt number with vibration

P_m = root-mean-square pressure, lb_f/ft^2

Note that these equations are dimensional.

Heat transfer from premixed propane/air flames to the water-cooled walls of a 5-in. inside diameter ramjet-type burner was studied by Zartman and Churchill[75] with and without flame-generated sonic oscillations. With this test equipment, intense longitudinal and transverse waves could be attained over a reasonable range of flows, transverse oscillations could be varied in intensity by the use of different flameholders and propane/air ratios, and longitudinal oscillations could be damped. Tests were conducted for Reynolds numbers from 35,000 to 48,000 and fuel/air equivalence ratios of 0.57 to 1.03. The flame-generated oscillations were measured with a microphone mounted flush with the inside tube surface at 22-in. from the exit. Frequency and amplitude measurements revealed that both transverse and longitudinal waves are resonant. The screeching flame, due to transverse oscillations, produced a sound level of 151 dB with a dominant frequency of 4150 Hz, as compared to 130 dB with no dominant frequency for the quiet flame. The heat-flux density was observed to be about 60% greater in the presence of this resonant oscillation. With longitudinal oscillations, an increase in sound level from 130 to 155 dB occurred along with a 73% increase in heat flux.

The ratio of the resonant-oscillation heat-transfer coefficient to that for a quiet flame (130 dB) can be expressed as:

$$\frac{h_o}{h} = 0.044 \frac{P_o}{P} + 1.08 \qquad (6.40)$$

where:

h = heat-transfer coefficient for a quiet flame, Btu/h-ft^2-°F

h_o = heat-transfer coefficient for resonant oscillation, Btu/h-ft^2-°F

P = sound-pressure amplitude for a quiet flame, lb_f/ft^2

P_o = sound-pressure amplitude for resonant oscillation, lb_f/ft^2

Thus, the heat-transfer coefficient for resonant oscillation appears to be independent of the resonant frequency; longitudinal (organ-pipe) oscillations are just as effective as transverse (screeching) oscillations.

The resonant oscillations may produce the observed changes in the heat-transfer coefficient by either or both of two mechanisms: changes in the combustion process (e.g., in flame speed, flame shape, and combustion efficiency) and changes in the dynamics of the hot-gas stream downstream from the flame (e.g., in boundary-layer thickness and intensity of turbulence). Similarity in the temperature profiles and the relative invariance of the combustion

efficiency suggest that fluid-dynamic effects, rather than combustion and thermal effects, are primarily responsible for the changes in heat flux.

Applying the quasi-steady-state concept (i.e., the heat-transfer coefficient at any instant can be predicted from the fluid velocity at that instant by means of the steady-flow relationship between heat-transfer coefficient and velocity), Baird, Duncan, Smith, and Taylor[76] presented the following equation for the ratio of the pulsating to the steady-flow heat-transfer coefficient:

$$\frac{h_p}{h_s} = \frac{(2\pi)^{n-1} \int_o^{2\pi} V^n \, d(\omega t)}{\left(\int_o^{2\pi} V \, d(\omega t) \right)^n} \tag{6.41}$$

where:

h_p = pulsating heat-transfer coefficient, Btu/h-ft^2-°F

h_s = steady-flow heat-transfer coefficient, Btu/h-ft^2-°F

n = a constant

V = instantaneous flow velocity, ft/s

t = time, s

ω = angular frequency = $2\pi f$, s^{-1}

For the case of sinusoidal pulsations of amplitude A and frequency ω, the instantaneous velocity V is expressed by:

$$V = V_m (1 + B \cos \omega t) \tag{6.42}$$

where:

$B = \omega A / V_m$ = pulsation velocity (dimensionless)

V_m = mean velocity, ft/s

A = pulsation amplitude, ft

When the expression for instantaneous flow velocity given as Eq. 6.42 is substituted into Eq. 6.41, the following equation results:

$$\frac{h_p}{h_s} = \frac{1}{2\pi}\int_0^{2\pi} |1 + B\ \mathrm{Cos}(\omega t)|^n\ d(\omega t) \qquad (6.43)$$

The absolute value, $|1 + B\ \mathrm{Cos}(\omega t)|$, is used because when $B > 1$, reverse flow occurs for part of the cycle and the heat-transfer coefficient must remain real and positive in the reverse-flow period. Normally, $n < 1$. Thus, when $B < 1$, Eq. 6.43 predicts a decrease in the heat-transfer coefficient due to flow pulsations. Equation 6.43 cannot be solved analytically, but it has been solved numerically.

The effect of large flow pulsations on heat transfer was investigated by Baird et al.[76] for water flowing upwards in a 0.75-in. inside-diameter tube that was steam-heated. Sinusoidal pulsations were produced by means of an air pulser connected to the water line. Pulsations of 0.8 to 1.7 Hz could be obtained, and pulse amplitudes of 0.09 to 1.1 ft were achieved. Without pulsations the Nusselt numbers, for Reynolds numbers from 5000 to 50,000, were correlated by:

$$Nu = 8.4\ Re_m^{0.25} \qquad (6.44)$$

where:

Re_m = Reynolds number based on mean velocity.

This equation gives a substantially lower result than the Dittus-Boelter relation for the water-side heat-transfer coefficient because of a low condensing-steam coefficient. However, Eq. 6.44 was retained for comparison with the pulsating-flow coefficients, which were obtained for the range $4300 < Re_m < 16{,}200$. The experimental ratios of h_p/h_s agreed approximately with those obtained from Eq. 6.43 for $n = 0.25$ and $B > 2.5$. The maximum h_p/h_s ratio was 1.41 for a value of $B = 7$. The best empirical correlation for h_p/h_s was found to be:

$$\frac{h_p}{h_s} = 0.96 + 0.0077\ B(Re_m)^{0.25} \qquad (6.45)$$

The experimental values of h_p/h_s did not fall below unity for low values of B (as predicted by Eq. 6.43). This effect may have resulted from some of the eddies generated at peak velocities persisting during the slower parts of the cycle.

The experimental heat-transfer study by Reay[32] is discussed in Appendix E. Heat-transfer coefficients were measured in a water-cooled Schmidt tube fired with town gas. In general, the experimental heat-transfer coefficients were higher than the calculated steady-state values based on a turbulent-flow correlation. The variation of the heat-transfer coefficient along the burner

was oscillatory, and in some cases the value of the coefficient fell below the predicted steady-flow values.

Hanby[41] used the quasi-steady-state theory to assess the effect of pulsations on the heat-transfer coefficient in a propane-fired pulse combustor. This work is also described in Appendix E. Equation 6.43 was used to correlate the experimental data with a value of n = 0.8, and the results are shown in Fig. 6.4. The standard deviation of the data from the predictions of Eq. 6.43 was 5%, and the maximum deviation was 20%. A slight initial decrease in the h_p/h_s ratio was obtained, as predicted by Eq. 6.43. The highest measured value of h_p/h_s was about 2.4 for B = 4.8.

Experiments were conducted by Mamayev, Nosov, and Stromyatnikov[77] with air flowing vertically upward at Reynolds numbers of 540-11,000 inside an electrically heated pipe (3.1-in. inside diameter, 26.2-ft long) with pulsation frequencies of 5 to 24 Hz. The experiments were conducted at a constant heating rate of 341 Btu/h. Without pulsations, the measured heat-transfer coefficients were correlated by:

$$\text{Laminar Flow:} \quad Nu = 0.21\ Re^{0.4} \tag{6.46}$$

$$\text{Turbulent Flow } (Re \geq 8000): \quad Nu = 0.021\ Re^{0.8} \tag{6.47}$$

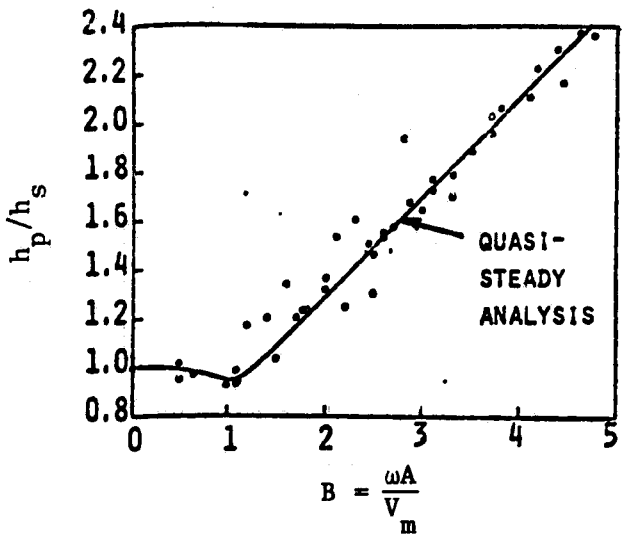

Fig. 6.4 Ratio of Pulsating to Steady-State Heat-Transfer Coefficient as a Function of a Dimensionless Pulsation Velocity (Source: Ref. 41)

For laminar flow with frequencies > 2 Hz, the h_p/h_s ratio rises steeply as the Reynolds number is increased until a critical value, depending on frequency, is reached; the ratio then declines rapidly. As the frequency is increased, the critical Reynolds number is reached at lower values and is indicative of flow transition. For frequencies $\leq$ 2 Hz, the h_p/h_s ratio is less than 1. As the frequency is increased from 5 to 24 Hz, the h_p/h_s ratio increases and the highest value (1.44) is obtained at a frequency of 12 Hz. As the frequency is increased to between 20 and 24 for a constant Reynolds number, the h_p/h_s ratio decreases. For Reynolds numbers beyond its critical value, the h_p/h_s ratio drops steeply and then levels off towards unity for frequencies of 0.5 to 11 Hz, but drops below unity for frequencies $\geq$ 20 Hz. Apparently at frequencies of 20 to 24 Hz, the forced fluctuations somewhat damp out the high-frequency turbulent fluctuations.

Ahrens[78] described the development of a thermal model, based on the quasi-steady-state approach reported by Baird et al.[76] and Hanby,[41] for prediction of the performance of a Helmholtz-type pulse combustor. Some preliminary heat-transfer results are presented. This work was the basis for the computer program described in Appendix C.

The studies of Dhar et al.[30] are described in Appendix E for single- and dual-chamber, natural-gas-fired, Helmholtz-type pulse combustors with a corebustor in the tailpipe. The authors found that the overall heat rate was 21.5% higher for pulse combustion than for steady burning. The percentage of heat transferred in the corebustor region was 63.4% for pulse combustion and 62.1% for steady burning. The average overall heat-transfer coefficient in this region was 10.98 Btu/h-ft^2-°F for pulse combustion and 9.68 Btu/h-ft^2-°F for steady combustion (a 13.5% increase under pulsating conditions).

Alhaddad and Coulman[55] measured the heat-transfer coefficient for a natural-gas-fired, Helmholtz-type pulse combustor. The burner consisted of a 4-in. schedule (sch) 40, 12-in long combustion chamber, a 1 1/2-in. sch 40, 71-in. long tailpipe and a 12-in. inside-diameter cylindrical exhaust-decoupling chamber that was 12-in. long and had a 1 1/2-in. sch 40 exhaust pipe. A set of gas orifices allowed the heat-input rate to be varied from 20,300 Btu/h to 65,000 Btu/h. The mean Reynolds number ranged from 2432 to 7892, the pressure was ±0.9 psig, and the burner frequency range was 45-60 Hz. The heat-transfer coefficient was determined from exhaust-gas, wall, and room temperature measurements and the computed heat loss to the room by free convection. These temperature measurements were taken at the mid-length of the combustion chamber, 7 in. and 49 in. from the tailpipe entrance. The authors found that the pulsation amplitude was the main parameter affecting the heat-transfer coefficient. In the range of Reynolds numbers studied, the heat-transfer coefficient decreased as the Reynolds number increased. The ratio of h_p/h_s ranged from 0.20 to 0.80, where h_s was calculated for laminar flow by Eq. 6.8 with a viscosity multiplier, by Eq. 6.25 for turbulent flow, and by an equation given in McAdams[56] for mixed-convection laminar flow in a horizontal tube. The authors conclude that the h_p/h_s ratio of less than unity

is consistent with the idea that the main resistance to the flow of heat from the fluid is in the viscous sublayer adjacent to the wall.

Several concerns arise over this study. The method of measuring the heat loss from the burner is subject to large errors. Wall and gas temperatures are difficult to measure accurately. The use of unshielded thermocouples could result in significantly lower gas-temperature measurements, as will be discussed in Sec. 6.5.1. The equation for laminar-flow heat transfer (Eq. 6.8) can result in errors of up to 250% at large diameters and temperature differences, according to McAdams[56] (page 237). Alhaddad's and Coulman's equation for turbulent flow (Eq. 6.25) is listed by McAdams for the transition region, and its accuracy is questionable. The equation for mixed convection was based on data for petroleum oils with Prandtl numbers ranging from 140 to 15,200 (see page 235 of McAdams); its use for gases is highly questionable.

Severyanin[60] states that oscillations in gas velocity intensify heat transfer in the laminar-flow regime by 100-300% and in the turbulent regime by 20-30%, compared to heat transfer with steady-state flow conditions.

From all these studies, it appears that pulsating flow enhances heat transfer, but conditions exist where it can cause decreases. The frequency range of most of the studies lies either below or above the normal operating frequencies of pulse combustors. Heat-transfer investigations with pulse combustors are few, and the data conflict. Therefore, more detailed studies are needed.

6.4 HEAT-TRANSFER MEASUREMENTS

For each of the 54 cooling channels on the ANL experimental pulse combustion burner, the flow rate and the inlet and outlet temperatures of the water were measured. The rate of heat removal from each channel was calculated from

$$Q_w = m_w C_p(t_o - t_i) \qquad (6.48)$$

where:

C_p = specific heat of water, 1 Btu/lb_m°F

m_w = mass flow rate of water, lb_m/h

Q_w = heat removed by the water, Btu/h

t_i = water inlet temperature, °F

t_o = water outlet temperature, °F

The data obtained from each test are presented in Appendix D (Figs. D.1-D.33). (Note that the straight lines connecting the data points do not have any special significance but were added only to clarify the trend of the data.) The surface area corresponding to the water-cooled part of the burner is 0.878 ft^2 for the combustion chamber and 1.656 ft^2 for the tailpipe. Axial heat transfer between cooling channels is negligible for parallel-flow operation, because any difference in the temperature of the water in adjacent channels will be small. For the series-flow arrangement, it is possible for the water temperature in two adjacent channels to be considerably different. However, the low thermal conductivity of the rubber O-rings between the channels minimizes the axial heat transfer between coolant streams. Table 6.2 indicates the total quantity of heat removed from the burner by the cooling water and the percentage of the heat input to the burner from combustion of the gas. This table also gives the amount of heat removed by the water from the combustion chamber and from the tailpipe, together with the corresponding percentages of the total heat transferred to the cooling water.

Table 6.2 Burner Heat-Transfer Data

		Heat Removed from Burner						
		Total		Combustion Chamber		Tailpipe		
Heat Input (Btu/h)	Air/Fuel Ratio	Btu/h	% of Input	Btu/h	% of Total	Btu/h	% of Total	Burner Configuration
32,887	13.21	27,227	82.8	13,134	48.2	14,093	51.8	Standard Burner
50,245	9.89	34,515	68.7	13,907	40.3	20,608	59.7	Standard Burner
54,194	12.48	40,447	74.6	16,679	41.2	23,768	58.8	Standard Burner
58,665	10.08	37,749	64.4	14,115	37.4	23,634	62.6	Standard Burner
95,458	11.89	55,044	57.7	19,627	35.7	35,417	64.3	Standard Burner
96,782	10.34	57,603	59.5	20,346	35.3	37,257	64.7	Standard Burner
97,464	7.90	44,773	45.9	17,076	38.1	27,697	61.9	Standard Burner
99,577	10.05	59,641	59.9	20,381	34.2	39,260	65.8	Standard Burner
100,215	9.89	62,130	62.0	23,547	37.9	38,583	62.1	Standard Burner
100,941	10.13	55,967	55.4	19,169	34.3	36,798	65.7	Standard Burner
101,713	9.87	63,642	62.6	24,242	38.1	39,400	61.9	Standard Burner
103,576	10.12	64,427	62.2	21,911	34.0	42,516	66.0	Standard Burner
194,371	9.38	101,260	52.1	32,541	32.1	68,719	67.9	Standard Burner
98,013	9.96	58,562	59.7	20,370	34.8	38,192	65.2	Insulated Standard Burner
53,589	12.50	30,910	57.7	13,340	43.2	17,570	56.8	No Flapper Valves
102,645	11.39	45,050	43.9	16,354	36.3	28,696	63.7	No Flapper Valves
50,418	10.02	38,476	76.3	16,216	42.1	22,260	57.9	Tailpipe Aspirator
98,620	9.60	64,844	65.8	22,356	34.5	42,480	65.5	Tailpipe Aspirator
53,116	11.03	42,320	79.7	18,794	44.4	23,526	55.6	Inlet Muffler
103,728	10.10	--	--	--	--	--	--	Inlet Muffler
101,532	10.09	66,122	65.1	22,688	34.3	43,434	65.7	Inlet Muffler
53,429	11.50	41,182	77.1	17,274	41.9	23,908	58.1	Exhaust Muffler
50,227	9.42	36,091	71.9	15,229	42.2	20,862	57.8	Inlet and Exhaust Mufflers
100,580	8.86	61,012	60.7	23,693	38.8	37,319	61.2	Inlet and Exhaust Mufflers
49,867	9.93	42,161	84.5	17,532	41.6	24,629	58.4	48-in-Long Corebustor
50,341	9.82	39,051	77.6	16,115	41.3	22,936	58.7	48-in-Long Corebustor
50,882	10.13	42,614	83.8	18,463	43.3	24,151	56.7	48-in-Long Corebustor
99,996	9.73	72,583	72.6	23,915	32.9	48,668	67.1	48-in-Long Corebustor
101,248	10.09	73,750	72.8	24,398	33.1	49,352	66.9	48-in-Long Corebustor
50,042	10.07	36,231	72.4	13,853	38.2	22,378	61.8	36-in-Long Corebustor
97,009	10.11	62,245	64.2	19,361	31.1	42,884	68.9	36-in-Long Corebustor
100,553	9.82	--	--	--	--	--	--	36-in-Long Corebustor
100,794	10.45	67,145	66.6	19,333	28.8	47,812	71.2	Air Decoupling Chamber

From the test data in Appendix D, it was found that in most cases the heat rate in the combustion chamber reached a maximum a few inches above the gas-supply tube head and then decreased as the exhaust gas funneled toward the tailpipe entrance. This decrease is associated with the recirculation region near the top of the burner (see Fig. 3.1 and discussion in Sec. 3.2). At the tailpipe entrance, the sudden contraction in diameter from that of the combustion chamber resulted in added turbulence and a corresponding increase in heat transfer for that region. The quasi-oscillatory pattern of increasing and decreasing heat-transfer rate along the burner is a real effect, not experimental error; this pattern was observed in all of our experiments. A phasing effect has also been observed (i.e., for similar burner conditions, the rise and fall in heat rate for the same cooling channel can be 180° out of phase). This oscillatory effect should not have been unexpected, given the pulsating nature of the gas flow. An examination of the data of West and Taylor[71] indicates an obvious oscillatory effect, even though the authors drew a smooth curve through their data. The heat-transfer-coefficient data of Reay[32] also display an oscillatory pattern. The frequency of the oscillations of the heat-transfer rate is much smaller than the firing frequency of the burner and may result more from the modulated pressure wave that was noted in Chapter 5. The increase in heat transfer at the tailpipe exit is attributed to the increased velocity of the combustion gases as they are accelerated toward the pressure node at the exit.

Even without the flapper valves, the burner operated somewhat as a pulse combustor, because the gas and air inlet holes functioned as an aerodynamic valve. The heat-transfer data are also oscillatory, as can be seen from Figs. D.15 and D.16. The pulsating and steady-flow heat-transfer rates are compared for pulse operation at 95,458 Btu/h heat input and an air/fuel ratio of 11.89 (Fig. D.5) and at 54,194 Btu/h heat input and an air/fuel ratio of 12.48 (Fig. D.3). From these data and the data in Table 6.2, the enhancement in total heat transfer is found to be 22% for a heat-input rate of approximately 99,000 Btu/h.

The heat-transfer rates from the combustion chamber and tailpipe were 20% and 23% higher, respectively, for pulsating operation. For this comparison the heat input to the burner under steady operation was 7.5% higher, so one may assume that the enhancement under pulsating conditions would have been slightly higher than the percentages listed. At a heat input rate of about 54,000 Btu/h, the total heat-transfer enhancement was 31%. The heat-transfer rates from the combustion chamber and tailpipe were 25% and 35% higher, respectively, for pulsating operation. Hence, these data confirm that pulse combustion does enhance heat transfer, albeit not by as much as might have been expected. These enhancement numbers are in agreement with those of Dhar et al.,[30] who obtained a 21.5% increase in the total heat transfer for pulse combustion with a Helmholtz-type combustor as compared with steady operation of the same burner.

Some observations on the heat-transfer data obtained in the ANL pulse combustion experiments are:

- As the heat input to the burner increases, the percentage of heat removal from the burner decreases.
- The percentage of heat removed in the combustion chamber decreases as the heat input increases.
- The use of a corebustor increases the heat removed from the burner.
- The 48-in.-long corebustor results in a 5 to 10% greater increase in heat removal than does the 36-in.-long corebustor.
- There is no significant difference in heat removal between the standard burner and one with both an inlet and an exhaust muffler installed, or an inlet decoupling chamber.
- Heat loss from the uninsulated burner is not significant.
- The high heat-transfer rates observed for gas entering the tailpipe result from the abrupt entrance.
- A sudden, low value of the local heat rate is probably caused by a partially blocked cooling channel.
- The burner heat transfer is slightly enhanced by the addition of a tailpipe aspirator.

Even though the use of a corebustor increased burner heat transfer, most of this increase occurred in the combustion chamber, not in the tailpipe (where it was expected). The 1-in.-diameter corebustor reduces the 1.75-in. diameter tailpipe to an equivalent diameter of 0.75 in. For the 50,000-100,000 Btu/h heat-input experiments, the estimated steady-flow Reynolds number of the combustion products in the tailpipe corresponds to the laminar and transition-flow regime. With equivalent mass flow and physical properties, the heat-transfer coefficient should increase by 50% when the corebustor is installed. Consequently, an increase in heat transfer from the tailpipe was to have been expected unless the gas-wall temperature difference had decreased proportionately. An examination of the experimental data does show a temperature decrease, due to the increase in combustion-chamber heat transfer, but the temperature difference alone should not fully account for the lack of an increase in tailpipe heat transfer. Turbulence effects associated with the corebustor and tube inlet should increase the heat-transfer coefficient. Radiative heat transfer from the hot gases accounts for approximately 10% of the total heat transfer in the standard burner. The addition of the

corebustor will reduce the radiative heat transfer from the gas, but this loss should be offset by the radiative heat transfer from the corebustor to the tailpipe wall. Conventional radiative and convective heat-transfer mechanisms cannot explain the failure of the corebustor to enhance the tailpipe heat transfer; the solution must be sought in the effect of pulsating flow on heat transfer. The corebustor may be suppressing pulsation effects in one of the directional modes to a greater extent than would be anticipated by its 17% reduction of the operating frequency. Another explanation may lie in the velocity-profile results of Belter,[38] which indicated that the greatest flow in a pulse combustor is at the duct walls and the lowest net flow is in the tube center, or the reverse of normal flow profiles. If the highest velocities do indeed occur adjacent to the tube wall, then a corebustor would not have a significant effect. An additional investigation of this phenomenon is required.

6.5 GAS-TEMPERATURE MEASUREMENTS

The temperature of combustion products was initially measured at two positions (3.5 and 7.5 in.) in the combustion chamber and 8 positions (12.5, 17.5, 18.5, 24.5, 30.5, 36.5, 42.5, 48.5, and 52.5 in.) in the tailpipe. Chromel-alumel thermocouples (1/4-in. diameter Inconel sheath, grounded junction, 0.040-in. wire diameter) were used for the measurements. The thermocouples were inserted through the cooling-water channels and into the center of the combustion chamber or tailpipe. Because of the difficulty of removing these thermocouples from the burner and the lack of replacements, thermocouples that failed were not replaced. Measured temperature data are presented in Appendix D (Figs. D.34-D.44).

The measured exhaust-gas temperatures presented in this section are mean values, because the thermocouple time constant is much larger than the time period of the fluctuating gas temperature. The thermocouples were unshielded, so the temperatures measured are lower than the actual values. A comparison of the data in Table 4.3 with that in Figs. D.34-D.44 reveals that the measured gas temperature at the tailpipe exit agrees reasonably well with the calculated values based on the adiabatic flame temperature. However, the measured temperatures in the combustion chamber and entrance region of the tailpipe are considerably lower than the calculated values in Table 4.3.

From the temperature data, the highest gas temperatures appear to be in the 3.5 to 7.5-in. region of the combustion chamber; the highest heat-transfer rates were in the 2.5 to 5-in. region. In general, the higher heat-input rate produced a slightly higher gas temperature in the combustion chamber. Along the tailpipe the gas temperatures were higher for the higher firing rates. There was considerable scatter in the data for similar conditions (see Fig. D.34). Equivalence ratios >1 or <1 resulted in lower gas temperatures (see Fig. D.36). The gas temperature at the 3.5-in. position in the combustion chamber was approximately the same for pulsating and steady combustion. When

the burner was operated with a tailpipe aspirator or with both mufflers, the gas temperature in the combustion chamber dropped rapidly.

Dhar et al.[30] measured an exhaust-gas temperature of 2100°F at the start of the corebustor region of the tailpipe, which was about 12 in. from the combustion chamber. They estimated the gas temperature to be 2600°F at the entrance to the tailpipe. Their combustion chamber was cooled by natural convection to the atmosphere.

In Ref. 51 (page 2/138), it is stated that the amount of heat lost by a flame before it reaches its maximum temperature ranges from 14 to 25% of the gross heating value of the gas burned. A graph showing the maximum temperature rise of the combustion gases, assuming a 20% heat loss, as a function of the percentage of carbon dioxide in the flue gas is given. The temperature rise of the gas is entirely dependent on the ratio of the total air supplied to the volume of gas burned. The curve presented only applies to small domestic and commercial types of appliances using atmospheric burners with a natural-draft secondary-air supply. Power burners with turbulent flames constitute an exception to this rule, for which the true theoretical flame temperature will give more satisfactory results. For the stoichiometric combustion of methane, the amount of carbon dioxide in the exhaust gas is 9.5% on a wet basis. Hence, the exhaust-gas temperature from Ref. 75 would be 2450°F.

A steady-state heat balance on the thermocouple probe consists of: (1) heat transfer to or from the probe by radiation, (2) heat transfer from the probe by conduction, (3) heat transfer to the probe by the conversion of kinetic energy of the flow into thermal energy, and (4) heat transfer to the probe by convection. The conversion of kinetic energy into thermal energy occurs for high flow velocities and can be neglected for the ANL experimental burner. Whereas conduction errors can be significant depending on the probe mounting temperature, they are estimated to be small for these measurements. Therefore the heat balance becomes

$$Q_{gp} + Q_c = Q_{pw} \tag{6.49}$$

where:

Q_c = convective heat transfer from gas to probe, Btu/h

Q_{gp} = net radiative heat transfer from gas to probe, Btu/h

Q_{pw} = net radiative heat transfer from the probe to the surfaces, Btu/h

For the simplified case of a transparent gas flowing through a tube whose diameter is large compared with that of the thermocouple and whose surface is at a constant temperature, $Q_{gp} = 0$ and Eq. 6.49 becomes

$$h_c A_p (T_g - T_p) = 0.71 \varepsilon_p A_p \left[\left(\frac{T_p}{100}\right)^4 - \left(\frac{T_w}{100}\right)^4\right] \quad (6.50)$$

where:

A_p = probe surface area, ft^2

h_c = convective heat-transfer coefficient, $Btu/h\text{-}ft^2{}^\circ R$

T_g = gas temperature, °R

T_p = thermocouple temperature, °R

T_w = tube-wall temperature, °R

ε_p = emissivity of probe surface

The thermocouple sheath is Inconel®, and its emissivity after repeated heating is approximately 0.65 (page 473 of McAdams[56]). Assuming that the wall temperature is 610°R, Eq. 6.50 can be arranged to become:

$$T_g = T_p + \frac{0.111}{h_c}\left[\left(\frac{T_p}{100}\right)^4 - 1384.6\right] \quad (6.51)$$

The value of h_c can be obtained from the following equation (page 260 of McAdams):

$$\frac{h_c d_p}{k_f} = 0.615 \left(\frac{d_p G}{\mu_f}\right)^{0.466} \quad (6.52)$$

where:

d_p = thermocouple diameter, ft

G = mass velocity of the gas, $lb_m/ft\text{-}h$

k_f = gas thermal conductivity at the film temperature, Btu/h-ft-°F

μ_f = gas absolute viscosity at the film temperature, $lb_m/ft\text{-}h$

Using mass velocities for methane combustion at heat rates of 50,000, 100,000, and 200,000 Btu/h with Eqs. 6.51 and 6.52, the thermocouple temperature was calculated for various gas temperatures. These temperatures are shown in Fig. 6.5. The thermal conductivity and viscosity values were obtained from page 2/97 of Ref. 51.

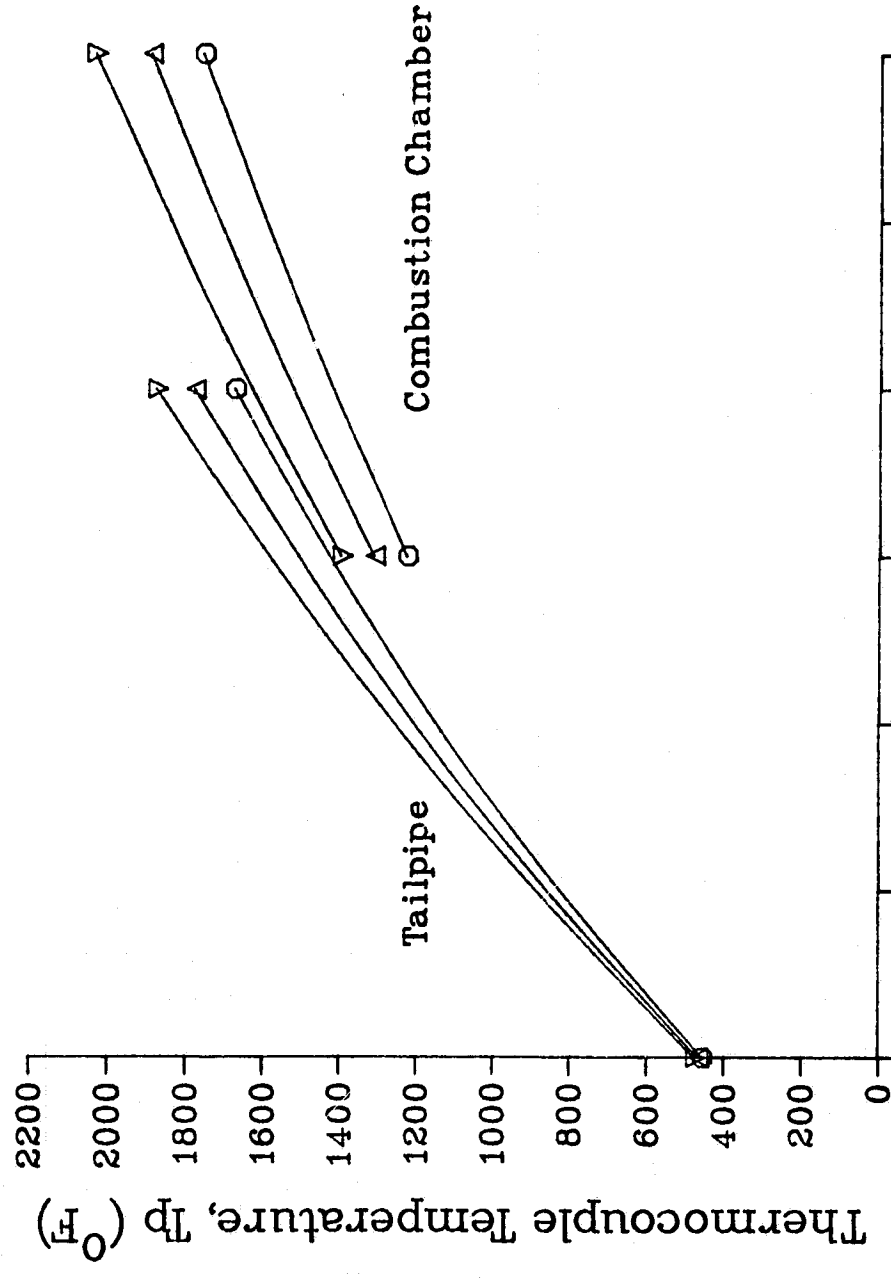

Fig. 6.5 Error in Unshielded Thermocouple Temperature for Various Heat-Input Rates to the Burner

From Fig. 6.5, it can be seen that large differences can exist between the measured and actual gas temperatures. The difference increases with increasing gas temperature. For the same gas temperature, the difference is larger in the combustion chamber than in the tailpipe because of the lower convective heat transfer to the thermocouple. These calculated temperature differences are high because of the assumption of a transparent gas. Applying these temperature differences to the measured temperatures in the combustion chamber would result in temperatures indicative of the adiabatic flame temperature.

For a participating medium, the radiant heat transfer adds additional complexity. Significant simplifying assumptions are made, and Q_{gp} in Eq. 6.49 is expressed by:

$$Q_{gp} = 0.171\ A_p \left[\varepsilon_g \left(\frac{T_g}{100} \right)^4 - \left(\frac{1 + \varepsilon_p}{2} \right) (\alpha_{gp}) \left(\frac{T_p}{100} \right)^4 \right] \tag{6.53}$$

where:

ε_g = gas emissivity

α_{gp} = gas absorptivity at the probe temperature

The gas absorptivity is a function of T_g/T_p, as discussed in Sec. 6.2. Combining Eqs. 6.50 and 6.53, substituting the values of $\varepsilon_p = 0.65$ and $T_w = 610°R$, and rearranging terms results in the following equation:

$$h_c\ T_g + 0.171\ \varepsilon_g \left(\frac{T_g}{100} \right)^4 = h_c\ T_p + (0.111 + 0.141\ \alpha_{gp}) \left(\frac{T_p}{100} \right)^4 - 153.7 \tag{6.54}$$

The solution of this equation is cumbersome, because the temperature-dependent emissivity and absorptivity are functions of the gas composition and the product of its partial-pressure mean-path length and must be obtained from curves presented in Refs. 57, 69, or 70. For stoichiometric methane combustion, the gas emissivity as a function of temperature is shown in Fig. 6.6 for both the tailpipe and combustion chamber. Based on these data and values of h_c calculated from Eq. 6.52, the thermocouple temperature as a function of the gas temperature for a 100,000 Btu/h heat-input rate is shown in Fig. 6.7. From this figure, it can be seen that by taking into account the radiative heat transfer from the gas one reduces the thermocouple error. However, a significant difference between the gas and thermocouple temperature still exists at higher temperatures.

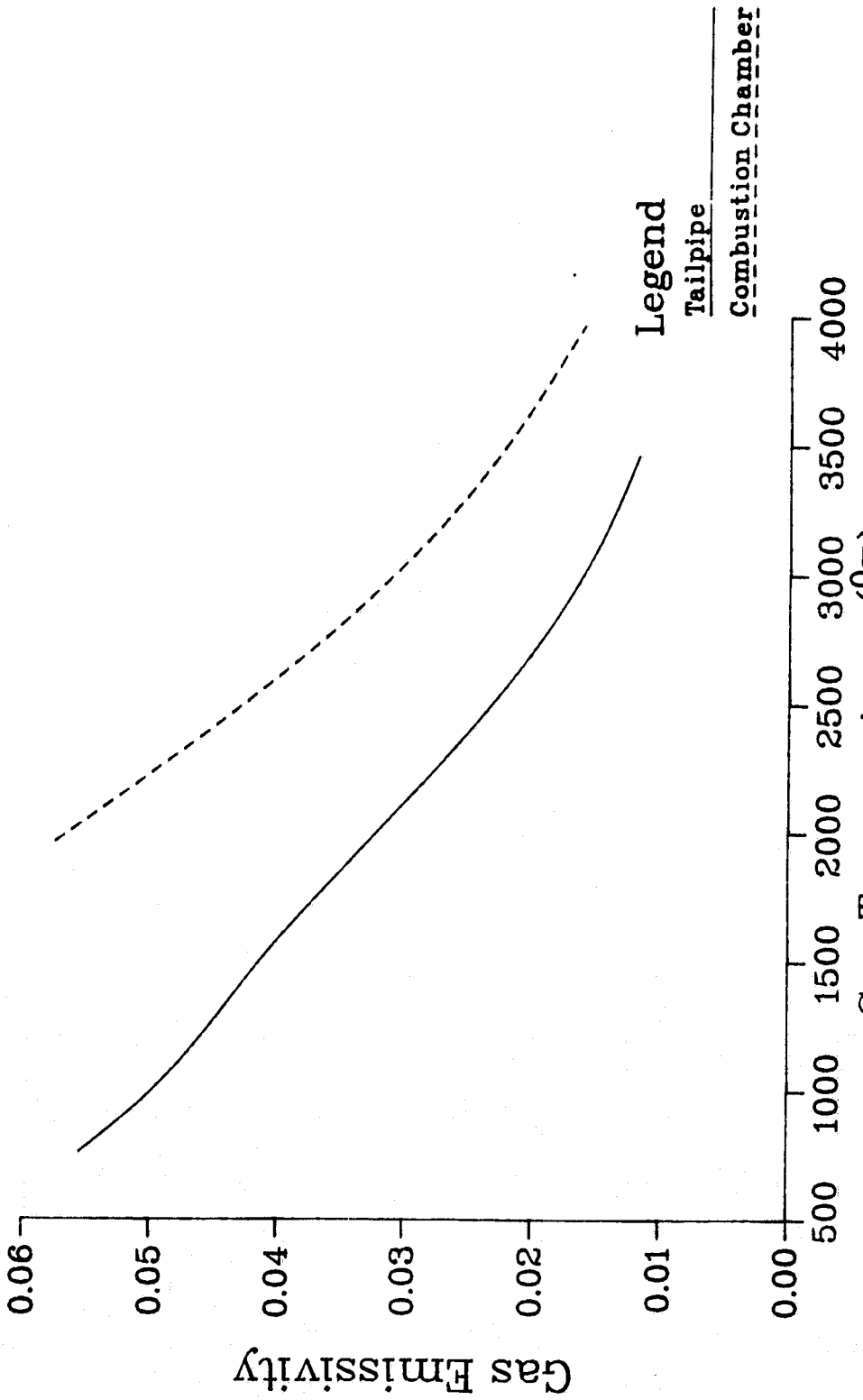

Fig. 6.6 Exhaust-Gas Emissivity for Radiative Heat Transfer to the Thermocouples

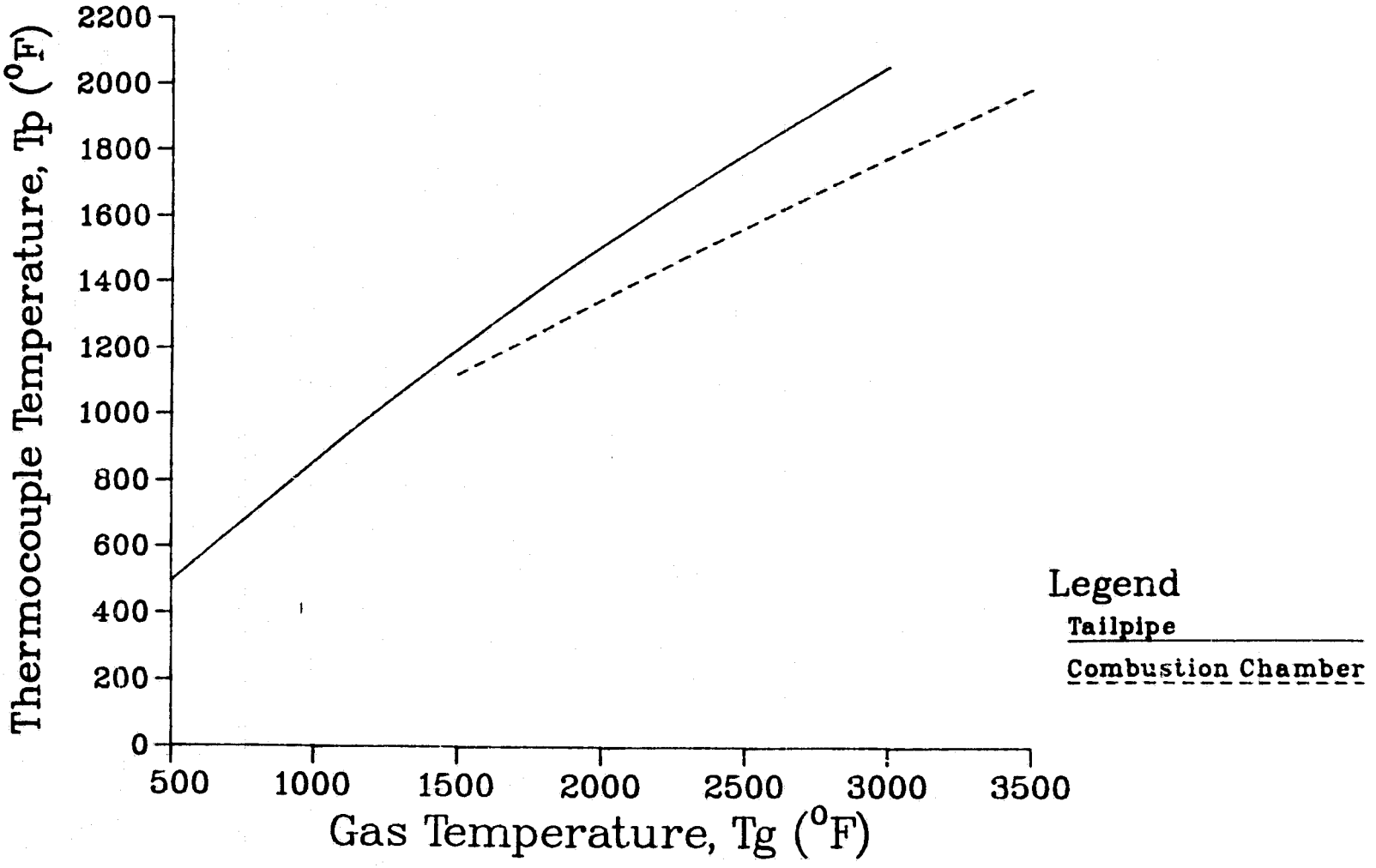

Fig. 6.7 Error in Unshielded Thermocouple Temperature When Radiative Heat Transfer for the Gas Is Considered

6.6 HEAT-TRANSFER PREDICTIONS

The amount of heat transferred by convection can be determined from the following equation:

$$Q_c = UA(\Delta t) \tag{6.55}$$

where:

A = surface area, ft^2

Q_c = convective heat-transfer rate, Btu/h

Δ_t = temperature difference, °F

U = overall heat-transfer coefficient, Btu/h-ft^2°F

For a cylindrical tube, the overall heat-transfer coefficient (based on the inside surface area of the tube) is given by:

$$\frac{1}{U} = \frac{1}{h_i} + \frac{1}{h_{fi}} + \frac{A_i \ln\left(\frac{D_o}{D_i}\right)}{2\pi k_w L} + \frac{A_i}{h_o A_o} + \frac{A_i}{h_{fo} A_o} \tag{6.56}$$

where:

A_i = inside surface area, ft^2

A_o = outside surface area, ft^2

D_i = tube inside diameter, ft

D_o = tube outside diameter, ft

h_i = film coefficient on inside of tube, Btu/h-ft^2-°F

h_o = film coefficient on outside of tube, Btu/h-ft^2-°F

h_{fi} = fouling coefficient on inside of tube, Btu/h-ft^2-°F

h_{fo} = fouling coefficient on outside of tube, Btu/h-ft^2-°F

k_w = tube-wall thermal conductivity, Btu/hr-ft-°F

L = length, ft

If fouling is negligible, the tube-wall conductivity is large, and if $h_o >> h_i$, then

$$U \cong h_i \tag{6.57}$$

Hence, h_i can be obtained from Eq. 6.55.

The temperature difference, Δt, is a log-mean difference; for a constant-temperature tube wall, it is expressed by:

$$\Delta T = \frac{t_2 - t_1}{\ln\left(\frac{t_2 - t_w}{t_1 - t_w}\right)} \tag{6.58}$$

where:

t_1 = fluid temperature at section outlet, °F

t_2 = fluid temperature at section inlet °F

t_w = wall temperature, °F

The heat-transfer rates presented in Sec. 6.4 contain a radiative contribution, which can be estimated by the techniques of Sec. 6.2. Both the radiative and convective heat transfer depend on the gas temperature, whose value is not exactly known (as discussed in Sec. 6.5). Therefore, the calculated gas temperatures listed in Table 4.3 based on the adiabatic flame temperature will be used to determine the convective heat-transfer coefficients. Because of these assumptions, average heat-transfer coefficients will be computed (instead of local coefficients) from representative samples of the data.

Table 6.3 contains the gas temperatures (T_g) used for the fluid properties and the radiative heat transfer (Q_r) calculations, the convective heat transfer rate (Q_c), the convective heat-transfer coefficient (h_c), and the Reynolds, Prandtl, and Grashof numbers (Re, Pr, and Gr). Similar data for the tailpipe are presented in Table 6.4. The convective heat-transfer rate was obtained by subtracting the radiative heat-transfer rate from the measured heat-transfer rate (Q) for the combustion chamber and the tailpipe. Based on the convection-region map for flow through vertical tubes given in Ref. 58 (p. 7-53), the number (Gr Pr D/L) and the Reynolds number for the combustion chamber are indicative of the mixed-turbulent convection region. For the tailpipe, the convection region is turbulent except for the 50,882 Btu/h heat-input case, which is in the laminar region. Radiative heat transfer accounts for about 23-36% of the combustion-chamber heat transfer but only 3-9% of the tailpipe heat transfer.

Since the convective conditions in the combustion chamber represent mixed convection, an attempt to predict the heat-transfer coefficient from Eq. 6.27 was unsuccessful, because the subtraction of $0.0722\ F_2\ (Gr_d Pr\ D/L)_w^{0.84}$ from WC_p/kL resulted in a negative number, which would predict a negative Nusselt number. The only other equation for mixed convection is Eq. 6.31, which was developed for highly turbulent flow and is not applicable to the

Table 6.3 Combustion-Chamber Heat-Transfer Data

Heat Input (Btu/h)	Air/Fuel Ratio	Tg (°R)	Q (Btu/h)	Q_r (Btu/h)	Q_c (Btu/h)	h_c (Btu/h ft^2-°F)	Re	Pr	Gr	Burner Configuration
53,589	12.50	3,150	13,340	4,534	8,806	3.99	1,349	0.756	8.60(104)	No flapper valves
54,194	12.48	3,050	16,679	4,204	12,474	5.89	1,396	0.759	9.56(104)	Standard Burner
102,645	11.39	3,500	16,354	5,861	10,493	4.19	2,178	0.758	6.07(104)	No flapper valves
95,458	11.89	3,350	19,627	5,276	14,351	6.10	2,184	0.756	7.04(104)	Standard Burner
101,713	9.87	3,600	24,242	6,662	17,580	6.78	1,844	0.769	5.42(104)	Standard Burner
194,371	9.38	3,760	32,541	7,421	25,120	9.14	3,241	0.775	4.63(104)	Standard Burner
50,882	10.13	3,280	18,463	5,679	12,784	5.49	1,011	0.773	7.50(104)	48-in. Long Corebustor
99,996	9.73	3,620	23,915	6,938	16,977	6.46	1,782	0.772	5.38(104)	48-in. Long Corebustor

Table 6.4 Tailpipe Heat-Transfer Data

Heat Input (Btu/h)	Air/Fuel Ratio	Tg (°R)	Q (Btu/h)	Q_r (Btu/h)	Q_c (Btu/h)	h_c (Btu/h ft^2-°F)	Re	Pr	Gr	Burner Configuration
53,589	12.50	2,220	17,570	1,317	16,253	6.29	3,983	0.782	2.21(104)	No flapper valves
54,194	12.48	1,850	23,768	663	23,105	13.11	4,552	0.792	3.71(104)	Standard Burner
102,645	11.39	2,750	28,696	2,647	26,049	7.53	5,982	0.771	1.11(104)	No flapper valves
95,458	11.89	2,330	35,417	1,469	33,948	12.33	6,537	0.780	1.89(104)	Standard Burner
101,713	9.87	2,380	39,400	1,552	37,848	13.74	5,749	0.794	1.73(104)	Standard Burner
194,371	9.38	2,710	68,719	2,461	66,258	19.72	9,528	0.791	1.15(104)	Standard Burner
50,882	10.13	1,660	24,151	1,898	22,253	21.40	2,310	0.852	0.37(104)	48-in. Long Corebustor
99,996	9.73	2,190	48,668	4,297	44,371	19.61	3,781	0.802	0.18(104)	48-in. Long Corebustor

low-flow conditions in the combustion chamber. Therefore, the heat-transfer coefficients for laminar flow were obtained from Fig. 6.1 and Eqs. 6.8 and 6.10. These values, along with coefficients for free convection calculated from Eq. 6.2, are given in Table 6.5. Values of hc calculated from Eq. 6.9 were unrealistically high, so this equation is not applicable. It can be seen that the measured coefficients for the non-pulsating conditions are best represented by Fig. 6.1, which predicts the coefficient's value to be too low by about 13% for the 53,589 Btu/h heat-input case but also gives a coefficient value too high by 19% for the 102,645 Btu/h heat-input case. Pulsating-flow heat-transfer coefficients are about 50 to 70% higher than values predicted from Fig. 6.1. The heat-transfer coefficient for the 194,371 Btu/h heat-input case was also calculated from Eqs. 6.13-6.18; results were 2.69, 3.25, 2.82, 3.49, 3.77, and 2.76 Btu/h-ft^2°F, respectively. Therefore, laminar forced convection for this case with h_c = 6.09 Btu/h-ft^2°F is more appropriate. No doubt free convection has some effect on the heat-transfer coefficient, but accounting for this effect will require further investigation.

Mean heat-transfer coefficients for the tailpipe were predicted by Eqs. 6.13-6.18 for turbulent flow conditions and augmented by Eq. 6.21; results are listed in Table 6.6. The annular space formed by the corebustor was treated by the use of an equivalent diameter as the characteristic dimension for the Reynolds and Nusselt numbers. There is an approximate 40% difference between the low and high values of the predicted heat-transfer coefficient. Because most of these correlations were developed for Reynolds numbers greater than 10,000, using them for values as low as 2310 is somewhat questionable. However, for the 50,882 Btu/h heat-input case a value of h_c = 3.49 Btu/h-ft^2°F for laminar flow was obtained from Fig. 6.1. When one compares the high measured heat-transfer coefficients, the use of the turbulent-flow correlations appears to be justified. For the nonpulsating cases, h_c calculated from the augmented Eq. 6.14 agrees with the measured value at the 53,589 Btu/h heat input, but the predicted heat-transfer coefficient exceeds the measured value by about 36% at the heat-input rate of 102,645 Btu/h. The use of an augmented Eq. 6.13 results in a prediction 19% too low at the low heat-input rate and a prediction 19% too high at the high heat-input rate. This outcome is somewhat similar to the case of predictions involving the combustion chamber. Hence, with this equation, the measured heat-transfer coefficients under pulsating conditions are 50 to 250% higher than the predicted steady-flow values. With the corebustor installed, measured heat-transfer coefficients are 80-370% higher than predicted values. The use of Eq. 6.26 for the tailpipe conditions gives excessively high heat-transfer coefficients.

Table 6.5 Steady-State Heat-Transfer Coefficients Predicted for the Combustion Chamber

Heat Input (Btu/h)	Air/Fuel Ratio	h_c, Btu/h-ft^2°F				Burner Configuration
		Fig. 6.1	Eq. 6.8	Eq. 6.10	Eq. 6.2	
53,589	12.50	3.46	2.73	2.57	2.38	No flapper valves
54,194	12.48	3.41	2.68	2.53	2.39	Standard Burner
102,645	11.39	5.00	3.55	3.61	2.44	No flapper valves
95,458	11.89	4.31	3.40	3.46	2.43	Standard Burner
101,713	9.87	4.40	3.47	3.44	2.45	Standard Burner
194,371	9.38	6.09	4.37	4.76	2.47	Standard Burner
50,882	10.13	3.22	2.59	2.33	2.42	48-in. Long Corebustor
99,996	9.73	4.35	3.45	3.40	2.46	48-in. Long Corebustor

Table 6.6 Steady-State Mean Heat-Transfer Coefficients Predicted for the Tailpipe

Heat Input (Btu/h)	Air/Fuel Ratio	h_c, Btu/h-ft^2°F						Burner Configuration
		Eq. 6.13	Eq. 6.14	Eq. 6.15	Eq. 6.16	Eq. 6.17	Eq. 6.18	
53,589	12.50	5.33	6.30	5.47	6.71	7.46	5.46	No flapper valves
54,194	12.48	5.03	5.86	5.10	6.21	7.03	5.15	Standard Burner
102,645	11.39	9.00	10.26	8.68	10.75	12.64	9.23	No flapper valves
95,458	11.89	8.28	9.36	7.93	9.77	11.60	8.49	Standard Burner
101,713	9.87	7.83	8.93	7.43	9.36	10.93	8.01	Standard Burner
194,371	9.38	13.05	14.32	12.02	14.76	18.24	13.36	Standard Burner
50,882	10.13	5.82	7.17	6.79	7.86	8.01	5.91	48-in. Long Corebustor
99,996	9.73	10.83	12.82	11.20	13.69	15.09	11.07	48-in. Long Corebustor

7 ACOUSTICS

One of the most characteristic aspects of pulse combustion is noise generation. Sound-level measurements were reported in a number of the studies surveyed in Chapter 1 and in Appendix E, and some attempts to attenuate the noise were made.

7.1 RESULTS FROM PREVIOUS EXPERIMENTS

Francis, Hoggarth, and Reay[31] used Burgess-type ADS straight-through absorption-type silencers on both the exhaust and intake of their pulse combustion burners equipped with flapper valves. The average sound-level attenuation over the spectrum was about 15 dB. The intake silencer slightly lowered the combustion frequency and slightly reduced the air input but had no after-effect on combustion conditions. An intake muffler couldn't be used on a burner with an aerodynamic valve, because the combustion products accumulated in the muffler and eventually choked the combustor.

For Helmholtz burners with flapper valves, Griffiths, Thompson, and Weber[21] reported exhaust-noise levels from about 95 to 110 dB. Noise level at the burner inlet was about 5 dB less than at the outlet. At the midpoint between inlet and outlet of the combustor, the noise level was about 10 dB lower than at the exhaust. With a straight-through automobile muffler installed on both the inlet and outlet, one combustor operated with a noise level of 80 dB. When an exhaust muffler was installed on a combustor, the heat input increased by about 8% and the fundamental frequency increased by about 13% for the same operating conditions. Expansion chambers between the burner and the mufflers minimized the effects of the muffler on the combustor operation.

Griffiths and Weber[23] found that restrictions and/or automotive mufflers attached to the tailpipe of Helmholtz-type pulse combustors with flapper valves could cause a reduction in the peak and mean pressures in the burner, as well as reductions in the gas- and air-flow rates. However, the pressure in the burner could be restored to its unrestricted value by increasing the gas-supply pressure. The authors state that noise is directly related to the burner operating pressure: the lower the pressure, the lower the noise level. The simplest method of reducing peak and mean pressure is to use relatively larger combustion chambers and larger tailpipe diameters.

For a Schmidt-type burner fired with town gas and having aerodynamic valves, Reay[32] measured overall sound-pressure levels of 114 dBC at 4 ft from the burner inlet and 118 dBC at 7 ft from the exhaust. Mineral-wool-lined sound-enclosure boxes installed on the inlet and outlet of the burner produced a considerable but not a sufficient noise reduction. Therefore, 3-ft long Burgess straight-through absorptive silencers were fitted to both sound enclosures. At 3 ft from the burner exit, the noise level was 86dB, and at 3 ft from the air intake, the noise level was 82 dB. Noise measurements 3 in.

from the inlet and exit were 78 and 80 dB, respectively, indicating that the noise from these sources had been effectively attenuated.

Briffa[3] coupled two Schmidt-type combustors and obtained a noise reduction of about 15 dB. When the spacing between the exhaust exits was decreased from 1.48-in. to 0.04-in., a noise reduction of 6.5 dB occurred. This small reduction resulted because coupling essentially reduces the noise due to the fundamental frequency but not from the higher harmonics. Therefore, to achieve substantial noise reductions, careful attention must be given to the magnitude of the sound-pressure level of the other pressure peaks in comparison with the fundamental.

For a natural-gas-fired Helmholtz pulse combustor with flapper valves, Vogt[26] reported that peaks in sound-pressure level occur approximately at frequencies that are harmonics of the firing frequency. The highest sound level was ahead of the air-decoupling chamber, and its source appears to be the flapper valves. The lowest noise source is at the exhaust and results from noise generated at the combustor inlet. Opposite the combustion chamber, the noise source probably is the combustion reaction itself. The highest A-weighed sound-pressure level was 87 dBA and the average of all tests was 77 dBA.

Assuming uniform hemispherical radiation over a non-absorbing surface, Brown[79] presents the following relationship between the sound power and the sound level:

$$\frac{SPL}{10} = 12 + \log_{10} W - \log_{10} 2\pi r^2 \qquad (7.1)$$

where:

r = distance from sound source, m

SPL = sound pressure level, dB

W = external sound power, W

Using data from published studies with four different pulse combustors, the sound power was computed from Eq. 7.1, and the acoustic efficiency (external sound-power/thermal-input rate) was determined. The average of these acoustic efficiencies was 1×10^{-4}, and there was no obvious variation of acoustic efficiency with fuel or combustor throughput.

Hanby and Brown[43] investigated the effect of coupling two identical propane-fired, aerodynamically valved, Schmidt-type pulse combustors together, and the effect of decreasing the diameter of the combustor outlet. The burner had a 2-in. internal diameter, was 74-in. long, and operated at a resonant frequency of 64 Hz. Coupling was effected by bolting the tubes to a

semicircular section of pipe, with a 3-in. diameter exit pipe. The exit diameter of the single or coupled combustors could be reduced by sections attached with bolts. Additional lengths of tube were used such that the total length remained constant. Results of these tests are shown in Table 7.1. The internal acoustic efficiency is defined as:

$$\eta_i = \frac{P^2 \pi D^2}{4 c Q_i} \tag{7.2}$$

where:

c = sound velocity

D = combustor internal diameter

P = root-mean-square pressure

Q_i = heat-input rate

η_I = internal acoustic efficiency

The external acoustic efficiency, η_E, was the conventional total radiated sound power divided by the heat-input rate.

From an octave band analysis, the effect of reducing the exit diameter of the single combustor from 2 in. to 1 3/8 in. was a noise reduction of up to 10 dB at all frequencies below 5 kHz. With two combustors coupled at their exit, no amplitude reduction in the fundamental frequency was observed, and the external sound field was not greatly altered. However, the coupling had considerably increased the pressure amplitude, as can be seen in Table 7.1, and this pressure increase should have led to an increased noise emission. A comparison of η_E and η_I revealed that more effective silencing is obtained at the expense of reduced combustor performance. An external acoustic efficiency of about 0.3×10^{-4} is considered reasonable. From the data in Table 7.1, it can also be seen that reducing the exit-pipe diameter reduces both the radiated noise and the pressure amplitude in the combustor. The authors also showed that the maximum pressure amplitude of a single combustor varies linearly with the heat-input rate.

Belles, Vishwanath, and Ives[80] present noise measurements at the inlet and outlet ends of a series of Helmholtz-type pulse combustion burners assembled from cylindrical components. Combustion chambers and exhaust-decoupling chambers had length-to-diameter ratios of approximately 3 and 1, respectively. The exhaust pipe varied in diameter but was 6 ft long in all cases. Each burner was operated at several input rates, with the carbon dioxide level in the exhaust gas held between 9 and 9.5%. Noise levels for the reference burner fired at 65,000 Btu/h were 91 dBA at the inlet and 77 dBA at the outlet. From a statistical analysis of noise measurements for 20

Table 7.1 Combustor Sound-Pressure Level, Pressure, and Acoustic Efficiency

Configuration	Broad-Band Sound-Pressure Level (dB)	Maximum RMS Pressure Amplitude In Combustor (psi)	Combustor Internal Acoustic Efficiency η_I	Combustor External Acoustic Efficiency η_E
Single combustor	112.4	1.84	5.2×10^{-3}	0.30×10^{-4}
Two combustors side by side	115.6	1.84	5.2×10^{-3}	0.29×10^{-4}
Two combustors coupled	116.3	3.43	18.2×10^{-3}	0.34×10^{-4}
Single combustor with a 1 3/8-in. exit	106.7	0.92	1.3×10^{-3}	0.08×10^{-4}
Two coupled combustors with a 1 7/8-in. exit	115.7	2.68	10.1×10^{-3}	0.30×10^{-4}
Two coupled combustors with a 1 3/8-in. exit	114.1	1.98	6.1×10^{-3}	0.21×10^{-4}

Source: Ref. 43.

burner configurations, the authors conclude that that heat input rate is important for both inlet and exhaust noise. Parameters significant for outlet noise are exhaust and tailpipe areas. At the inlet, air-valve spacing is rather significant. A further conclusion is that there is considerable flexibility in designing pulse combustion burners with noise as a constraint.

7.2 NOISE MEASUREMENTS IN ANL EXPERIMENTS

Near-field sound-level measurements were made with a Bruel and Kjaer Model 2218 precision integrating sound-level meter; these data are presented in Table 7.2. Typical noise spectra in the narrow (3% bandwith) and 1/3 octave band are shown in Fig. 7.1. No attempt was made to attenuate the noise from the burner beyond the use of an inlet or an exhaust muffler as described in Chapter 2. These mufflers are low-pass noise filters that are effective in reducing the air-inlet or exhaust-gas noise but not the structural noise. Therefore, large reductions in the burner noise level were not anticipated, but a significant noise reduction was achieved when both mufflers were installed (see Table 7.2). In fact, the two-muffler combination reduced the noise

Table 7.2 Measured Noise Level of Experimental Pulse Combustor

Heat Input (Btu/h)	Air/Fuel Ratio	Noise Level, dBA, for Microphone Position[a] A	B	C	D	E	Burner Configuration
32,887	13.21	-	-	-	84.9	85.1	Standard Burner
50,245	9.89	-	-	-	79.9	84.7	Standard Burner
54,194	12.48	-	-	-	86.6	94.4	Standard Burner
58,655	10.08	82.3	84.3	-	-	-	Standard Burner
95,458	11.89	94.3	96.3	-	-	-	Standard Burner
96,782	10.34	93.8	93.8	-	-	-	Standard Burner
97,464	7.90	88.4	90.2	-	-	-	Standard Burner
99,577	10.05	-	-	-	88.3	91.7	Standard Burner
100,215	9.89	-	-	-	91.3	95.1	Standard Burner
100,941	10.13	-	-	91.5	-	93.5	Standard Burner
101,713	9.87	-	-	-	94.6	99.3	Standard Burner
103,576	10.12	-	-	-	89.9	91.8	Standard Burner
194,371	9.38	-	106.9	-	-	-	Standard Burner
98,013	9.96	-	-	-	92.0	94.0	Insulated Standard Burner
53,589	12.50	-	-	-	70.0	-	No Flapper Valves
102,645	11.39	-	-	-	77.5	-	No Flapper Valves
50,418	10.02	-	-	-	79.9	83.3	Tailpipe Aspirator
98,620	9.60	-	-	-	94.9	93.0	Tailpipe Aspirator
53,116	11.03	-	-	-	78.7	79.2	Inlet Muffler
103,728	10.10	-	-	-	92.7	93.5	Inlet Muffler
101,532	10.09	-	-	-	90.1	90.8	Inlet Muffler
53,429	11.50	-	-	-	82.3	87.0	Exhaust Muffler
50,227	9.42	-	-	-	71.3	71.9	Inlet and Exhaust Mufflers
100,580	8.86	-	-	-	76.9	79.5	Inlet and Exhaust Mufflers
49,867	9.93	-	-	-	80.7	84.5	48-in. Long Corebustor
50,341	9.82	-	-	-	76.5	80.8	48-in. Long Corebustor
50,882	10.13	-	-	-	80.0	84.4	48-in. Long Corebustor
99,996	9.73	-	-	-	89.5	94.6	48-in. Long Corebustor
101,248	10.09	-	-	-	90.3	96.7	48-in. Long Corebustor
50,042	10.07	-	-	-	78.3	83.5	36-in. Long Corebustor
97,009	10.11	-	-	-	86.3	91.2	36-in. Long Corebustor
100,553	9.82	-	-	-	89.1	94.1	36-in. Long Corebustor
100,794	10.45	-	-	-	88.7	89.8	Air Decoupling Chamber

[a]A: 36-in. in front of burner, 36-in. above floor
B: 36-in. in front of burner, 66-in. above floor
C: 84-in. in front of burner, 48-in. above floor
D: 72-in. in front of burner, 48-in. above floor
E: 36-in. in front of blower, 12-in. above floor

Fuel Input = 100,000 Btu/hr
Air/Fuel = 10:1

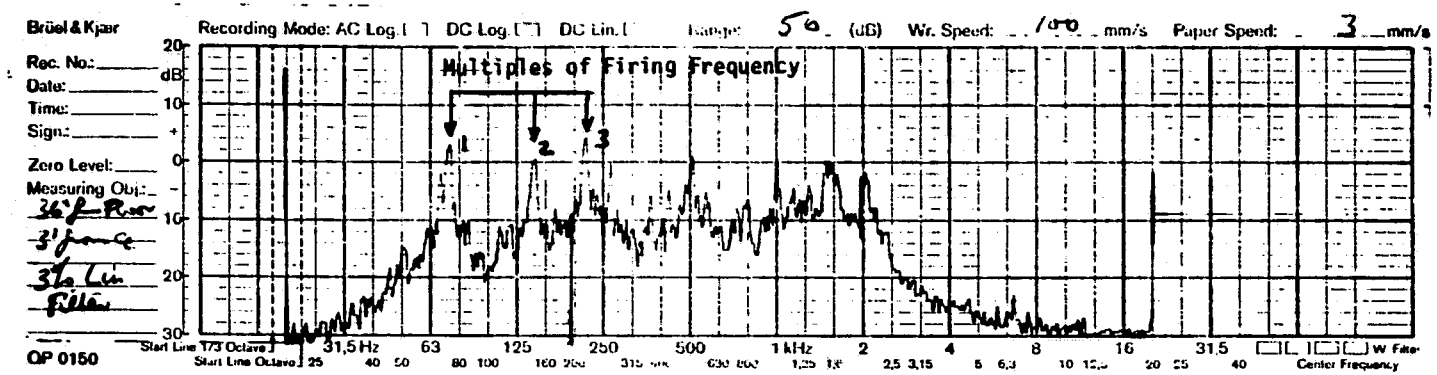

NOISE SPECTRUM IN NARROW FREQUENCY BAND

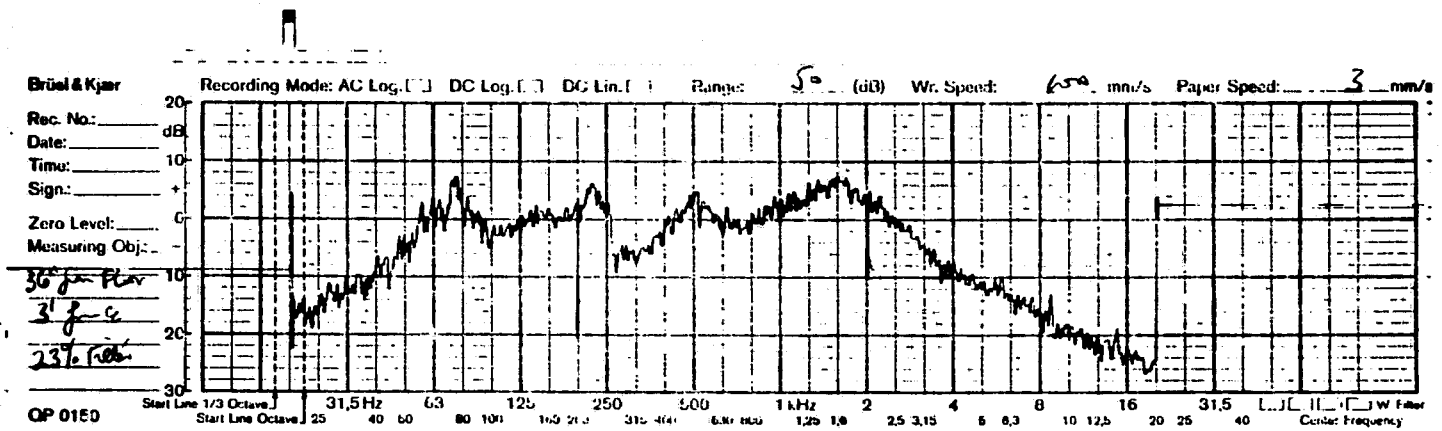

NOISE SPECTRUM IN 1/3-OCTAVE FREQUENCY BAND

Fig. 7.1 Typical Noise-Spectrum Data

level to that of the burner operating without flapper valves, and the reduction agrees with the measurements of Francis et al.[31] and Griffiths et al.[21]

The noise level opposite the air intake (position E in Table 7.3) was approximately 5 dBA higher than the level at the exhaust. This result is similar to the findings of Vogt[26] but in opposition to those of Griffiths et al.[21] Contrary to the findings of Griffiths et al., the burner heat transfer did not change with the addition of an exhaust muffler; our data are insufficient to confirm a frequency increase.

With the corebustor installed, the measured noise was essentially the same as that emitted by the standard burner. For the 100,000 Btu/h heat-input test with the tailpipe aspirator, the noise level measured at Position "A" was about 5 dB higher than that obtained with the standard burner; there was no increase in noise level when the burner was operated at 50,000 Btu/h. The high noise levels measured for the 32,890 Btu/h heat-input experiment are attributed to the high air/fuel ratio. The inlet decoupling chamber acts as an inlet muffler.

In Chapter 5, it was shown that the maximum positive combustion-chamber pressure appears to be a linear function of the heat-input rate to the burner. This behavior was also shown by Hanby and Brown.[43] Since the noise is directly related to the burner pressure, the sound-power level should be a linear function of the heat-input rate. Selected sound data from Table 7.2 are plotted against heat-input rate in Fig. 7.2; a straight line can be drawn through the data. Note that the air/fuel ratio has an effect on the burner pressure, and consequently on the noise level.

Using the information given in Fig. 7.2, Chiu, Clinch, Blomquist, and Croke[81] presented the following empirical correlations for the sound-pressure level at a near-field point:

Steady Combustion:

$$SPL = 23.08 \log_{10} Q - 39.38 \qquad (7.3)$$

Pulsating Combustion:

$$SPL = 29.20 \log_{10} Q - 51.40 \qquad (7.4)$$

where:

SPL = sound power level, dB

Q = mean firing rate, Btu/h

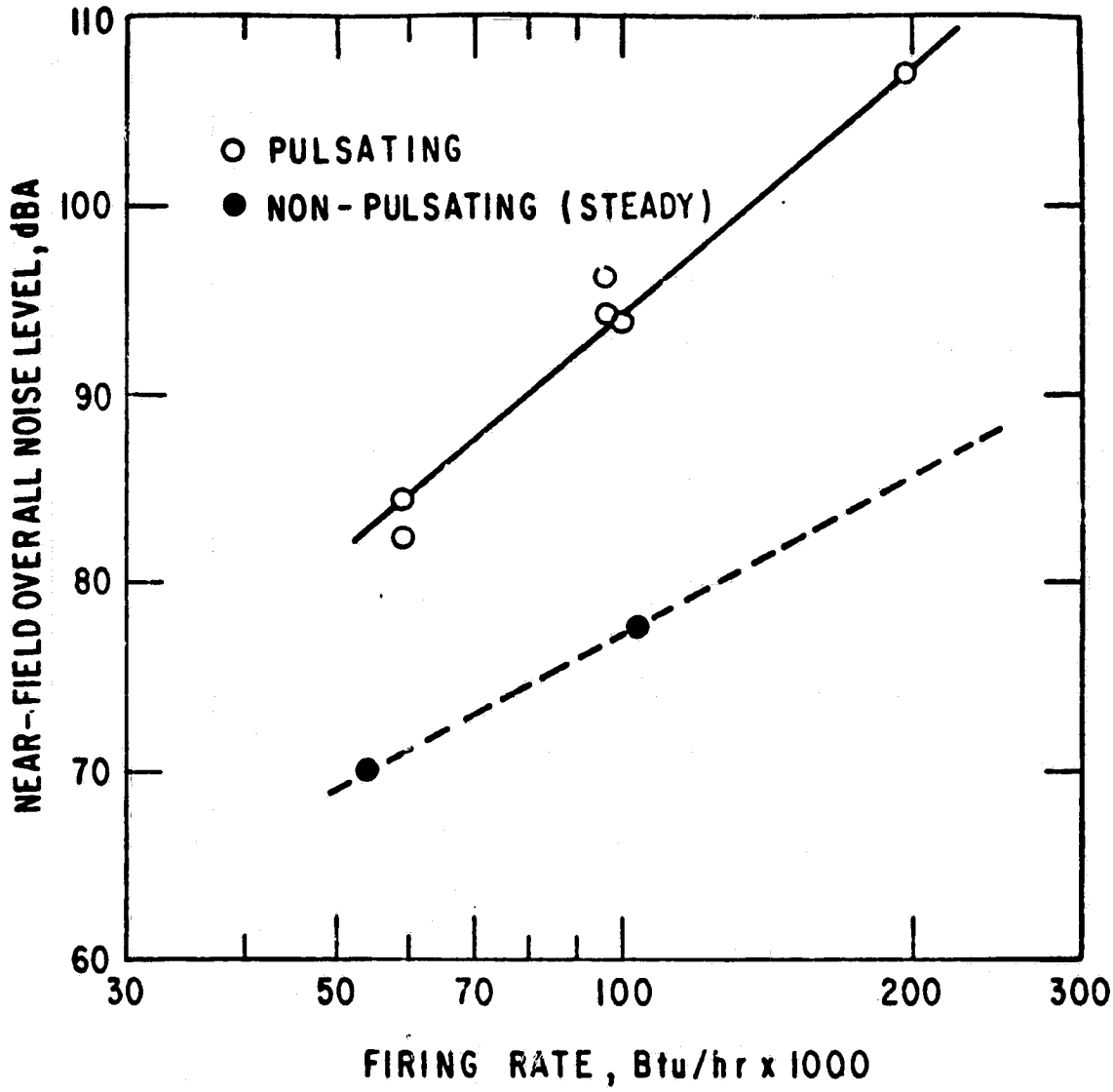

Fig. 7.2 Near-Field Overall Noise Level vs. Heat-Input Rate

8 INLET DECOUPLING CHAMBER

The air-inlet decoupling chamber was a 15 1/2-in. inside diameter cylinder with a length of 47 in. and containing a movable piston. The chamber was attached to the side branch of the air-inlet tee. Connected to the movable piston were a piece of 1-in. sch 40 pipe, the air flowmeter, another section of pipe, and the starting blower.

The volume in the air-inlet tee was approximately 197 $in.^3$ Prior to the burner test with the air-decoupling chamber, the effect on the pressure in the air-inlet tee was investigated at different volumes in the decoupling chamber. With the burner operating at about 100,000 Btu/h, an air/fuel ratio of 10, and the piston all the way forward (zero decoupling-chamber volume), the pressure pulse shown in Fig. 8.1 was obtained.

Next the piston was moved outward 3 in. to create a decoupling-chamber volume of 566 $in.^3$; the resulting pressure pulse is shown in Fig. 8.2.

With the piston withdrawn 5 in. to create a decoupling-chamber volume of 944 $in.^3$, the pressure pulse shown in Fig. 8.3 was observed.

The pressure pulse obtained with the piston withdrawn 8 in. to give a 1510-$in.^3$ decoupling-chamber volume is shown in Fig. 8.4, and the pulse obtained with the piston withdrawn 12-in. to create a 2264-$in.^3$ decoupling-chamber volume is shown in Fig. 8.5.

The pressure pulses cannot be compared directly, because of the short time duration (as discussed in Chapter 5). However, the filtered signal does show the amplitude reduction as the piston is withdrawn. Hence, the 8-in. piston position (1510-$in.^3$ volume) was selected for the test reported on in earlier sections. These data, along with those from the standard burner and the burner with an inlet muffler (928-$in.^3$ volume) are shown in Table 8.1. From the data in this table, it appears that the use of an air-inlet decoupling chamber is similar to the use of an inlet muffler.

The pressure pulse in the air-inlet tee was monitored for two additional burner heat-input rates. The piston was withdrawn until the amplitude of the pressure signal was observed to be a minimum. For a burner heat-input rate of 151,814 Btu/h with a 9.8 air/fuel ratio, the minimum pressure pulse occurred with the piston withdrawn 12-3/4 in. for a 2406-in.3 decoupling-chamber volume. The pressure waveforms are shown in Figs. 8.6 and 8.7.

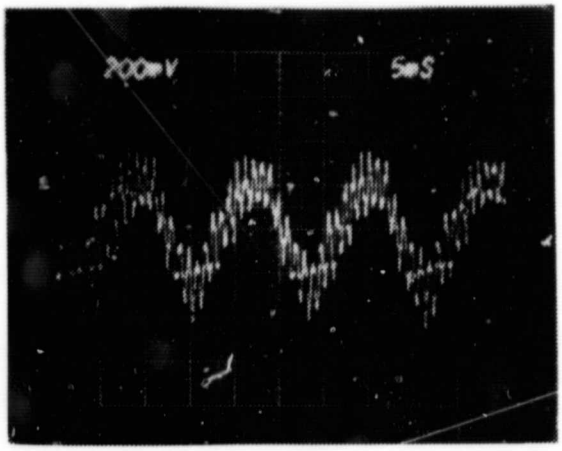

(a) Unfiltered

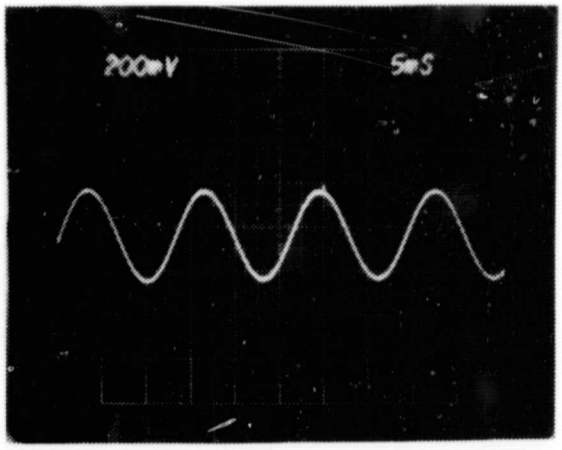

(b) 3% Filter
(1 unit vert. = 200 mV,
1 unit horiz. = 5 ms)

Fig. 8.1 Pressure Pulse in Air-Inlet Tee
for a Zero-Volume Decoupling Chamber
(1 V = 1 psi)

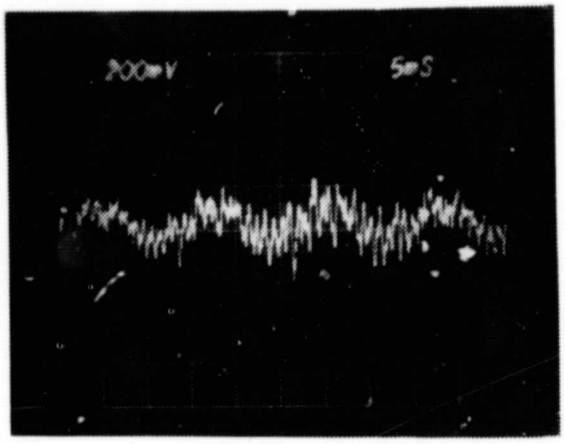

(a) Unfiltered
(1 unit vert. = 200 mV,
1 unit horiz. = 5 ms)

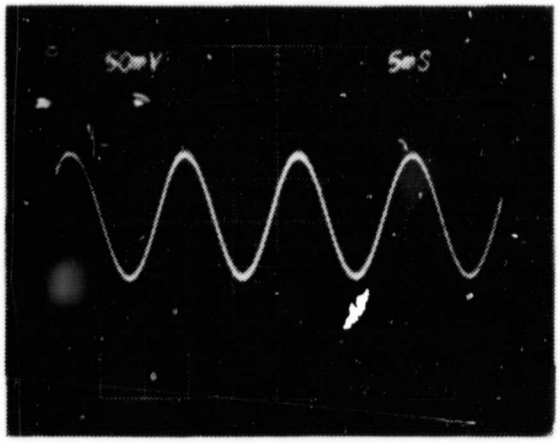

(b) 3% Filter
(1 unit vert. = 50 mV,
1 unit horiz. = 5 ms)

Fig. 8.2 Pressure Pulse in Air-Inlet Tee for a 566-in.^{3} Decoupling-Chamber Volume (1 V = 1 psi)

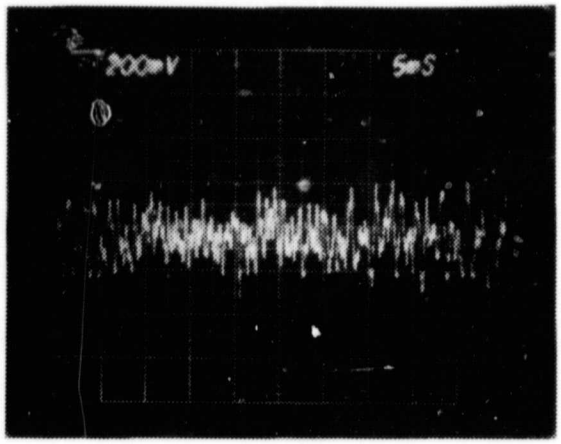

(a) Unfiltered
(1 unit vert. = 200 mV,
1 unit horiz. = 5 ms)

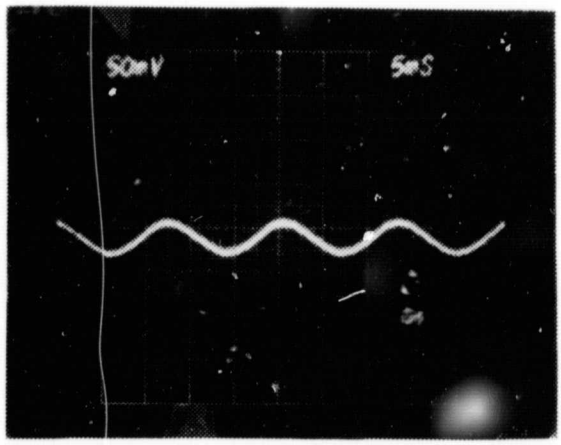

(b) 3% Filter
(1 unit vert. = 50 mV,
1 unit horiz. = 5 ms)

Fig. 8.3 Pressure Pulse in Air-Inlet Tee for a 944-in.^{3} Decoupling-Chamber Volume (1 V = 1 psi)

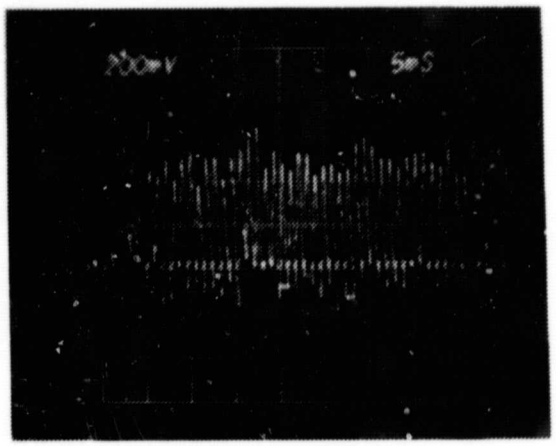

(a) Unfiltered
(1 unit vert. = 200 mV,
1 unit horiz. = 5 ms)

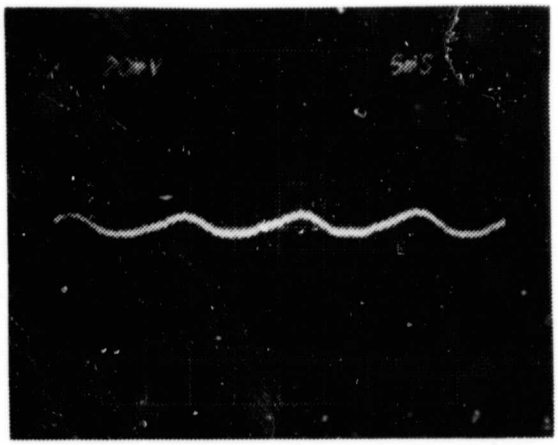

(b) 3% Filter
(1 unit vert. = 20 mV,
1 unit horiz. = 5 ms)

Fig. 8.4 Pressure Pulse in Air-Inlet Tee for a 1510-in.^{3} Decoupling-Chamber Volume (1 V = 1 psi)

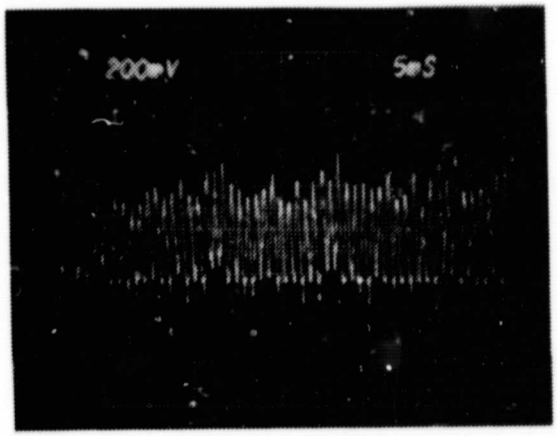

(a) Unfiltered
(1 unit vert. = 200 mV,
1 unit horiz. = 5 ms)

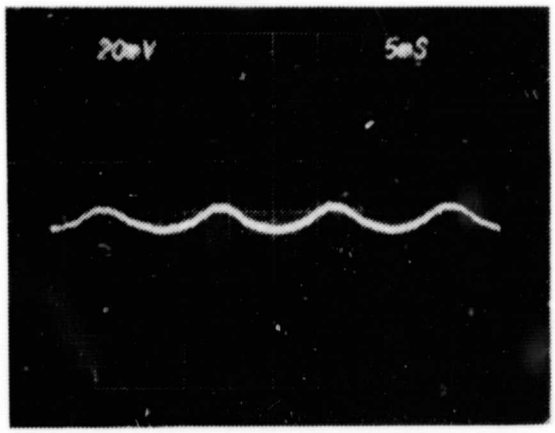

(b) 3% Filter
(1 unit vert. = 20 mV,
1 unit horiz. = 5 ms)

Fig. 8.5 Pressure Pulse in Air-Inlet Tee for a 2264-in.^{3} Decoupling-Chamber Volume (1 V = 1 psi)

Table 8.1 Performance Data for Three Inlet Configurations

Performance	Standard Burner	Burner with Inlet Muffler	Burner with Air-Decoupling Chamber
Heat input rate, Btu/h	100,941	101,532	100,794
Volumetric air/fuel rate	10.13	10.09	10.45
Frequency, Hz	74.0	79.0	76.0
Combustion-chamber pressure, psi	1.4	1.7	0.9
Heat-transfer rate from combustion chamber, Btu/h	19,169	22,688	19,333
Heat-transfer rate from tailpipe, Btu/h	36,798	43,434	47,812
Inlet noise level, dBA	93.5	90.1	89.8
Exhaust noise level, dBA	91.5	90.8	88.7

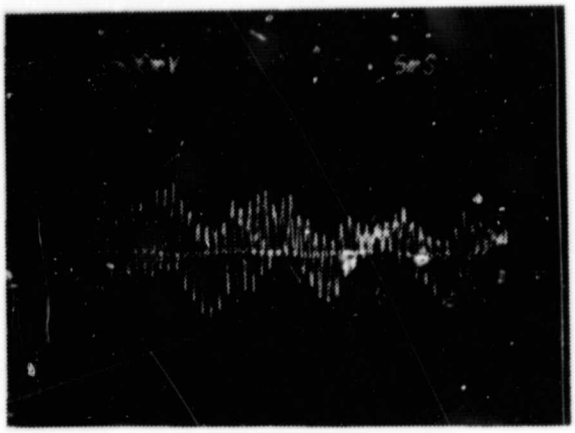

Unfiltered
(1 unit vert. = 500 mV,
1 unit horiz. = 5 ms)

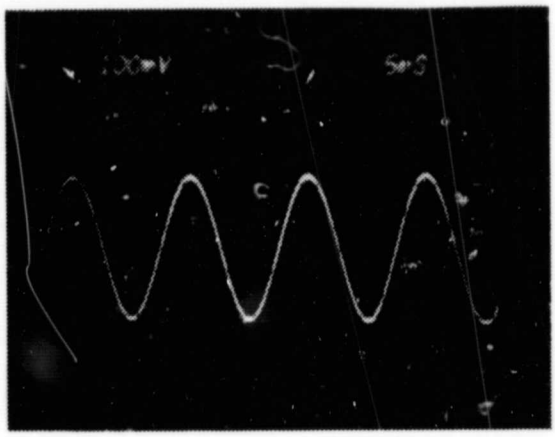

3% Filter
(1 unit vert. = 100 mV,
1 unit horiz. = 5 ms)

Zero-in.^{3} Chamber Volume

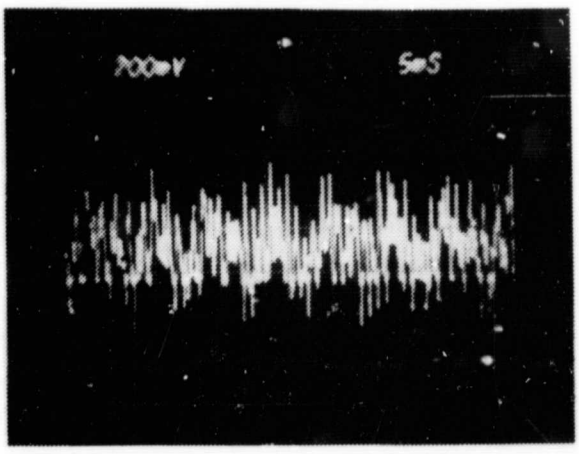

Unfiltered
(1 unit vert. = 200 mV,
1 unit horiz. = 5 ms)

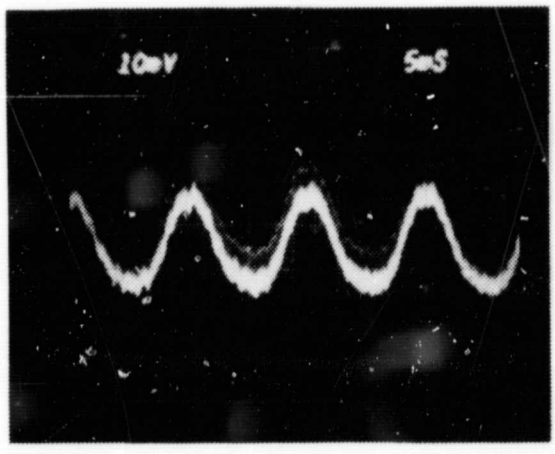

3% Filter
(1 unit vert. = 10 mV,
1 unit horiz. = 5 ms)

2406-in.^{3} Chamber Volume

Fig. 8.6 Air-Inlet-Tee Pressure Pulses for the Burner with an Inlet Decoupling Chamber, a 151,814 Btu/h Heat-Input Rate, a 9.8 Air/Fuel Ratio, and a 75-Hz Frequency

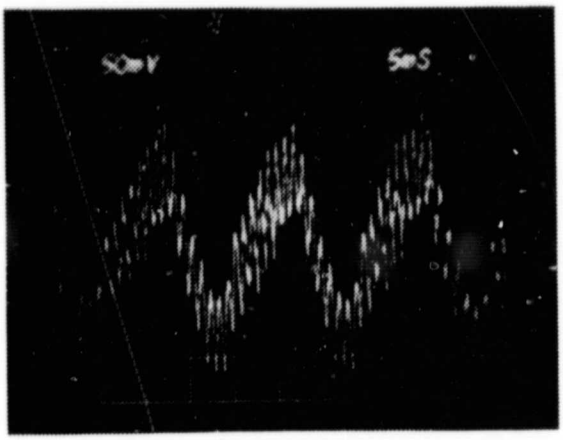

Unfiltered
(1 unit vert. = 50 mV,
1 unit horiz. = 5 ms)

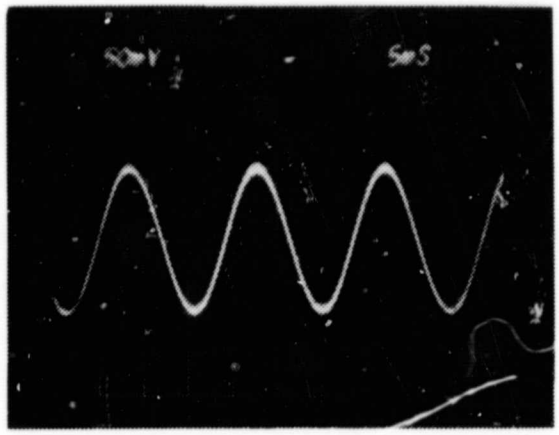

3% Filter
(1 unit vert. = 50 mV,
1 unit horiz. = 5 ms)

Zero-in.^{3} Chamber Volume

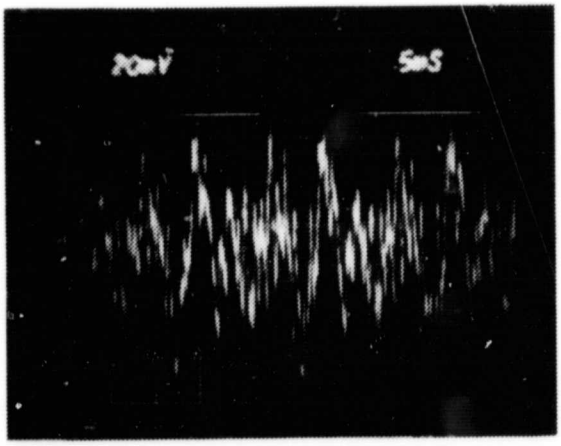

Unfiltered
(1 unit vert. = 20 mV,
1 unit horiz. = 5 ms)

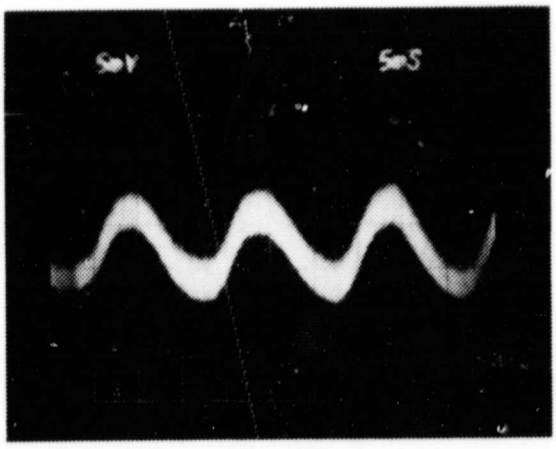

3% Filter
(1 unit vert. = 5 mV,
1 unit horiz. = 5 ms)

2830-in.^{3} Chamber Volume

Fig. 8.7 Air-Inlet-Tee Pressure Pulses for the Burner with an Inlet Decoupling Chamber, a 49,160 Btu/h Heat Input Rate, a 10.1 Air/Fuel Ratio, and a 70-Hz Frequency

9 CONCLUSIONS AND RECOMMENDATIONS FOR FUTURE STUDIES

9.1 CONCLUSIONS

A survey of pertinent literature on pulse combustion has revealed the diversity of the equipment, fuels, and studies. There has been no unification of these efforts, and conflicting results exist. Applications of pulse combustors for space heating are appearing; however, it appears that the trial-and-error approach and repeated testing, instead of the application of theory, was required for these developments. The literature survey was biased toward experimental studies and applications rather than theory. Additional information on pulse combustion theory is included in Winiarski[82,83]; Edelman, Turan, and France;[84] and Chiu.[85] Also of interest is the work of Kitchen[86] on pulsating-combustion chambers.

The ANL experiments, performed with a Helmholtz-type pulse combustion burner, demonstrated the enhanced heat-transfer capability of this type of combustor. Reliable operation was achieved for a range of heat inputs, air/fuel ratios, and geometrical configurations. However, a number of problem areas still exist: The high carbon monoxide content of the exhaust gas, the structurally emitted noise, the lack of tailpipe heat-transfer enhancement by the corebustor, and the difficulty of finding the appropriate gas temperature for predicting the acoustic velocity. These areas and others related to the close-coupled nature of pulse combustors will require more systematic research and study than the more common performance evaluations undertaken thus far have given them.

9.2 RECOMMENDATIONS FOR FUTURE STUDIES

Even though the pulse combustion phenomenon has been known for about three quarters of a century and numerous investigations have been conducted, detailed understanding of this mode of combustion and ability to design and predict the performance of these combustors are still lacking. To alleviate this situation, a well-instrumented experimental program (in conjunction with analytical modeling) is required. Such a program should include, but not be limited to, the following:

- Characterization of the three basic types of pulse combustors (Reynst tube, Schmidt tube, and Helmholtz combustor), delineating their differences, advantages and disadvantages, potential applications, limitations, etc. (For completeness, the Rijke tube should also be included.)

- Determination, for each type of burner, of its performance with solid, liquid, or gaseous fuels. Specifically, determine the techniques of supplying the fuel to the combustor, its limitations, the air requirements, and the combustor configuration.

- Determination of the limits of air and fuel preheating and the limits of self-aspiration.

- Determination of the effects of combustor geometry and peripherals (such as the size and shape of the combustion chamber, the type of valving, the size and shape of resonance tubes, size of decoupling chambers, type of secondary heat exchangers, use of flame holders, presence of multiple inlets or exhausts, etc.).

- Improved understanding of noise generation and improved techniques for attenuation of noise.

- Characterization of valving requirements and development of methods for the design and performance evaluation of aerodynamic and flapper valves.

- Investigation of the kinetics of combustion for the three classes of fuels.

- Determination of the effects of combustor coupling.

- Development of analytical models, both detailed and simplified, for the combustors.

- Investigation of effects of horizontal and vertical position on combustor performance.

- Determination of limits of convective and radiative heat transfer.

The experimental program should be well planned and the combustor designed to obtain data required for analytical models. Ease and completeness of data acquisition will be important design criteria, as will the ability to change components. Experimental measurements should be taken continuously, should be time-relatable, and (as a minimum) should include:

- Frequency.

- Air/fuel ratio.

- Air and fuel flow rates.

- Fuel analysis.
- Exhaust-gas analysis (in combustion chamber and at a minimum of three locations in tailpipe).
- Exhaust-gas temperatures.
- Noise measurements.
- Pressure measurements (at air and fuel inlets, at two locations in the combustion chamber, and at a minimum of four tailpipe positions).
- Heat-transfer measurements, both convective and radiative.
- Burner wall temperatures.

A program like that outlined here would require a considerable investment in equipment and instrumentation and several years of effort. Anything short of such an investigation would probably result in just another study to be added to the existing list. Prior to the start of such a program, a detailed review of all available literature should be conducted. This report includes such a survey for a significant portion of the published investigations, but it lacks a review of the studies related to propulsion. Undoubtedly there are some important unpublished works that are still considered proprietary. The existing literature should form a basis for the design of the combustors and planning of the experiments.

APPENDIX A: DRAWINGS

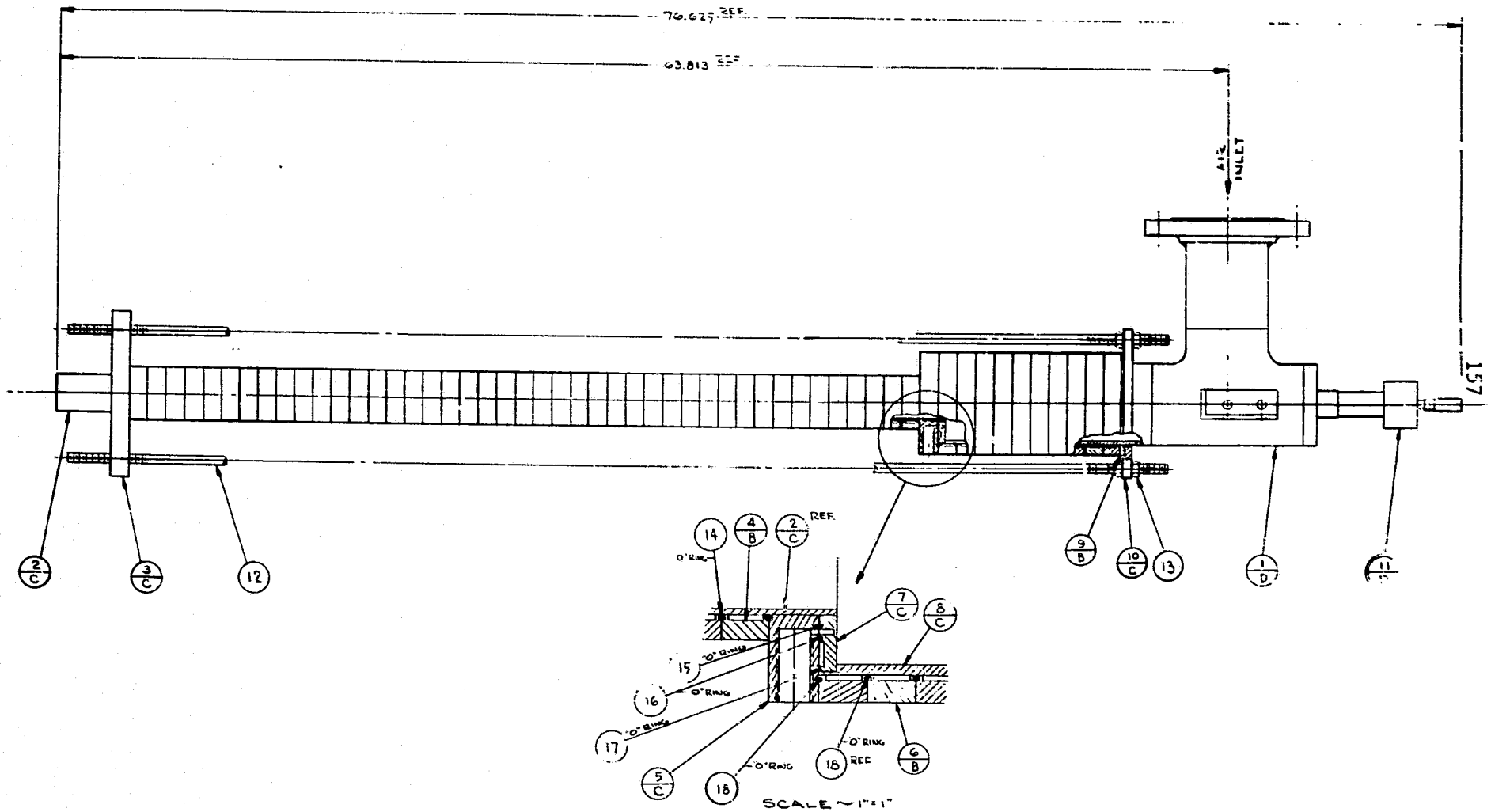

Pulse Combustion Burner Assembly

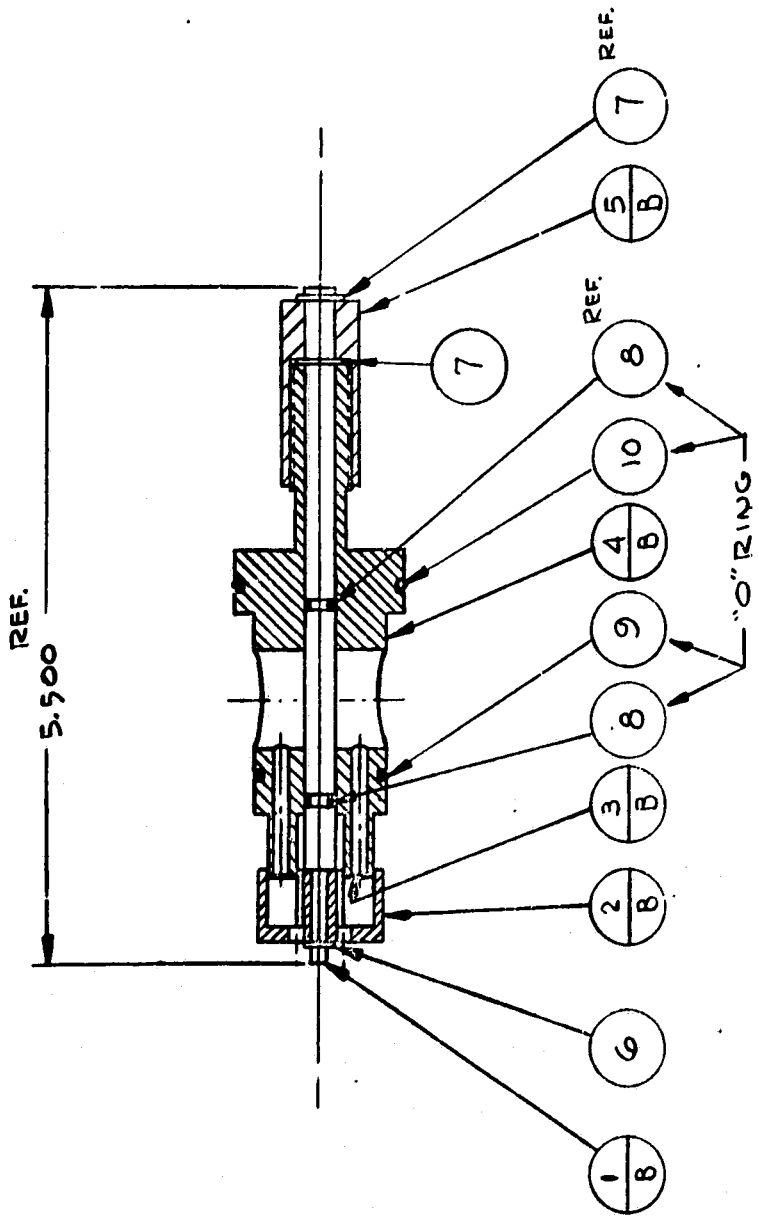

Gas-Valve Assembly

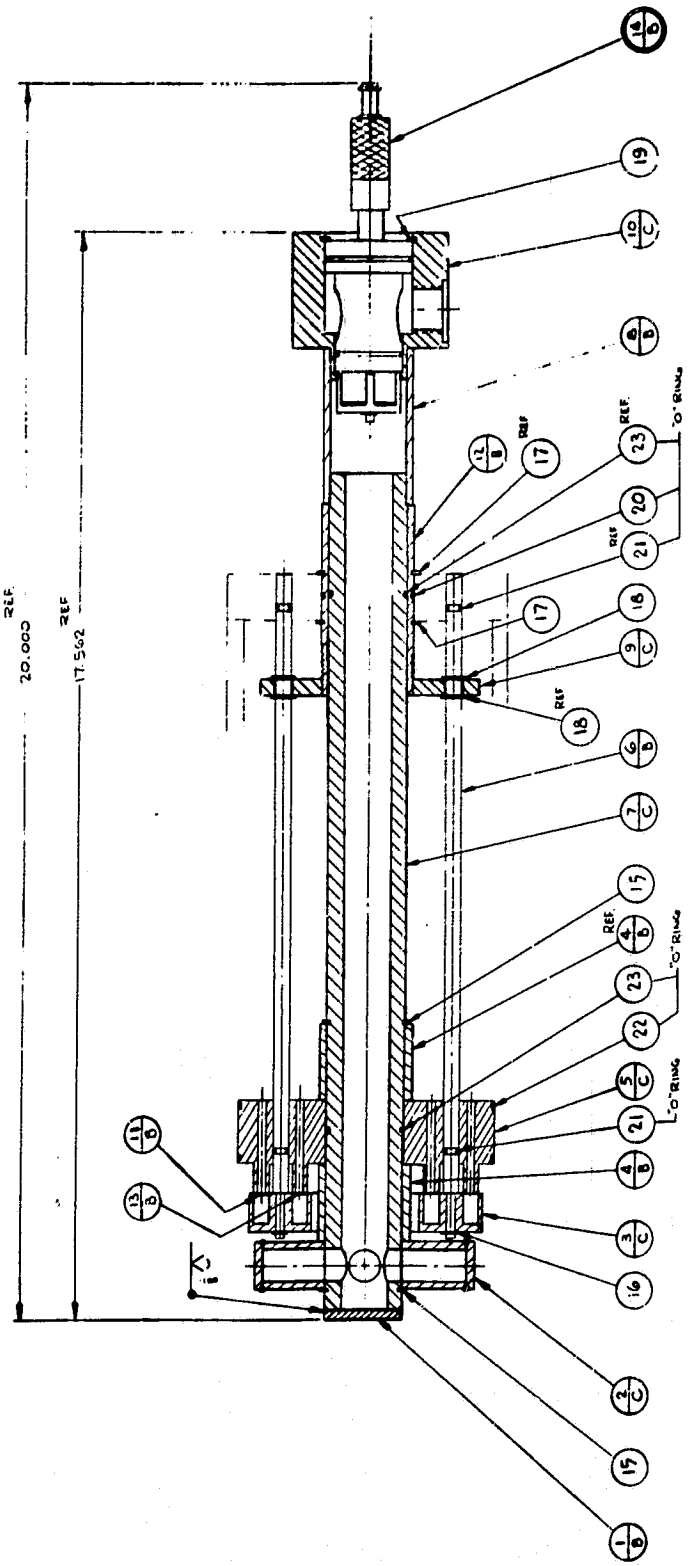

Gas- and Air-Valve Assembly

APPENDIX B

SELECTED EXPERIMENTAL DATA

A typical set of data obtained using the ANL experimental pulse combustion burner follows. A cooling-channel set covers nine cooling channels for which flow measurements were taken. Six channel sets were taken per test. The number of data sets varied for each cooling-channel set. The data are for the standard burner with a heat-input rate of 103,576 Btu/h, an air/fuel ratio of 10.12, and an operating frequency of 75.5 Hz.

PULSE COMBUSTION BURNER OPERATING TEMPERATURES,FLOWS AND Q'S.
RUN # : 28 DATE : 12/ 5/80 TIME : 12:18:25 PAGE # 11
COOLING CHANNEL SET : 1 DATA SET : 6

CHNL	FLOW (LB/HR)	OUTPUT (DEG.F)	EX.GAS (DEG.F)	INLET (DEG.F)	WALL (DEG.F)	DELTA (DEG.F)	(Q)
54	0.0001	204.9	0.0	190.5	0.0	14.4	0.0
53	0.0001	200.0	363.7	174.9	0.0	25.1	0.0
52	0.0001	194.0	0.0	172.1	0.0	21.9	0.0
51	0.0001	190.5	0.0	171.6	0.0	18.9	0.0
50	0.0001	186.4	0.0	168.8	0.0	17.6	0.0
49	46.350	190.6	0.0	173.5	260.2	17.1	792.6
48	0.0001	194.3	0.0	172.7	0.0	21.6	0.0
47	0.0001	175.2	0.0	155.4	0.0	19.8	0.0
46	0.0001	173.3	0.0	152.8	0.0	20.5	0.0
45	0.0001	172.9	0.0	153.7	0.0	19.2	0.0
44	0.0001	169.7	0.0	152.0	0.0	17.7	0.0
43	46.350	175.9	2015.6	155.0	261.8	20.9	968.7
42	0.0001	173.6	0.0	151.5	0.0	22.1	0.0
41	0.0001	176.0	0.0	154.0	0.0	22.0	0.0
40	0.0001	154.0	0.0	133.1	0.0	20.9	0.0
39	0.0001	154.9	0.0	134.5	0.0	20.4	0.0
38	0.0001	153.0	0.0	131.2	0.0	21.8	0.0
37	46.350	154.2	1471.1	132.1	147.7	22.1	1024.3
36	0.0001	152.6	0.0	130.5	0.0	22.1	0.0
35	0.0001	134.7	0.0	109.5	0.0	25.2	0.0
34	0.0001	133.8	0.0	112.2	0.0	21.6	0.0
33	0.0001	135.2	0.0	114.1	0.0	21.1	0.0
32	0.0001	131.8	0.0	111.2	0.0	20.6	0.0
31	46.350	132.7	180.4	112.0	0.0	20.7	959.4
30	0.0001	131.4	0.0	93.7	0.0	37.7	0.0
29	0.0001	109.9	0.0	86.9	0.0	23.0	0.0
28	0.0001	112.5	0.0	90.0	0.0	22.5	0.0
27	0.0001	114.4	0.0	89.8	0.0	24.6	0.0
26	0.0001	111.4	0.0	88.7	0.0	22.7	0.0
25	46.350	112.3	0.0	91.9	180.4	20.4	945.5
24	0.0001	93.7	0.0	64.0	0.0	29.7	0.0
23	0.0001	86.8	0.0	63.7	0.0	23.1	0.0
22	0.0001	90.0	0.0	63.6	0.0	26.4	0.0
21	0.0001	89.7	0.0	63.5	0.0	26.2	0.0
20	0.0001	89.2	0.0	64.0	0.0	25.2	0.0
19	46.350	92.1	60.4	63.9	0.0	28.2	1307.1
18	0.0001	112.1	0.0	105.0	0.0	9.1	0.0
17	0.0001	127.6	0.0	116.4	0.0	11.2	0.0
16	0.0001	134.0	0.0	115.7	0.0	18.3	0.0
15	0.0001	117.4	0.0	105.2	0.0	12.2	0.0
14	0.0001	122.5	0.0	109.3	0.0	13.2	0.0
13	88.278	118.0	663.9	103.4	0.0	14.6	1288.9
12	0.0001	102.5	0.0	84.4	0.0	18.1	0.0
11	0.0001	116.7	0.0	90.5	0.0	26.2	0.0
10	0.0001	116.7	0.0	96.7	0.0	20.0	0.0
9	0.0001	105.9	0.0	89.0	0.0	16.9	0.0
8	0.0001	109.8	2026.3	89.2	109.5	20.6	0.0
7	88.278	104.6	0.0	86.5	0.0	18.1	1597.8
6	0.0001	84.8	0.0	63.9	0.0	20.9	0.0
5	0.0001	90.9	0.0	63.9	0.0	27.0	0.0
4	0.0001	98.0	0.0	63.8	88.0	34.2	0.0
3	0.0001	89.3	0.0	63.8	0.0	25.5	0.0
2	0.0001	89.8	0.0	63.7	0.0	26.1	0.0
1	88.278	86.5	0.0	63.7	0.0	22.8	2012.7

*** PULSE COMBUSTION BURNER ***

(FLOWS,PRESSURES AND MISCELLANEOUS TEMPERATURES)

RUN # : 28 DATE : 12/ 5/80 TIME : 12:18:25 PAGE # 12
COOLING CHANNEL SET : 1 DATA SET : 6

FLOWS :	LEGEND	VALUE	UNITS
GROUP 'C'	FM1	5.584	GPH
GROUP 'B'	FM2		GPH
GROUP 'A'	FM3	10.636	GPH
AIR	FM3	977.31	CFH
GAS	FM4	98.31	CFH

PRESSURE :	LEGEND	VALUE	UNITS
AIR PRESSURE	AP		PSI
GAS SUPPLY TUBE PRESSURE	GSP		PSI
GAS PRESSURE	GP		PSI
GAS DELIVERY TUBE PRESSURE	GDT		PSI

TEMPERATURES :	LEGEND	VALUE	UNITS
AIR TEMPERATURE	AT	0.0	DEG.F
GAS DELIVERY TUBE TEMPERATURE	GDT	70.4	DEG.F
WATER SUPPLY TEMPERATURE	WST	62.9	DEG.F
WATER RETURN TEMPERATURE	WRT	115.9	DEG.F
ROOM TEMPERATURE	RT	56.3	DEG.F

MECHANICAL :	LEGEND	VALUE	UNITS
AIR VALVE LIFT	AVL	.014	INCH
GAS VALVE LIFT	GVL	0.000	INCH

MISCELLANEOUS :	LEGEND	VALUE	UNITS
CHAMBER HEIGHT		9.625	INCH
CHAMBER DIAMETER (ID)		4.0	INCH
TAILPIPE LENGTH		48.375	INCH
TAILPIPE DIAMETER		1.75	INCH
AIR/FUEL RATIO	A/F	9.9/1	
INPUT		100669.5	BTU/HR

PULSE COMBUSTION BURNER OPERATING TEMPERATURES,FLOWS AND Q'S.
RUN # : 28 DATE : 12/ 5/80 TIME : 12:24:26 PAGE # 32
COOLING CHANNEL SET : 2 DATA SET : 6

CHNL	FLOW (LB/HR)	OUTPUT (DEG.F)	EX.GAS (DEG.F)	INLET (DEG.F)	WALL (DEG.F)	DELTA (DEG.F)	(Q)
54	0.0001	213.4	0.0	198.8	0.0	14.6	0.0
53	0.0001	203.3	314.8	179.2	0.0	24.3	0.0
52	0.0001	197.1	0.0	175.0	0.0	22.1	0.0
51	0.0001	195.4	0.0	175.6	0.0	19.8	0.0
50	42.4421	193.1	0.0	174.0	0.0	19.1	830.7
49	0.0001	193.2	0.0	175.1	266.0	18.1	0.0
48	0.0001	203.6	0.0	180.4	0.0	23.2	0.0
47	0.0001	180.1	0.0	159.5	0.0	20.6	0.0
46	0.0001	176.2	0.0	155.4	0.0	20.8	0.0
45	0.0001	177.1	0.0	157.5	0.0	19.8	0.0
44	42.4421	175.5	0.0	157.0	0.0	18.5	785.2
43	0.0001	175.7	1011.7	154.0	240.5	21.7	0.0
42	0.0001	182.2	0.0	158.9	0.0	23.3	0.0
41	0.0001	160.4	0.0	137.0	0.0	23.4	0.0
40	0.0001	156.6	0.0	134.6	0.0	22.0	0.0
39	0.0001	158.7	0.0	137.1	0.0	21.6	0.0
38	42.4421	158.4	0.0	135.1	0.0	23.3	988.9
37	0.0001	155.2	1465.2	132.6	148.8	22.6	0.0
36	0.0001	160.6	0.0	136.9	0.0	23.7	0.0
35	0.0001	138.0	0.0	111.7	0.0	26.3	0.0
34	0.0001	135.1	0.0	113.3	0.0	21.8	0.0
33	0.0001	137.9	0.0	116.3	0.0	21.6	0.0
32	42.4421	135.8	0.0	114.4	0.0	21.4	908.3
31	0.0001	133.2	183.4	112.2	0.0	21.0	0.0
30	0.0001	138.2	0.0	97.2	0.0	41.0	0.0
29	0.0001	112.2	0.0	88.1	0.0	24.1	0.0
28	0.0001	113.6	0.0	90.2	0.0	23.4	0.0
27	0.0001	116.6	0.0	90.7	0.0	25.9	0.0
26	42.4421	114.8	0.0	90.4	0.0	24.4	1035.6
25	0.0001	112.6	0.0	91.6	183.4	21.0	0.0
24	0.0001	97.5	0.0	64.0	0.0	33.5	0.0
23	0.0001	87.9	0.0	63.8	0.0	24.1	0.0
22	0.0001	90.2	0.0	63.5	0.0	26.7	0.0
21	0.0001	90.7	0.0	63.5	0.0	27.2	0.0
20	42.4421	90.8	0.0	63.9	0.0	26.9	1141.7
19	0.0001	91.8	61.0	63.8	0.0	28.0	0.0
18	0.0001	113.6	0.0	104.1	0.0	9.5	0.0
17	0.0001	150.5	0.0	138.7	0.0	11.8	0.0
16	0.0001	139.4	0.0	119.9	0.0	19.5	0.0
15	0.0001	119.1	0.0	106.4	0.0	12.7	0.0
14	91.1791	123.0	0.0	109.4	0.0	13.6	1240.0
13	0.0001	120.1	1705.4	105.0	0.0	15.1	0.0
12	0.0001	103.7	0.0	85.1	0.0	18.6	0.0
11	0.0001	119.1	0.0	91.6	0.0	27.5	0.0
10	0.0001	121.0	0.0	99.3	0.0	21.7	0.0
9	0.0001	107.1	0.0	89.3	0.0	17.8	0.0
8	91.1791	110.2	2041.6	89.4	109.4	20.8	1896.5
7	0.0001	106.1	0.0	87.6	0.0	18.5	0.0
6	0.0001	85.4	0.0	63.9	0.0	21.5	0.0
5	0.0001	91.9	0.0	63.8	0.0	28.1	0.0
4	0.0001	100.1	0.0	63.9	89.4	36.2	0.0
3	0.0001	89.6	0.0	63.7	0.0	25.9	0.0
2	91.1791	89.8	0.0	63.7	0.0	26.1	2379.8
1	0.0001	87.6	0.0	63.7	0.0	23.9	0.0

*** PULSE COMBUSTION BURNER ***

(FLOWS,PRESSURES AND MISCELLANEOUS TEMPERATURES)

RUN # : 28 DATE : 12/ 5/80 TIME : 12:24:26 PAGE # 33
COOLING CHANNEL SET : 2 DATA SET : 6

FLOWS :	LEGEND	VALUE	UNITS
GROUP 'C'	FM1	5.114	GPH
GROUP 'B'	FM2		GPH
GROUP 'A'	FM5	10.985	GPH
AIR	FM3	1025.28	CFH
GAS	FM4	100.94	CFH

PRESSURE :	LEGEND	VALUE	UNITS
AIR PRESSURE	AP		PSI
GAS SUPPLY TUBE PRESSURE	GSP		PSI
GAS PRESSURE	GP		PSI
GAS DELIVERY TUBE PRESSURE	GDT		PSI

TEMPERATURES :	LEGEND	VALUE	UNITS
AIR TEMPERATURE	AT	0.0	DEG.F
GAS DELIVERY TUBE TEMPERATURE	GDT	71.9	DEG.F
WATER SUPPLY TEMPERATURE	WST	62.8	DEG.F
WATER RETURN TEMPERATURE	WRT	114.6	DEG.F
ROOM TEMPERATURE	RT	59.1	DEG.F

MECHANICAL :	LEGEND	VALUE	UNITS
AIR VALVE LIFT	AVL	.014	INCH
GAS VALVE LIFT	GVL	0.000	INCH

MISCELLANEOUS :	LEGEND	VALUE	UNITS
CHAMBER HEIGHT		9.625	INCH
CHAMBER DIAMETER (ID)		4.0	INCH
TAILPIPE LENGTH		48.375	INCH
TAILPIPE DIAMETER		1.75	INCH
AIR/FUEL RATIO	A/F	10.2/1	
INPUT		103362.8	BTU/HR

PULSE COMBUSTION BURNER OPERATING TEMPERATURES,FLOWS AND Q'S.
RUN # : 20 DATE : 12/ 5/80 TIME : 12:30:27 PAGE # 53
COOLING CHANNEL SET : 3 DATA SET : 6

CHNL	FLOW (LB/HR)	OUTPUT (DEG.F)	EX.GAS (DEG.F)	INLET (DEG.F)	WALL (DEG.F)	DELTA (DEG.F)	(Q)
54	0.0001	213.9	0.0	199.3	0.0	14.6	0.0
53	0.0001	209.9	306.8	184.7	0.0	25.2	0.0
52	0.0001	205.4	0.0	182.0	0.0	23.4	0.0
51	37.1481	202.2	0.0	181.4	0.0	20.8	772.7
50	0.0001	193.7	0.0	174.4	0.0	19.3	0.0
49	0.0001	194.4	0.0	176.3	267.6	18.1	0.0
48	0.0001	202.9	0.0	179.4	0.0	23.5	0.0
47	0.0001	185.2	0.0	164.0	0.0	21.2	0.0
46	0.0001	183.8	0.0	161.8	0.0	22.0	0.0
45	37.1481	183.1	0.0	162.5	0.0	20.6	765.2
44	0.0001	175.7	0.0	156.9	0.0	18.8	0.0
43	0.0001	176.5	1514.3	154.6	240.4	21.9	0.0
42	0.0001	180.3	0.0	156.4	0.0	23.9	0.0
41	0.0001	164.9	0.0	140.3	0.0	24.6	0.0
40	0.0001	163.3	0.0	139.8	0.0	23.5	0.0
39	37.1481	164.1	0.0	141.1	0.0	23.0	854.4
38	0.0001	157.9	0.0	134.5	0.0	23.4	0.0
37	0.0001	155.6	1465.0	132.7	149.1	22.9	0.0
36	0.0001	157.3	0.0	133.7	0.0	23.6	0.0
35	0.0001	141.1	0.0	114.0	0.0	27.1	0.0
34	0.0001	140.6	0.0	117.2	0.0	23.4	0.0
33	37.1481	142.2	0.0	119.5	0.0	22.7	843.3
32	0.0001	135.1	0.0	113.7	0.0	21.4	0.0
31	0.0001	133.3	183.3	112.2	0.0	21.1	0.0
30	0.0001	134.5	0.0	95.4	0.0	39.1	0.0
29	0.0001	114.5	0.0	89.2	0.0	25.3	0.0
28	0.0001	117.8	0.0	92.6	0.0	25.2	0.0
27	37.1481	119.9	0.0	92.2	0.0	27.7	1029.0
26	0.0001	114.1	0.0	89.9	0.0	24.2	0.0
25	0.0001	112.7	0.0	91.6	182.2	21.1	0.0
24	0.0001	95.5	0.0	65.9	0.0	29.6	0.0
23	0.0001	88.9	0.0	63.7	0.0	25.2	0.0
22	0.0001	92.6	0.0	63.6	0.0	29.0	0.0
21	37.1481	92.4	0.0	63.4	0.0	29.0	1077.3
20	0.0001	90.3	0.0	63.9	0.0	26.4	0.0
19	0.0001	91.8	61.4	63.7	0.0	28.1	0.0
18	0.0001	114.1	0.0	104.6	0.0	9.5	0.0
17	0.0001	131.3	0.0	119.4	0.0	11.9	0.0
16	0.0001	139.1	0.0	119.7	0.0	19.4	0.0
15	88.3861	119.8	0.0	106.8	0.0	13.0	1149.0
14	0.0001	124.1	0.0	110.2	0.0	13.9	0.0
13	0.0001	121.5	1683.9	105.8	0.0	15.7	0.0
12	0.0001	104.2	0.0	85.4	0.0	18.8	0.0
11	0.0001	119.7	0.0	91.9	0.0	27.8	0.0
10	0.0001	120.8	0.0	98.7	0.0	22.1	0.0
9	88.3861	107.5	0.0	89.6	0.0	17.9	1582.1
8	0.0001	110.9	2029.4	89.8	111.0	21.1	0.0
7	0.0001	107.0	0.0	88.4	0.0	18.6	0.0
6	0.0001	85.7	0.0	63.9	0.0	21.8	0.0
5	0.0001	92.2	0.0	63.7	0.0	28.5	0.0
4	0.0001	99.5	0.0	63.8	89.2	35.7	0.0
3	88.3861	89.8	0.0	63.7	0.0	26.1	2306.9
2	0.0001	90.3	0.0	63.7	0.0	26.6	0.0
1	0.0001	88.4	0.0	63.6	0.0	24.8	0.0

*** PULSE COMBUSTION BURNER ***

(FLOWS,PRESSURES AND MISCELLANEOUS TEMPERATURES)

RUN # : 28 DATE : 12/ 5/80 TIME : 12:30:27 PAGE # 54
COOLING CHANNEL SET : 3 DATA SET : 6

FLOWS :	LEGEND	VALUE	UNITS
GROUP "C"	FM1	4.476	GPH
GROUP "B"	FM2		GPH
GROUP "A"	FM5	10.649	GPH
AIR	FM3	1037.70	CFH
GAS	FM4	101.99	CFH

PRESSURE :	LEGEND	VALUE	UNITS
AIR PRESSURE	AP		PSI
GAS SUPPLY TUBE PRESSURE	GSP		PSI
GAS PRESSURE	GP		PSI
GAS DELIVERY TUBE PRESSURE	GDT		PSI

TEMPERATURES :	LEGEND	VALUE	UNITS
AIR TEMPERATURE	AT	0.0	DEG.F
GAS DELIVERY TUBE TEMPERATURE	GDT	73.8	DEG.F
WATER SUPPLY TEMPERATURE	WST	62.6	DEG.F
WATER RETURN TEMPERATURE	WRT	118.0	DEG.F
ROOM TEMPERATURE	RT	62.2	DEG.F

MECHANICAL :	LEGEND	VALUE	UNITS
AIR VALVE LIFT	AVL	.014	INCH
GAS VALVE LIFT	GVL	0.000	INCH

MISCELLANEOUS :	LEGEND	VALUE	UNITS
CHAMBER HEIGHT		9.625	INCH
CHAMBER DIAMETER (ID)		4.0	INCH
TAILPIPE LENGTH		48.375	INCH
TAILPIPE DIAMETER		1.75	INCH
AIR/FUEL RATIO	A/F	10.2/1	
INPUT		104433.6	BTU/HR

PULSE COMBUSTION BURNER OPERATING TEMPERATURES, FLOWS AND Q'S.
RUN # : 28 DATE : 12/ 5/80 TIME : 12:56:29 PAGE # 74
COOLING CHANNEL SET : 4 DATA SET : 6

CHNL	FLOW (LB/HR)	OUTPUT (DEG.F)	EX.GAS (DEG.F)	AMBT (DEG.F)	WALL (DEG.F)	DELTA (DEG.F)	(Q)
54	0.0001	215.6	0.0	200.8	0.0	14.8	0.0
53	0.0001	216.3	312.3	190.2	0.0	26.1	0.0
52	35.1821	211.9	0.0	187.6	0.0	24.3	854.9
51	0.0001	201.2	0.0	180.3	0.0	20.9	0.0
50	0.0001	195.6	0.0	176.1	0.0	19.5	0.0
49	0.0001	196.6	0.0	178.2	268.9	18.4	0.0
48	0.0001	205.3	0.0	181.6	0.0	23.7	0.0
47	0.0001	191.1	0.0	169.1	0.0	22.0	0.0
46	35.1821	189.7	0.0	166.9	0.0	22.8	802.2
45	0.0001	181.6	0.0	160.7	0.0	20.9	0.0
44	0.0001	177.3	0.0	158.4	0.0	18.9	0.0
43	0.0001	178.5	1305.8	156.3	242.0	22.2	0.0
42	0.0001	182.8	0.0	158.5	0.0	24.3	0.0
41	0.0001	170.1	0.0	144.6	0.0	25.5	0.0
40	35.1821	168.5	0.0	144.0	0.0	24.5	862.0
39	0.0001	161.8	0.0	139.0	0.0	22.8	0.0
38	0.0001	159.2	0.0	135.6	0.0	23.6	0.0
37	0.0001	157.2	1464.9	134.0	150.8	23.2	0.0
36	0.0001	160.0	0.0	135.7	0.0	24.3	0.0
35	0.0001	145.6	0.0	117.1	0.0	28.5	0.0
34	35.1821	145.5	0.0	120.8	0.0	24.7	869.0
33	0.0001	139.6	0.0	117.3	0.0	22.3	0.0
32	0.0001	136.1	0.0	114.6	0.0	21.5	0.0
31	0.0001	134.9	982.8	113.2	0.0	21.3	0.0
30	0.0001	136.8	0.0	96.7	0.0	40.1	0.0
29	0.0001	117.6	0.0	90.9	0.0	26.7	0.0
28	35.1821	121.2	0.0	94.7	0.0	26.5	952.3
27	0.0001	117.3	0.0	91.0	0.0	26.3	0.0
26	0.0001	114.8	0.0	90.3	0.0	24.5	0.0
25	0.0001	113.6	0.0	92.2	183.3	21.4	0.0
24	0.0001	96.7	0.0	63.9	0.0	32.8	0.0
23	0.0001	90.7	0.0	63.7	0.0	27.0	0.0
22	35.1821	94.8	0.0	63.3	0.0	31.5	1108.2
21	0.0001	91.0	0.0	63.3	0.0	27.7	0.0
20	0.0001	90.6	0.0	63.7	0.0	26.9	0.0
19	0.0001	92.4	61.5	63.6	0.0	28.8	0.0
18	0.0001	114.2	0.0	104.6	0.0	9.6	0.0
17	0.0001	133.1	0.0	120.9	0.0	12.2	0.0
16	52.7241	139.7	0.0	120.1	0.0	19.6	1033.4
15	0.0001	119.8	0.0	106.8	0.0	13.0	0.0
14	0.0001	124.7	0.0	110.8	0.0	13.9	0.0
13	0.0001	121.7	1707.3	106.2	0.0	15.5	0.0
12	0.0001	104.2	0.0	85.4	0.0	18.8	0.0
11	0.0001	121.2	0.0	92.8	0.0	28.4	0.0
10	52.7241	121.2	0.0	99.1	0.0	22.1	1165.2
9	0.0001	107.4	0.0	89.5	0.0	17.9	0.0
8	0.0001	111.4	2034.2	90.2	110.8	21.2	0.0
7	0.0001	107.3	0.0	88.6	0.0	18.7	0.0
6	0.0001	85.6	0.0	63.8	0.0	21.8	0.0
5	0.0001	93.0	0.0	63.7	0.0	29.3	0.0
4	52.7241	99.9	0.0	63.8	89.4	36.1	1903.3
3	0.0001	89.6	0.0	63.6	0.0	26.0	0.0
2	0.0001	90.5	0.0	63.6	0.0	26.9	0.0
1	0.0001	88.6	0.0	63.6	0.0	25.0	0.0

*** PULSE COMBUSTION BURNER ***

(FLOWS,PRESSURES AND MISCELLANEOUS TEMPERATURES)

RUN # : 28 DATE : 12/ 5/80 TIME : 12:36:29 PAGE # 75
COOLING CHANNEL SET : 4 DATA SET : 6

FLOWS :	LEGEND	VALUE	UNITS
GROUP 'C'	FM1	4.239	GPH
GROUP 'B'	FM2		GPH
GROUP 'A'	FM5	6.352	GPH
AIR	FM3	1032.60	CFH
GAS	FM4	101.38	CFH

PRESSURE :	LEGEND	VALUE	UNITS
AIR PRESSURE	AP		PSI
GAS SUPPLY TUBE PRESSURE	GSP		PSI
GAS PRESSURE	GP		PSI
GAS DELIVERY TUBE PRESSURE	GDT		PSI

TEMPERATURES :	LEGEND	VALUE	UNITS
AIR TEMPERATURE	AT	0.0	DEG.F
GAS DELIVERY TUBE TEMPERATURE	GDT	75.3	DEG.F
WATER SUPPLY TEMPERATURE	WST	62.6	DEG.F
WATER RETURN TEMPERATURE	WRT	115.6	DEG.F
ROOM TEMPERATURE	RT	64.0	DEG.F

MECHANICAL :	LEGEND	VALUE	UNITS
AIR VALVE LIFT	AVL	.014	INCH
GAS VALVE LIFT	GVL	0.000	INCH

MISCELLANEOUS :	LEGEND	VALUE	UNITS
CHAMBER HEIGHT		9.625	INCH
CHAMBER DIAMETER (ID)		4.0	INCH
TAILPIPE LENGTH		48.375	INCH
TAILPIPE DIAMETER		1.75	INCH
AIR/FUEL RATIO	A/F	10.2/1	
INPUT		103817.1	BTU/HR

PULSE COMBUSTION BURNER OPERATING TEMPERATURES,FLOWS AND Q'S.
RUN # : 28 DATE : 12/ 5/80 TIME : 12:42:30 PAGE # 95
COOLING CHANNEL SET : 5 DATA SET : 6

CHNL	FLOW (LB/HR)	OUTPUT (DEG.F)	EX.GAS (DEG.F)	INLET (DEG.F)	WALL (DEG.F)	DELTA (DEG.F)	(Q)
54	0.0001	220.1	0.0	207.7	0.0	12.4	0.0
53	35.0721	223.9	301.0	197.1	0.0	26.8	939.9
52	0.0001	214.5	0.0	190.0	0.0	24.5	0.0
51	0.0001	201.7	0.0	180.5	0.0	21.2	0.0
50	0.0001	197.6	0.0	177.4	0.0	20.2	0.0
49	0.0001	200.8	0.0	181.7	272.9	19.1	0.0
48	0.0001	211.8	0.0	187.2	0.0	24.6	0.0
47	35.0721	198.5	0.0	175.4	0.0	23.1	810.2
46	0.0001	192.3	0.0	168.9	0.0	23.4	0.0
45	0.0001	182.0	0.0	160.9	0.0	21.1	0.0
44	0.0001	179.0	0.0	159.6	0.0	19.4	0.0
43	0.0001	182.5	309.7	159.1	246.3	23.2	0.0
42	0.0001	188.6	0.0	163.0	0.0	25.6	0.0
41	35.0721	176.9	0.0	150.0	0.0	26.9	943.4
40	0.0001	170.5	0.0	145.4	0.0	25.1	0.0
39	0.0001	162.2	0.0	139.1	0.0	23.1	0.0
38	0.0001	160.7	0.0	136.7	0.0	24.0	0.0
37	0.0001	160.3	463.8	136.1	233.7	24.2	0.0
36	0.0001	164.3	0.0	138.7	0.0	25.6	0.0
35	35.0721	153.4	0.0	123.0	0.0	30.4	1066.2
34	0.0001	146.4	0.0	121.3	0.0	25.1	0.0
33	0.0001	139.8	0.0	117.4	0.0	22.4	0.0
32	0.0001	137.3	0.0	115.3	0.0	22.0	0.0
31	0.0001	136.7	195.6	114.7	0.0	22.0	0.0
30	0.0001	139.6	0.0	98.0	0.0	41.6	0.0
29	35.0721	121.8	0.0	93.1	0.0	28.7	1006.6
28	0.0001	122.0	0.0	95.0	0.0	27.0	0.0
27	0.0001	117.7	0.0	91.1	0.0	26.6	0.0
26	0.0001	115.6	0.0	90.8	0.0	24.8	0.0
25	0.0001	115.2	0.0	93.3	183.4	21.9	0.0
24	0.0001	98.0	0.0	64.0	0.0	34.0	0.0
23	35.0721	93.0	0.0	63.6	0.0	29.4	1031.1
22	0.0001	95.0	0.0	63.4	0.0	31.6	0.0
21	0.0001	91.1	0.0	63.2	0.0	27.9	0.0
20	0.0001	91.1	0.0	63.8	0.0	27.3	0.0
19	0.0001	93.5	61.7	63.6	0.0	29.9	0.0
18	0.0001	114.2	0.0	104.5	0.0	9.7	0.0
17	88.6001	129.9	0.0	118.1	0.0	11.8	1045.5
16	0.0001	140.9	0.0	121.0	0.0	19.9	0.0
15	0.0001	120.2	0.0	106.9	0.0	13.3	0.0
14	0.0001	125.0	0.0	111.0	0.0	14.0	0.0
13	0.0001	122.2	1714.3	106.4	0.0	15.8	0.0
12	0.0001	104.2	0.0	85.2	0.0	19.0	0.0
11	88.6001	118.3	0.0	90.8	0.0	27.5	2436.5
10	0.0001	122.0	0.0	99.6	0.0	22.4	0.0
9	0.0001	107.6	0.0	89.6	0.0	18.0	0.0
8	0.0001	111.6	1996.8	90.2	111.5	21.4	0.0
7	0.0001	107.4	0.0	88.9	0.0	18.5	0.0
6	0.0001	85.4	0.0	63.7	0.0	21.7	0.0
5	88.6001	91.0	0.0	63.7	0.0	27.3	2418.8
4	0.0001	100.2	0.0	63.7	89.7	36.5	0.0
3	0.0001	89.7	0.0	63.6	0.0	26.1	0.0
2	0.0001	90.7	0.0	63.6	0.0	27.1	0.0
1	0.0001	88.7	0.0	63.5	0.0	25.2	0.0

(PC2)

*** PULSE COMBUSTION BURNER ***

(FLOWS,PRESSURES AND MISCELLANEOUS TEMPERATURES)

RUN # : 28 DATE : 12/ 5/80 TIME : 12:42:30 PAGE # 96
COOLING CHANNEL SET : 5 DATA SET : 6

FLOWS :	LEGEND	VALUE	UNITS
GROUP 'C'	FM1	4.226	GPH
GROUP 'B'	FM2		GPH
GROUP 'A'	FM5	10.675	GPH
AIR	FM3	1033.62	CFH
GAS	FM4	102.02	CFH

PRESSURE :	LEGEND	VALUE	UNITS
AIR PRESSURE	AP		PSI
GAS SUPPLY TUBE PRESSURE	GSP		PSI
GAS PRESSURE	GP		PSI
GAS DELIVERY TUBE PRESSURE	GDT		PSI

TEMPERATURES :	LEGEND	VALUE	UNITS
AIR TEMPERATURE	AT	0.0	DEG.F
GAS DELIVERY TUBE TEMPERATURE	GDT	76.5	DEG.F
WATER SUPPLY TEMPERATURE	WST	62.5	DEG.F
WATER RETURN TEMPERATURE	WRT	118.9	DEG.F
ROOM TEMPERATURE	RT	65.1	DEG.F

MECHANICAL :	LEGEND	VALUE	UNITS
AIR VALVE LIFT	AVL	.014	INCH
GAS VALVE LIFT	GVL	0.000	INCH

MISCELLANEOUS :	LEGEND	VALUE	UNITS
CHAMBER HEIGHT		9.625	INCH
CHAMBER DIAMETER (ID)		4.0	INCH
TAILPIPE LENGTH		48.375	INCH
TAILPIPE DIAMETER		1.75	INCH
AIR/FUEL RATIO	A/F	10.1/1	
INPUT		104466.1	BTU/HR

PULSE COMBUSTION BURNER OPERATING TEMPERATURES,FLOWS AND Q'S.
RUN # : 28 DATE : 12/ 5/80 TIME : 12:48:31 PAGE #116
COOLING CHANNEL SET : 6 DATA SET : 6

CHNL	FLOW (LB/HR)	OUTPUT (DEG.F)	EX.GAS (DEG.F)	INLET (DEG.F)	WALL (DEG.F)	DELTA (DEG.F)	(Q)
54	30.2081	229.6	0.0	220.4	0.0	9.2	277.9
53	0.0001	232.4	300.6	204.7	0.0	27.7	0.0
52	0.0001	222.6	0.0	196.8	0.0	25.8	0.0
51	0.0001	208.6	0.0	186.4	0.0	22.2	0.0
50	0.0001	202.8	0.0	181.4	0.0	21.4	0.0
49	0.0001	207.0	0.0	187.0	278.6	20.0	0.0
48	30.2081	227.5	0.0	200.8	0.0	26.7	806.6
47	0.0001	207.0	0.0	182.6	0.0	24.4	0.0
46	0.0001	200.2	0.0	175.0	0.0	25.2	0.0
45	0.0001	188.3	0.0	166.1	0.0	22.2	0.0
44	0.0001	183.2	0.0	163.2	0.0	20.1	0.0
43	0.0001	187.5	349.2	163.2	211.9	24.3	0.0
42	30.2081	205.6	0.0	176.0	0.0	27.6	833.7
41	0.0001	184.6	0.0	156.2	0.0	28.4	0.0
40	0.0001	177.4	0.0	150.7	0.0	26.7	0.0
39	0.0001	167.6	0.0	143.3	0.0	24.3	0.0
38	0.0001	164.4	0.0	139.2	0.0	25.2	0.0
37	0.0001	164.4	461.0	138.8	197.8	25.6	0.0
36	30.2081	178.3	0.0	150.6	0.0	27.7	836.8
35	0.0001	157.9	0.0	125.0	0.0	32.9	0.0
34	0.0001	152.5	0.0	125.5	0.0	27.0	0.0
33	0.0001	144.2	0.0	120.4	0.0	23.8	0.0
32	0.0001	139.8	0.0	117.1	0.0	22.7	0.0
31	0.0001	139.4	192.6	116.4	0.0	23.0	0.0
30	30.2081	152.1	0.0	105.7	0.0	48.4	1462.1
29	0.0001	126.0	0.0	95.2	0.0	30.8	0.0
28	0.0001	126.8	0.0	97.5	0.0	29.3	0.0
27	0.0001	120.7	0.0	92.6	0.0	28.1	0.0
26	0.0001	117.5	0.0	91.7	0.0	25.8	0.0
25	0.0001	116.7	0.0	93.8	188.0	22.9	0.0
24	30.2081	104.4	0.0	64.1	0.0	40.3	1217.4
23	0.0001	95.2	0.0	63.7	0.0	31.5	0.0
22	0.0001	97.9	0.0	63.4	0.0	34.5	0.0
21	0.0001	92.8	0.0	63.2	0.0	29.6	0.0
20	0.0001	92.0	0.0	63.7	0.0	28.3	0.0
19	0.0001	93.9	62.0	63.6	0.0	30.3	0.0
18	100.9531	114.2	0.0	104.6	0.0	9.6	969.1
17	0.0001	151.3	0.0	139.5	0.0	11.8	0.0
16	0.0001	141.9	0.0	121.9	0.0	20.0	0.0
15	0.0001	120.2	0.0	107.0	0.0	13.2	0.0
14	0.0001	125.2	0.0	110.8	0.0	14.2	0.0
13	0.0001	122.3	214.3	106.2	0.0	15.8	0.0
12	100.9531	104.1	0.0	85.3	0.0	18.8	1897.9
11	0.0001	119.8	0.0	91.1	0.0	28.7	0.0
10	0.0001	123.0	0.0	100.0	0.0	23.0	0.0
9	0.0001	107.7	0.0	89.4	0.0	18.3	0.0
8	0.0001	111.7	2050.6	90.3	110.5	21.4	0.0
7	0.0001	107.6	0.0	88.9	0.0	18.7	0.0
6	100.9531	85.6	0.0	63.7	0.0	21.9	2210.9
5	0.0001	91.3	0.0	63.6	0.0	27.7	0.0
4	0.0001	100.6	0.0	63.7	89.9	36.9	0.0
3	0.0001	89.6	0.0	63.6	0.0	26.0	0.0
2	0.0001	90.7	0.0	63.5	0.0	27.2	0.0
1	0.0001	88.8	0.0	63.5	0.0	25.3	0.0

*** PULSE COMBUSTION BURNER ***

(FLOWS,PRESSURES AND MISCELLANEOUS TEMPERATURES)

RUN # : 28 DATE : 12/ 5/80 TIME : 12:48:31 PAGE #117
COOLING CHANNEL SET : 6 DATA SET : 6

FLOWS :	LEGEND	VALUE	UNITS
GROUP 'C'	FM1	5.640	GPH
GROUP 'B'	FM2		GPH
GROUP 'A'	FM3	12.163	GPH
AIR	FM3	1033.11	CFH
GAS	FM4	102.26	CFH

PRESSURE :	LEGEND	VALUE	UNITS
AIR PRESSURE	AP		PSI
GAS SUPPLY TUBE PRESSURE	GSP		PSI
GAS PRESSURE	GP		PSI
GAS DELIVERY TUBE PRESSURE	GDT		PSI

TEMPERATURES :	LEGEND	VALUE	UNITS
AIR TEMPERATURE	AT	0.0	DEG.F
GAS DELIVERY TUBE TEMPERATURE	GDT	77.4	DEG.F
WATER SUPPLY TEMPERATURE	WST	62.5	DEG.F
WATER RETURN TEMPERATURE	WRT	115.3	DEG.F
ROOM TEMPERATURE	RT	65.7	DEG.F

MECHANICAL :	LEGEND	VALUE	UNITS
AIR VALVE LIFT	AVL	.014	INCH
GAS VALVE LIFT	GVL	0.000	INCH

MISCELLANEOUS :	LEGEND	VALUE	UNITS
CHAMBER HEIGHT		9.625	INCH
CHAMBER DIAMETER (ID)		4.0	INCH
TAILPIPE LENGTH		48.375	INCH
TAILPIPE DIAMETER		1.75	INCH
AIR/FUEL RATIO	A/F	10.1/1	
INPUT		104709.4	BTU/HR

APPENDIX C

FORTRAN PROGRAM FOR ANALYSIS OF HEAT-TRANSFER DATA

The computer program listed in this section was developed by F.W. Ahrens as an aid in data reduction and to help in preliminary analysis. Basically, the program consists of the following:

- Input of pertinent dimensions, excess-air factor, fuel flow rate, combustion-chamber pressure, and the heat rate for each of the 54 cooling channels.
- Assumption of complete methane combustion.
- Treatment of radiative heat transfer as described in Sec. 6.2.
- Temperature of gas entering the tailpipe was 3500°R.
- Treatment of combustion-chamber heat transfer as one section (the tailpipe heat transfer is treated on a local basis per cooling-channel section).
- Assumption that radiating gas temperature in the combustion chamber was 3800°R.
- Assumption that combustor wall temperature was 150°F.
- Prediction of steady-state heat-transfer coefficients using Eq. 6.13.

Output from the program includes:

- Predicted radiant and convective heat transfer in combustion chamber
- Nusselt number for combustion chamber
- Gas temperature in tailpipe sections
- Radiant and convective heat rate in tailpipe sections
- Nusselt number in tailpipe sections
- Enhancement of heat-transfer coefficients due to pulsations in tailpipe sections
- Exhaust-gas velocity in tailpipe sections

```
C      PULSE COMBUSTION DOUBLER EXPT. DATA REDUCTION
0001        DIMENSION EQCH(50),EQTP(150),EHFCH(50),EHFTP(150)
0002        DIMENSION PSF(100)
0003        DIMENSION XNM(100)
0004        NAMELIST /INPUT/FI,X,DCH,XLCH,DTP,XLTP,NI,DELTA,PCHF,YEAR,ICH,ITP
0005        READ(5,INPUT)
0006        WRITE(6,INPUT)
0007        READ(5,125) (EQCH(I),I=1,ICH)
0008      125 FORMAT(F10.3)
0009        WRITE(6,127)
0010        READ(5,125)(EQTP(I),I=1,ITP)
0011        PI=3.14159
0012        ACHR=PI*DCH/12.
0013        AEP=PI*(DCH**2-DTP**2)/4.
0014        XNI=NI
0015        DX=XLTP/XNI
0016        ADX=PI*DTP*DX
0017        DO 30 I=1,10
0018     30   EHFCH(I)=EQCH(I)/ACHR
0019        EHFCH(11)=EQCH(11)/AEP
0020        DO 32 I=1,48
0021     32 EHFTP(I)=EQTP(I)/ADX
0022        EHFTP(1)=EHFTP(1)/1.375
0023        WRITE(6,126)( I,EQCH(I),EHFCH(I) ,I=1,ICH)
0024        WRITE(6,128)
0025        WRITE(6,126)( I,EQTP(I),EHFTP(I),I=1,ITP)
0026      126 FORMAT(9X,I5,2F15.1)
0027      127 FORMAT(///,' CHAMBER COOLING RING HT. TR. ')
0028      128 FORMAT(///,' TAILPIPE HT. TR. ')
0029        GAM=1.3
0030        PR=.75
0031        HHVCH4=23860.*16.04
0032        DHCH4=21502.*16.04
0033          TW=150.
0034        TWA=TW+460.
0035        PA=14.7
0036        SIG=.171E-8
0037        KMAX=10
0038        MMAX=5
0039        JMAX=3
0040        XNMOLS=10.52+9.52*X
C       PARTIAL PRESSURES --- ATM
0041        PCO2=1./XNMOLS
0042        PH2O=2./XNMOLS
C        MEAN BEAM LENGTHS
0043        CMBL=.73*DCH
0044        TMBL=.94*DTP
0045        PLCO2=PCO2*CMBL
0046        PLH2O=PH2O*CMBL
0047        PTLC=PLCO2+PLH2O
0048        PTLT=PTLC*TMBL/CMBL
C       MASS FLOW RATE = WDOT
0049        XNDCH4=FI/HHVCH4
0050        WDOT=XNDCH4*(16.+2.*(1.+X)*(32.+3.76*28.))
C        ER = DEGREE OF REACTION FOR CO --- CO2
```

```
0051                  S2=1.
C052                  DHCH=4344.*28.01
C053                  QCH=0.
                C     CHAMBER  HEAT  TRANSFER  RATE
C054                  DO 109  I=1,ICH
C055                  QCH=QCH+EQCH(I)
C056                109 CONTINUE
C057                  ALPHA=QCH/(XNDCH4*DHCH4)
C058                  T2=3500.
                C     CHAMBER ENERGY BALANCE
                C       TEMP. FROM ENERGY BALANCE . . .  ABS. TEMPS.
C059                  DO 10 K=1,KMAX
0060                  T=T2
0061                  CPCO2=16.2-6530./T+1.41E6/T**2
0062                  CPH2O=19.86-597./SQRT(T)+7500./T
0063                  CPO2=11.52-172./SQRT(T)+1530./T
0064                  CPN2=9.47-3470./T+1.16E6/T**2
0065                  CPCO=9.46-3290./T+1.07E6/T**2
0066                  HCO2=16.2*(T-520.)-6530.*ALOG(T/520.)+1.41E6*(1./520.-1./T)
0067                  HH2O=19.86*(T-520.)-1194.*(SQRT(T)-SQRT(520.))+7500.*ALOG(T/520.)
0068                  HO2=11.52*(T-520.)-344.*(SQRT(T)-SQRT(520.))+1530.*ALOG(T/520.)
0069                  HN2=9.47*(T-520.)-3470.*ALOG(T/520.)+1.16E6*(1./520.-1./T)
0070                  HCO=9.46*(T-520.)-3290.*ALOG(T/520.)+1.07E6*(1./520.-1./T)
0071                    F=2.*HH2O+7.52*(1.+X)*HN2+ER*HCO2+(1.-ER)*HCO
                     1  +(2.*X+.5-.5*ER)*HO2-(1.-ALPHA)*DHCH4+(1.-ER)*DHCO
0072                  FP=2.*CPH2O+7.52*(1.+X)*CPN2+ER*CPCO2
                     1  +(2.*X+(1.-ER)/2.)*CPO2+(1.-ER)*CPCO
0073                  T2N=T2-F/FP
0074                  DT=T2N-T2
0075                  T2=T2N
0076                  IF(ABS(DT).LE.1.) GO TO 50
C077                  IF(K.LT.KMAX) GO TO 10
C078                  WRITE(6,101)
0079                101 FORMAT(5X,' T2 DID NOT CONVERGE !//)
C080                 10 CONTINUE
C081                 50 CONTINUE
0082                  WRITE(6,102)T2     ,QCH
C083                102 FORMAT(5X,' T2  = ',F7.1,' R ',5X,'EXPT. QCH',F7.1,'BTU/HR')
                C       THEO.  HT.  TR.
0084                  T2=T2+DELTA
C085                  TDEL=T2
C086                  ETI=70.+70.*(PTLC-.02)/.04
0087                  ET=ETI/T2
C088                  T2F=T2-460.
0089                  T=T2F
0090                  COND=.04+.04*(T-1500.)/3000.
0091                  VIS=.08+.08*(T-500.)/3000.
0092                  ACH=PI*XLCH*DCH     +(PI/4.)*(DCH**2-DTP**2)
0093                  QCHR=      ET   *SIG*ACH*(T2**4-TWA**4)
0094                  RECH=4.*WDOT/(PI*DCH*VIS)
0095                  XNUCH=.021*RECH**.8*PR**.6
0096                  IF(XNUCH.LT.3.66)XNUCH=3.66
0097                  HCH=COND*XNUCH/DCH
0098                  QCHC=HCH*ACH*(T2-TWA)
0099                    T2=T2-DELTA
```

```
C100                    QCH=QCHR+QCHC
C101                    WRITE(6,300)T2,QCH,QCHP,QCHC,TPEL , ,DT  ,XPCL,XNUC
C102                300 FORMAT(5X,8F15.7)
C103                    WRITE(6,998)
C104                998 FORMAT(5X,'  TAILPIPE  HEAT TRANSFER  ')
C105                     QTOT=0.
C106                     AFTP= PI*DTP**2/4.
C107                    QTP=0.
C108                     DO 188 I=1,ITP
C109                    QTP=QTP+EQTP(I)
C110                188  CONTINUE
C111                    WRITE(6,189) QTP
C112                189  FORMAT(5X,' EXPT. QTP = ',F7.1)
C113                    TIN=T2
C114                     TOUT=T2
C115                    DO 80 N=1,ITP
C116                    XN=N-1
C117                    XXN=XN/12.
C118                    XXN=XN/12.+.375/12.
C119                    PAF=1.
C120                    XNB=XXN+DX/2.
C121                    IF(N.EQ.1) XNB=(DX+.375/12.)/2.
C122                    XOD=XNB/DTP
C123                    IF(XOD.LE.1.5)  ELAF=2.3
C124                    IF(XOD.GT.1.5.AND.XOD.LT.20.) ELAF=1.+1.3*(1./XOD=.051/.627
C125                    IF(XOD.GE.20.) ELAF=1.
C126                    ELAF=1.+.5*(ELAF-1.)
C127                     ELAF=1.
C128                    DO 333 J=1,JMAX
C129                    TX=(TIN+TOUT)/2.
C130                    RHO=PA*144./(53.3*TX)
C131                    USS=WDOT/(3600.*RHO*AFTP)
C132                    XB=XNB/XLTP
C133                     XBN(N)=XB
C134                    PBF(N)=COS(WBAR*XB)-SIN(WBAR*XB)/TAN(WBAR)
C135                    T=TX-460.
C136                    COND =.04+.04*(T-1500.)/3000.
C137                    COND =.04+.03*(T-1500.)/3000.
C138                    VIS=.08+.08*(T-500.)/3000.
C139                    T=TX
C140                    CPCO2=16.2-6530./T+1.41E6/T**2
C141                    CPH2O=19.86-597./SQRT(T)+7500./T
C142                    CPO2=11.52-172./SQRT(T)+1530./T
C143                    CPN2=9.47-3470./T+1.16E6/T**2
C144                    WDCP=XNDCH4*(7.52*(1.+X)*CPN2+2.*CPH2O+CPCO2+2.*X*CPO2)
C145                    RESS=4.*WDOT/(PI*DTP*VIS)
C146                    XNUSS=.021*RESS**.8*PR**.6
C147                    XNUSS=ELAF*XNUSS
C148                    HSS=XNUSS*COND/DTP
C149                    ETT=70.+70.*(PTLT-.02)/.04
C150                    ET=ETT/TX
C151                    QR=ET*SIG*ADX*(TX**4-TWA**4)
C152                    QR=QR*.85*.5
C153                    IF(N.EQ.1) QR=1.375*QR
C154                    QC=EQIP(N)-QR
```

```
C155                H=QC/((TX-TWA)*ADX)
C156              IF(N.EQ.1) H=H/1.375
C157                Q=EQTP(N)
C158              PAF=H/HSS
C159              TOUT=TIN-Q/WDCP
C160               WRITE(6,199) TOUT
C161          199 FORMAT(5X,F14.3)
C162          332 CONTINUE
C163          333 CONTINUE
C164              TIN=TOUT
C165              QTOT=QTOT+Q
C166              WRITE(6,999)XN,TX,Q,QR,QC,ELAF,PAF,H,USS
C167          999 FORMAT(8X,9F14.3)
C168          808 CONTINUE
C169           80 CONTINUE
C170              WRITE(6,995) QTOT
C171          995 FORMAT(///,10X,'  QTOT  =  ',F15.2)
C172              DO 99 I=1,ITP
C173              WRITE(6,98) I,XBN(I),PBF(I)
C174           99 CONTINUE
C175           98  FORMAT(5X,I3,2F10.3)
C176              END
```

NOMENCLATURE USED IN COMPUTER PROGRAM

ACH	Surface area (sidewall and top) of combustion chamber, ft^2
ACHR	Inside surface area of a 1" long segment of combustion chamber, ft^2
ADX	Surface area of tailpipe section whose length is the total tailpipe length divided by number of increments (i.e., cooling channels)
AEP	Area of top combustion chamber, ft^2
AFTP	Cross-sectional area of tailpipe, ft^2
ALPHA	Ratio of heat loss through combustion-chamber walls to burner heat input, based on the lower-heating value of methane. Fraction of heat loss in combustion chamber
CMBL	Combustion-chamber mean beam length
COND	Thermal conductivity of gas in combustion chamber at radiating temperature, Btu-ft/hr-ft^2-°F
COND	Thermal conductivity of gas in tailpipe section at mean gas temperature, Btu-ft/hr-ft^2-°F
CPCO	Molal heat capacity of CO, Btu/lb-mole-°R
CPCO2	Molal heat capacity of CO_2, Btu/lb-mole-°R
CPH2O	Molal heat capacity of H_2O, Btu/lb-mole-°R
CPN2	Molal heat capacity of N_2, Btu/lb-mole-°R
CPO2	Molal heat capacity of O_2, Btu/lb-mole-°R
DCH	Inside diameter of combustion chamber = 4" = 0.333 ft
DELTA	300°R minus the difference between radiation gas temperature and leaving gas temperature, °R
DHCH4	Lower heating value for methane, Btu/lb-mole
DHCO	Gross heating value for carbon monoxide, Btu/lb-mole
DT	T2N-T2 = difference between adjusted and previous temperature in the combustion chamber, °R

DTP	Inside diameter of tailpipe = 1.75" = 0.146 ft
DX	Length of tailpipe divided by number of increments along pipe. Incremented length of tailpipe.
EHFCH(1)	Heat flux through combustion chamber section, Btu/h-ft^2
EHFCH(11)	Heat flux through top of combustion chamber, Btu/h-ft^2
EHFTP(I)	Heat flux through tailpipe section, Btu/h-ft^2
EHFTP(1)	Heat flux through 1st tailpipe section, Btu/h-ft^2
ELAF	Nusselt number multiplier for tailpipe entrance effects
EQCH(I)	Heat rate from combustion-chamber cooling channel "I", Btu/h
EQTP(I)	Heat rate from tailpipe cooling channel "I", Btu/h
ER	Degree of reaction for $CO \longrightarrow CO_2$
ET	Gas emissivity (ETT/T2) in combustion chamber and tailpipe section (ETT/TX)
ETT	Gas emissivity-temperature product in either tailpipe section or combustion chamber based on Fig. 6.14 in Hottel and Sarofim[70]
F	Sum of the product of the number of moles times the molal enthalpy of the flue-gas components, Btu
FI	Fuel input rate, Btu/h
FP	Sum of the product of the number of moles times the molal specific heat of the flue-gas components, Btu/°R
GAM	Specific heat ratio for combustion gases = 1.3
H	Convective heat-transfer coefficient in tailpipe section, Btu/h-ft^2-°R
HCH	Combustion-chamber convective heat-transfer coefficient, Btu/h-ft^2-°R
HCO	Molal enthalpy for CO, Btu/lb-mole
HCO2	Molal enthalpy for CO_2, Btu/lb-mole
HH2O	Molal enthalpy for H_2O, Btu/lb-mole

HHVCH4	Higher heating value for methane, Btu/lb-mole
HN2	Molal enthalpy for N_2, Btu/lb-mole
HO2	Molal enthalpy for O_2, Btu/lb-mole
I	Counter in first part of program
ICH	Number of combustion-chamber cooling rings = 11
ITP	Number of tailpipe cooling rings = 43
J	Counter in tailpipe heat balance per section
JMAZ=3	Maximum number of iterations on heat balance in tailpipe section
KMAX	Counter used in chamber energy-balance do-loop = 10
MMAX	5
N	Do-loop counter in tailpipe heat-transfer section
NI	Number of tailpipe cooling channels
PA	Ambient pressure = 14.7 psia
PAF	Ratio of pulse combustion heat-transfer coefficient to steady-state heat-transfer coefficient
PBF(N)	Part of instantaneous pressure fluctuation term
PCHF	Maximum combustion-chamber pressure, psig
PCO2	Partial pressure of CO_2 in combustion products, atm
PH2O	Partial pressure of H_2O in combustion products, atm
PI	π = 3.14159 (approximately)
PLCO2	Partial-pressure/mean-beam-length product for CO_2, atm-ft
PLH2O	Partial-pressure/mean-beam-length product for H_2O, atm-ft
PR	Prandtl number for combustion gas = 0.75
PTLC	Total-path-length/partial-pressure product of $CO_2 + H_2O$ in combustion chamber, atm-ft

PTLT	Total-path-length/partial-pressure product for $CO_2 + H_2O$ in tailpipe, atm-ft
Q	Heat transferred from tailpipe section to cooling channel, Btu/h
QC	Convective heat transfer from gas to tailpipe-section wall, Btu/h
QCH	Combustion-chamber heat-transfer rate, Btu/h (actual and theoretical)
QCHC	Convective heat transfer from gas to combustion-chamber wall and top, Btu/h
QCHR	Radiant heat transfer from gas to combustion-chamber wall and top, Btu/h
QR	Radiant heat transfer from gas to tailpipe-section wall, Btu/h
QTOT	Total calculated tailpipe heat-transfer rate, Btu/h
QTP	Total measured tailpipe heat-transfer rate, Btu/h
RECH	Gas Reynolds number in combustion chamber
RESS	Gas Reynolds number in tailpipe section
RHO	Gas density in combustion-chamber/tailpipe section, lb_m/ft^3
SIG	Stefan-Boltzmann constant = 0.1714×10^8 Btu/h-ft^2-$°R^4$
T	Fahrenheit value of mean gas temperature in tailpipe section, °F, for conductivity and viscosity computation. T = TX, °R, for specific-heat calculations
T	Temperature for molal specific heat and enthalpy calculations in chamber energy balance, °R. Also radiating gas temperature for conductivity and viscosity calculation
TDEL	(T2 + DELTA): Radiating gas temperature in combustion chamber, °R
TIN	Inlet temperature at tailpipe section, °R
TMBL	Tailpipe mean beam length, ft
T2	3500 °R initial assumption: temperature of gas leaving combustion chamber. Also radiating gas temperature.
T2F	Radiating gas temperature in Fahrenheit degrees, °F

T2N	T2 - (F/FP) = Adjusted combustion gas temperature, °R
TX	Mean gas temperature in tailpipe section, °R
TW	Wall temperature, °F
TWA	Absolute wall temperature, °R
USS	Gas velocity in a tailpipe section, ft/s
VIS	Viscosity of gas in combustion chamber at radiating temperature, lb_m/ft-h
VIS	Viscosity of gas in tailpipe section at mean gas temperature, lb_m/ft-h
WBAR	Omega bar term = $2\pi\omega L/c$ and $\bar{\omega}$ tan $\bar{\omega} = \frac{1}{\bar{v}}$
WDCP	Heat rate of combustion product in tailpipe section at temperature T, Btu/h
WDOT	Mass flow of gas and air, lb_m/h
X	Fraction of excess air
XB	Distance from combustion chamber to center of a tailpipe section divided by total length of tailpipe
XBN(N)	XB for section N of tailpipe
XLCH	Length of combustion chamber = 10" = 0.833 ft
XLTP	Length of tailpipe = 48" = 4 ft
XN	N-1: Counter used in tailpipe-section 1
XNB	Distance from top of combustion chamber to center of tailpipe section, ft
XNDCH4	Molal flow rate of methane gas, lb-mole/h
XNI	NI = Decimal equivalent of number of tailpipe increments
XNMOLS	Total number of moles in combustion reaction
XNUCH	Gas Nusselt number in combustion chamber for turbulent flow

XNUSS	Nusselt number in tailpipe section
XOD	XNB/DTP: Distance from top of combustion chamber to center of tailpipe section, divided by tailpipe inside diameter

APPENDIX D

EXPERIMENTAL DATA ON HEAT TRANSFER AND EXHAUST-GAS TEMPERATURES

Figures D.1-D.33 present heat-transfer results obtained in the ANL pulse combustion experiment under stated conditions of heat input and air/fuel ratio. Figures D.34-D.44 give measured exhaust-gas temperatures and effects of various parameters on those temperatures. (Note that the straight lines connecting the data points do not have any special significance. These lines were added merely to make the trend of the data clearer.)

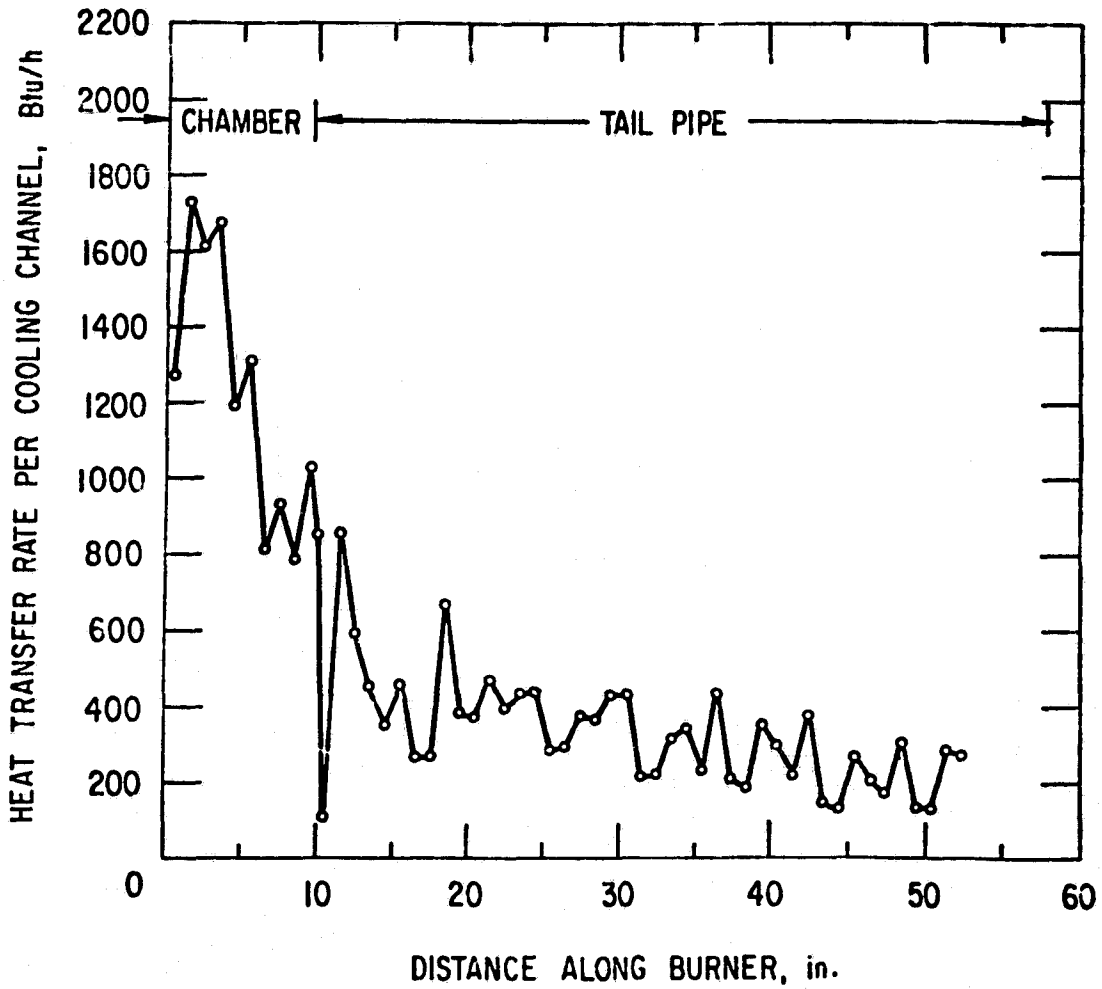

Fig. D.1 Heat Transfer along Burner for a 32,887 Btu/h Heat Input and a 13.2 Air/Fuel Ratio

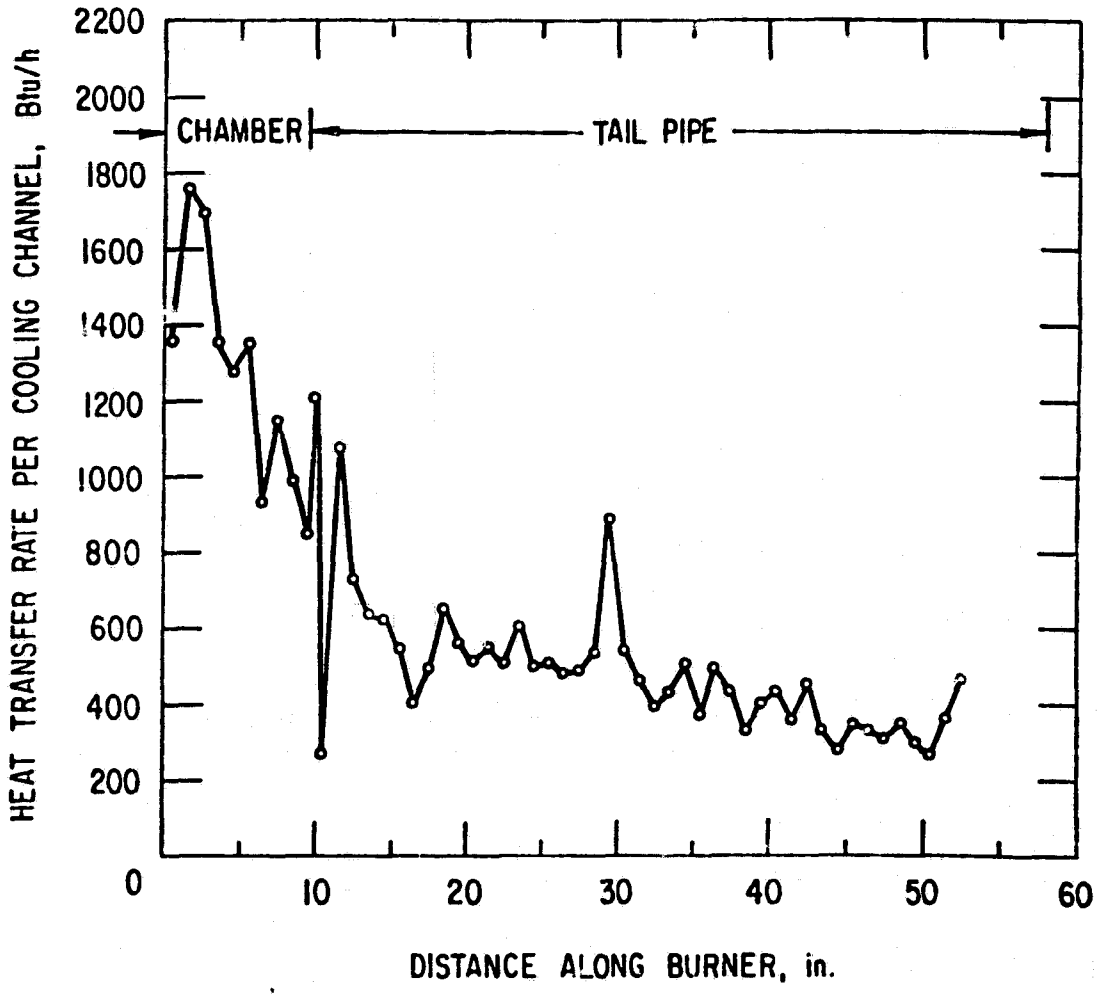

Fig. D.2 Heat Transfer along Burner for a 50,245 Btu/h Heat Input and a 9.9 Air/Fuel Ratio

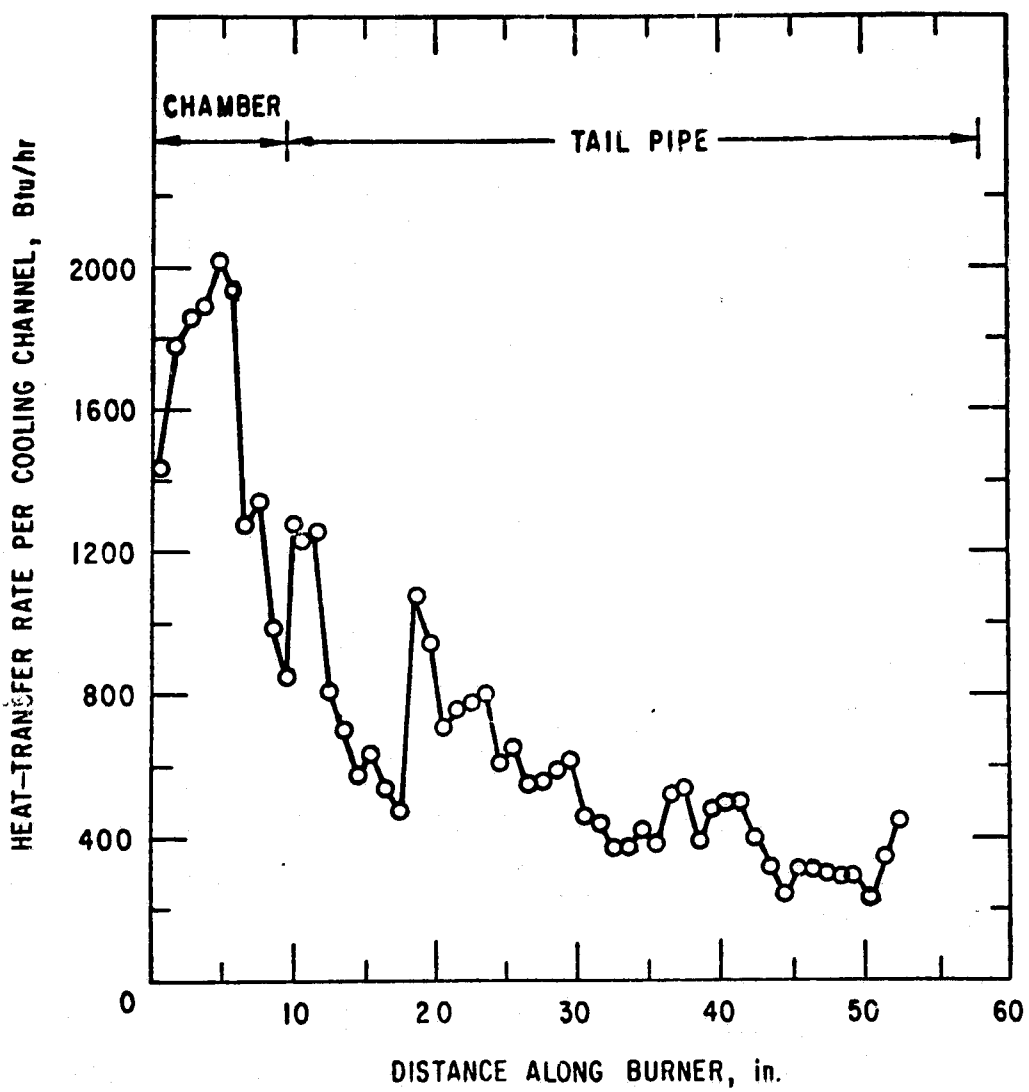

Fig. D.3 Heat Transfer along Burner for a 54,194 Btu/h Heat Input and a 12.5 Air/Fuel Ratio

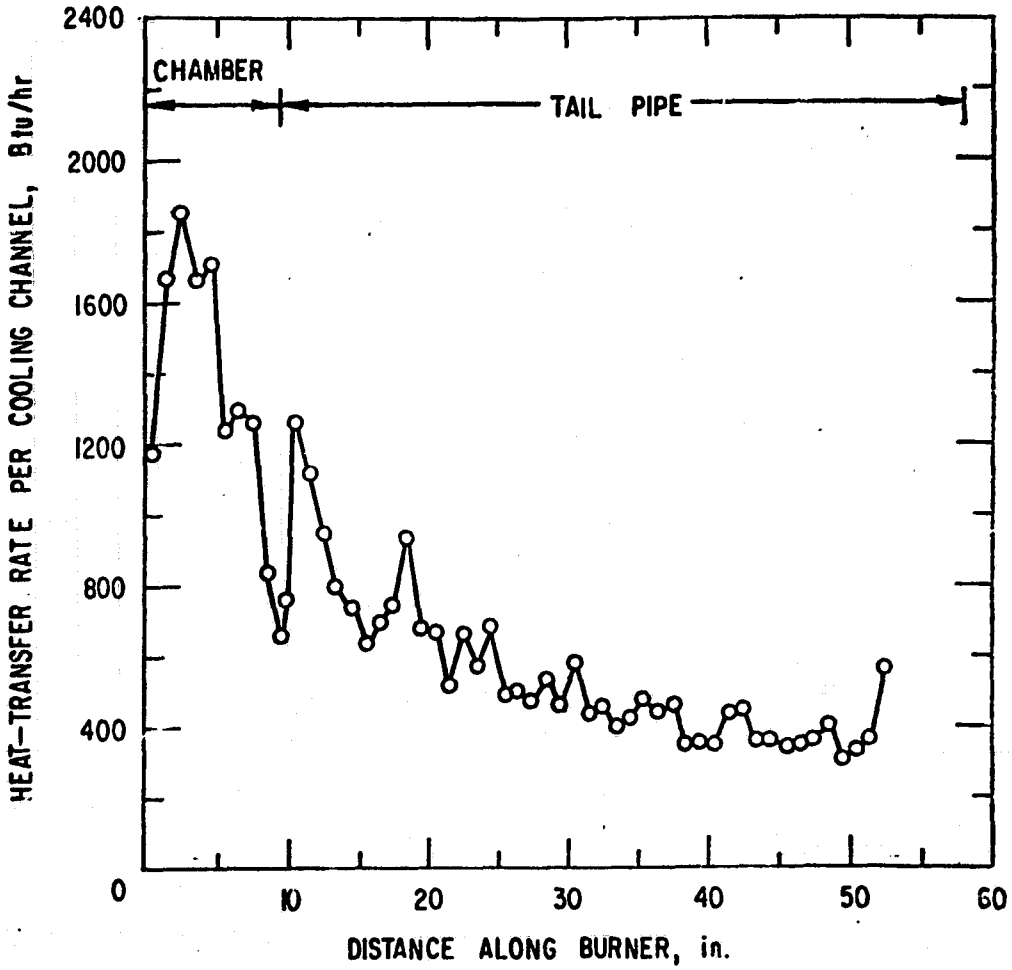

Fig. D.4 Heat Transfer along Burner for a 58,655 Btu/h Heat Input and a 10.1 Air/Fuel Ratio

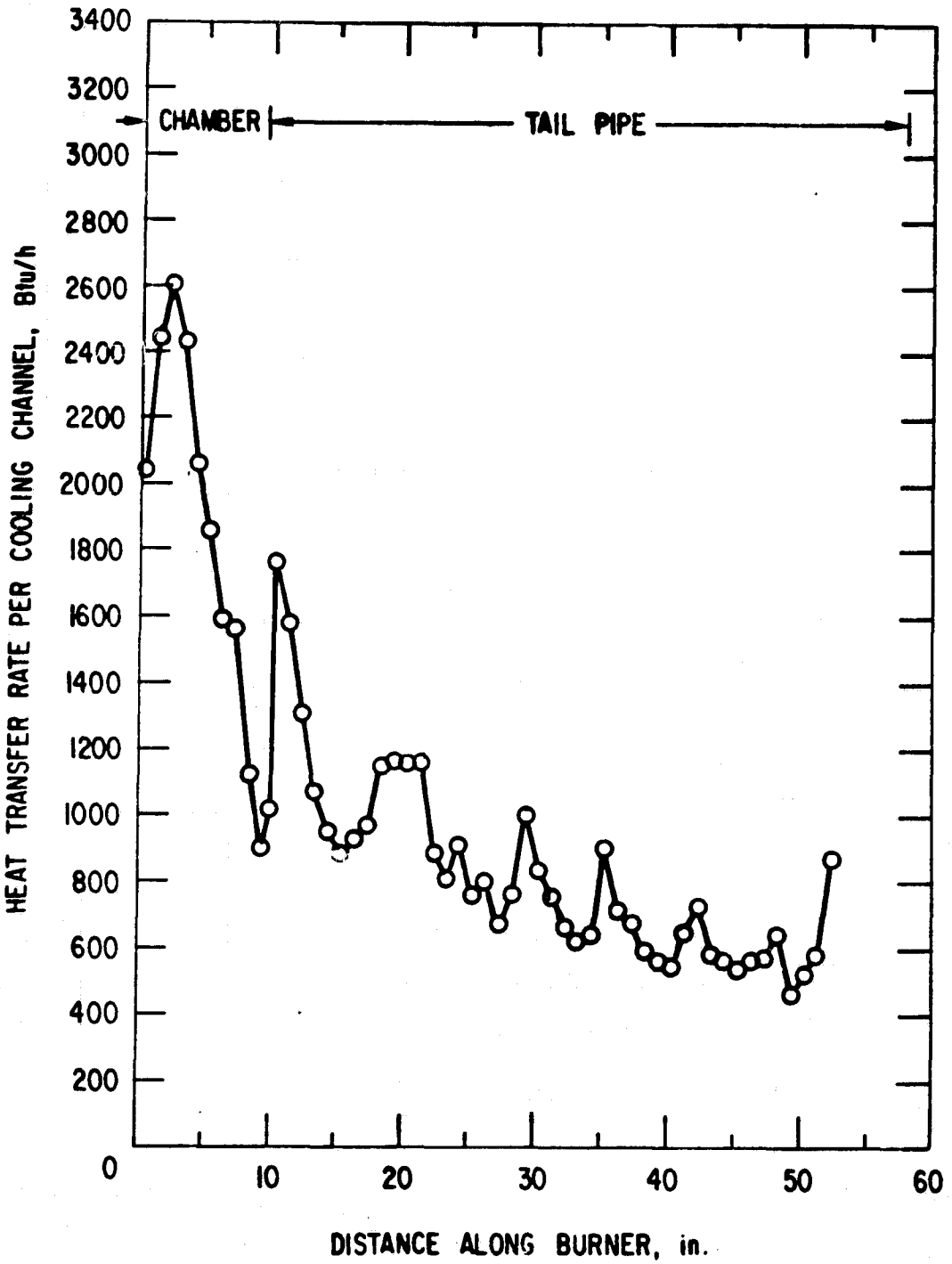

Fig. D.5 Heat Transfer along Burner for a 95,458 Btu/h Heat Input and an 11.89 Air/Fuel Ratio

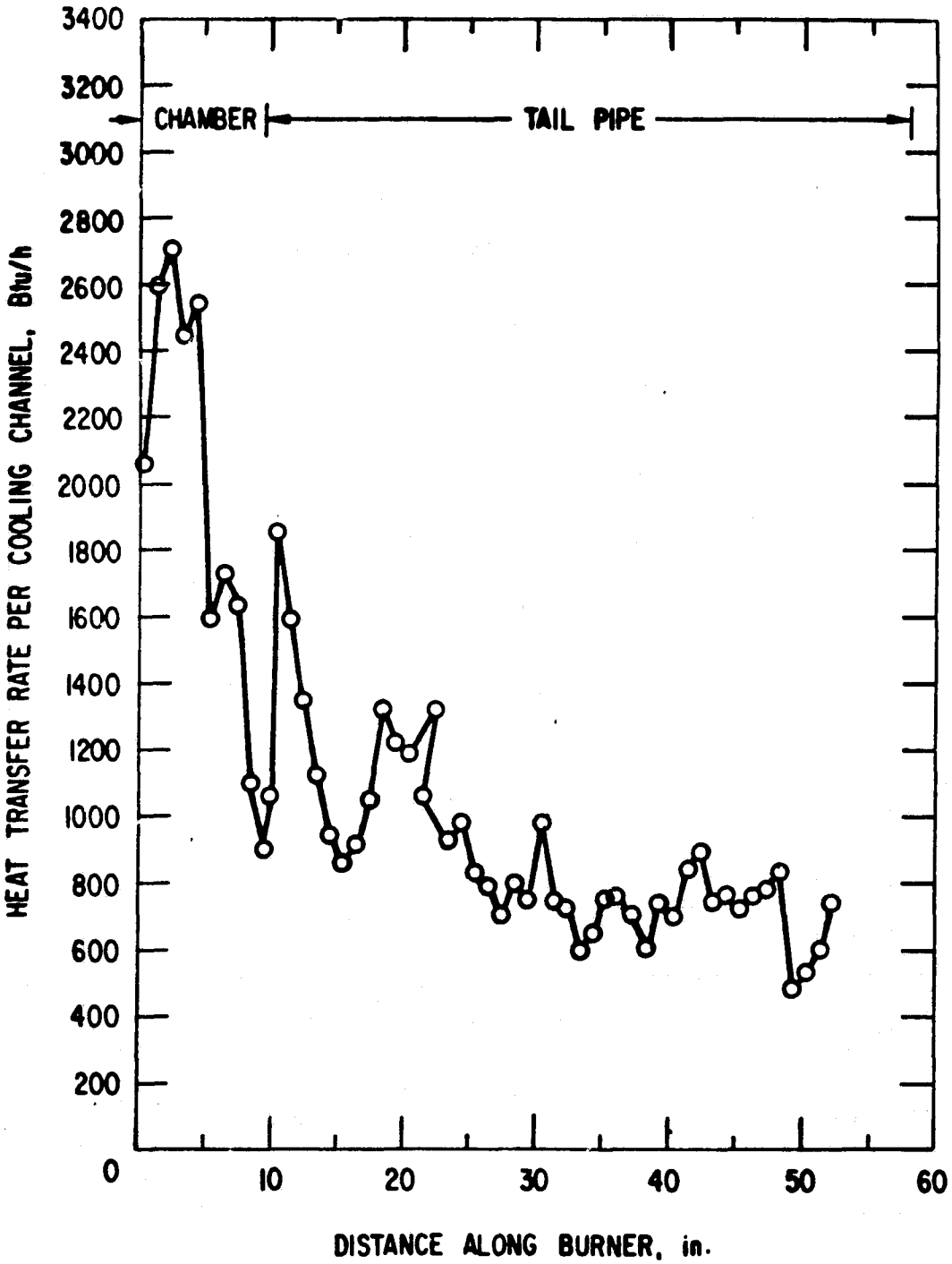

Fig. D.6 Heat Transfer along Burner for a 32,887 Btu/h Heat Input and a 13.2 Air/Fuel Ratio

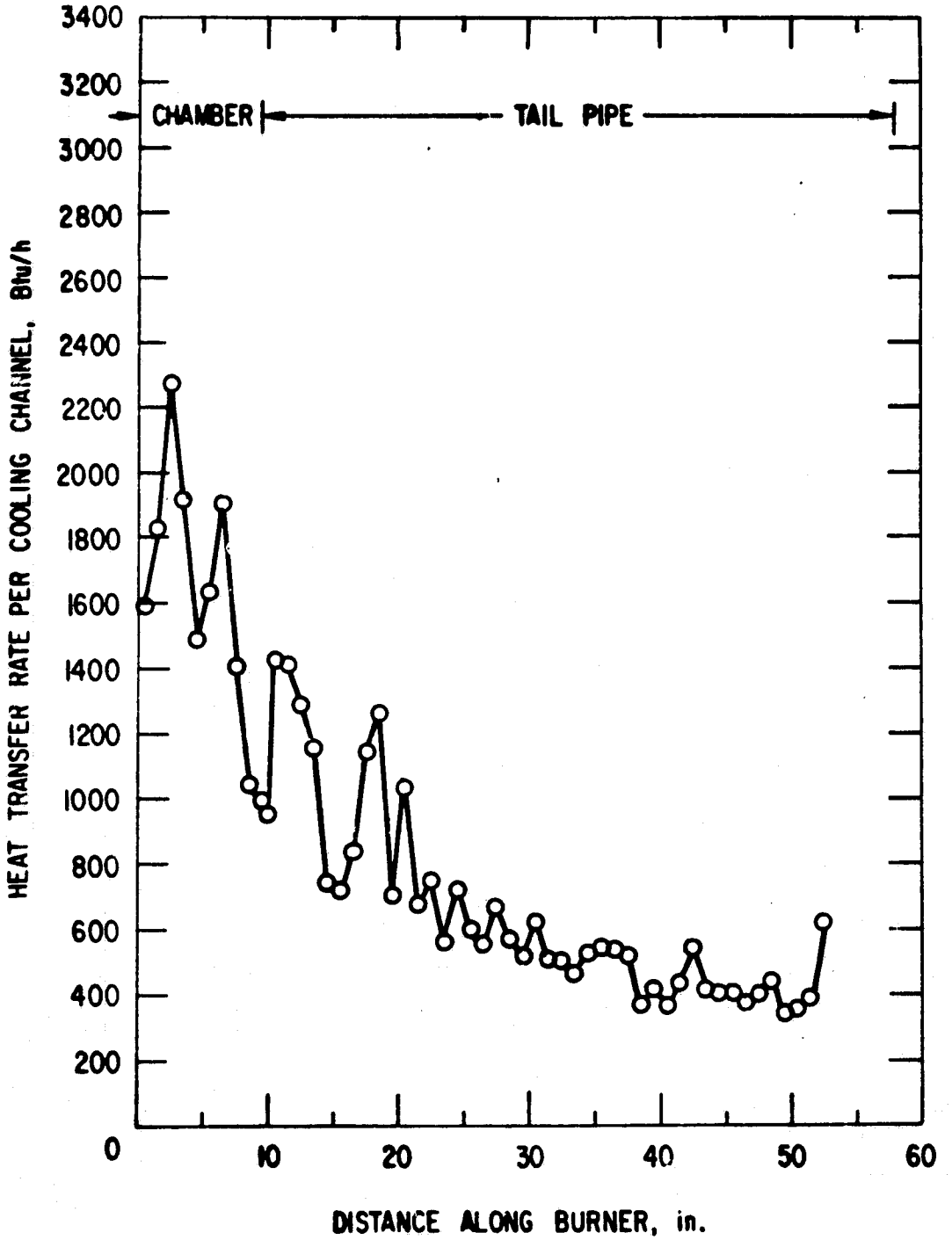

Fig. D.7 Heat Transfer along Burner for a 96,782 Btu/h Heat Input and a 10.3 Air/Fuel Ratio

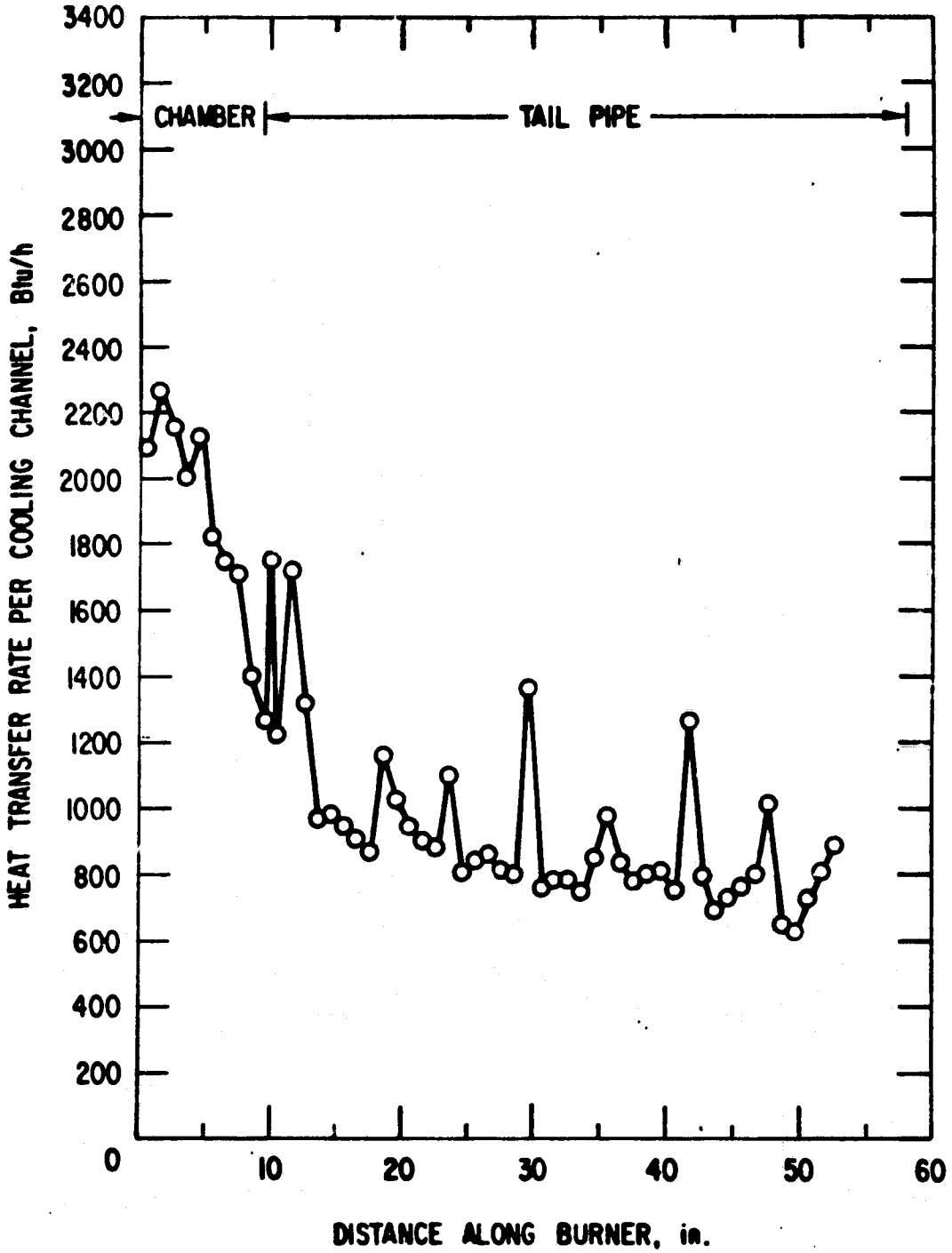

Fig. D.8 Heat Transfer along Burner for a 99,577 Btu/h Heat Input and a 10.1 Air/Fuel Ratio

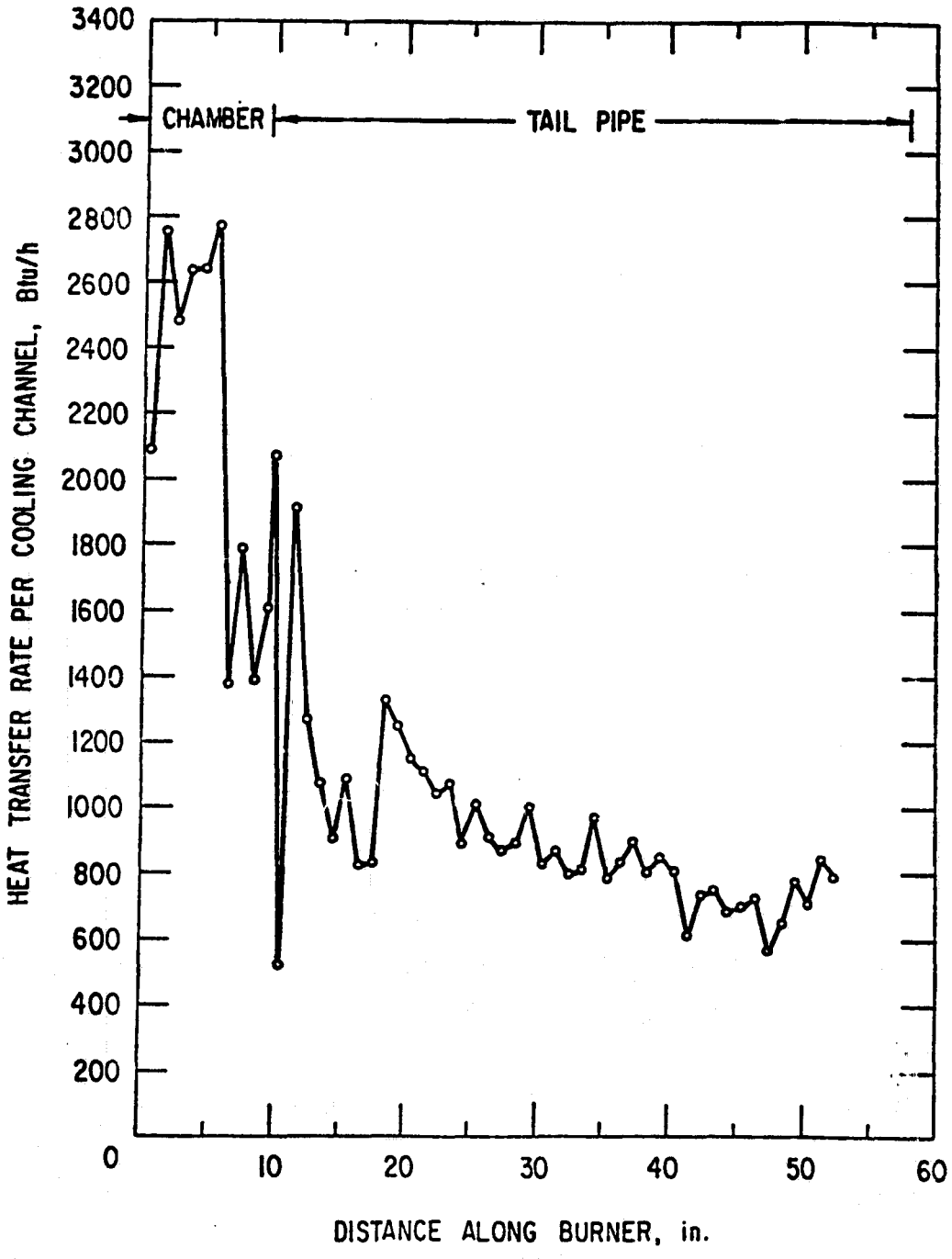

Fig. D.9 Heat Transfer along Burner for a 100,215 Btu/h Heat Input and a 9.9 Air/Fuel Ratio

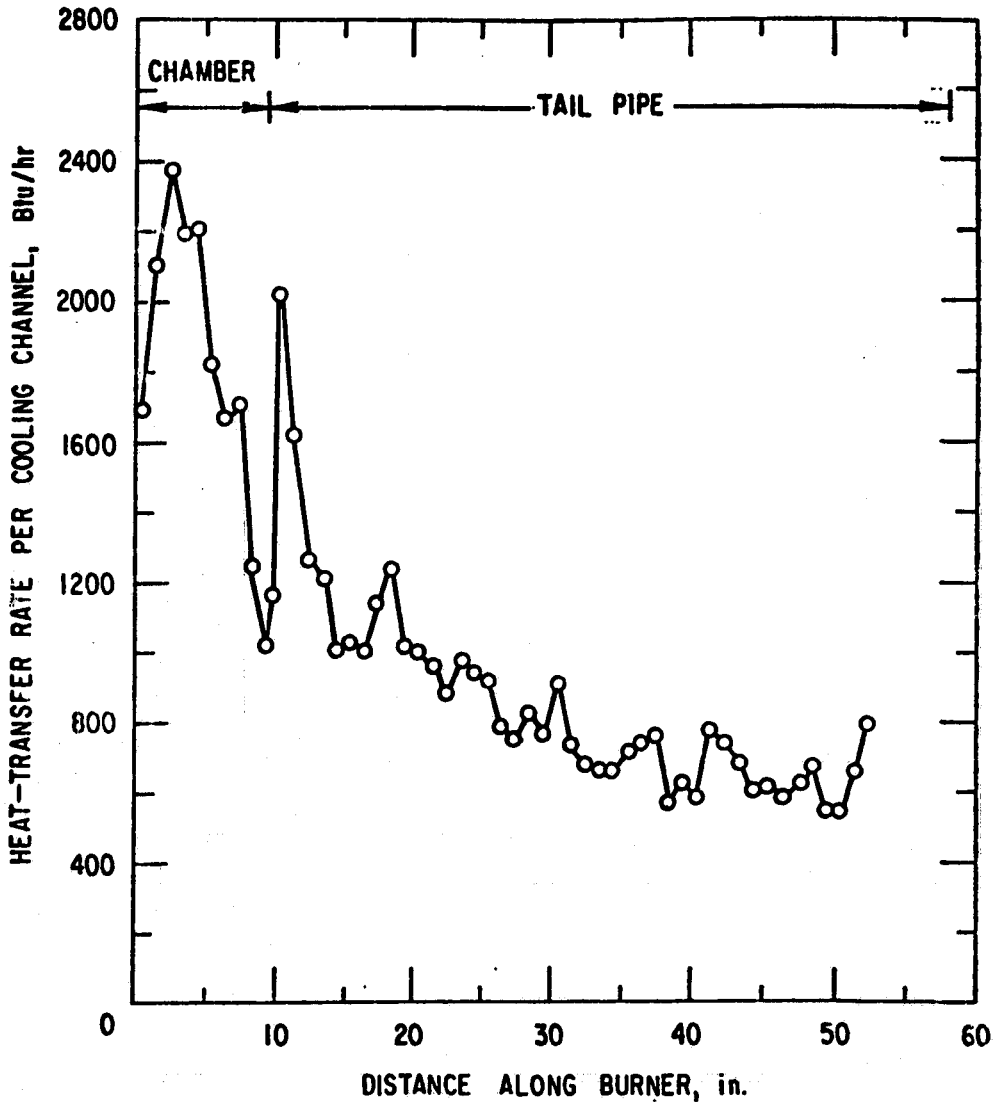

Fig. D.10 Heat Transfer along Burner for a 100,941 Btu/h Heat Input and a 10.1 Air/Fuel Ratio

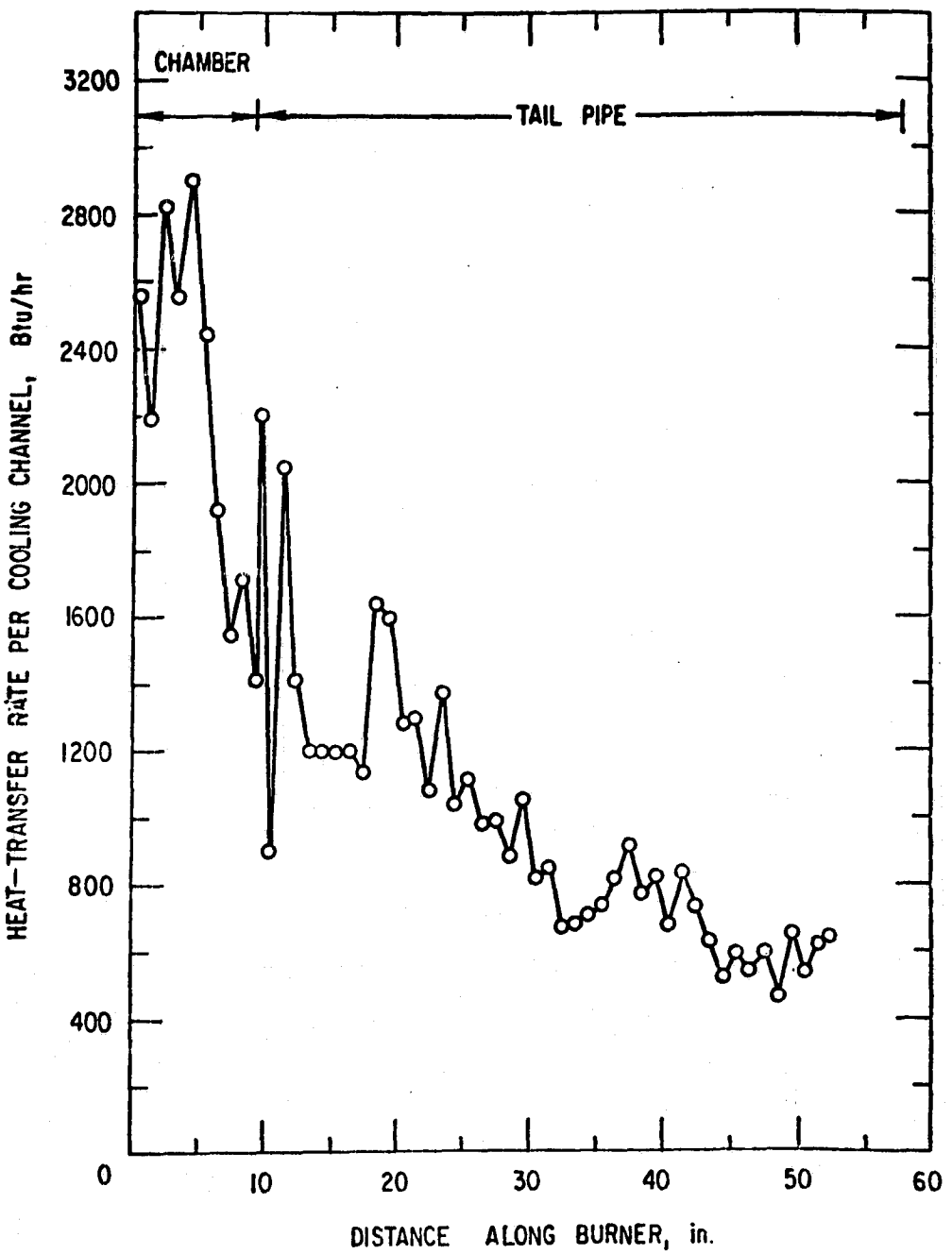

Fig. D.11 Heat Transfer along Burner for a 101,713 Btu/h Heat Input and a 9.9 Air/Fuel Ratio

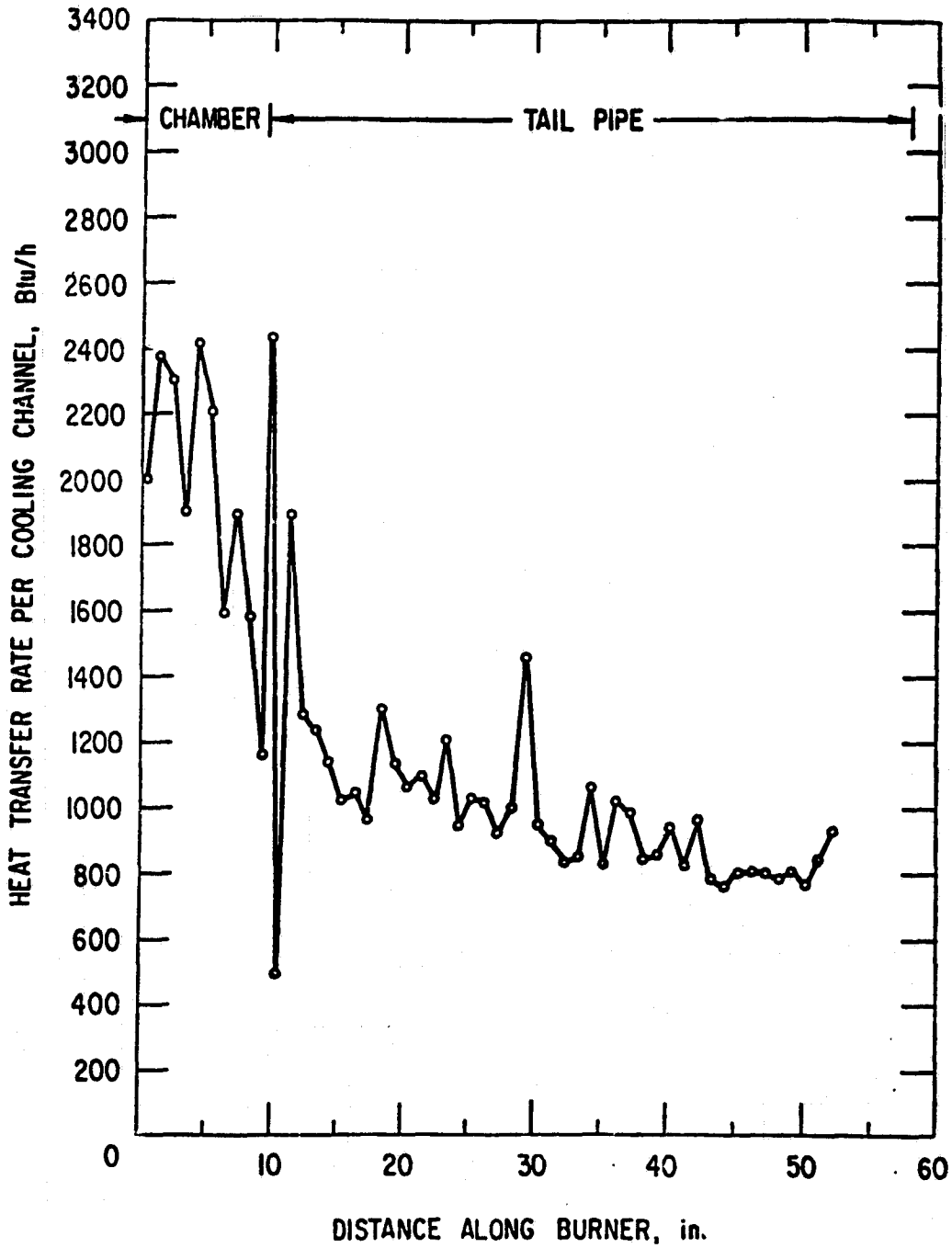

Fig. D.12 Heat Transfer along Burner for a 103,576 Btu/h Heat Input and a 10.1 Air/Fuel Ratio

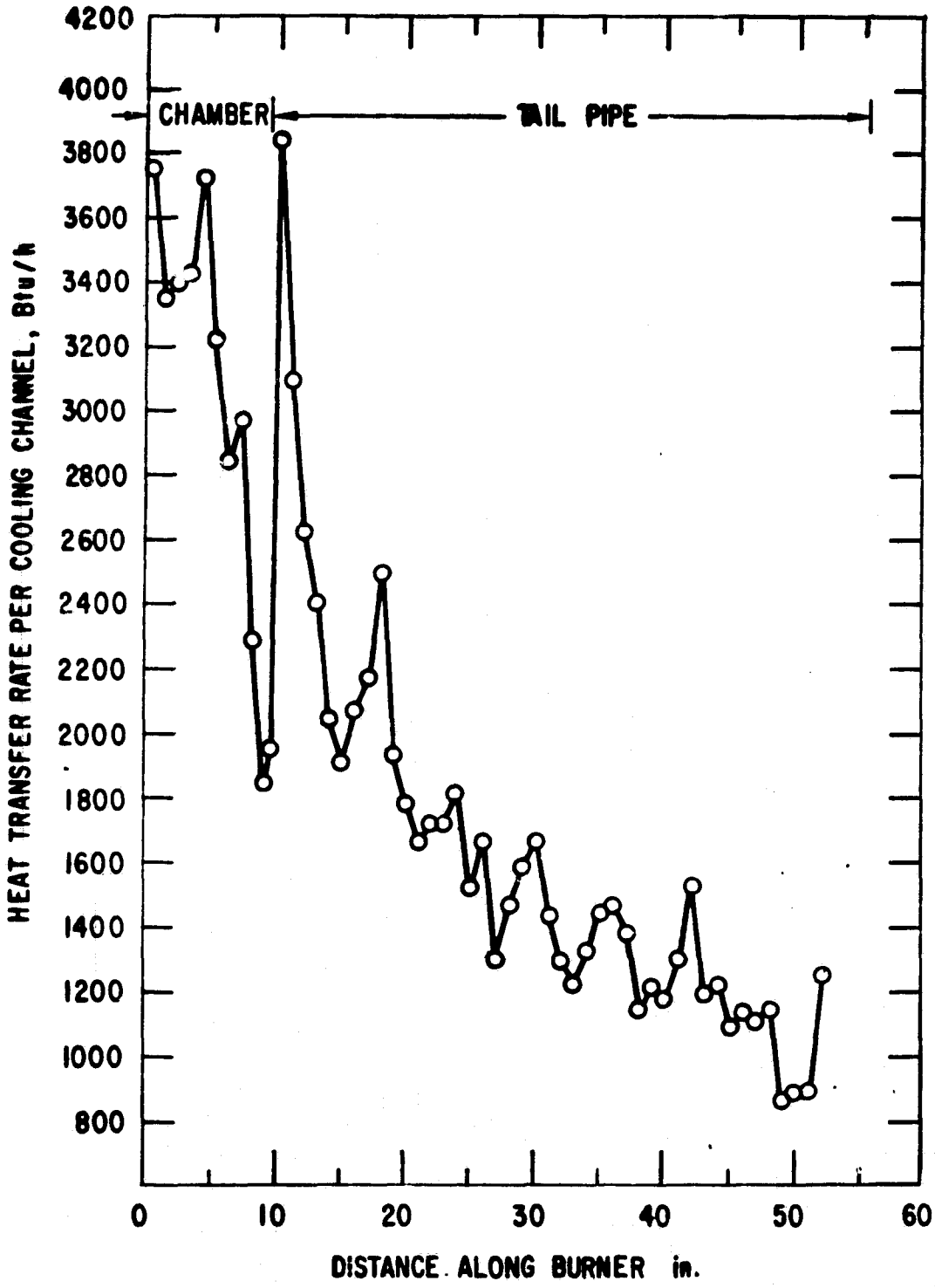

Fig. D.13 Heat Transfer along Burner for a 194,371 Btu/h Heat Input and a 9.38 Air/Fuel Ratio

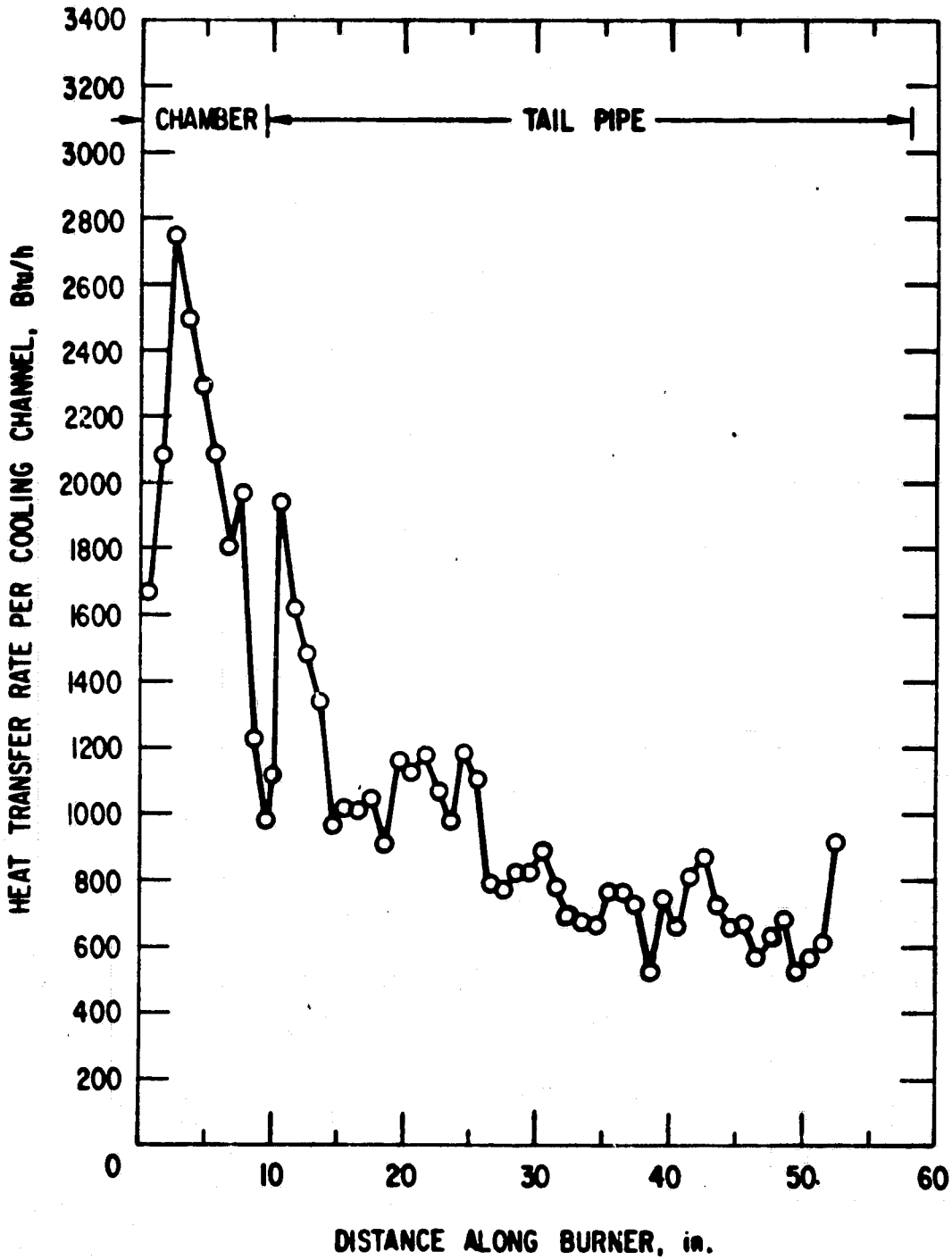

Fig. D.14 Heat Transfer along Burner for a 98,013 Btu/h Heat Input and a 9.96 Air/Fuel Ratio

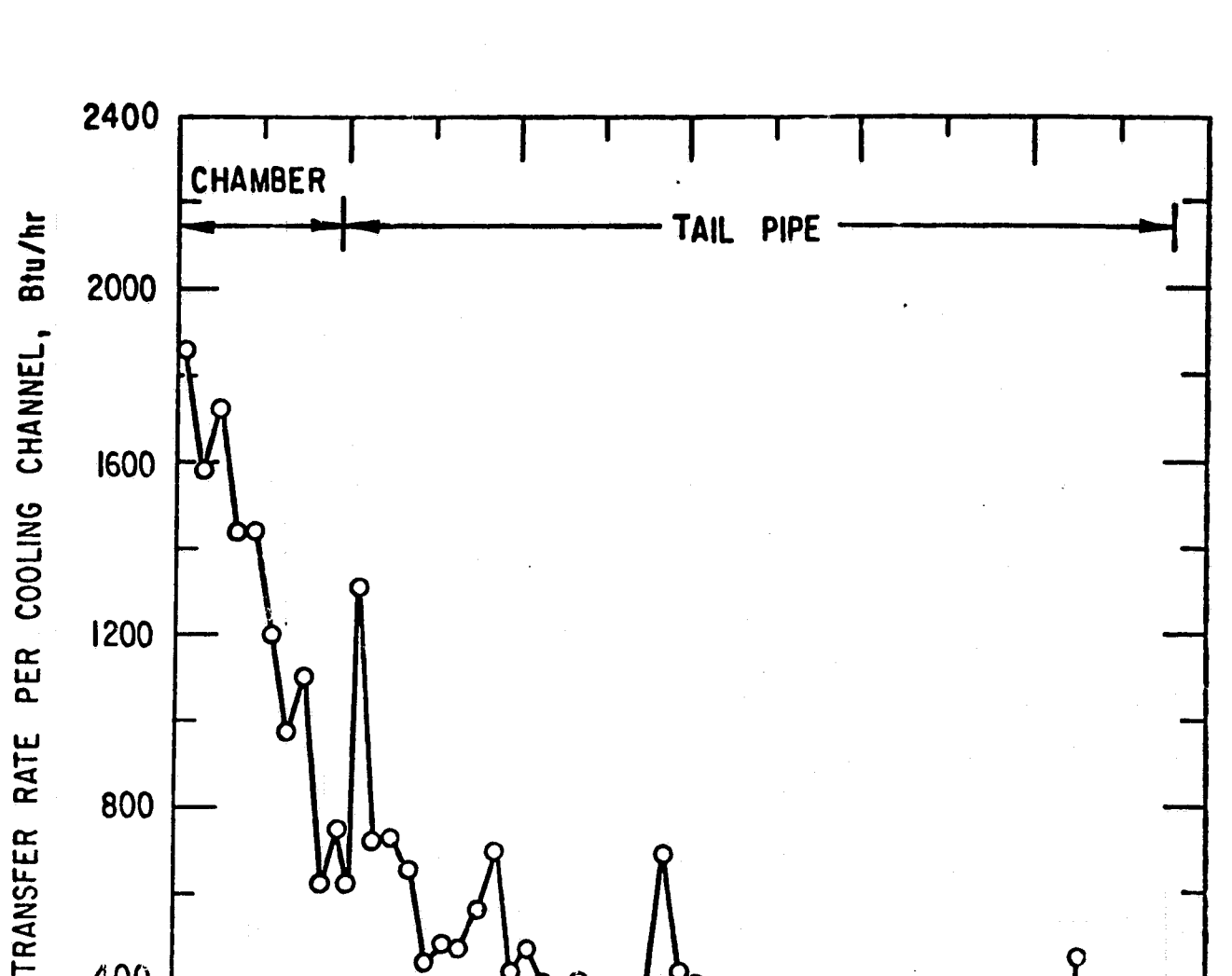

Fig. D.15 Heat Transfer along Burner without Flapper Valves for a 53,589 Btu/h Heat Input and a 12.5 Air/Fuel Ratio

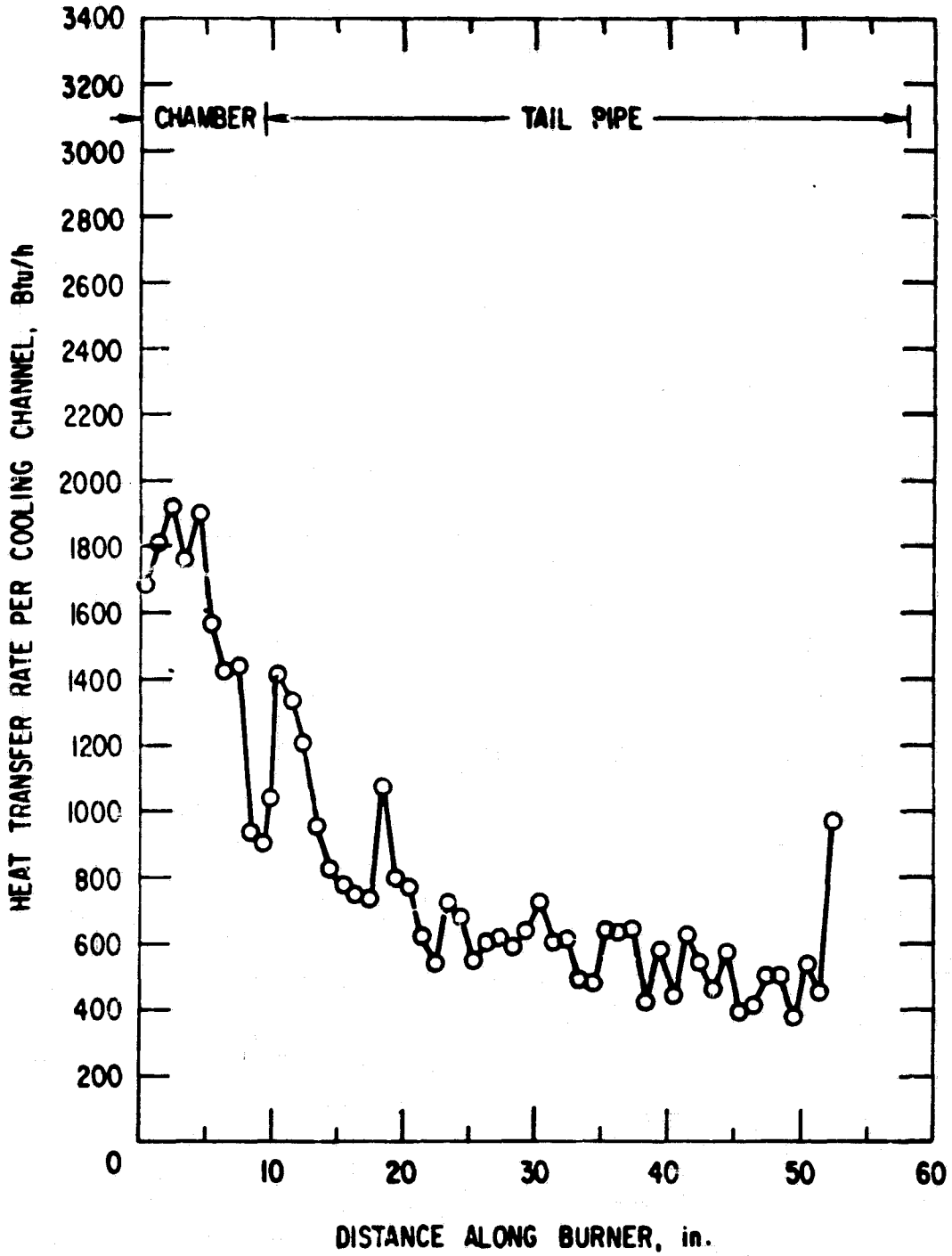

Fig. D.16 Heat Transfer along Burner without Flapper Valves for a 102,645 Btu/h Heat Input and an 11.39 Air/Fuel Ratio

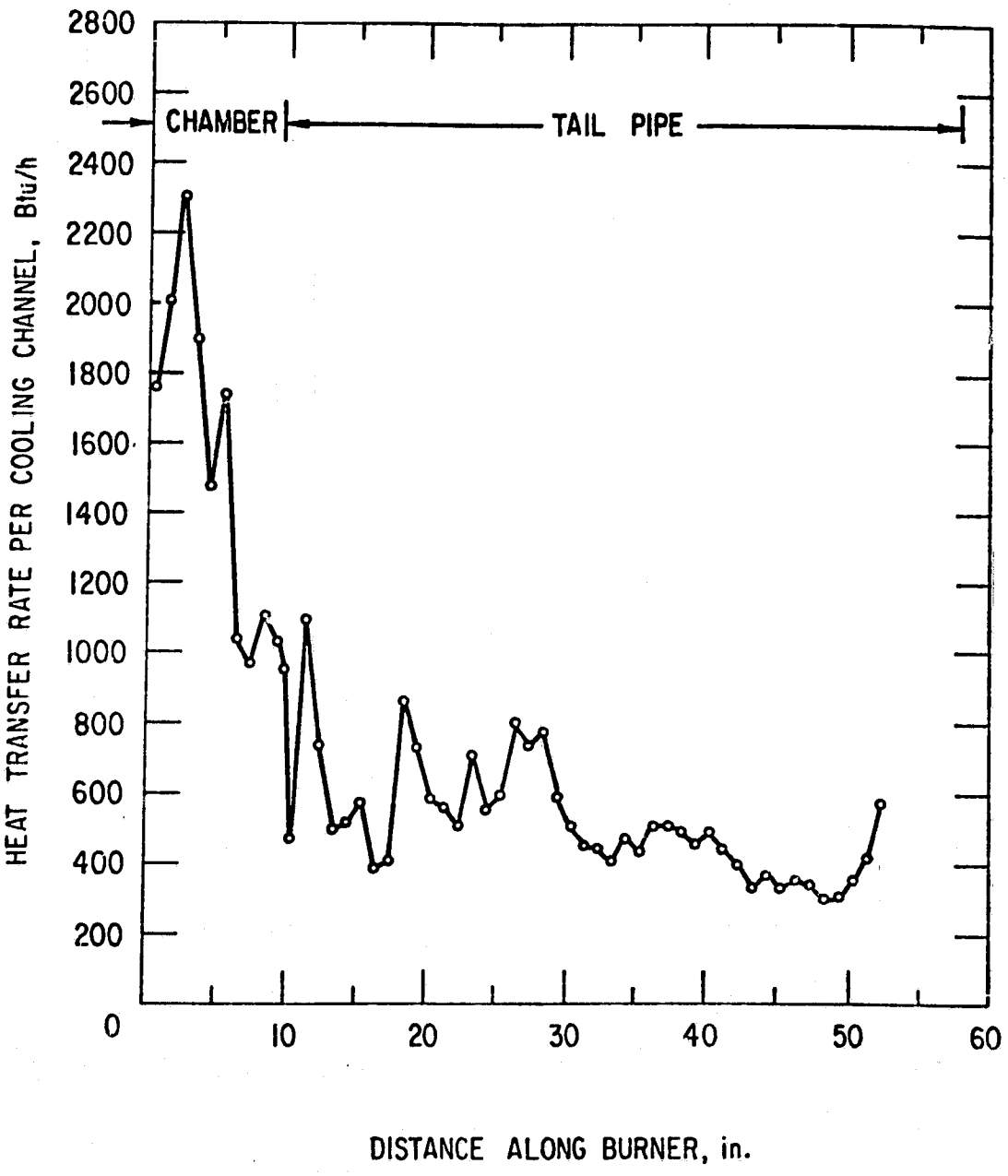

Fig. D.17 Heat Transfer along Burner with a Tailpipe Aspirator for a 50,418 Btu/h Heat Input and a 10.0 Air/Fuel Ratio

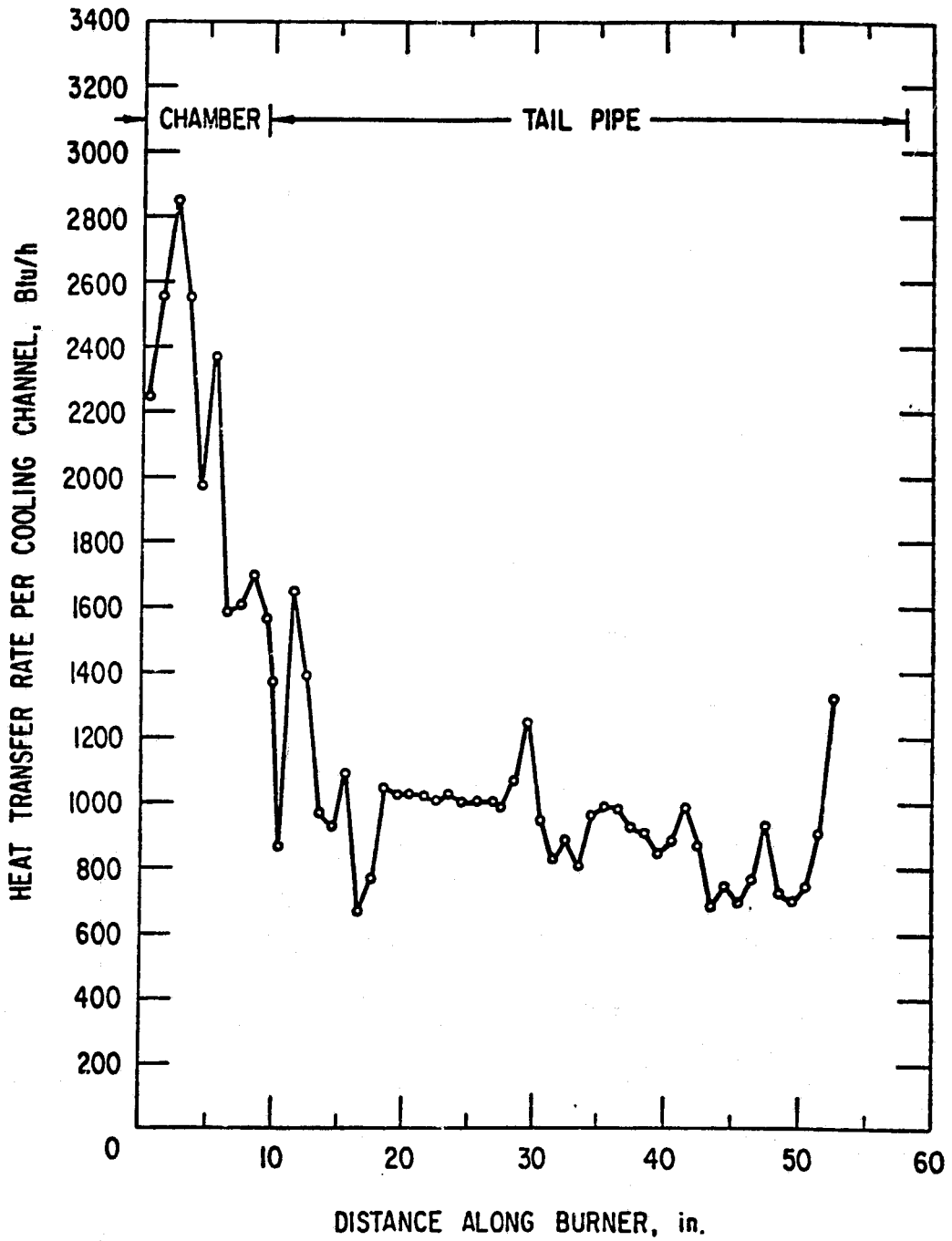

Fig. D.18 Heat Transfer along Burner with a Tailpipe Aspirator for a 98,620 Btu/h Heat Input and a 9.6 Air/Fuel Ratio

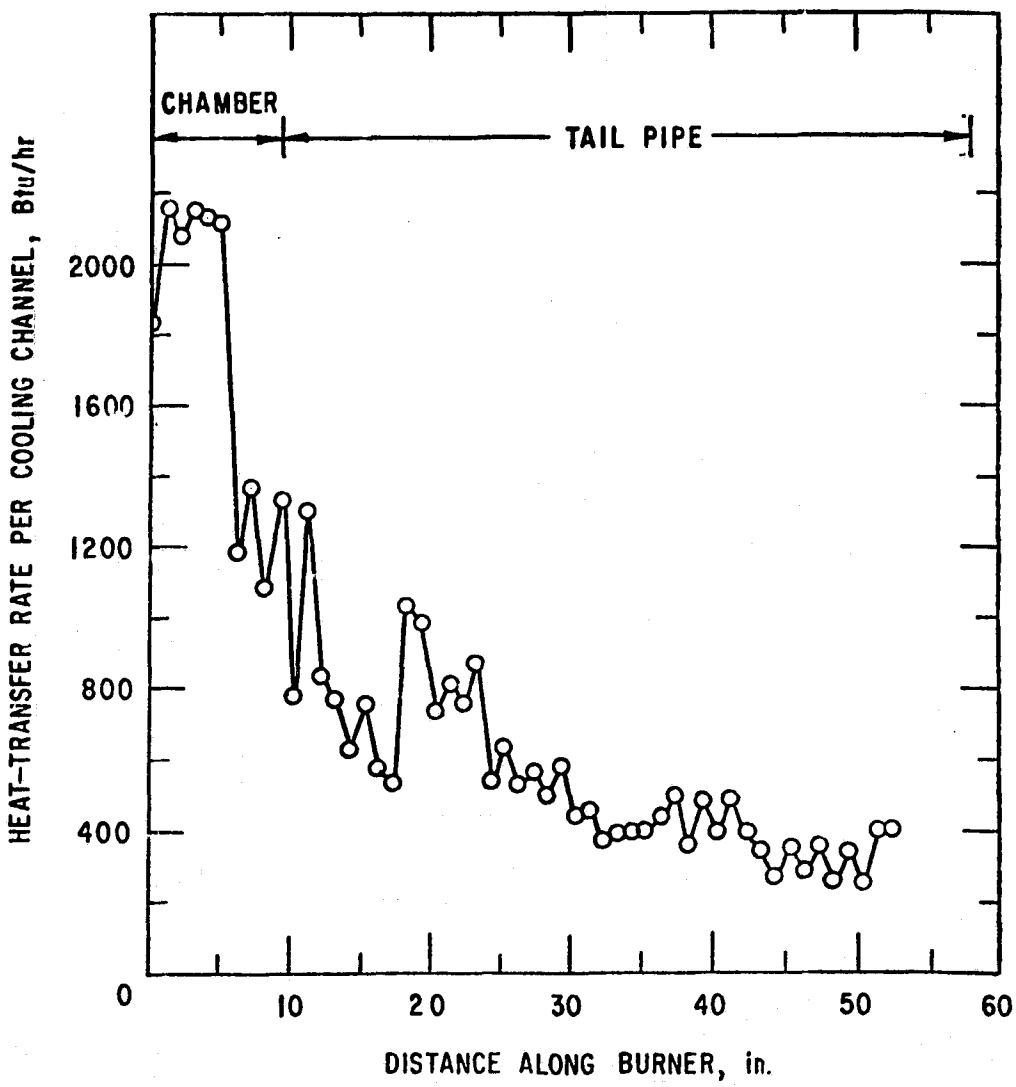

Fig. D.19 Heat Transfer along Burner with an Inlet Muffler for a 53,116 Btu/h Heat Input and an 11.0 Air/Fuel Ratio

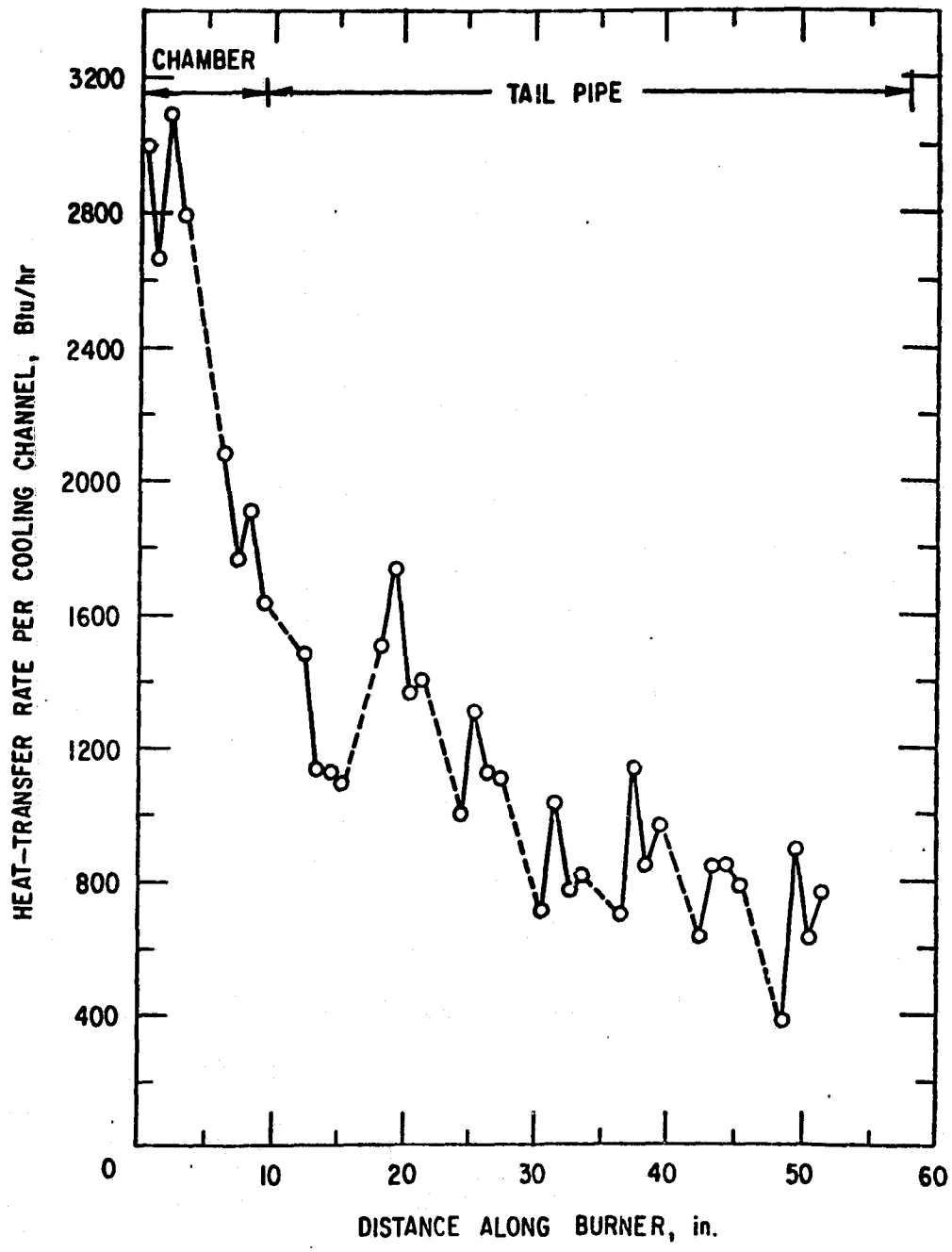

Fig. D.20 Heat Transfer along Burner with an Inlet Muffler for a 103,728 Btu/h Heat Input and an 10.1 Air/Fuel Ratio (partial data set)

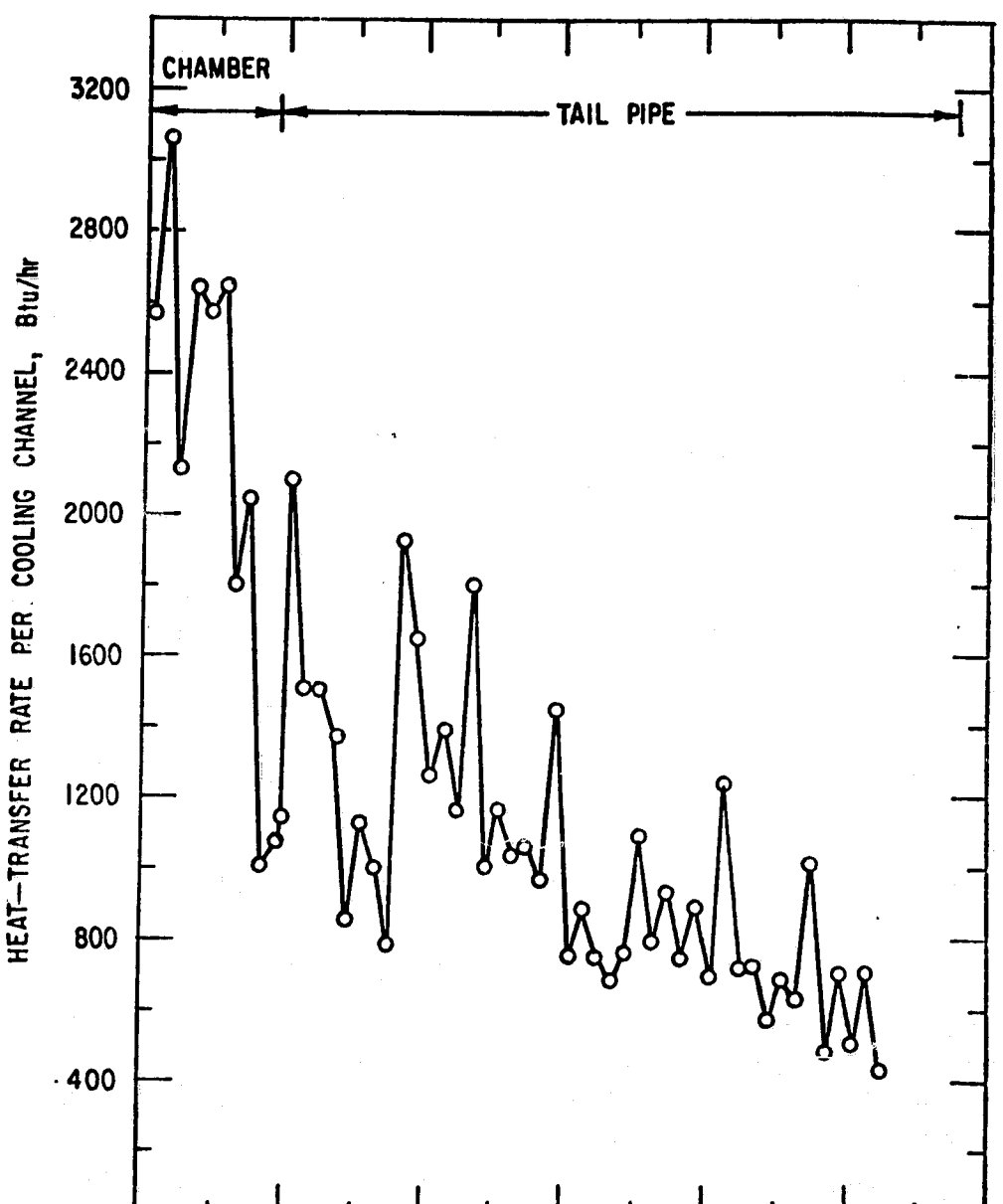

Fig. D.21 Heat Transfer along Burner with an Inlet Muffler for a 101,532 Btu/h Heat Input and a 10.1 Air/Fuel Ratio

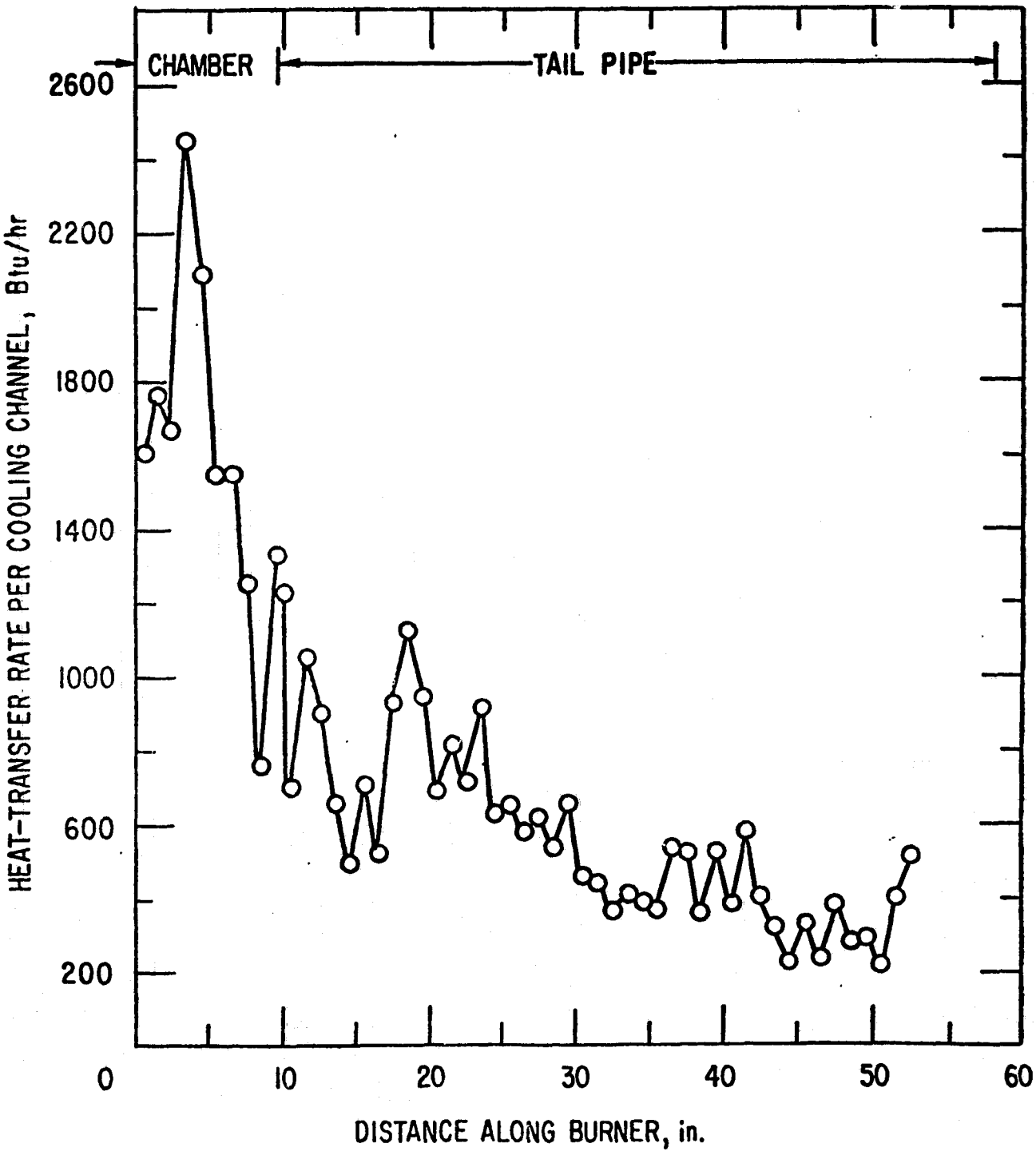

Fig. D.22 Heat Transfer along Burner with an Exhaust Muffler for a 53,429 Btu/h Heat Input and an 11.5 Air/Fuel Ratio

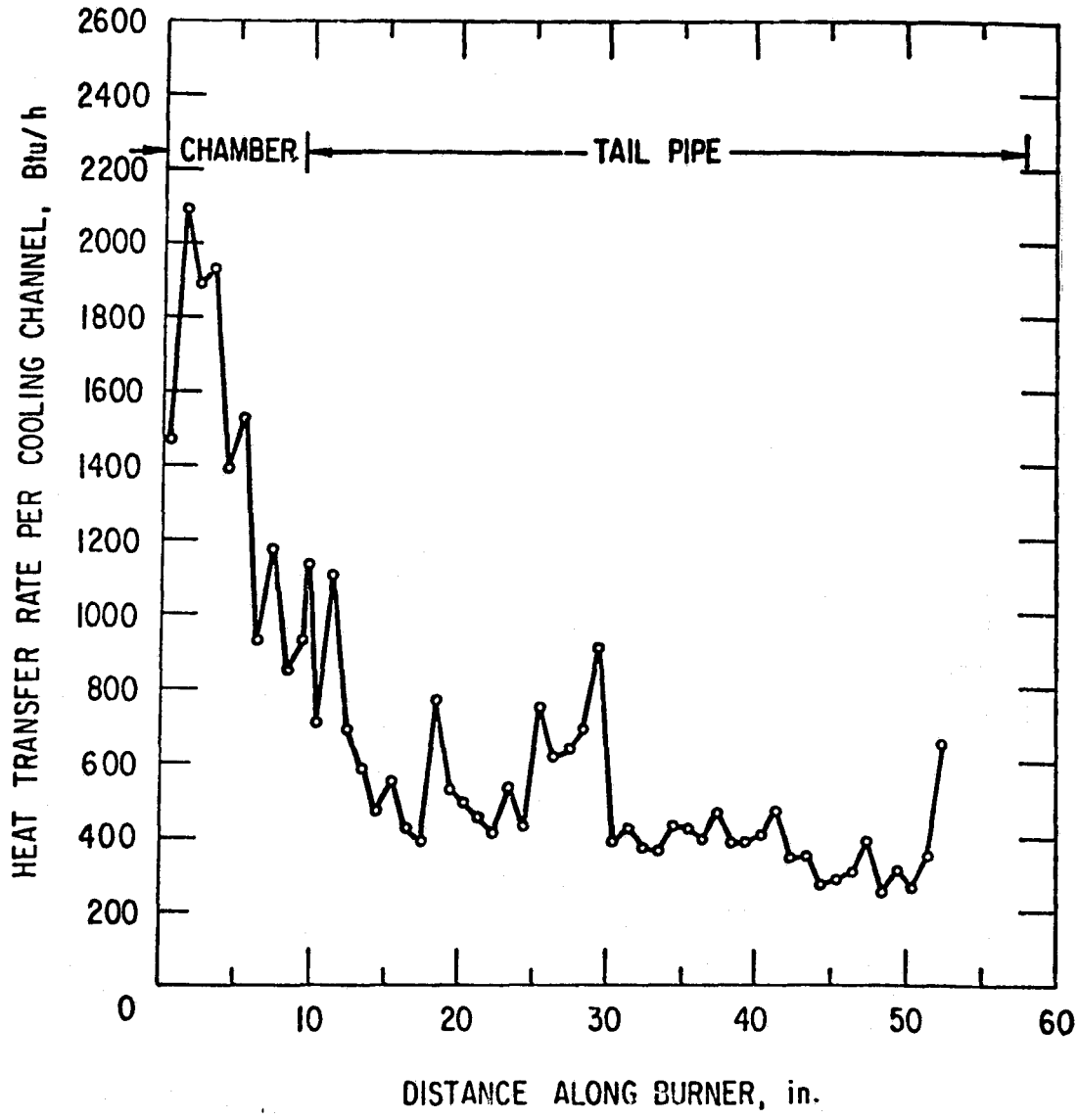

Fig. D.23 Heat Transfer along Burner with Inlet and Exhaust Mufflers for a 50,227 Btu/h Heat Input and a 9.4 Air/Fuel Ratio

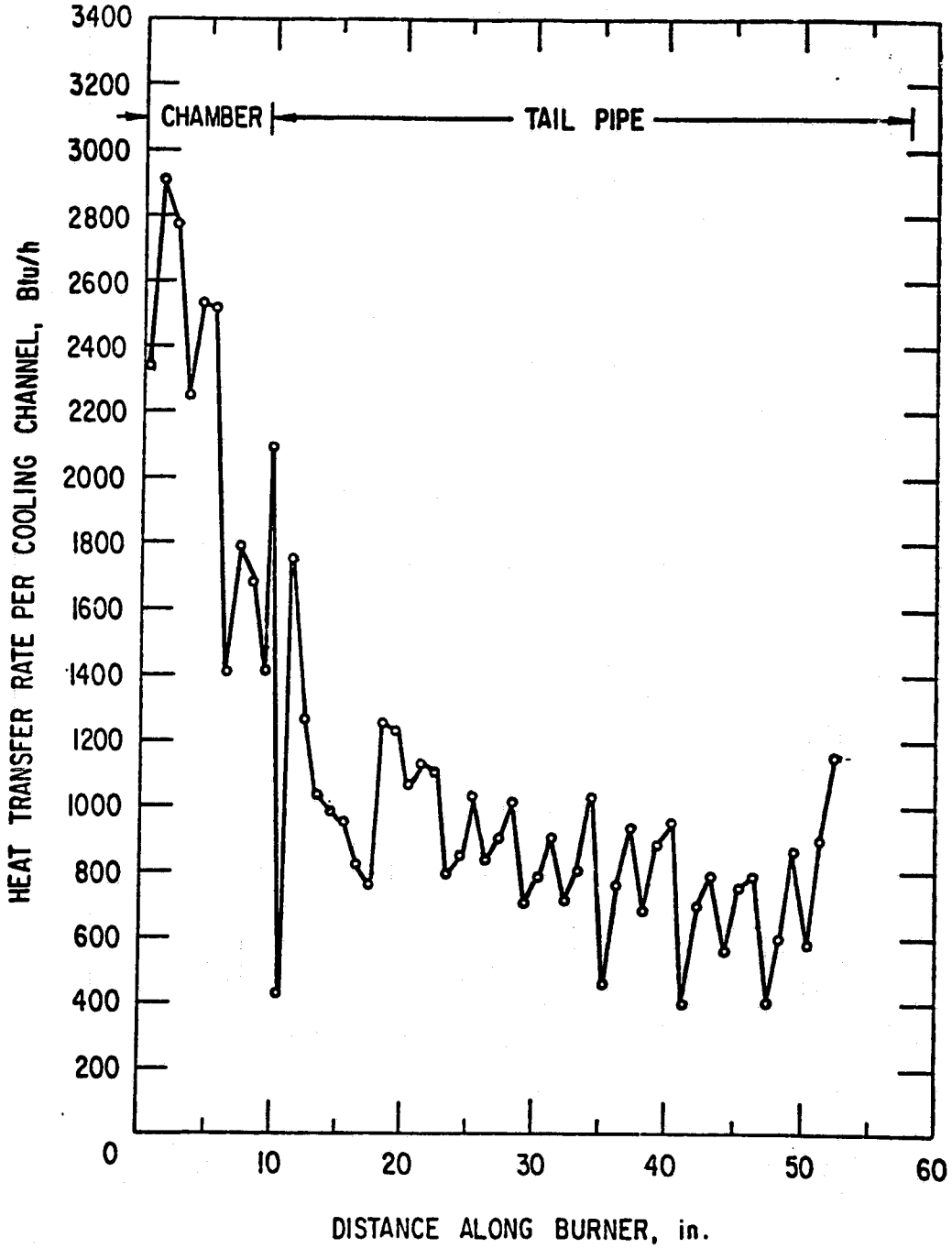

Fig. D.24 Heat Transfer along Burner with Inlet and Exhaust Mufflers for a 100,580 Btu/h Heat Input and an 8.9 Air/Fuel Ratio

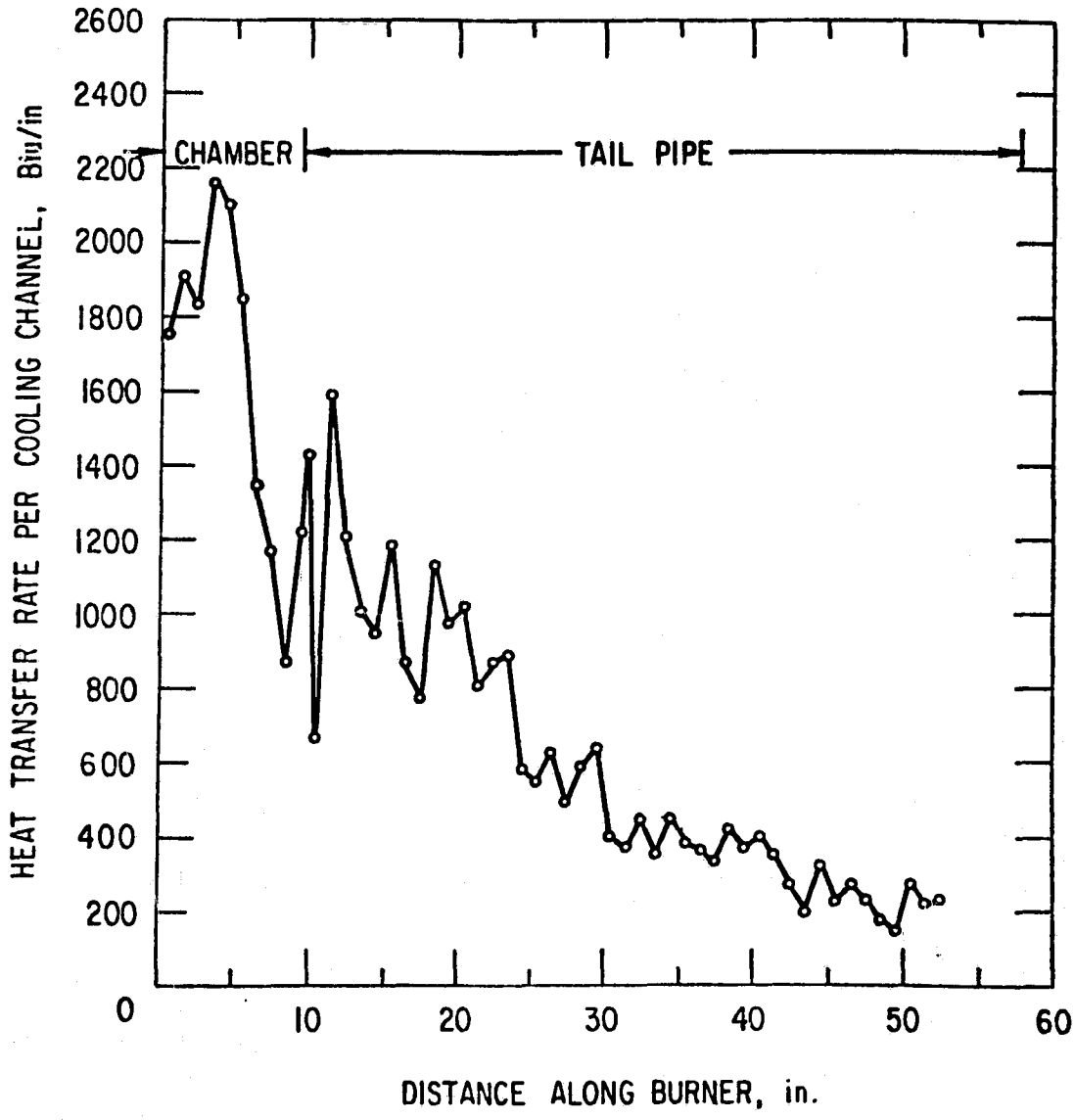

Fig. D.25 Heat Transfer along Burner with a 1-in.-Diameter, 48-in.-long Corebustor for a 49,867 Btu/h Heat Input and a 9.9 Air/Fuel Ratio

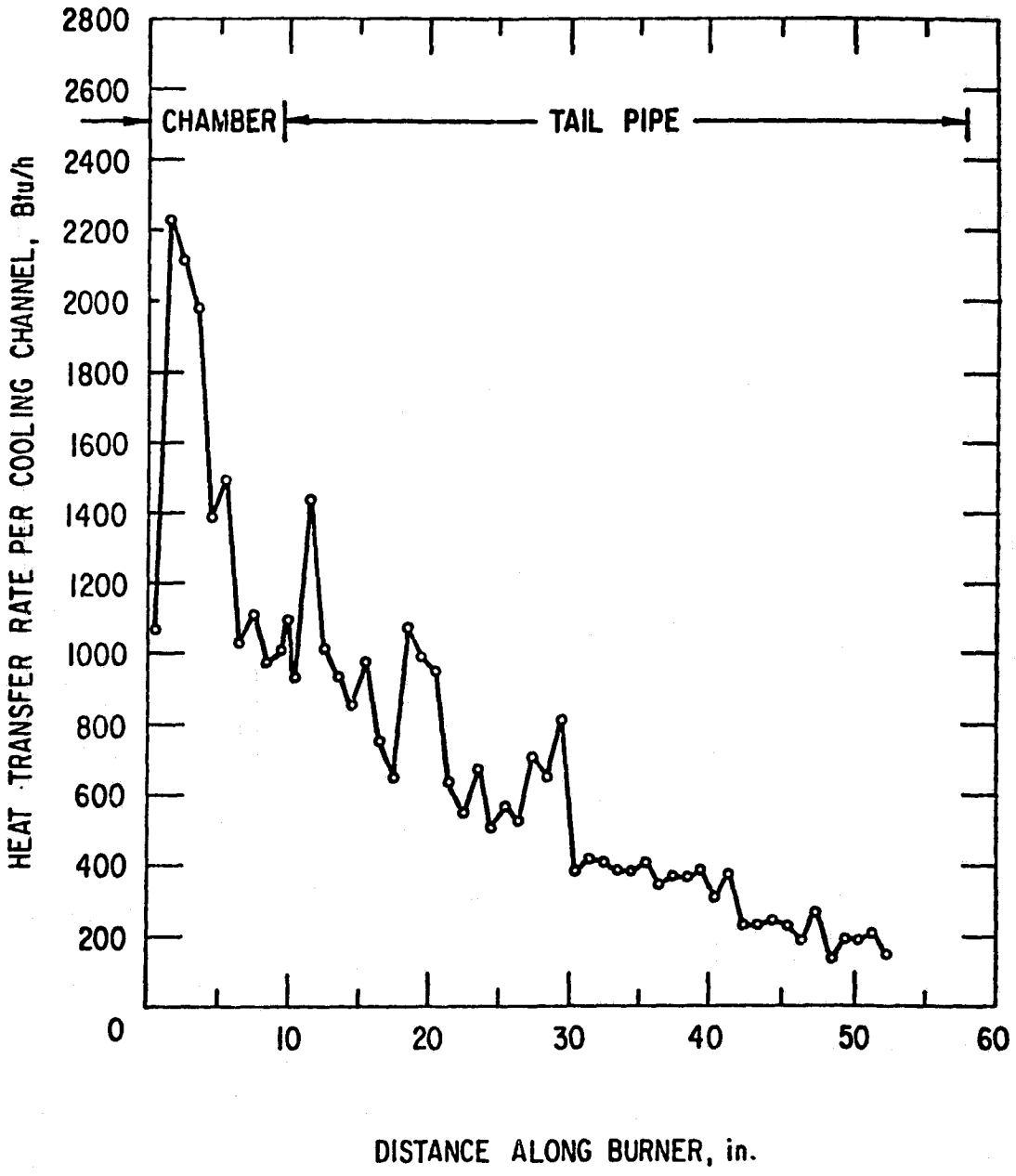

Fig. D.26 Heat Transfer along Burner with a 1-in.-Diameter, 48-in.-long Corebustor for a 50,341 Btu/h Heat Input and a 9.8 Air/Fuel Ratio

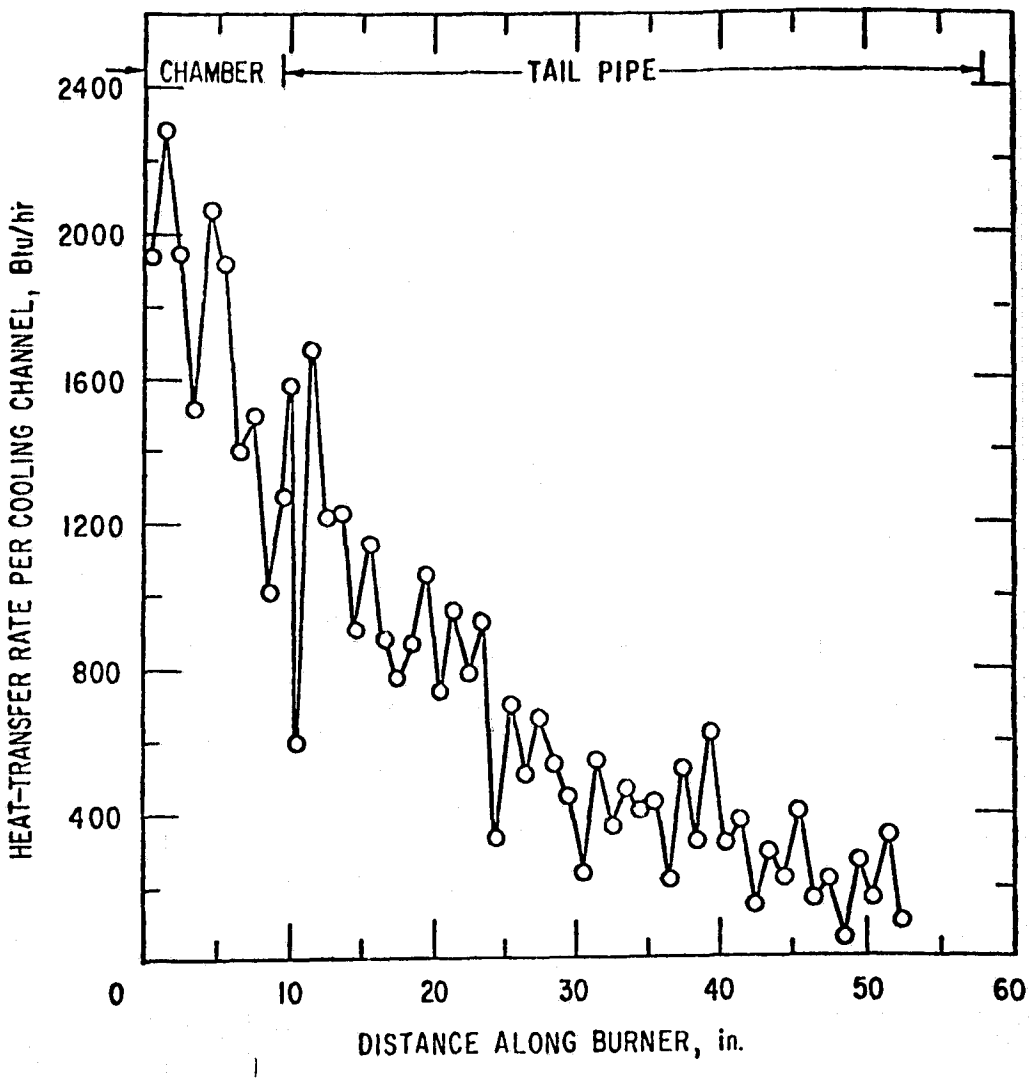

Fig. D.27 Heat Transfer along Burner with a 1-in.-Diameter, 48-in.-long Corebustor for a 50,882 Btu/h Heat Input and a 10.1 Air/Fuel Ratio

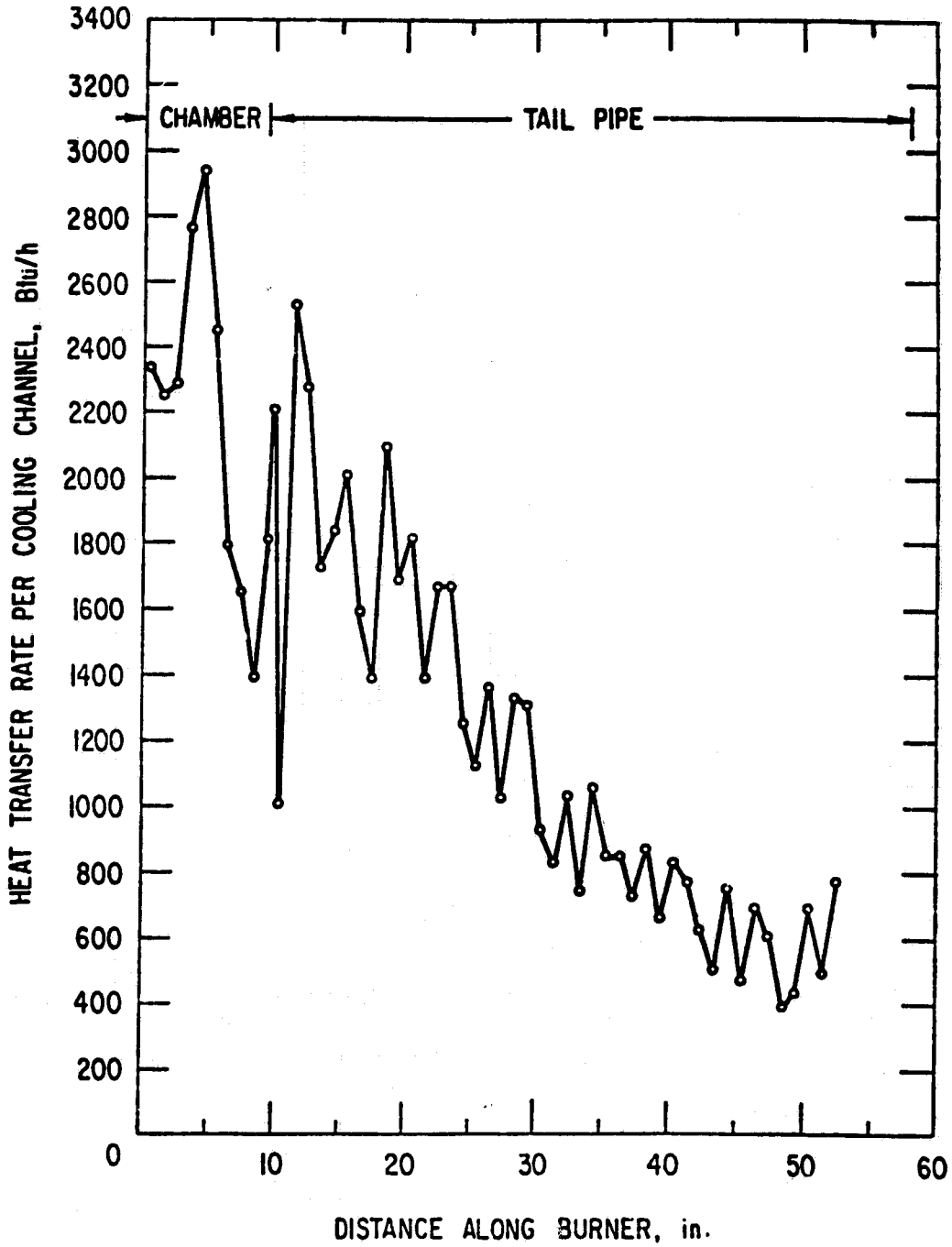

Fig. D.28 Heat Transfer along Burner with a 1-in.-Diameter, 48-in.-long Corebustor for a 99,996 Btu/h Heat Input and a 9.7 Air/Fuel Ratio

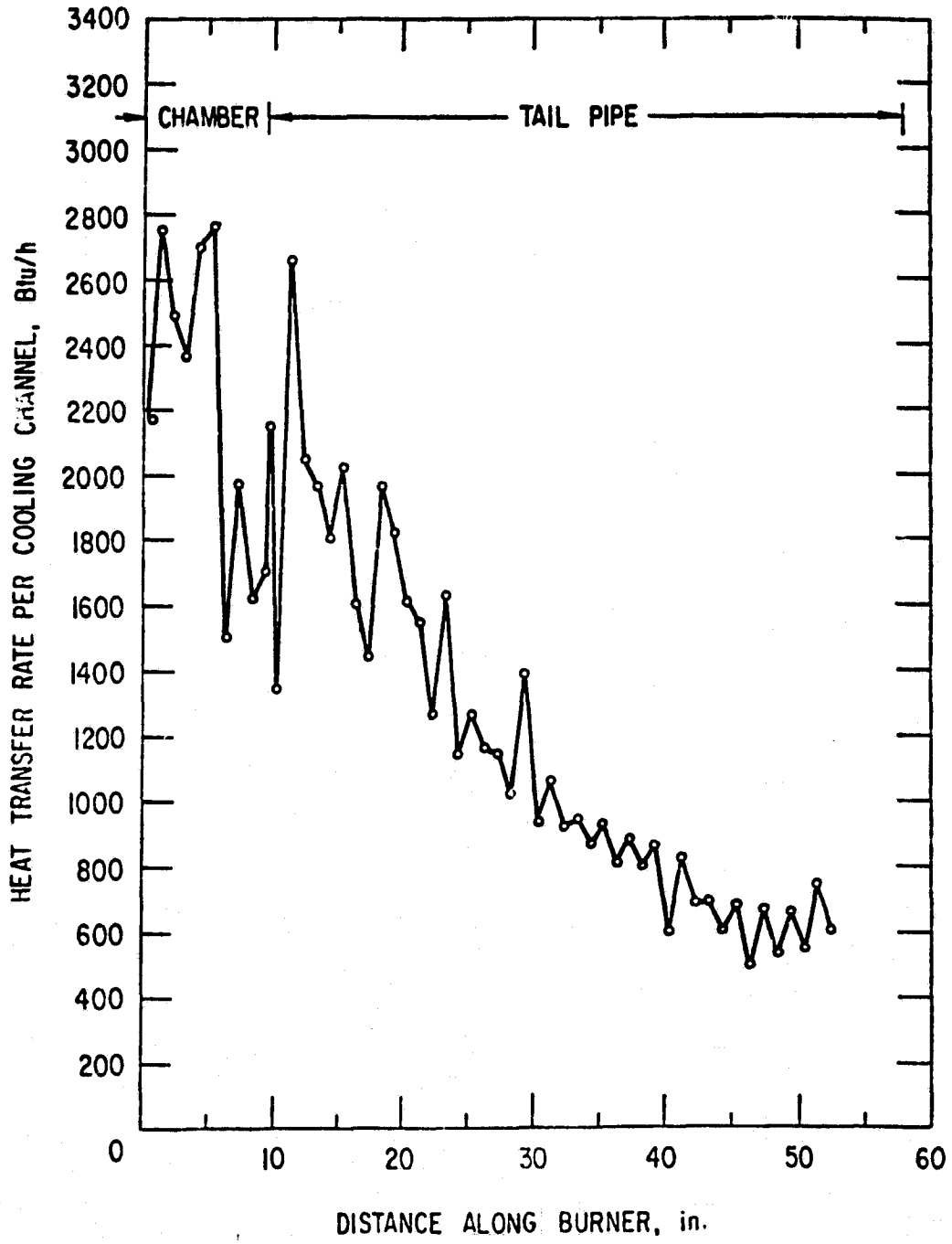

Fig. D.29 Heat Transfer along Burner with a 1-in.-Diameter, 48-in.-long Corebustor for a 101,248 Btu/h Heat Input and a 10.1 Air/Fuel Ratio

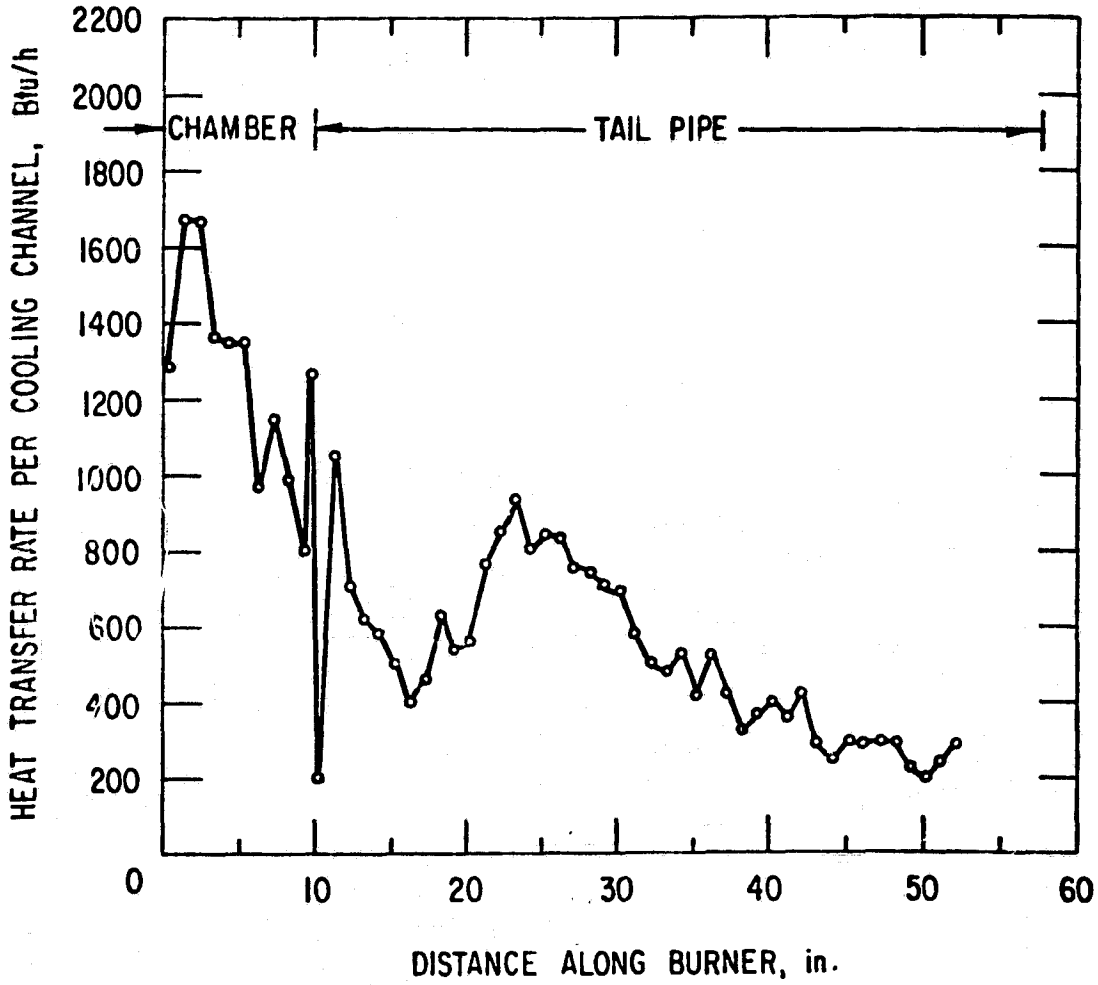

Fig. D.30 Heat Transfer along Burner with a 1-in.-Diameter, 36-in.-long Corebustor for a 50,042 Btu/h Heat Input and a 10.1 Air/Fuel Ratio

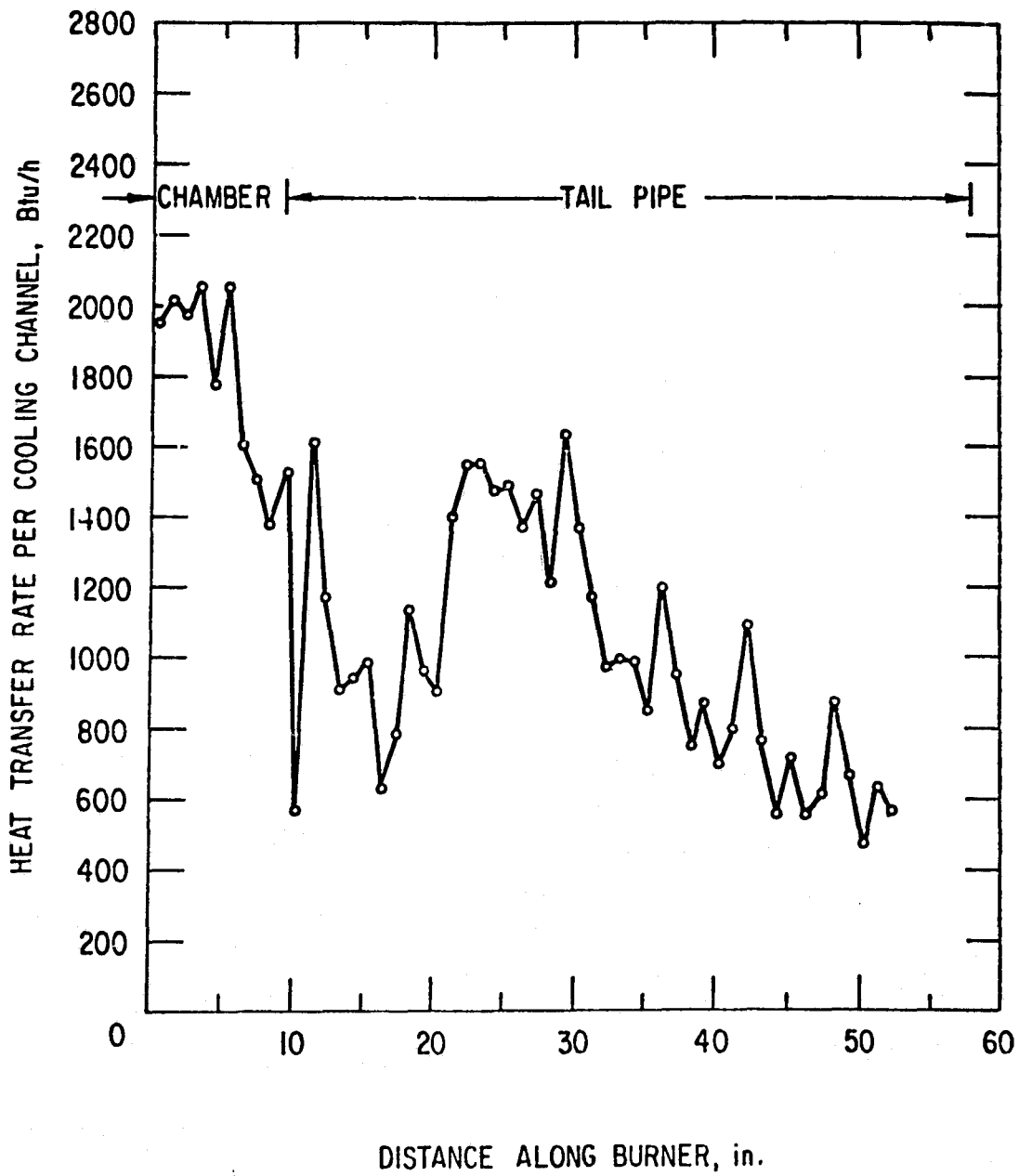

Fig. D.31 Heat Transfer along Burner with a 1-in.-Diameter, 36-in.-long Corebustor for a 97,009 Btu/h Heat Input and a 10.1 Air/Fuel Ratio

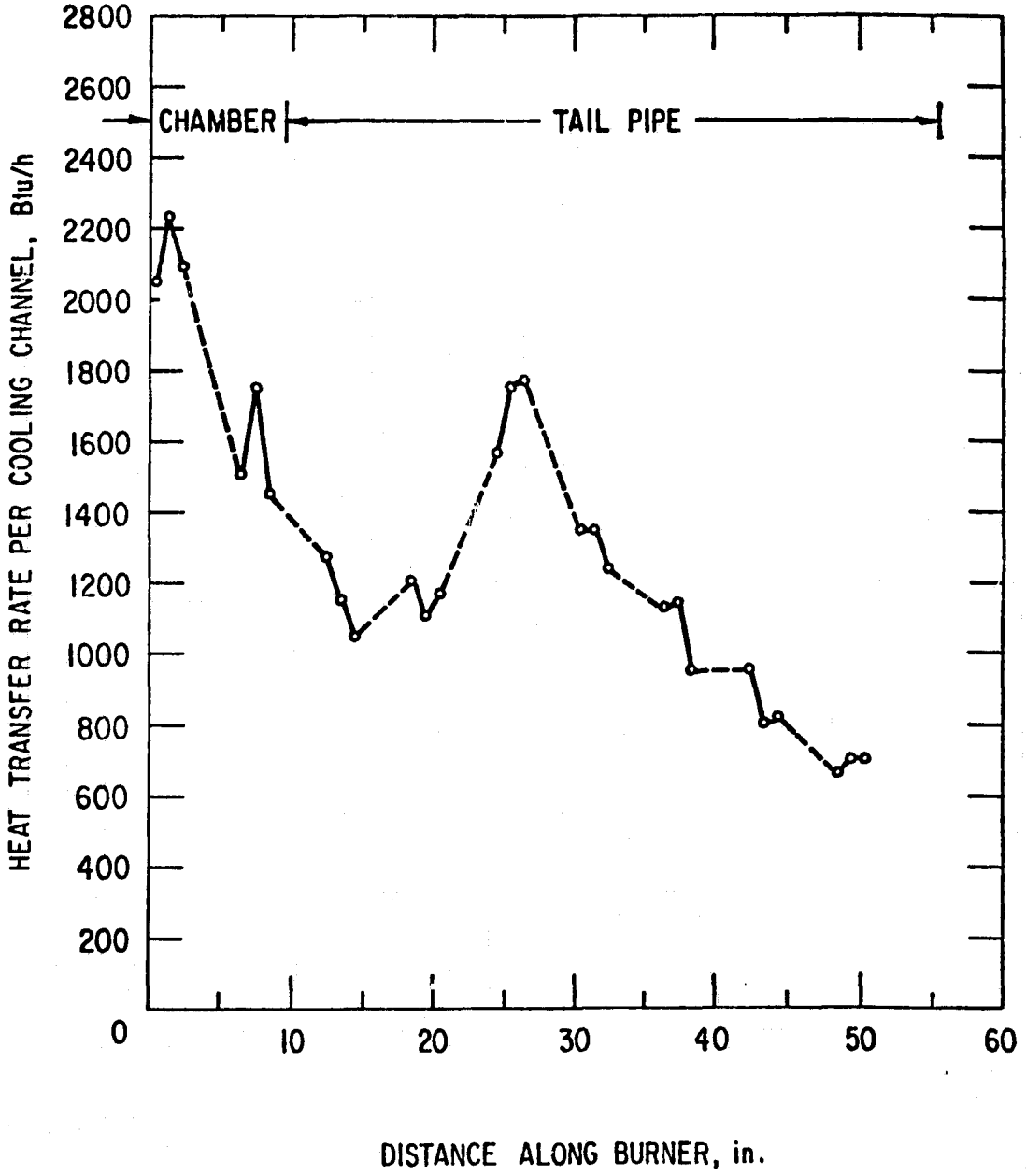

Fig. D.32 Heat Transfer along Burner with a 1-in.-Diameter, 36-in.-long Corebustor for a 100,553 Btu/h Heat Input and a 9.8 Air/Fuel Ratio

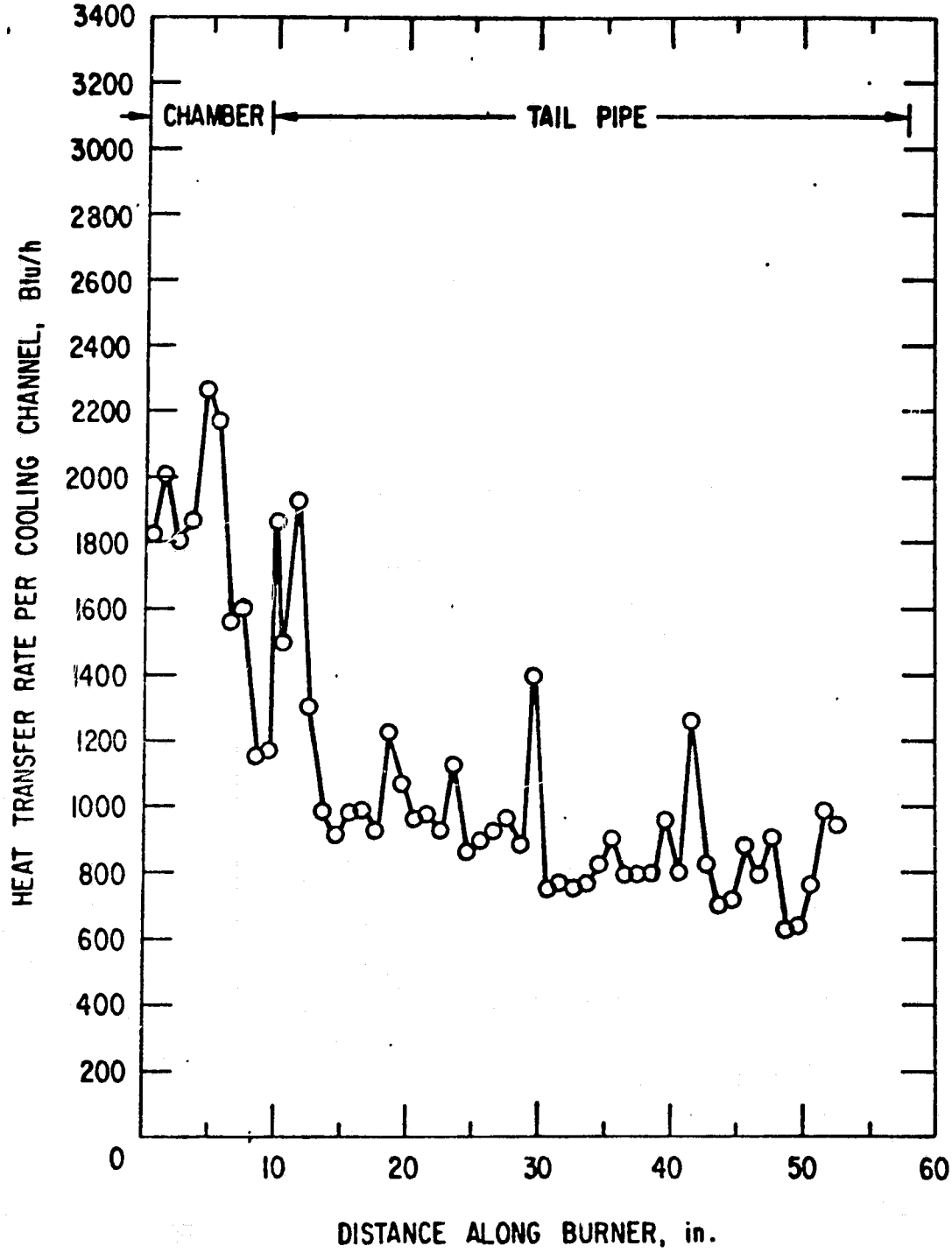

Fig. D.33 Heat Transfer along Burner with an Air-Decoupling Chamber for a 100,794 Btu/h Heat Input and a 10.5 Air/Fuel Ratio

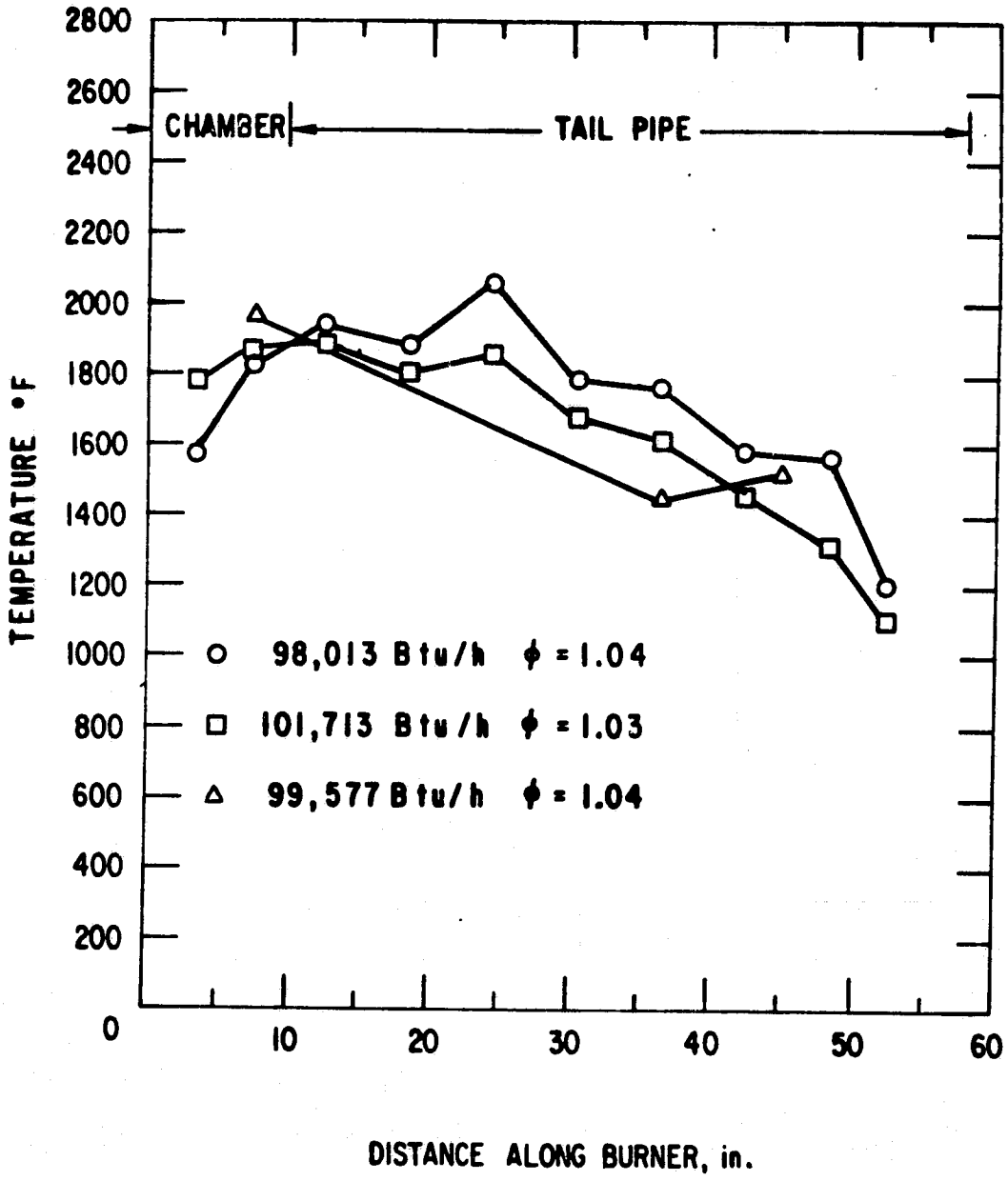

Fig. D.34 Measured Exhaust-Gas Temperature for the Burner Operating at Approximately 100,000 Btu/h

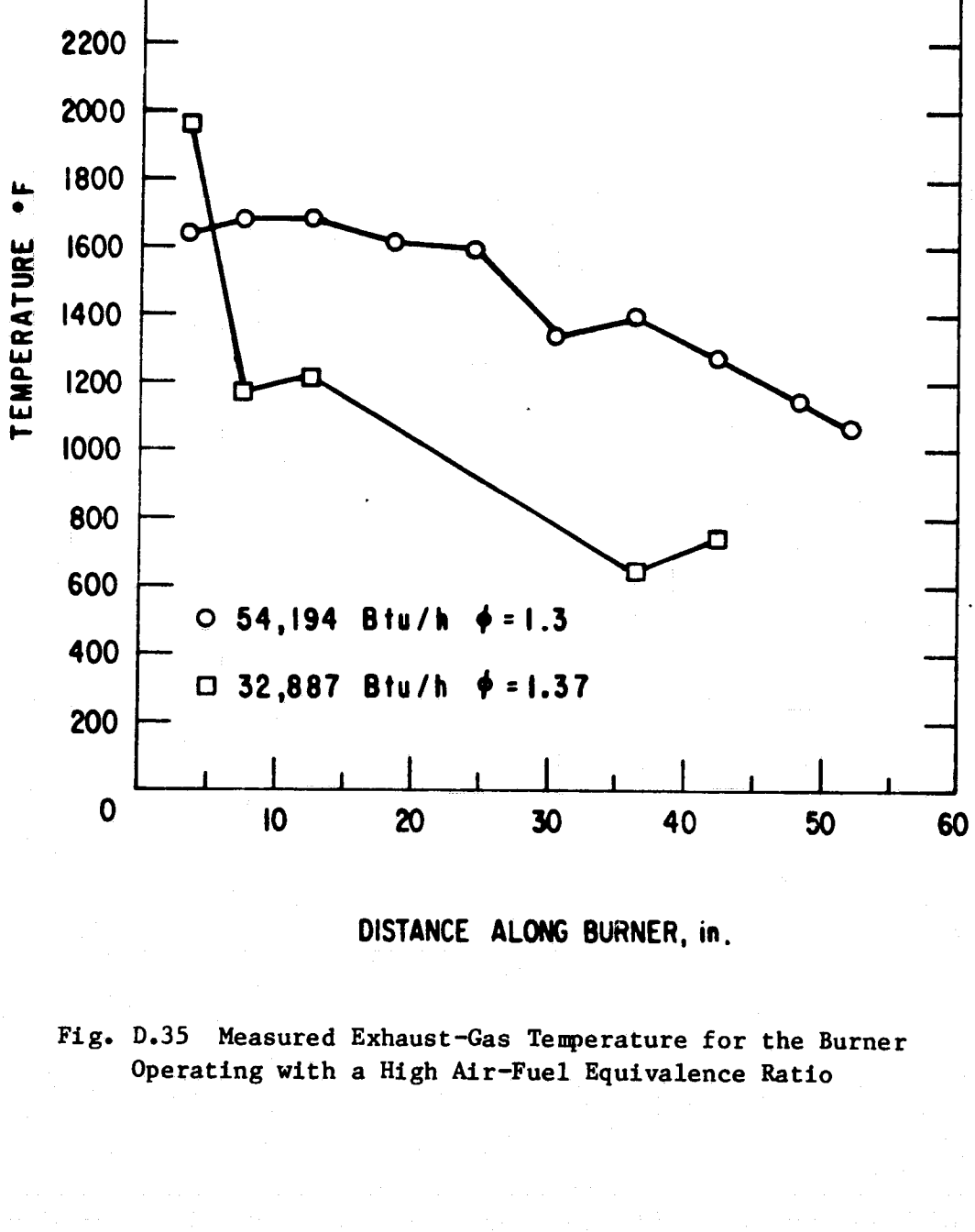

Fig. D.35 Measured Exhaust-Gas Temperature for the Burner Operating with a High Air-Fuel Equivalence Ratio

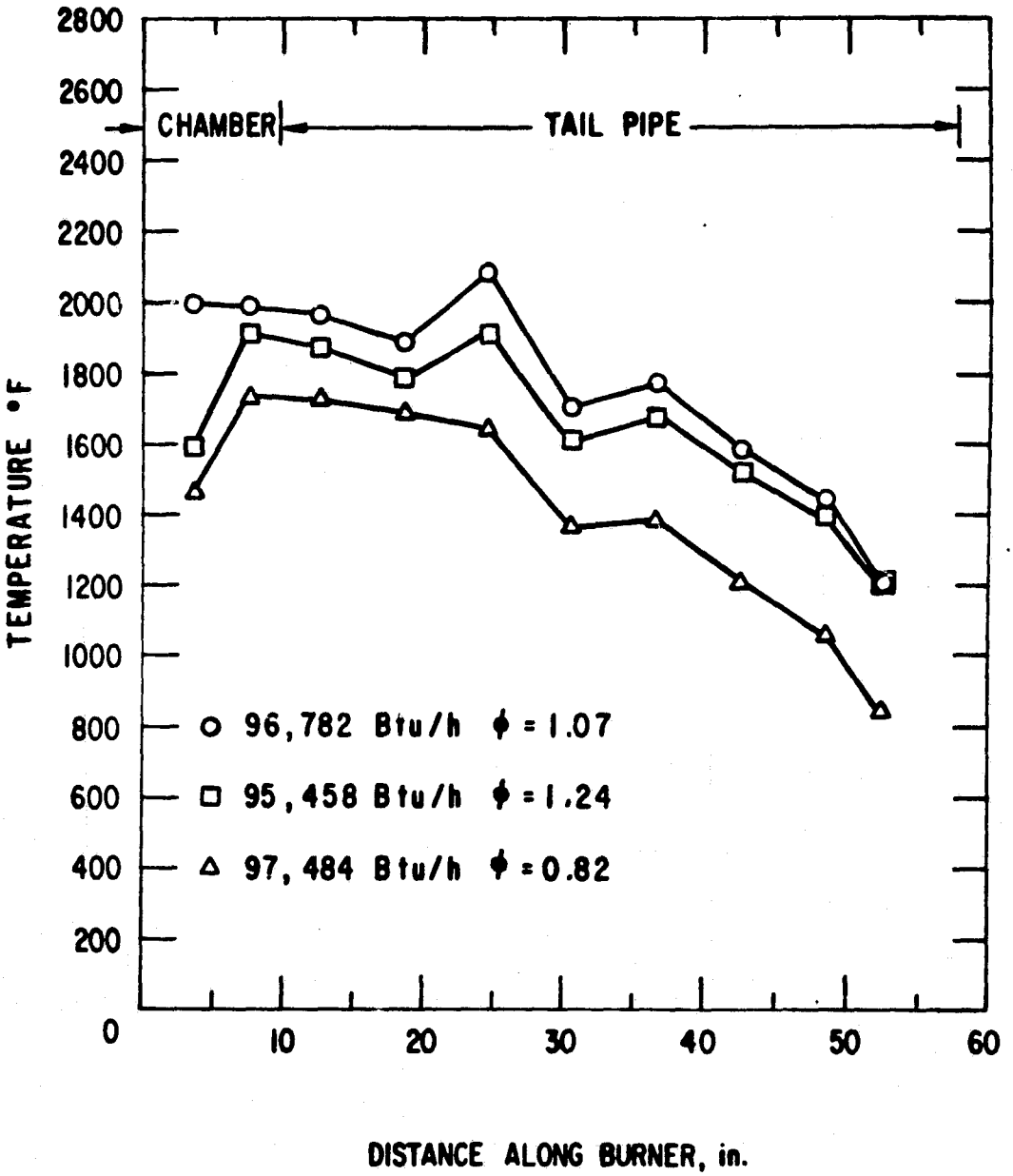

Fig. D.36 Effect of Air-Fuel Equivalence Ratio on the Measured Exhaust-Gas Temperature

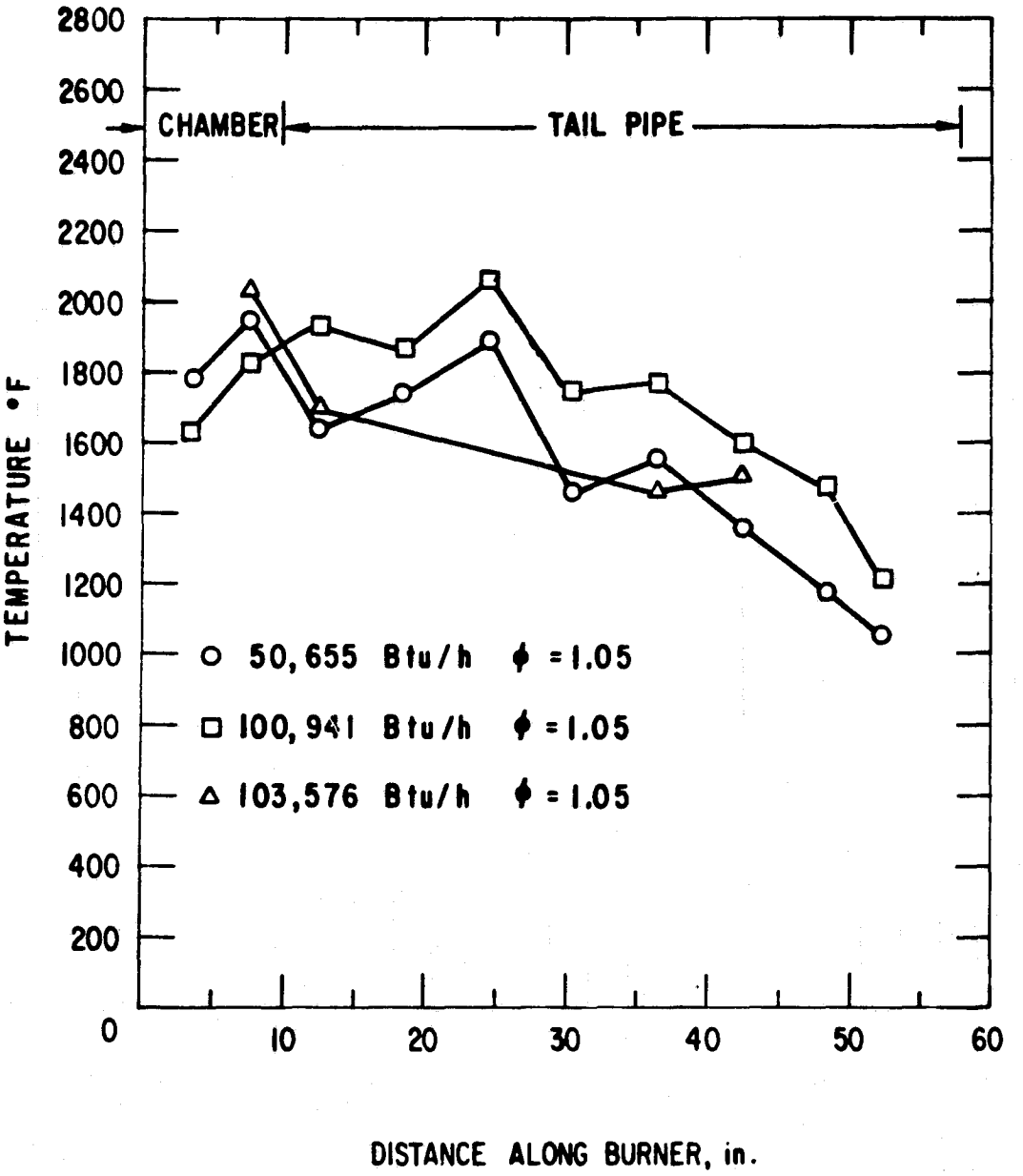

Fig. D.37 Measured Exhaust-Gas Temperature for the Burner Operating with an Equivalence Ratio of 1.05

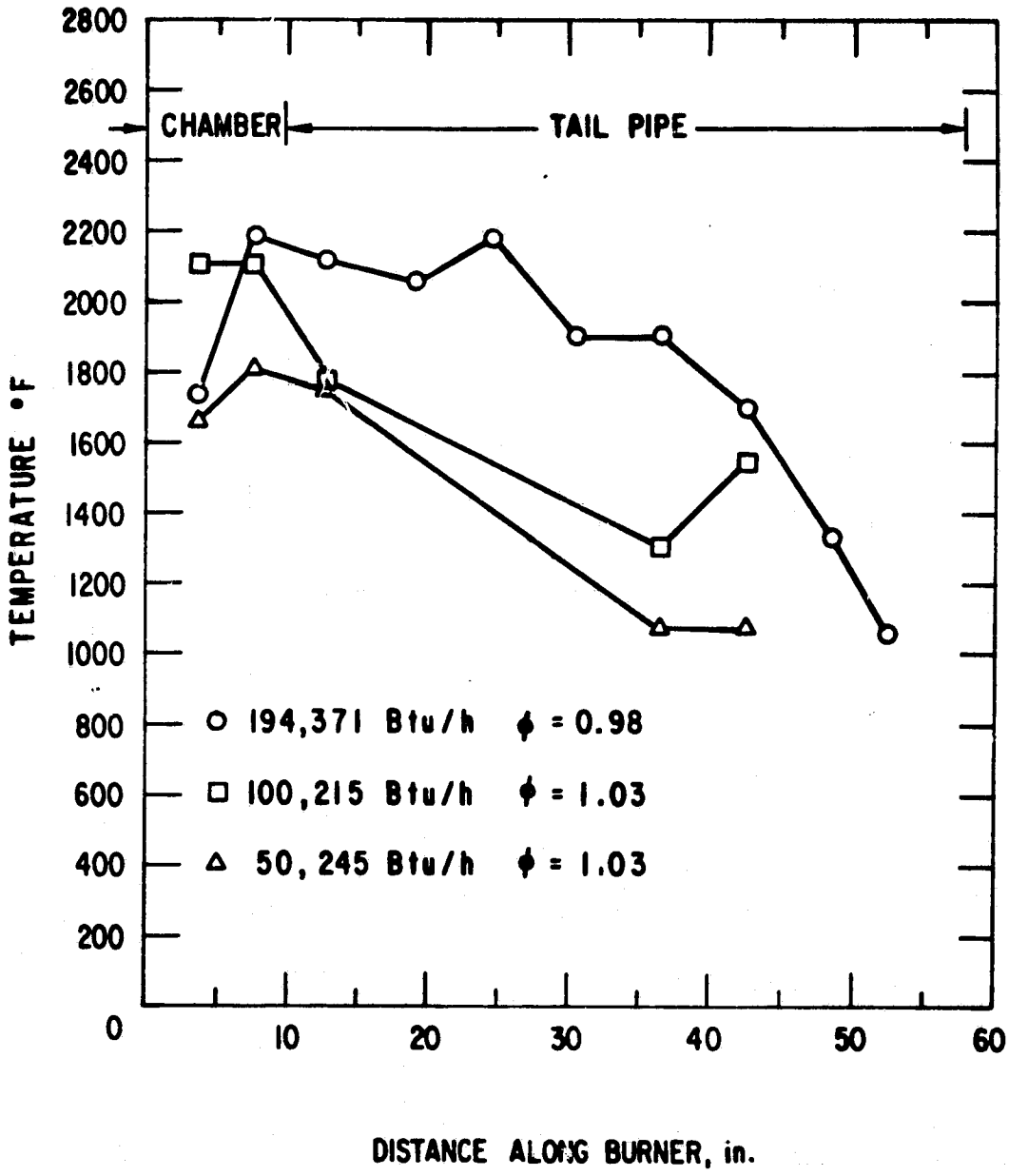

Fig. D.38 Effect of Heat Input to the Burner on the Measured Exhaust-Gas Temperature

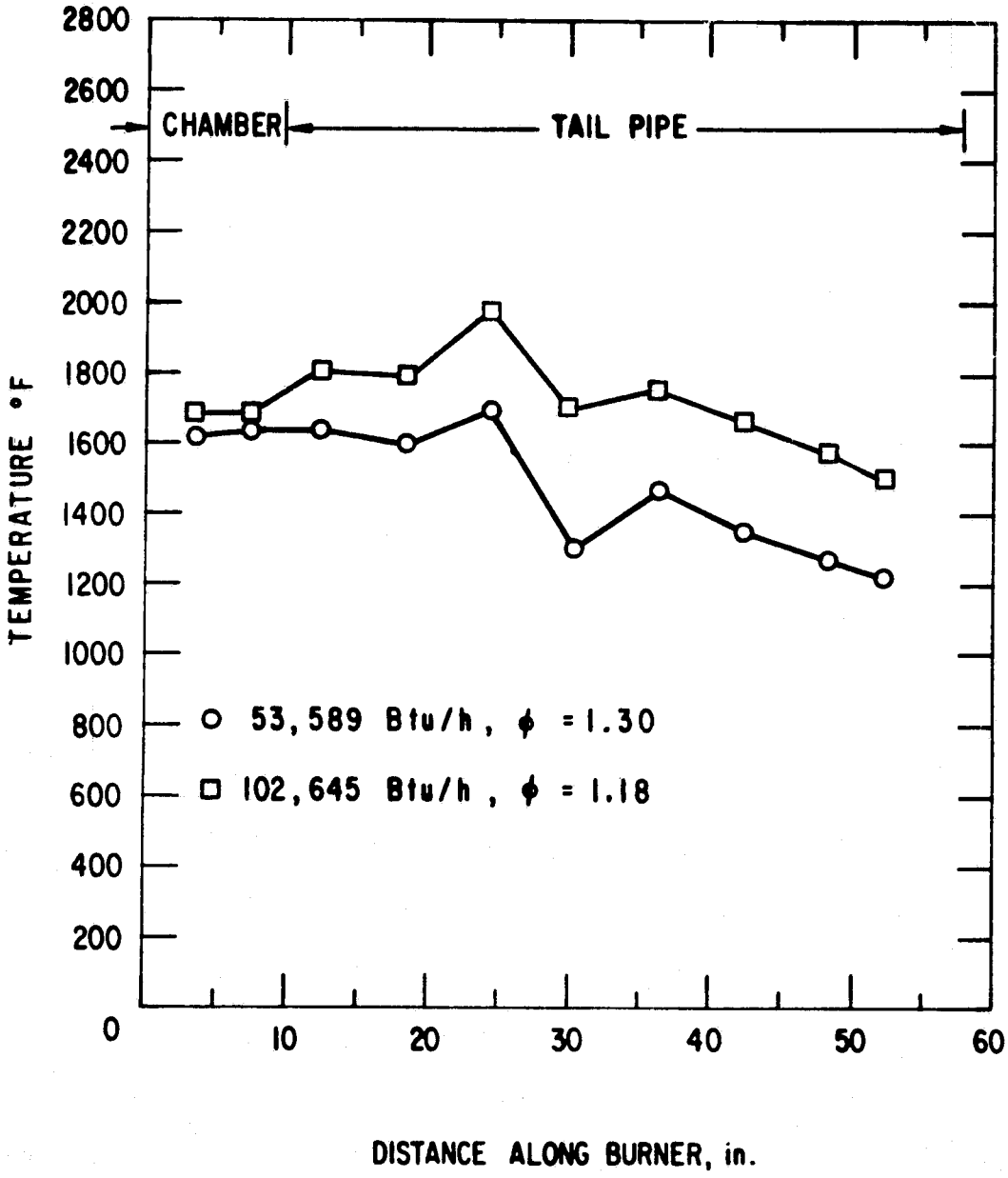

Fig. D.39 Measured Exhaust-Gas Temperature for the Burner without Flapper Valves

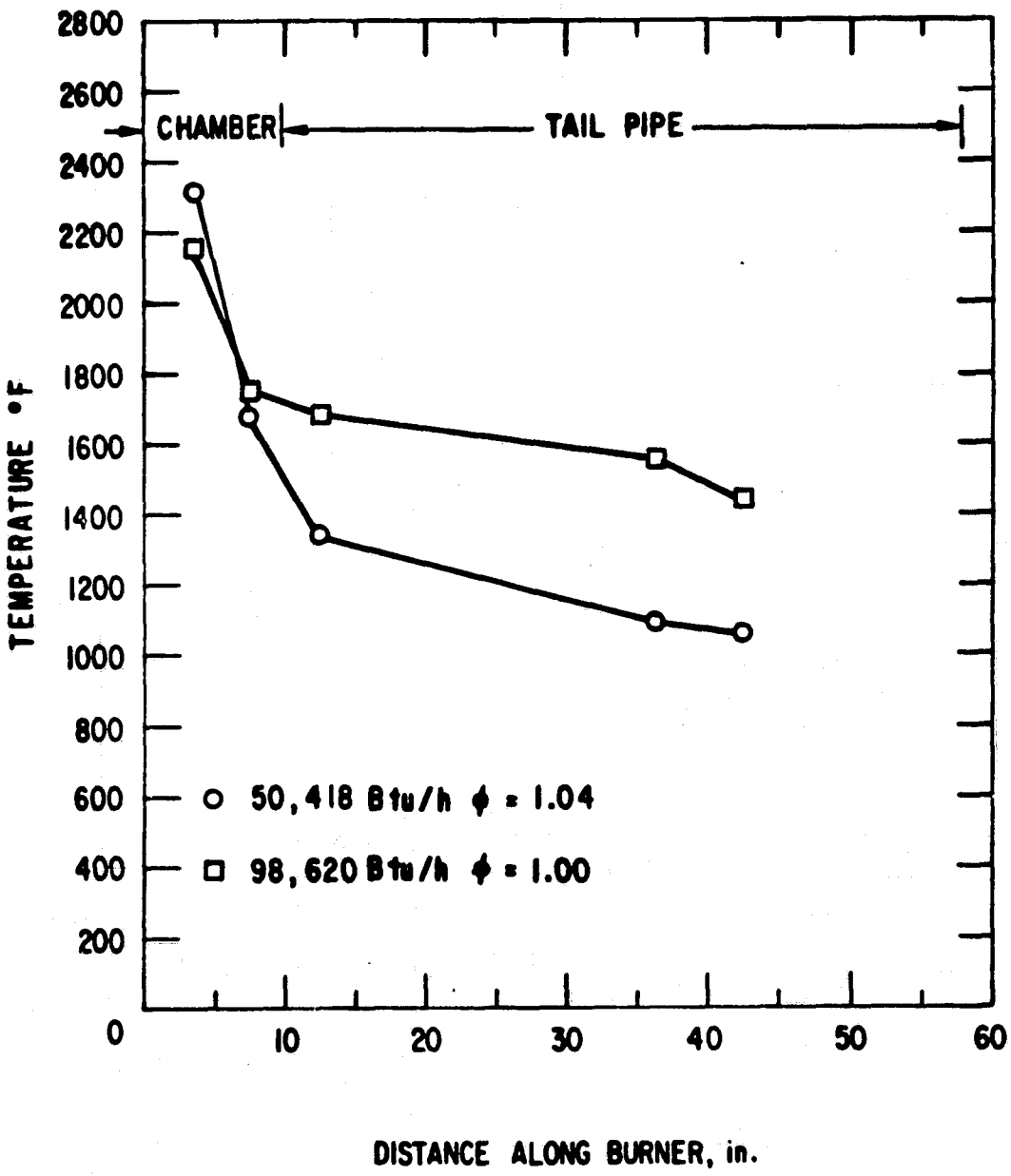

Fig. D.40 Measured Exhaust-Gas Temperature for the Burner with a Tailpipe Aspirator

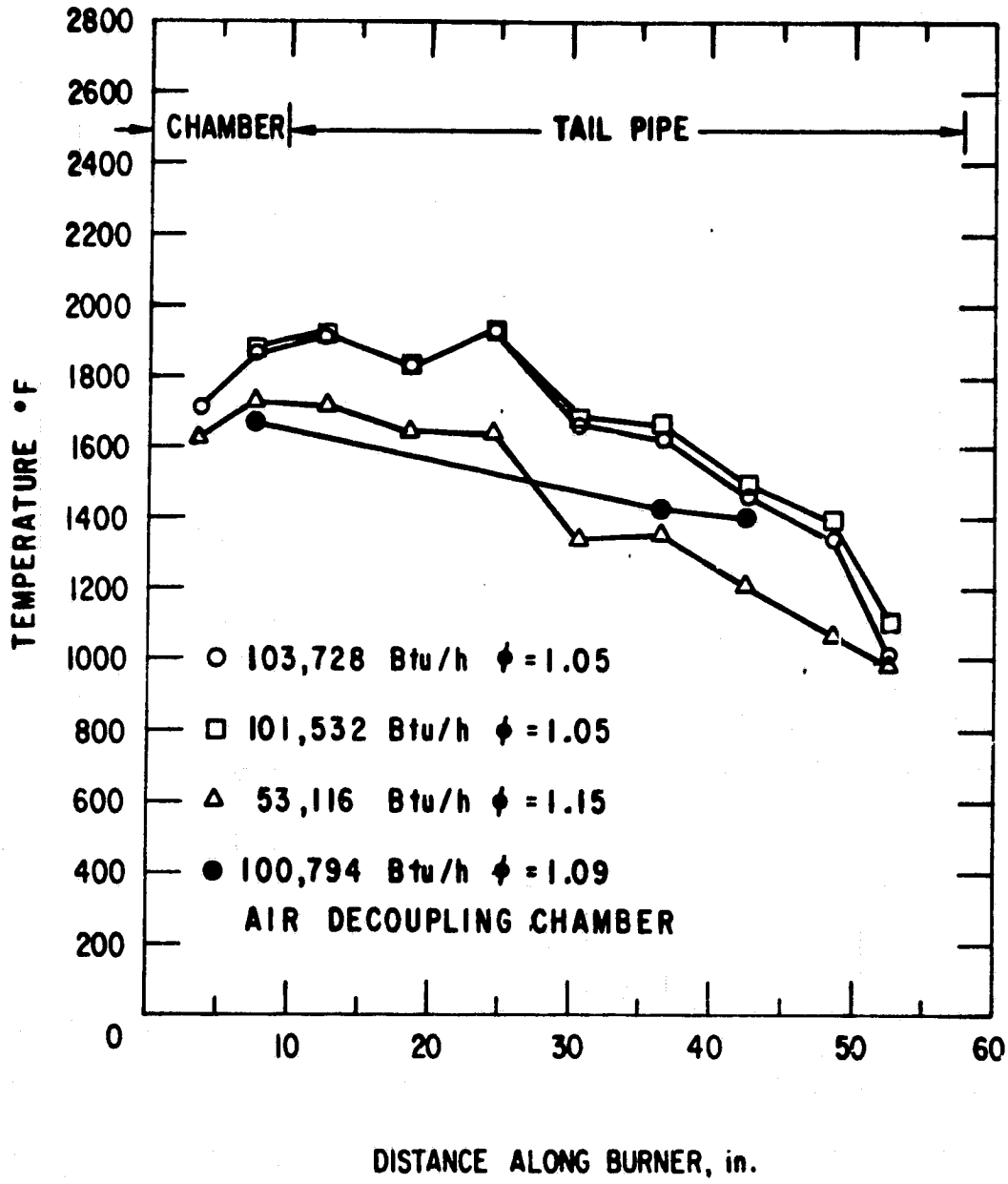

Fig. D.41 Measured Exhaust-Gas Temperature for the Burner with an Inlet Muffler or Air-Decoupling Chamber

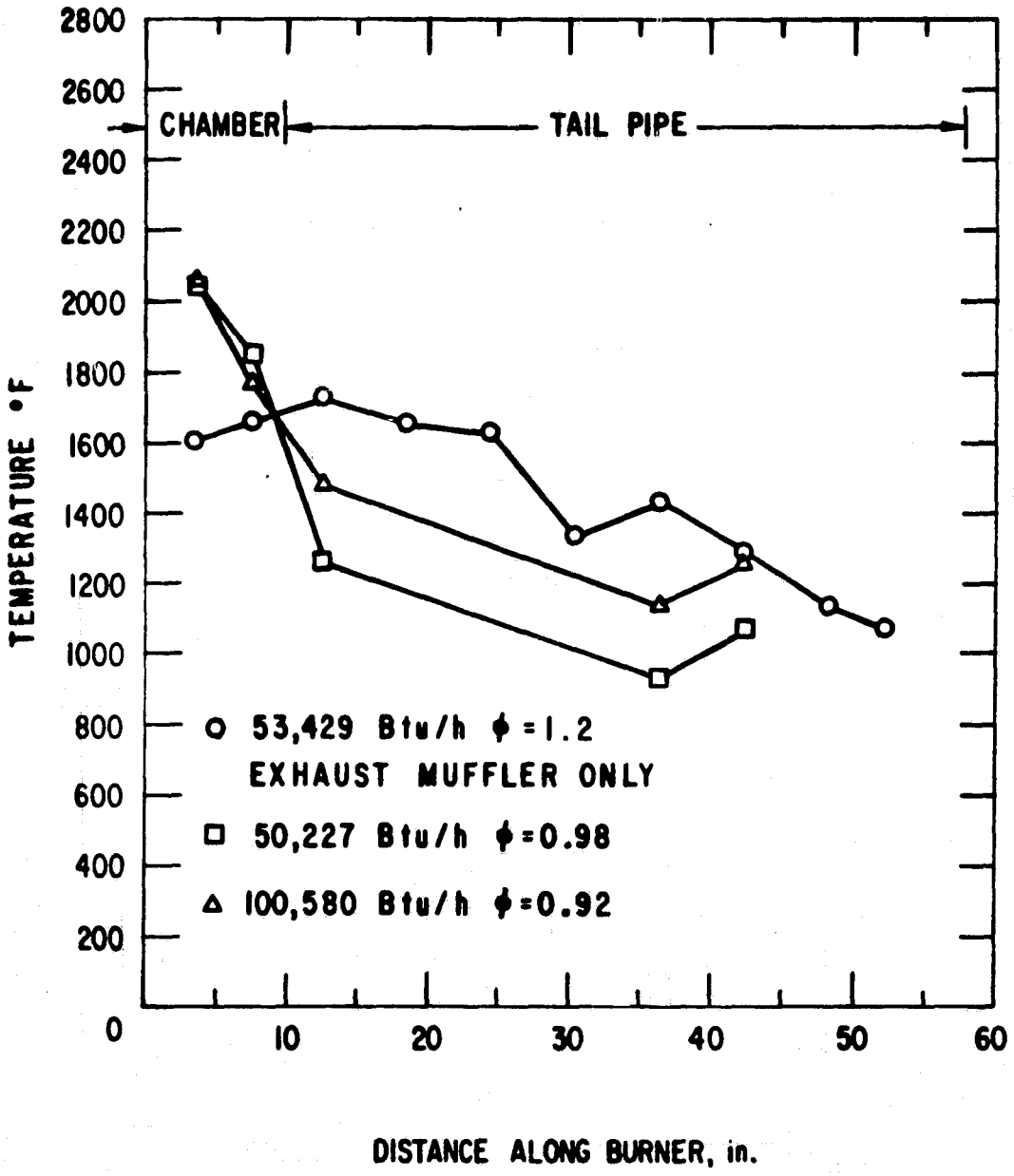

Fig. D.42 Measured Exhaust-Gas Temperature for the Burner with Inlet and Exhaust Mufflers

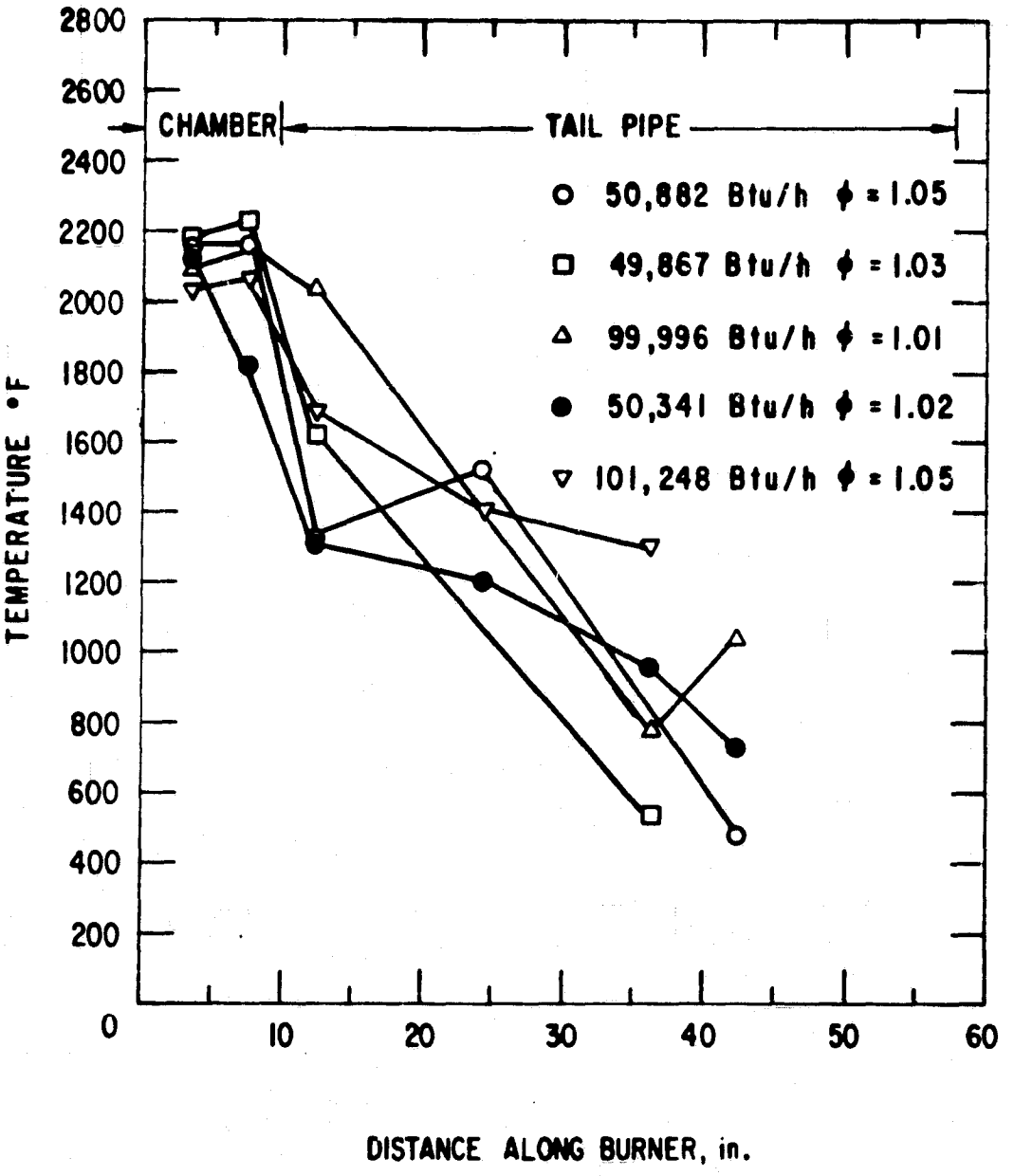

Fig. D.43 Measured Exhaust-Gas Temperature for the Burner with a 48-in.-long Corebustor

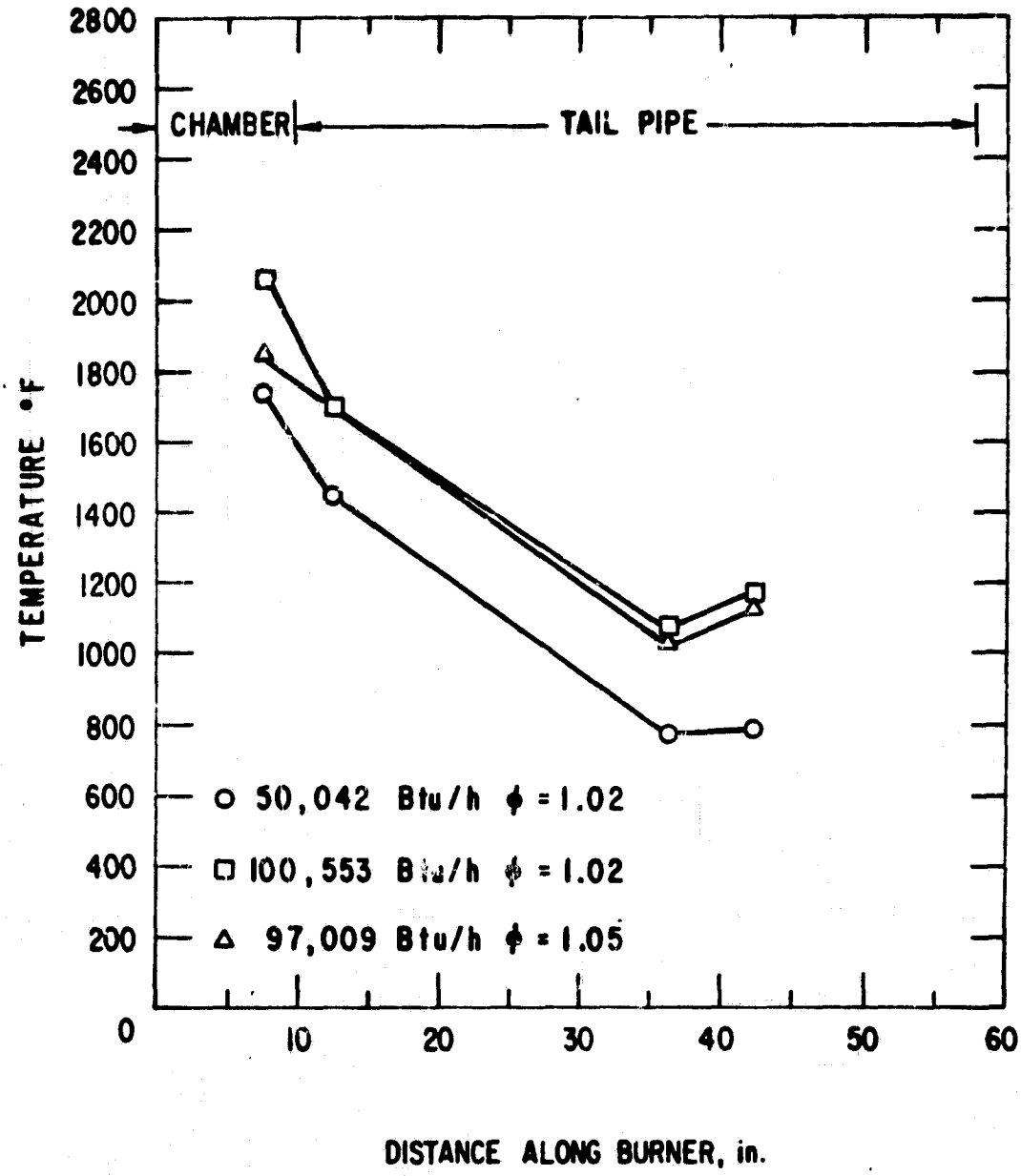

Fig. D.44 Measured Exhaust-Gas Temperature for the Burner with a 36-in.-long Corebustor

APPENDIX E

REVIEW OF STUDIES OF GAS-FIRED PULSE COMBUSTION

APPENDIX E: REVIEW OF STUDIES OF GAS-FIRED PULSE COMBUSTION

In Sec. 1.3 a summary of the studies conducted with liquid- and solid-fuel-fired pulse combustion systems was presented. This appendix contains a review of the principal experimental studies conducted with gas-fired pulse combustors.

E.1 WORK OF FRANCIS, HOGGARTH, AND REAY[31]

These investigators performed a preliminary study of Schmidt-type and Helmholtz-type pulse combustors (Fig. E.1) with the intent of assessing possible uses in industry, particularly for indirectly fired heating of water or air. The diameters of the Schmidt burners were 1 1/2, 2, 3, and 6 in., with a concentration on the 2- and 3-in. tubes. Burners with a nominal bore of 3/4 in. and 1 in. were also tried but were found to be unstable under nearly all conditions. For the Helmholtz burners, combustion chambers of 1 1/2, 2, and 3 in. were mainly used, with tailpipe diameters of 3/4, 1, 1 1/2, and 2 in. A tailpipe diameter of 1/2 in. was tried, but pulsating combustion was not obtained. Maximum town-gas rates ranged from 140 ft^3/h for a 3/4-in. diameter resonance tube to 2500 ft^3/h for a 6-in. diameter tube.

The mechanical flapper valves used were of the multiple-reed type mounted in the end of a conical section attached to the air-inlet pipe. The reeds were made of paper and were suitable for experimental purposes but would be useless for any continuous, practical applications. A number of single-reed valves were tried; the most promising one consisted of a circular reed of a synthetic rubberized fabric that was fixed in the center by a backstop that limited its lift. For the aerodynamic valve, the air-inlet pipe without the conical section was used.

The most satisfactory gas-nozzle arrangement was an evenly spaced ring of nozzles on a constant pitch-circle diameter that is slightly larger than the air-inlet-tube diameter. The holes are angled at 45 degrees (not critical) to the incoming air stream so that the gas-air stream impinges on a stabilizer. The diameter of the individual nozzles was kept small (up to 3/32 in.) to give even distribution. The number of nozzles used was dependent on the maximum gas rating of the burner. The stabilizer bar was a 3/8-in. diameter rod welded diametrically across the combustion chamber from 1- to 2-in. downstream of the gas valve for rates of 100 ft^3/h and to 4-in. downstream for gas rates of 2500 ft^3/h. Its action as a flame stabilizer is obscure but when it was removed, irregular firing occurred. To dampen pulsations in the gas line, a mechanical flapper valve of the type used for the air supply was installed in the line. A gas pressure of 1 to 2 in. H_2O gage at the nozzles was sufficient to give good combustion.

Pressure and frequency measurements were taken on a Schmidt burner with a 3-in. ID exhaust tube of varying lengths and a 3/4-in. ID, 10-in. long air

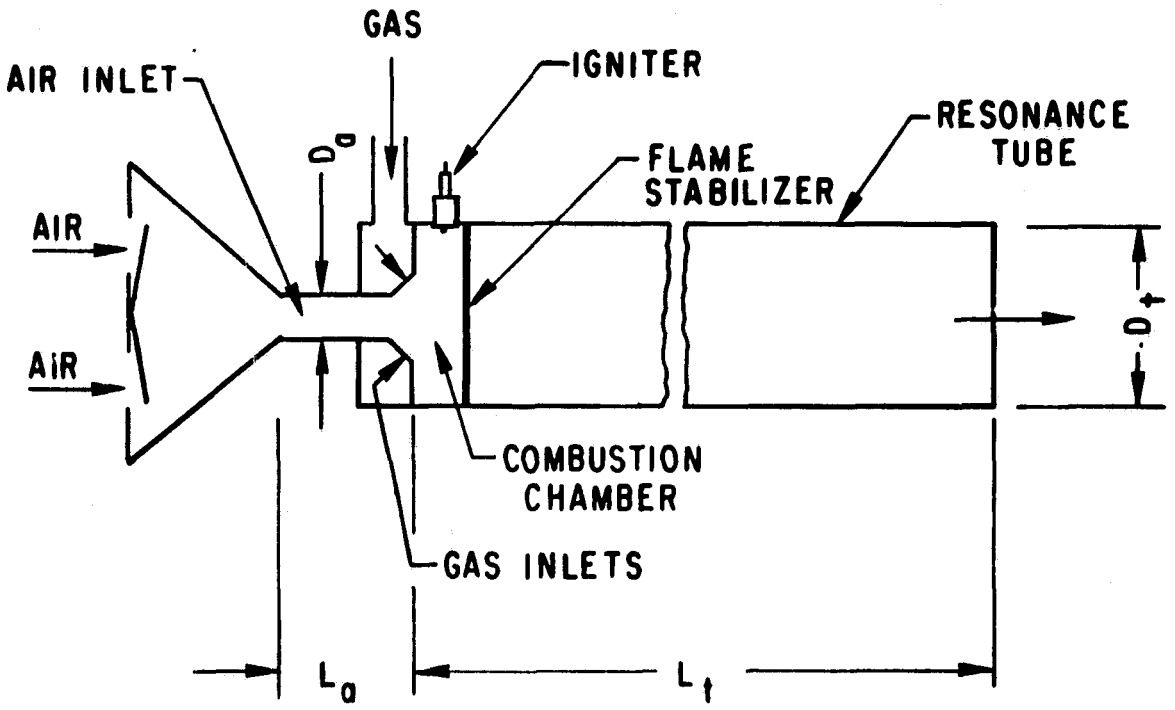

(a) Schmidt Burner

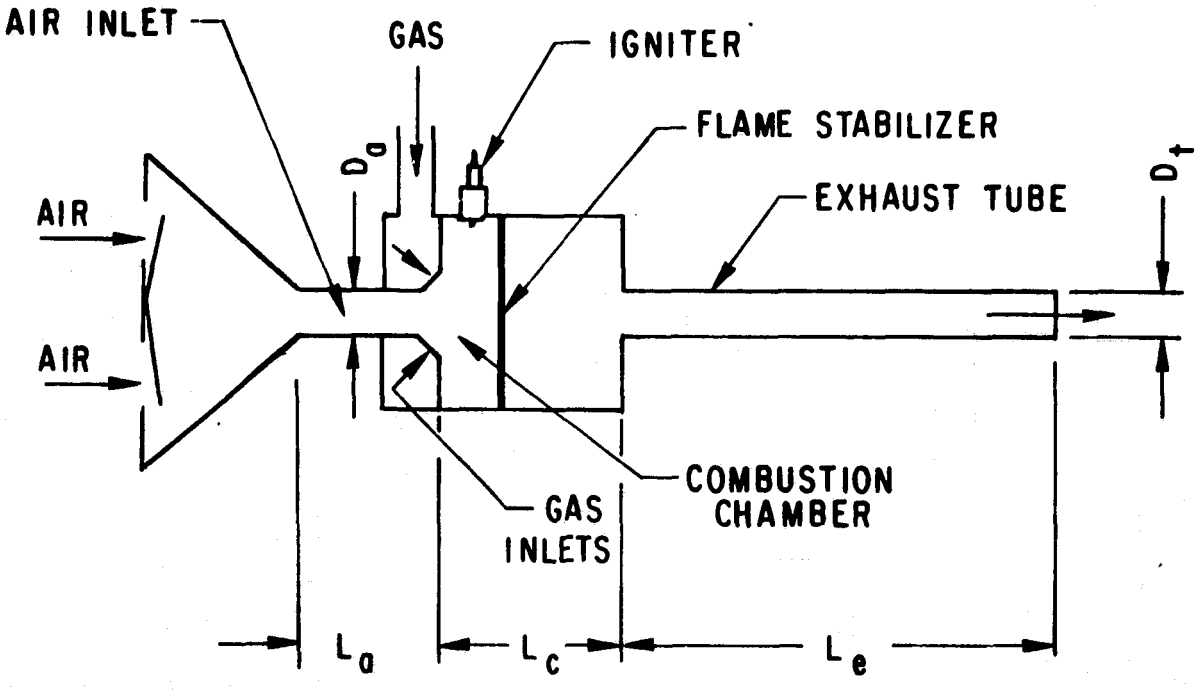

(b) Helmholtz Burner

Fig. E.1 Pulse Combustors used by Francis, Hoggarth, and Reay[31]

tube. With a 17-ft long exhaust tube, pressure nodes were found at about 5 ft, 11.5 ft, and at the end of the tube. Antinodes were at the beginning of the exhaust tube and at approximately 8.3 and 14.3 ft. The pressure waveform was sinusoidal with the axis of the curve slightly exceeding zero pressure. Distortions in the wave occurred when the burner was not properly tuned and fired irregularly. Mean static pressure at the combustion zone decreased as the length of the exhaust tube increased until the half-wave addition brought the antinode back to the combustion zone with a consequent sharp increase in pressure at exhaust tube lengths of 10 ft and 17 ft. The maximum gas rate varied inversely as the static pressure in the combustion chamber.

The fundamental frequency of the burner at a gas rate of 100 ft^3/h decreased from 120 Hz for a 4-ft long exhaust tube to about 60 Hz for a 9-ft long tube. Between a tube length of 9 and 10 ft, the addition of an extra half wavelength to the standing wave pattern caused the fundamental frequency to roughly double. Such a transition also occurred between a tube length of 14 and 15 ft, with a frequency jump of about 50%. The effect of an aerodynamic valve, the air-inlet tube length (3.5 and 7 in.), and the exhaust-tube length on the frequency of a Schmidt burner with a 2-in. ID was investigated. Higher frequencies were obtained with the multiple-reed flapper valve than with the aerodynamic valve. With either type of valve, the shorter-length air tube resulted in higher operating frequencies. However, with reed valves, stable burner operation is achieved over a wider range of exhaust tube lengths when the longer air-tube length is used. The acoustic valve provides a wider range of stable operation than does the mechanical flapper valve.

With a Helmholtz burner the pressure amplitude is relatively constant in the acoustic volume of the combustion chamber. The constriction between the chamber and tailpipe had little effect on the total amplitude of the fluctuating pressure, but the mean pressure fell due to the increase in mean velocity. As the gas rate was increased, the positive maximum pressure increased, while the negative maximum tended to stay constant. Mean pressure therefore increased to drive a greater volume of exhaust gases through the exhaust tube. For stable burners, the pressure waveform was a regular sine wave.

The effect of combustion-chamber length and tailpipe length on the resonant frequency of a Helmholtz burner with a multiple-reed flapper valve, a 3/4-in. ID air-delivery tube that is 10-in. long, and a 3-in. ID combustion chamber was investigated. The gas rate for all these tests was constant at 100 ft^3/h. These measurements indicated that the fundamental frequency of the burner decreases with increasing length; this effect was more pronounced with increasing combustion-chamber length than for increasing tailpipe length. The frequency does not depend on the overall length of the burner, but on the individual lengths of chamber and tailpipe; the sharp frequency jumps that affect the Schmidt burner are absent.

The authors state that the Helmholtz burner is ideally a Helmholtz resonator formed by the acoustic mass of the air-inlet pipe and the compliance

of the combustion-chamber volume, coupled to a quarter-wave exhaust tube. If the exhaust tube is untuned, stable pulsating combustion may still be obtained. Combustion appears to be more stable for burners that have too short exhaust lengths than for burners with over-long exhausts. Transition from a Helmholtz burner to a Schmidt burner occurred when the exhaust-tube diameter was half the diameter of the combustion chamber.

The quality of combustion was normally very good, provided that the air-inlet valve was efficient and the air-inlet diameter was large enough to admit the full air requirement. With multiple-reed valves, the air intake for the Schmidt burner was governed by the air-inlet diameter as the number of reeds was usually greater than necessary to supply the required amount of air for the burner. The maximum air-inlet diameter that can be used appears to be not greater than about one half the exhaust-tube diameter. If the diameter is too large, the exhaust tube becomes effectively open at each end, and will not function as a quarter-wave tube. For the Helmholtz burner, air intake was governed by the air-intake-tube diameter (D_a) in conjunction with the tailpipe diameter (D_e). Normally, $D_a = D_e$ because if $D_a > D_e$, the flame would normally light back to the valve. If $D_a < D_e$ the burner functioned satisfactorily, but the air supply was limited. The function of the volume between the inlet pipe and the valve plate (plate containing the ring of air holes and the reed valves) is somewhat obscure, but single-reed valves functioned with more regularity with a small volume between the valve plate and the inlet pipe. This volume, which has an effect on the phase and duration of the valve opening, may produce a cushioning effect for the backflow of combustion products.

The degree to which the gas rate can be turned down is dependent on the maintenance of sufficient velocity through the gas nozzles. Turn-down rates varied widely from burner to burner but usually were 2 to 3. A ratio of nearly 5:1 was obtained with a separately fed low-flow nozzle, mounted through the combustion-chamber wall an inch or so downstream of the main gas nozzles.

Tests were conducted with the 3-in. diameter, 7-ft long Schmidt burner fitted with aerodynamic valves of various diameters and lengths. Observations from these tests indicate that the length of the valve (air-inlet tube) is important and that a diameter of 1 1/4 in. provides the greatest flexibility in choosing this length, because stable operation was obtained with lengths from 9 to 13 in. A smaller or larger valve diameter gives less operational latitude. This valve design was inefficient, as backflow of the exhaust through the valve was considerable. With small-diameter valves, the flame remained in the combustion chamber for small gas rates, but as the gas rate increased, the flame appeared at the entrance of the valve.

Burgess-type ADS "straight-through" absorption silencers were used on both the exhaust and intake of the burners with flapper valves. With this type of muffler, it was impossible to silence the intake of a burner with an aerodynamic valve, because combustion products emitted by the valve were trapped by the silencer and then sucked back into the combustion chamber on the next half-cycle, effectively choking combustion. The diameter of silencer

used on the exhaust was larger than the exhaust-tube diameter (e.g., a 1-1/2 in. diameter silencer for a 3/4-in. diameter exhaust) to prevent the silencer from becoming part of the acoustic system. The inlet silencer was upstream of the flapper valve, and for a 3-in. diameter Helmholtz burner with a 3/4-in. tailpipe, a 1 1/2-in. diameter silencer was suitable. The intake silencer slightly lowered the combustion frequency and reduced the air input slightly, but it had no other effect on combustion conditions. The average sound-level attenuation over the spectrum was about 15 dB.

Heat transfer experiments were carried out with the 3-in. ID Schmidt burner and the 3-in. diameter Helmholtz burner (3/4-in. diameter tailpipe), fitted with sectionalized water-cooling jackets. In addition, attempts were made to operate the Schmidt burner under non-pulsating conditions. These tests were largely unsuccessful, due to high noise levels (115 dB), and also some pulsations were still evident. It was not possible to operate the Helmholtz burner at all without violent pulsations. Heat-transfer coefficients varied from 5 to 12 Btu/h-ft^2-°F and were highest at the two ends of the Schmidt tube. For the Helmholtz burner the measured heat-transfer coefficients are shown to be less than values predicted for steady-flow conditions. The overall thermal efficiency achieved experimentally did not appear to be greatly influenced by the effect of pulsations. The values of thermal efficiency for the Helmholtz burner were considerably larger than those for the Schmidt burner. This increase is attributed to the larger ratio of length to diameter of the Helmholtz burner.

E.2 WORK OF GRIFFITHS, THOMPSON, AND WEBER[21]

The experimental burners used were of the Helmholtz type with either separate flapper valves for the air and gas stream (Fig. E.2) or a single flapper valve (Fig. E.3) to control admission of an air-gas mixture into the combustion chamber. The valve was a ring of holes drilled through a plate and intermittently sealed by a flapper, which was a ring of fabric coated with a synthetic polymer. A backer plate limited the travel of the flapper and could be adusted to provide a lift of 1/32 to 3/32 in. A metal flapper was tried but inadequate sealing resulted from the metal-to-metal contact and permanent deformation of the metal flapper occurred.

A flame trap was installed inside the combustion chamber and the air-gas mixture burned at or near its surface. Some success was obtained using a triple layer of 40-mesh nickel/stainless-steel screen as a flame trap. However, the air-gas mixture's flow was apparently restricted by this arrangement. Ceramic grid-type flame traps were also used with some success. Most of the experimental burners used a crimped, stainless-steel-ribbon flame trap, about 1/2 in. deep, wrapped into a circular pattern. The positioning of the flame trap with respect to the flapper valve appeared to be somewhat critical. When this separation was too large, the unit would not operate. The combustor could be operated without a flame trap, but the flapper was quickly destroyed by flame impingement.

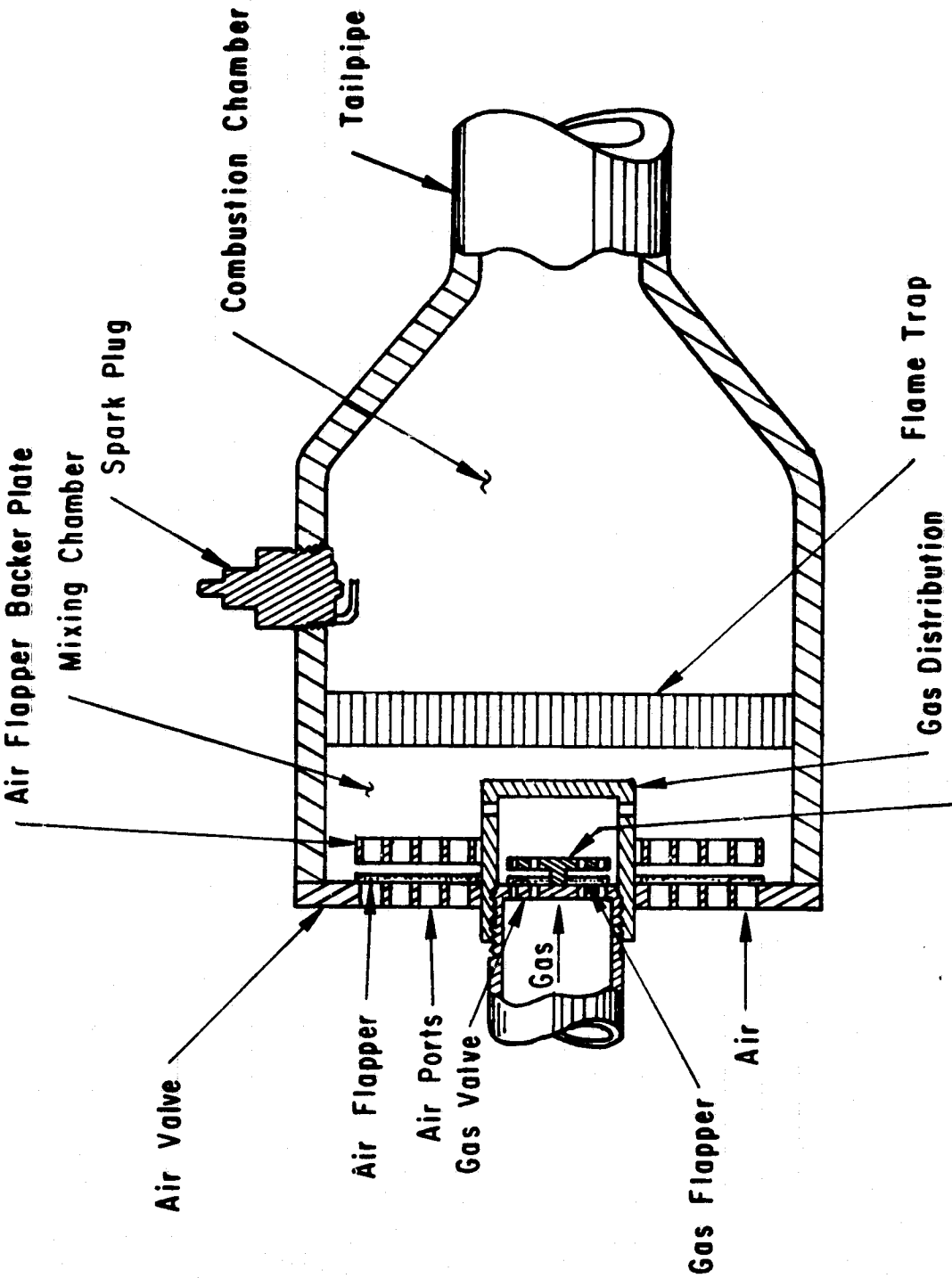

Fig. E.2 Pulse Combustion Device Using Separate Air- and Gas-Flapper Valves (Source: Ref. 23)

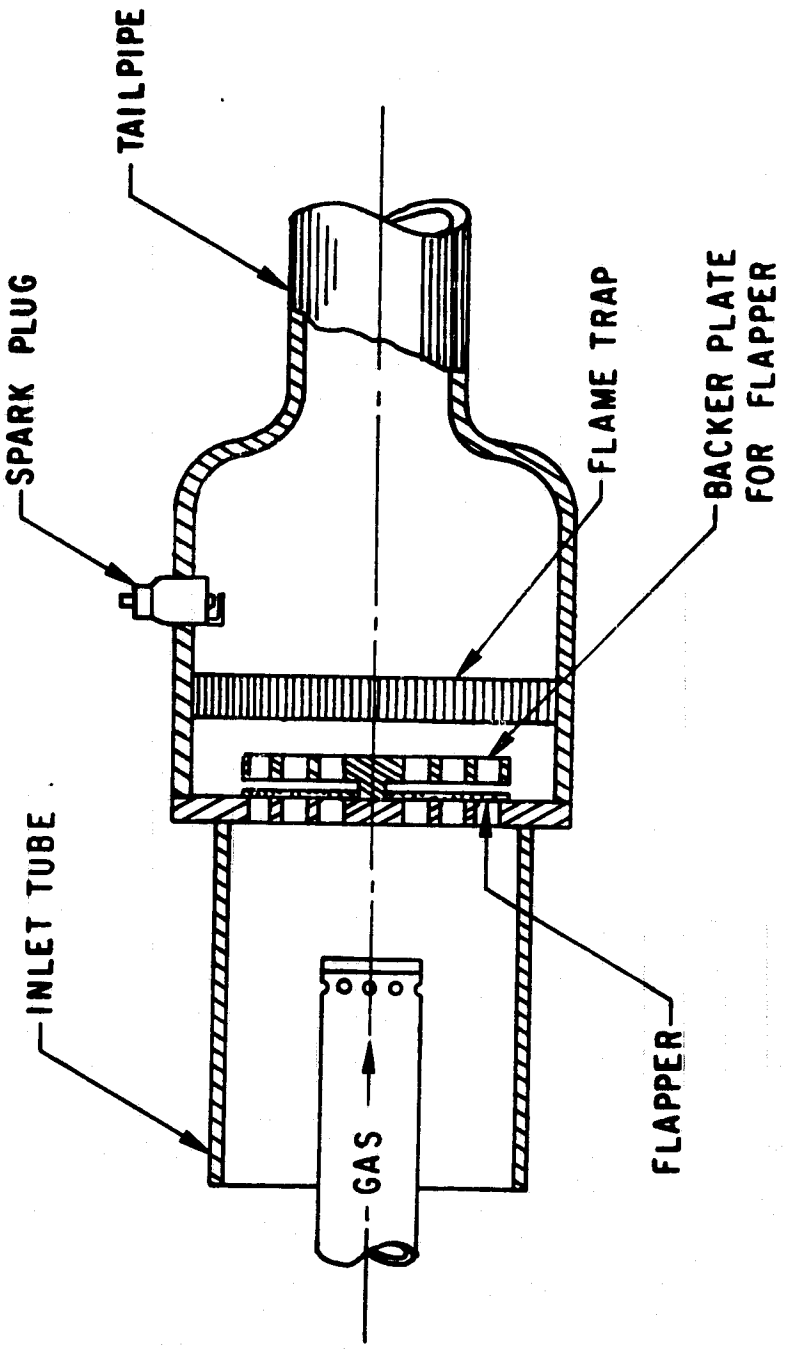

Fig. E.3 Pulse Combustion Devise Using a Single Flapper Valve (Source: Ref. 21)

Frequency data and the CO_2 content of the exhaust products were given for various tailpipe lengths, air lifts, and gas lifts as a function of the heat-input rate. The burner had a 3-in. diameter combustion chamber, about 6-in. long, and a 1-in. diameter tailpipe. The frequency was determined by observing the air-flapper motion with a stroboscopic-light counter. Combustion samples were taken at least 1 ft. inside the tailpipe to prevent dilution from the air drain into the exhaust end of the pipe during the reverse cycle. Air-flow rates ranged from a minimum of about 108 to 112% of theoretical air for complete combustion up to a maximum of about 136 to 170%. Unfortunately the data presented do not indicate the air/fuel ratio used.

Some general observations were:

- The burner operated over a span of gas-input rates for a number of tailpipe lengths and lifts of the critical gas flappers. In some instances this span was quite small, and for others the minimum input tube ranged from about 50 to 60% of the maximum rate.

- An increase in gas-input rate for a given design arrangement resulted in a higher operating frequency, except for a portion of the input range of a couple of burners, where a decrease was obtained.

- Longer tailpipes generally resulted in lower operating frequencies, other conditions being the same. With most of the burners the tailpipe length was limited to 9 or 10 ft. With a 1/32 in. air and gas valve lift, the burner would not operate for more than a few seconds with tailpipe lengths of about 11, 12 or 13 ft. With a 14.4 ft tailpipe, the combustor operated with a higher frequency than that of units with 5 to 9-ft. long tailpipes. The span of operating gas-input rates was reduced to about 30,000 to 45,000 Btu/hr as compared to about 45,000 to 65,000 Btu/hr for the burners with shorter tailpipes. Increasing the tailpipe length to 15.5 ft further reduced the span of operating frequencies.

- No consistent effects of increased tailpipe lengths on the CO_2 concentration in the combustion products were evident.

- Restriction of the air-flapper lift appeared to have a greater effect on the operating span of gas-input rates than did restriction of the gas-flapper lift.

- Reduction of the gas-flapper lift, while maintaining the same air-flapper lift, apparently did not reduce the span of operating rates for the spacings used. In some

instances higher maximum gas-input rates were obtained with smaller gas-flapper lifts.

- Lower CO_2 concentrations in the exhaust gas were observed with larger air-flapper lifts. However, with the largest air-flapper lift of 3/32 in., a minimum tailpipe length of 5 ft was necessary for combustor operation. Other combustors could operate with a minimum tailpipe length of 2 ft.

A few observations were made of noise levels near the inlet, outlet, and middle of operating burners with straight tailpipes. The exhaust-noise level ranged from about 95 to 110 dB, with quasi peaks ranging from about 100 to 130 dB. In general, the noise level at the inlet was about 5 dB less than at the outlet. At the midpoint between inlet and outlet of the combustor, the noise level was about 10 dB lower than that at the exhaust. A radical reduction in noise level could be obtained by installing mufflers at the inlet and outlet of the combustor. With two straight-through automobile mufflers installed, one combustor operated at 80 dB with quasi peaks of 85 dB. Mufflers can have an effect on the operating frequency and gas-input rate of the combustor. When an exhaust muffler was installed on a combustor with a 6-ft long tailpipe, the heat-input rate increased from 85,000 Btu/h to 92,000 Btu/h, and the frequency increased from 47 Hz to 53 Hz for the same operating conditions. It was also noted that placement of expansion chambers between the burner and the mufflers minimized the effects of the mufflers on the combustor operation as well as any effect of inlet and exhaust conduits attached to the unit.

E.3 WORK OF HANBY[41]

The objective of this investigation was to measure the local heat-transfer coefficients and values of the oscillating-pressure amplitude in a Schmidt-tube combustor. The combustor consisted of a 74-in. long, 2-in. ID, 2 1/2-in. OD, stainless-steel tube that was water-jacketed for most of its length. The open end was connected to a brick furnace and the other end was acoustically closed by a constriction to 3/4-in. diameter, with a 5/8-in. diameter central propane jet. Two water-cooled cylinders with pistons for varying their length were mounted perpendicular to the combustor just downstream of the inlet to act as damping tubes or acoustic filters. By altering the length of these cylinders the amplitude of the oscillations could be changed. At a damping-tube length of 44 in., standing waves were set up in opposition to that in the combustor so that the combustor oscillations were almost completely damped out. With this arrangement the amplitude of oscillation in the combustor could be controlled without affecting other burner variables. Air and propane were delivered under high pressure through closed nozzles to prevent the flow oscillations from interfering with the flowmeter readings. Tests were conducted over the range of fuel/air equivalence ratios of 0.95-1.1 and exhaust-gas Reynolds numbers of 6,000-16,000 (for the heat

input rates given in the paper, calculated Reynolds numbers are much lower than these values).

Pressure measurements confirmed a standing quarter wave in the combustor with a pressure antinode at the inlet and a pressure node at the outlet. The resonant frequency was about 100 Hz. A comparison of heat fluxes for pulsating and nonpulsating combustion reveals that about a 45% increase in heat flux near the combustion zone is obtained with pulsating operation. At the combustor exhaust the increase in heat flux for pulsating operation is about 130%. This large increase occurs because for non-pulsating combustion, the heat flux decreases along the length of the combustor, whereas with pulsating combustion this does not occur. As the velocity antinode at the open end of the combustor is approached, the increasing heat-transfer coefficient fortuitously tends to cancel out the decreasing gas temperature, giving a roughly constant heat flux. Heat-transfer coefficients near the entrance of the combustor (velocity node, pressure antinode) were roughly the same for both pulsating and nonpulsating combustion. This is somewhat contrary to the 45% increase in heat flux. The heat-transfer coefficient decreases along the combustor length for nonpulsating combustion but increases for pulsating combustion and is about four times higher near the exhaust exit.

A quasi-steady-state theory provided a satisfactory prediction of the effects of longitudinal combustion-driven oscillations on the turbulent convective heat-transfer coefficients in the combustor. At locations where the dimensionless pulsation velocity is less than 1, a slight decrease in convective heat-transfer rates is obtained; at values greater than 1, an almost linear increase occurs. The quasi-steady-state theory is based on the assumption that the heat-transfer coefficient in any instant can be calculated from the instantaneous value of the velocity by means of an appropriate steady-state relationship. Knowing the waveform of the velocity, this relationship can be integrated over one cycle to give a time-averaged heat-transfer coefficient.

E.4 WORK OF KATSNEL'SON, MARONE, AND TARAKANOVSKII[34]

The authors used a water-cooled Helmholtz-type combustor for studying combustion in a pulsating flow. The combustion chamber was a truncated cone with a 12.6-in. diameter base, a 9.8-in. diameter top and a length of 23.6-in. It was studded and refractory lined. The resonance tube was 51-in. diameter, 45.3-in. long, and terminated in a 16.5 in. diameter exhaust duct. The heated air (68-86°F) entered the combustion chamber axially through a tube of unspecified diameter. No mention of flapper or aerodynamic valves was given. A fuel-burner was installed at 3.5-in. above the top of the combustion chamber. The fuel-air mixture was ignited by an electric-arc igniter in the combustion chamber.

At the maximum fuel (unspecified) rate of 264.6 lb/h, the combustor operated stably, the mean air velocity at the combustion-chamber entrance was

about 378 ft/s, the volume heat release was 5.62×10^6 Btu/h-ft^3 (3.71×10^6 Btu/h-ft^3 if the resonance tube is included), and the combustion-chamber surface heat release was 7.38×10^6 Btu/h-ft^2. There were no unburnt gases at the end of the resonance tube with an air-equivalence ratio of 1.05. Doubling the heat release of the burner had little effect on the amplitude of the pressure oscillation in the combustion chamber. The authors state that the amplitude depends mainly on the air-equivalence ratio. The pulsation frequency varied from 62 to 100 Hz as the heat rate of the combustor increased.

To study the effect of tangential air entry to the combustion chamber, a number of small combustors were built. The combustion-chamber diameter varied from 2 to 3.9 in., with lengths from 3.9 to 9.9 in. The resonance-tube diameters were 1.2 in. and 2 in., with lengths from 15.7 in. to 59.1 in. A large number of tests were conducted with varying air-inlet tube diameter, intake of the fuel-air mixture, length of the resonance tube, and composition of the fuel-air mixture. Fuels used were acetylene, hydrogen, and methane. Similar tests were conducted with an axial inlet of the air. No details of these tests were presented. From the test results, it was established that combustors with a tangential air supply operate much more stably in the whole range of air-equivalence ratio variations at which the fuel can burn. For acetylene the air-equivalence ratio variation was 0.4 to 2.8; for hydrogen it was 0.42 to 2.8. With methane and an air-equivalence ratio of 0.85, the flame lifted off the burner and gas was burning at the outlet of the resonance tube. Lean mixtures having an air-equivalence ratio of 2.3 could still burn. The dependence of the pressure amplitude on the air-equivalence ratio was also investigated for the three fuels. Two pressure peaks were obtained with each fuel, one for lean mixtures and one for rich mixtures. For acetylene and hydrogen, the lean mixture produced about a 1/3 higher pressure-amplitude peak than the rich mixture. With methane, the peaks were almost identical in magnitude for the rich and lean mixtures. For acetylene the pressure antinodes occurred at air-equivalence ratios of about 1.7 and 0.6; for methane the ratios were 1.5 and 0.8; for hydrogen the ratios were 2.3 and 0.5. Pressure nodes occurred at the following air-equivalence ratios: acetylene, 0.9; methane, 1.2; and hydrogen, 0.8.

E.5 WORK OF GRIFFITHS AND WEBER[23]

On the basis of about six years of active pulse combustion research, the authors of this report present experimental data and design guidelines for Helmholtz-type pulse combustors. Combustors used for the experimental studies were assembled from standard pipe and fittings and were equipped with gas-and-air flapper valves. The basic configuration of the burner is shown in Fig. E.4. Combustion chambers were made from 3, 4, 6, and 8-in. diameter standard steel pipes with lengths ranging from about 4 to 18 in. Bell reducers were used to connect the combustion chambers to tailpipes and to the air-chamber neck. Standard 1 1/4, 1 1/2, 2, and 3-in. diameter steel pipes were used for tailpipes, with lengths varying from about 4 to 12 ft. (Note: Pipe diameters

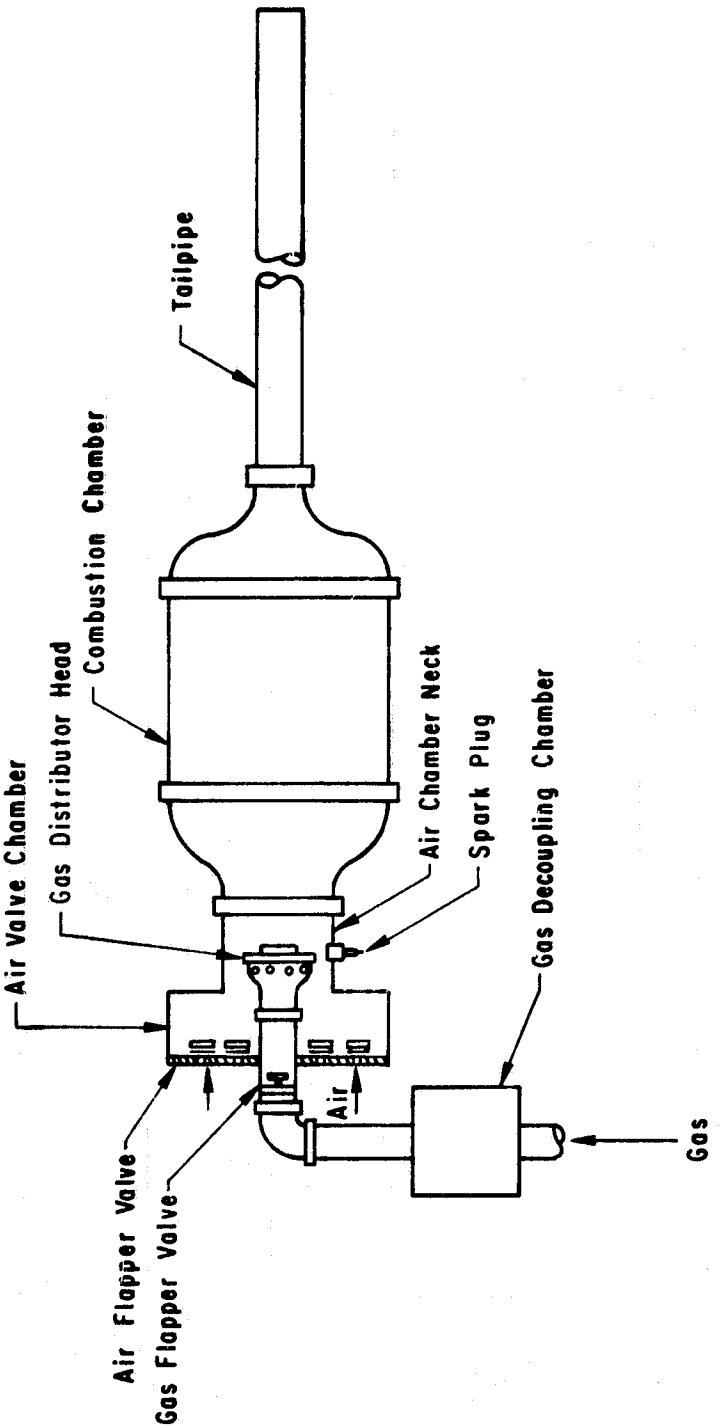

Fig. E.4 Pulse Combustion Burner Studied by American Gas Association (Source: Ref. 23)

are the nominal outside diameter. The wall thickness varies with the diameter. Standard pipe is schedule 40 in these sizes.)

The air-valve chamber is simply the housing for mounting the air-flapper valve. Within reasonable limits, the volume of this chamber does not appear to affect burner operation. The air-chamber neck connects the air-valve to the combustion chamber. In most of the experimental studies a 3-in. diameter close steel nipple was used for the air-chamber neck. A few units used a 2-in. diameter close nipple for the neck. The length of the neck, within reasonable limits, does not appear to affect burner operation.

The gas decoupling chamber is simply an expansion chamber that damps out pulsations in the gas line. The size of the chamber depends on the magnitude of the pressure pulsations originating from the combustion chamber and on the flapper-valve design. Two sizes of gas decoupling chambers were used. A 4-in. diameter by 3 1/2-in. long chamber was adequate for gas rates up to about 350,000 Btu/h, but this might be adequate for even higher rates.

The gas distributor head is positioned inside the air-chamber neck so that the gas and air mix and burn several inches away from the air-flapper valve. Thus, a flame trap is not necessary to protect the air flappers. Gas-distributor heads were fabricated from standard 1 1/2 or 1 1/4 by 3/4-in. bell reducers with the large end capped for use with the 3-in. air-chamber neck. For the 2-in. neck the distributor head was made from a capped standard 3/4-in. pipe coupling. The number and size of ports in the head did not critically affect burner performance as long as the total port area was the same. Configurations with 4, 8, 16, and 32 ports were used, but 8 or 16 would be a reasonable number. Clearance between the gas-distributor head and the inner wall of the air-chamber neck should be about 1/4 to 1/2 in. for proper mixing of the air and gas.

Air and gas flappers should be made as light as possible so that they will respond quickly to pressure changes. They must be durable, able to withstand impact, and completely free to move in a back-and-forth motion with a minimum of bending. A variety of flapper materials were tried. Metal flappers, including stainless steel, deteriorated after only minutes of operation. Some flexible materials, such as rubber or nylon, appeared to resist impact stresses to a greater degree than metals but eventually failed, apparently because of age hardening or temperature embrittlement. A Teflon-coated fiberglass material, 0.010-in. thick and weighing 0.355 g/in.^{2}, was used in most of the testing. For ring-shaped flappers a reasonable width is 3/8 to 1/2 in. The flapper lift should be 0.025 to 0.055 in.

The use of relatively high gas-supply pressure will facilitate the use of smaller gas-flapper valves. However, the gas pressure will ordinarily be much smaller than the negative pressure created by the pulse combustion process, so that its effect on gas-input rate, and consequently valve size, will not be appreciable. The magnitude of the supply pressure becomes increasingly significant for burners with relatively low peak and mean pressures. A low

gas-supply pressure generally improves the starting characteristics of a pulse combustion burner and reduces the size of the starting blower, because only a small quantity of air is required for combustion of the small initial gas flow into the combustor. Therefore, a reasonable design gas-supply pressure would be 2 to 4-in. H_2O except for very large burners (greater than 10^6 Btu/h), where a higher supply pressure may be required.

The combustion-chamber volume and tailpipe diameter were found to have the greatest effect on operating pressures in a pulse combustor. Data are presented on the mean positive pressure (arithmetic mean of positive and negative peak pressures: the negative peak pressure is less than the positive peak pressure) in the air-chamber neck as a function of the combustion-chamber volume (includes the reducers at the air-chamber neck and tailpipe) and gas-input rate. Data are also given for the peak pressure in the combustion chamber as a function of the mean positive pressure and combustion-chamber volume. For a given gas-input rate, burner operating pressures are usually higher for combustors with smaller combustion chambers and smaller tailpipe diameters. These pressure data are intended only to provide the designer with approximate values of the peak and mean positive pressure for use in initial design calculations for the gas- and air-valve systems. These pressure data are somewhat lacking as the effect of tailpipe length, the length/diameter ratio of the combustion chamber, and the air/fuel ratio are not addressed.

The pressure data, along with air and gas flow rates, are used to size the flow areas for the air- and gas-flapper valves. The gas- or air-valve system is really a series of orifices from which an equivalent orifice area can be calculated. Modified orifice equations that account for the fraction of the operating cycle that the flapper valve is open were developed. These equations permit the calculation of the required equivalent orifice area. A considerable part of the report deals with the sizing of the gas and air valves.

The combustion chamber size, tailpipe diameter, and tailpipe length generally establish the fundamental operating frequency of the burner. Combustors with larger chambers and small-diameter and/or longer tailpipes normally operate at lower frequencies. Occasionally some pulse combustion burners operate at a harmonic of the fundamental frequency, for an undetermined reason. When this occurs, the operating pressures in the burner decrease, with a corresponding decrease in flow of gas and air into the burner. This harmonic mode of operation does not occur except with relatively long tailpipes (10 to 12 ft.or longer). Large combustion chambers have a more pronounced effect on the burner frequency than tailpipe length. For example, the operating frequency of a combustor with a 4-in. diameter, 12.6-in. long chamber (163 $in.^3$ volume) was reduced from 78 to 48 Hz when its 1 1/4-in. diameter tailpipe was lengthened from 4 to 12 ft. Correspondingly, the same diameter tailpipe and length change on a burner with an 8-in. diameter, 23.3-in. long combustion chamber (1,186 $in.^3$ volume) resulted in a frequency reduction from 33 to 31 Hz.

A limited amount of data were collected for pulse combustion burners equipped with simple chambers, restrictions, and/or automotive mufflers attached to the tailpipe exhaust. In some cases, these additions caused a reduction in the peak and mean pressures in the burner, and a reduction in the gas and air flow rates. When the gas rate was restored (by increasing the supply pressure) to its unrestricted rate, the peak and mean pressures were also restored to their unrestricted values. Consequently, the effects of mufflers and other exhaust-system restrictions can be offset by simple adjustments in the air- and/or gas-valve designs or adjustments to their lifts.

The experimental studies indicated that the operating noise level in a pulse combustion burner can be reduced by its design. Noise is directly related to the burner operating pressures; the lower the operating pressures, the lower the noise level. The simplest method of reducing peak and mean pressures is to use relatively larger combustion chambers and larger tailpipe diameters. However, there are other factors which will limit the size of the burner. Noise reduction may also be achieved by design changes that offset the mixing of combustion air and gas, with the subsequent reduction in operating pressures.

E.6 WORK OF REAY[32]

This study is a continuation of the work of Francis, Hoggarth, and Reay[31] discussed in Sec. E.1. In the previous study cited, some of the heat-transfer data given were in error due to inaccurate gas-rate measurements, resulting from an effect of pulsations in the flow-measuring equipment. Therefore, this study was initiated to further investigate the effect of flow pulsations on heat transfer.

Reay chose to use the 3-in. diameter Schmidt burner described in Ref. 31, because he claimed that heat inputs for a Helmholtz burner were low, and thus the burner was less attractive as a practical unit for industrial applications. This statement is unsupported by any specific data and is contrary to other studies and applications of pulse combustors. The exhaust-tube length for the burner was either 7 ft or 11 ft. The 7-ft length was chosen because in the work of Francis et al.[31] for burner lengths of 8 to 10 ft, the pressure antinode drifted away from the flame zone and the burner was unstable. For an 11 ft length, an additional half wavelength was added to the standing wave so that a three-quarter wave was set up in the exhaust tube and the pressure antinode was again at the flame zone. Both burners were water-cooled along their entire lengths by a series of 1-ft long jackets.

Town gas with a heating value of 485 Btu/ft^3 was used in all the experiments. The tests were carried out under both condensing and noncondensing conditions of the exhaust gas. Under noncondensing conditions, the thermal efficiency of the 7-ft long burner was about 70%, and for the 11-ft long burner, it was about 80%. For both burners these efficiencies are about 1/3 higher than was predicted for steady-flow conditions. When an exhaust

silencer was added to the 11-ft long burner, its overall thermal efficiency dropped to about 70%. Under condensing conditions, the overall thermal efficiencies of the 7-ft long burner were 70-80%, and for the 11-ft long burner, the efficiencies were 80-90%. In all measurements, carbon monoxide was found to be negligible, but the percentage of excess air was 15 to 60, decreasing as the gas rate increased.

From the measured heat transfer to the water in each section of the cooling jacket, the exhaust gas temperatures and the pulsating-flow heat-transfer coefficients were calculated. A turbulent-flow correlation was used to predict the steady-flow heat-transfer coefficient. (Estimates from the data provided indicate that the exhaust-gas Reynolds Number corresponds to the the transition-flow regime and not turbulent flow). In general, the experimental heat-transfer coefficients are higher than the calculated steady-state values. Repeated tests with the same gas and air rates but different water-flow rates produced some significant differences in the heat-transfer results. For all the tests, high heat-transfer coefficients were obtained for the first foot of the burner. The variation of the local heat-transfer coefficient along the burner was oscillatory with a sharp rise in values over the last foot of the burner. The author suggests that this rise is due to the approach of the velocity antinode of the burner. For the 11-ft long burner, heat-transfer coefficients were below predicted steady-flow values in the 7-10-ft region of the burner. An attempt was made to relate the heat-transfer coefficient to the peak-to-peak pressure amplitude, but the results were somewhat inconclusive. High pressures exist in the 1-3 ft and 7-10 ft regions of the burner, and a pressure node exists around the 5-ft length. Generally the heat-transfer coefficients are lower in these regions, especially the 7-10-ft section (as was mentioned earlier).

With a gas-input rate of 375 ft^3/h, overall sound-pressure levels of 114 dBC were obtained 4-ft from the inlet of the burner and 118 dBC at 7-ft from the exhaust. A 3 x 2 x 2 ft sound enclosure box with a 3-in. diameter inlet and exit opening was used for the burner exhaust. A 1 1/2-ft diameter x 1-ft long cylinder with 2-in. diameter openings was used to enclose the air-inlet valve. Both of these devices were lined with a 3-in. thickness of mineral-wool insulation. A considerable, but not sufficient, noise reduction occurred. Therefore, Burgess straight-through absorptive silencers, 3-ft long, were fitted to the outlet and inlet sound enclosures. Sound pressure levels measured 3-ft from the exhaust exit and air inlet were 86 dB and 82 dB respectively. Noise measurements 3-in. from the inlet and exit were 78 and 80 dB, which indicates that the noise from these sources had been effectively attenuated. The majority of the remaining noise was being transmitted from the burner ports.

A Schmidt burner (3-in. diameter, 7-ft long, 275,000 Btu/h heat input, 5.5 ft^2 of heating surface) was installed in a 200-gal water tank (4 x 3 x 3 ft). Silencing consisted of lined expansion chambers and straight-through silencers on both the inlet and outlet. Sound-pressure levels measured 3 ft

from the burner varied from 80 to 85 dB with low-frequency noise predominating. To raise the water temperature from 70 to 180°F in an uncovered tank took 1 3/4 h. The heating efficiency was 49%, the tube efficiency 73%, and the surface heat-release rate was 36,510 Btu/h-ft^2. Similarly an 11-ft long burner (240,000 Btu/h heat input, 8.6 ft^2 of heating surface) was installed in a 735-gal water tank (8 x 4.5 x 3 ft). It took six hours to heat the water from 70 to 180°F in this uncovered tank. The heating efficiency was 58%, the tube efficiency was 79%, and the heat release per unit area was 22,000 Btu/h-ft^2. This burner exhibited an instability and could not be operated without failure for any length of time. On the hypothesis that this instability was caused by operation in a transitional mode, the burner length was increased to 13 ft. Stability was not improved, and random failure occurred occasionally (on the average, after several hours of running).

For comparative purposes, a Temgas unit consisting of three tubes of 4-in. diameter and a length of 11 ft (includes the header for the two-pass unit) was installed in the 735-gal tank. The unit had an input rating of 311,000 Btu/h, a heating surface of 44.2 ft^2 and required 3 1/2 h to heat the water from 70 to 180°F. The heating efficiency was 65%, the tube efficiency was 78%, and the surface heat-release rate was 6,019 Btu/h-ft^2. Thus, the pulse combustion burner provided a large reduction in immersion tube area for a comparable thermal rating and efficiency of a more conventional heater.

E.7 FURTHER WORK OF HANBY[42]

With a 2-in. inside diameter, 75-in. long, propane-fired, Schmidt-type pulse combustor with a resonant frequency of about 90 Hz, Hanby conducted experiments to investigate the effect of heat-release rate and air/fuel ratio on the frequency and pressure amplitude of the burner.

The operating frequency of the burner could be predicted within 5% if the mean-square root gas temperature was used in the following equation:

$$f = \sqrt{\frac{\gamma g_c RT}{4L}} \qquad \text{(E.1)}$$

where:

f = frequency

$g_c = 32.2 \dfrac{\text{lb}_m\text{-ft}}{\text{lb}_f\text{-s}^2}$

L = tube length, ft

R = individual gas constant, $\dfrac{\text{lb}_f\text{ft}}{\text{lb}_m\,^\circ\text{F}}$

T = absolute temperature, °R

γ = specific-heat ratio

The mean root gas temperature is obtained from the area under the curve of the square root of the gas temperature in the combustor as a function of the distance along the combustor. Variations in the resonant frequency of oscillation of the combustor, which occurred when either the heat-input rate or the equivalence ratio was changed, could be attributed to the resultant variation in the exhaust-gas temperature.

For a constant equivalence ratio of 1.05, the maximum pressure amplitude was found to increase linearly with increasing heat-input rates. The maximum pressure amplitude was also found to increase linearly with increasing equivalence ratios above 0.95 for a constant heat-input rate of 27,500 Btu/h. The increased amplitude resulting from increasing air flow alone suggests that the kinetic energy of the flow plays an important part in the combustion oscillation mechanism. Unfortunately, altering the flow rate of either air or fuel also changes the speed of flame propagation. Thus, the possibility arises that the efficiency of coupling between heat release and pressure fluctuation is responsible for the increase in maximum pressure amplitude with increasing equivalence ratio. Experimentally, the pressure amplitude was found to be strongly dependent on the fuel injector and the type of fuel used. For example, at a constant heat-input rate, a different propane injector reduced the amplitude from 3 to 1 psi, but an amplitude of 14 psi was obtained when kerosene was burnt in a pressure jet.

The sound power radiated from the open end of a tube is proportional to the square of the pressure amplitude at that point. The ratio formed by the pressure amplitude at the open end of the combustor divided by the pressure amplitude at the antinode was shown to increase for increasing heat-input rates above 70,000 Btu/h. This indicates that the amplitude at the open end rises disproportionately higher than does the amplitude at the antinode; this phenomenon may be thought of as the pressure node moving further away from the open end of the tube. These results also indicate that the acoustic efficiency of the pulse combustor is not constant but increases with the heat-input rate. Thus, very high combustion intensities and heat-input rates will be obtained at the expense of increased sound radiation from the combustor.

E.8 WORK OF BRIFFA[33]

In this study, experiments were conducted with the object of reducing noise from pulse combustors by combining the out-of-phase exhaust stream from two similar units. This coupling arrangement for silencing was first suggested in 1910 by M. Ensault-Pelterie as mentioned in Ref. 1. Both Helmholtz-type and Schmidt-type pulse combustors were used, but most of the testing was done with the Schmidt tube. For a single uncoupled Helmholtz pulse combustor,

the fluctuating pressure wave was modulated by a much lower frequency than the fundamental frequency. When two Helmholtz combustors were coupled together, the noise reduction obtained was about 15 dB, but the simultaneously recorded pressure fluctuations in the combustors were not opposed in phase.

The Schmidt combustors were quarter-wave steel tubes having a length of 43.3 in. and an inside diameter of 1.48 in. Each tube was enclosed by a 3.97-in. diameter steel water jacket divided into eight separate sections. Methane fuel and air were supplied to each combustor through a 0.98-in. diameter, 6.89-in. long, steel mixing tube. The fuel and air were supplied under sufficient pressure to ensure that the supply was not influenced by the fluctuating pressures. Air-fuel mixtures close to stoichiometric were used, because deviations of more than 5% from this level led to a deterioration in the acoustic quality of the signal produced. Gas supply rates were 20.5 to 35.3 ft^3/h per combustor.

Each combustor was connected to a 1.48-in. diameter 90° pipe elbow, which passed through the side of a ceramic-wool-lined cylindrical metal coupling chamber, 7.87-in. long and 6.89-in. diameter. The exhaust ends of the elbows faced each other with an annular clearance area of one third of the combustor's cross-sectional area. The coupling chamber had one exhaust outlet of 1.48-in. diameter. Another coupling chamber of 4.92-in. diameter and length was used for tests when the separation distance of the exhaust elbows was varied by threaded inserts from 1.48-in to 0.04-in.

Sound measurements were made at a position of 39.4-in. away from, but level with and normal to, the coupling-chamber exhaust axis. At a gas-input rate of 35.3 ft^3/h per combustor, an overall noise reduction of 6.5 dB occurred when the spacing between the exhaust elbows was decreased from 1.48 in. to 0.04 in. This rather small noise reduction resulted because coupling essentially reduces the noise due to the fundamental frequency, and at the maximum gas intake, the noise amplitude between the fundamental frequency and its first harmonic is only 8 dB. With a gas input of 55 ft^3/h, the fundamental frequency of the uncoupled combustor is some 23 dB higher than that of the first harmonic. With a fixed-gap coupling of the combustors, the fundamental is suppressed, the harmonic is reduced by 12 dB, and an overall noise reduction from 113 dB to 78 dB occurs. The ceramic lining contributed about 5 dB to the noise reductions. Therefore, to achieve substantial noise reduction, careful attention must be given to the magnitude of the sound pressure level of the other resonance peaks in comparison with that of the fundamental frequency.

Coupling of the combustors had no effect on the mean pressure; measurements of about 2.36 in. H_2O were obtained for both coupled and uncoupled burners. The essential change obtained with coupling was the elevation of the fluctuating pressure in the vicinity of the combustor exits. Whereas the magnitude of the positive pressure is similar for both coupled and uncoupled combustors, the negative pressure in the coupled combustor is about 15.7 in. H_2O less than in the uncoupled combustor until the exit is approached.

Heat-transfer measurements along the tube were conducted at gas-input rates of 27.5, 24.4, and 20.5 ft^3/h for both the coupled and uncoupled burners. For both burners, the heat-transfer rate is greatest at the inlet end of the burner but decreases very rapidly. With the uncoupled burner, the heat-transfer rate is relatively constant along the burner but increases at the exhaust end. The author attributes this increase to the increase in the local pressure, which is contrary to heat-transfer theory (i.e., high local pressure means a lower velocity, which reduces heat transfer).

The amount of NO_x was measured with a Thermo Electron Corp. model 10A chemiluminescent analyzer over an excess-air range of 0 to 10% and varied between 0.084 and 0.0970 lb $NO_x/10^6$ Btu. These results are similar to values quoted for natural-gas-fired domestic burners.

An alternative approach to achieving the opposed-phase coupling was investigated. A fluid-logic circuit that employs a bistable amplifier for switching the gas supply from one combustor to the other was used. The control signal for switching was derived from the pressure pulse generated by the combustion process. Regular operation was achieved, but the pressure trace exhibited a fine structure that was correlated with the resonant frequency of the combustor cavity. Although regular alternating operation was obtained, switching at the frequency of the fine structure would be necessary to simulate the opposed-phase operation.

E.9 WORK OF READER[3]

The specific objectives of this study were to determine the empirical data required for numerical solutions of a mathematical model, and to measure cyclic pressures and temperatures for comparison with those predicted by the model. The equations summarizing the one-dimensional model were given, but no results were presented, as the computer program was incomplete. With one-dimensionality in mind, a cylindrical-combustion system was chosen for its axial symmetry and so that longitudinal wave motion predominated. To ensure insignificant radial temperature gradients, the combustion chamber was lined with an alumina-based ceramic. This liner was found to improve the starting characteristics of the burner and to reduce the noise level.

A double-necked Helmholtz combustor was constructed based on the work of Francis, Hoggarth, and Reay[31]. The combustion-chamber was mild steel with a 3.5-in. ID and a 0.25 in. thick ceramic liner. Its length was 16-in., because a longer chamber would have required an excessively long tuned exhaust duct, while a shorter chamber would have restricted the temperature measurements. Based on an operating frequency of 50 Hz and an equation given by Francis et al., the air-intake duct length was found to be 6-in. for an inside diameter of 0.91 in. A 0.25-in. ID copper pipe was mounted at an angle into the wall of the air-intake duct so that pressurized air could be fed into the combustion chamber during the starting sequence. The length of the exhaust tube was calculated as 100-in. using the formula for a quarter-wavelength

tube. Valving for the combustor is unspecified but must be aerodynamic, because the equations of Francis et al. were for this type of valve.

For air measurement, an orifice was installed at the inlet of an air box of sufficient capacity so that it would not affect the system acoustic frequency and operating characteristics. This box was connected to the air-intake duct, but a steady flow through the box was not obtained. Back flow from the combustor eventually filled the air box, and combustion ceased. There was no noticeable static pressure rise inside the box, so the average cyclic consumption of air was determined from the equivalent air depletion of the air box, the running time of the combustor, and its operating frequency.

The average operating frequency of the burner over some twenty experimental runs was 43.5 Hz. Using the temperatures obtained from these tests and the frequency equation of Francis et al.[31], the calculated frequency of the burner was 45.2 Hz. Using the air-box data, the average equivalence ratio was 1.04; from exhaust-gas analyses, it was 1.05. No combustibles or carbon monoxide were detected in the exhaust gas.

The pressure wave in the combustion chamber was sinusoidal and regular with almost equal amplitude swings. Along the combustion-chamber length the mean cyclic pressure was about 0.07 psi above atmospheric pressure. At the two exhaust locations, the pressure waveform was also sinusoidal, but both locations exhibited a second smaller pressure peak lagging the main peak by three quarters of a cycle. The reason for the second peak is not clear, but it may be caused by either secondary burning or air intrusion up the exhaust tube. The ratio of the mean outlet pressure to the mean inlet pressure was found to be marginally greater than 1, thus indicating a slight pressure gain. Along the combustion-chamber length, the maximum pressure range was 0.64 to 0.83 psi above atmospheric, while the minimum pressure range was 0.30 to 0.41 psi below atmospheric. However, at the location a quarter of the way along the chamber from the inlet, the maximum, minimum, and cyclic pressure swings were less than at all other locations. Although the minimum pressure amplitudes were less than the maximum pressure amplitudes, invariably for some 60% of each cycle the pressure was below atmospheric. Therefore, a net inflow of air and gas took place, and in the most extreme case, combustion was completed within 0.4 cycles.

The gas temperature in the combustion chamber was measured through sapphire windows by an infrared-radiation spectroscopy technique. The mean temperatures varied from 1430-1880°F, depending on chamber location. (Note: These values are quite low; the adiabatic flame temperature for methane is about 3509°F.) Mean cyclic temperatures along the combustor were very similar except at those locations approximately 1/4 way along the chamber, where they were somewhat less. This is the location where the pressure data were also lower. The maximum cyclic temperatures were 1916-2654°F, and the minimum cyclic temperatures were 800-1430°F. Temperature-time results show cyclic peaks and troughs that are very roughly sinusoidal. The phase lag between the

temperature and pressure peaks was found to vary between 20° and 230° at different locations and cycle times.

Assuming that the temperature peaks indicate the presence of the flame front, a rough estimate of 98 ft/s for the flame speed was obtained. The author concludes that this flame speed indicates that pulse combustion is neither a form of controlled detonative combustion nor constant-volume combustion. Furthermore, on a time-averaged basis for the pressure data, it could be inferred that the system operated as a constant-pressure device. (Reynst[1] considered that pulse combustion was constant-volume combustion.) From the experimental data, a combustion-zone length of 1/5 of the combustion chamber length was inferred. Estimates of the gas residence time show that on the average a fuel-air change takes about 3.5 cycles to pass through the system.

E.10 WORK AT RAY W. HERRICK LABORATORIES[25-30]

A number of research studies were conducted and are being conducted at the Ray W. Herrick Laboratories, School of Mechanical Engineering, Purdue University. The combustor utilized (shown schematically in Fig. E.5) is of the Helmholtz type and is natural-gas-fired. The single combustion chamber can be converted to a dual chamber by the addition of a central divider, which allows the unit to be operated as two out-of-phase combustors. A water jacket encases the two flue tubes, which are 2.8 in. ID and contain a 2-in. square corebustor. The fundamental frequency of this combustor is approximately 65 Hz.

The contents of Refs. 25 and 26 are identical and are summarized in Ref. 28. These works describe some of the preliminary thermal, pressure, and acoustical measurements that were performed. For the single combustion chamber, the maximum pressure varied from 13 to 26 inches of water gage. The mean combustion-chamber pressure was 2 to 5 inches of water gage. The maximum exhaust-chamber pressure occurred about four or five milliseconds after the maximum combustion-chamber pressure. From this time lag and the distance between the pressure transducers, a pressure-wave velocity of 1500 ft/s was estimated. For the dual-combustion chamber, the pressure traces showed equal amplitudes but were 180 degrees out of phase.

For the single combustion chamber, the average heat input to the burner was 176,000 Btu/h (based on a 980 Btu/ft^3 natural gas), and a mean thermal efficiency of 71% was obtained. The average excess air was 12%. A mean overall heat-transfer coefficient of 14 Btu/h-ft^2-°F, based on an assumed 2600°F temperature of the gases entering the flue tube, was obtained. The mean heat-input rate for the dual-combustion-chamber tests was 253,000 Btu/h with a mean excess air of only 6%. The mean efficiency was 79%, and the estimated mean heat-transfer coefficient was 21.2 Btu/h-ft^2-°F.

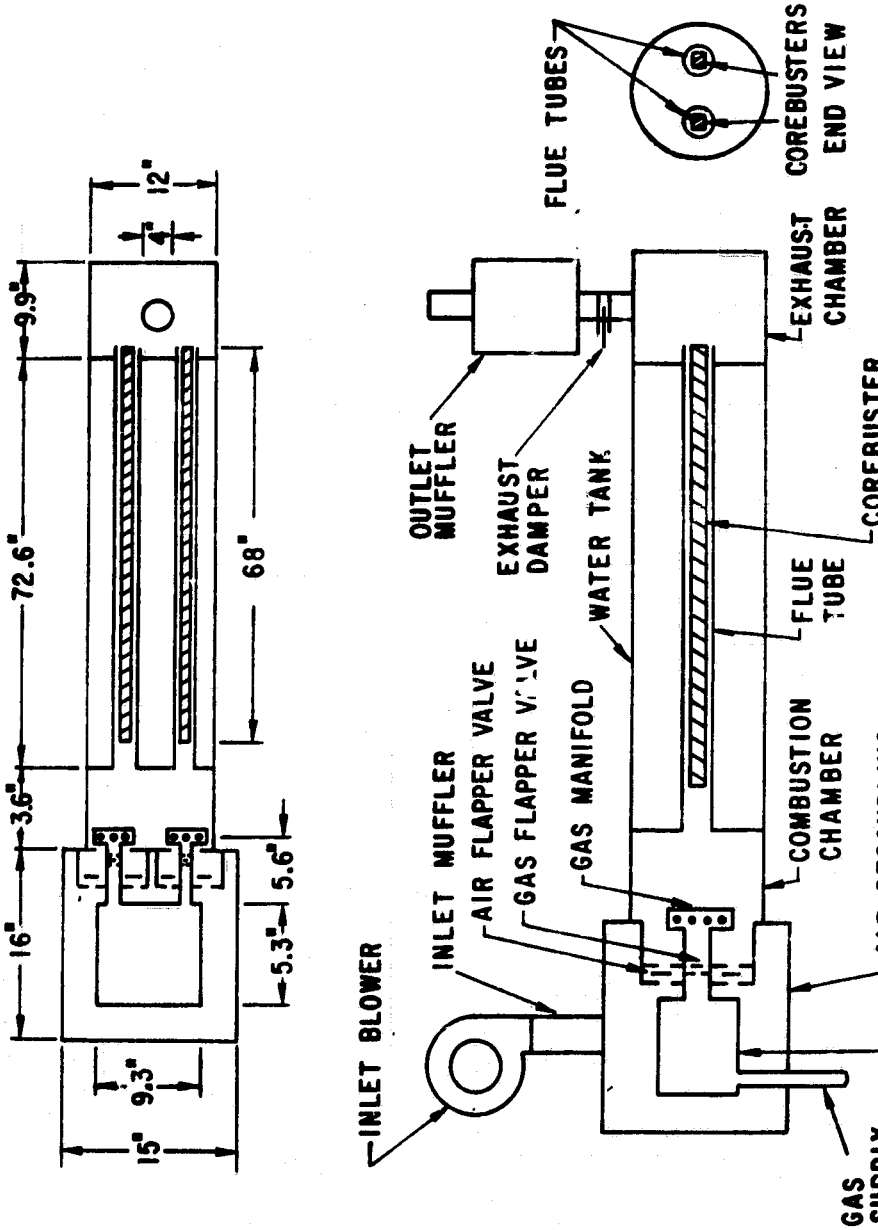

Fig. E.5 Schematic Diagram of Ray W. Herrick Laboratories Experimental Pulse Combustor (Source: Ref. 28)

One-third-octave band sound-pressure-level measurements were taken at three different positions around the unit (opposite the air decoupling chamber, the combustion chamber, and exhaust chamber). The microphone was always located in the horizontal plane passing through the centerline of the unit and approximately 2 feet from the surface. The sound-pressure-level peaks occur approximately at frequencies that are harmonics of the firing frequency. The highest sound level was ahead of the air-decoupling chamber, and its source appears to be the flapper valves. The lowest-noise source is at the exhaust and results from noise generated at the combustor inlet. Opposite the combustion chamber, the noise source probably is the combustion reaction itself. The highest A-weighed sound pressure level was 87 dBA, and the average of all runs was 77 dBA.

Dhar et al.[27,29] continued performance studies with this combustor and encountered unstable burning. The combustor would not operate without the aid of an auxiliary blower for more than 10 minutes, and no more than 25 to 30 minutes with the blower. The problem appeared to be an insufficient amount of combustion air for stable burning. Therefore, the air valve lift was increased from 0.06 in. to 0.112 in., but the combustor could not be started because of a very lean air-fuel mixture. Reducing the valve lift to 0.05 in. resulted in smooth burner operation for a few minutes without the use of an auxiliary blower. Further investigations revealed that as the combustion chamber heats up, the temperature inside the closely-coupled air and gas decoupling chamber rises and the volumetric efficiency of the burner is drastically reduced. Thus, the actual mass flow of air and gas into the combustion chamber becomes less than that theoretically required for sustaining combustion. Therefore, a cooling circuit was placed between the gas and air decoupling chamber, and fiberglass insulation was removed from the air decoupling chamber. These changes (along with an air valve lift of 0.05 in. and a gas valve lift of 0.025 in.) resulted in continuous stable operation without a blower.

Investigation of the pressure signal revealed that the adaptor pipe used to mount the pressure transducer on the combustion chamber introduced a cut-off frequency limitation. It was shown that sizeable high-frequency oscillations were due to a resonance amplification by the adaptor pipe. In addition, the adaptor began to act as a filter at frequencies corresponding to its natural frequency, so that harmonics at higher frequencies were partially suppressed. The length of the adaptor only had an effect beyond the second harmonic. The maximum pressure amplitude was approximately 16.5 in. of water in the combustion chamber and 1.2 in. of water in the exhaust chamber. Hence the exhaust chamber decoupled the burner from the rest of the exhaust system. The phase lag of the fundamental exhaust-chamber wave with respect to the fundamental combustion-chamber wave was $3\ \pi/2$.

Noise spectrum peaks were observed at 65, 130, 195, 260, 325, and 390 Hz. The 390-Hz peak is not as dominant as found in earlier measurements, and its suppression is probably related to the changes in the air intake. An air-

intake resonance in this frequency region is suspected. Resonance conditions occur in the vicinity of 1100 Hz and 2000 Hz and appear to be of a structural nature. The 1100-Hz resonance band may be due to a natural frequency of the cover plate for the air-decoupling chamber. The 2000-Hz resonances are unidentified. In any case, the structural resonances are at a fairly low level and are not of much concern. Noise spectrum data are also presented for measurements taken on the flat roof of the laboratory. The microphone was located about 85 in. from the exhaust pipe at a height of 39 inches above the roof level.

Dhar et al.[30] present additional measurements related to the thermal performance of the combustor and also describe the development of a computer simulation of the combustor that incorporates the dynamics of the system.

In order to compare pulsating and nonpulsating burner operation, the single combustion chamber had the flapper valves removed. Both methane and air had to be supplied under pressure to obtain gas and air flow rates comparable with pulsating operating conditions. Thus, it was shown that under pulsating conditions, air and fuel were pumped into the combustor to provide a higher burning rate for equivalent fuel and air pressures. Removal of the flapper valves did not completely eliminate pressure oscillations in the combustion chamber. At a heat input rate of about 208,000 Btu/h with 29% excess air, the pressure amplitude in the combustion chamber was 0.75 in. of water for steady burning and 21 in. of water for pulse combustion. The overall heat rate to the water was 21.5% higher under pulse combustion conditions than under steady burning conditions. Correspondingly, the overall thermal efficiencies were 78.6% and 64.9%. The percentage of heat transferred to the water in the region of the corebustor was 63.4% for pulsating conditions and 62.1% for steady burning. For the corebustor region of the flue tubes, the average overall heat-transfer coefficient (based on the outside area of the flue tubes) was 10.98 Btu/h-ft^2-°F for pulse combustion and 9.68 Btu/h-ft^2-°F for steady combustion, or a 13.5% increase with pulsations.

A shielded-junction Chromel-Alumel®* thermocouple mounted on a long rod was used to measure the gas temperature at various axial locations in one of the flue tubes. The time constant of the thermocouple was on the order of 1 s, whereas the cycle period was about 0.015 s, so time-averaged gas temperatures were obtained. At the start of the corebustor region of the tube, the gas temperature was about 2100°F for pulse combustion and 1830°F for steady combustion. However, near the exhaust end of the flue tubes, the temperatures were essentially the same, about 630°F.

The computer simulation program is based on a Helmholtz-resonator approach and is presently limited primarily to the internal dynamics of the combustion and flow pulsations. Coupling of the dynamic and heat-transfer effects is not included. It was shown that an exhaust decoupling chamber has

*Chromel-Alumel® is a registered tradename of the Hoskins Manufacturing Co., Detroit, Mich.

to be included in the computer model, otherwise oscillations cannot be predicted. (Pulse combustors can operate without an exhaust decoupling chamber).

For the single combustion chamber, predicted pressure amplitude in the chamber was 0.69 psi as compared to a measured value of 0.61 psi. The predicted pressure amplitude in the exhaust chamber was 0.18 psi as compared to a measured value of about 0.05 psi. This large discrepancy could result from the corebustor acting as a side-branch resonator, which the model does not consider. The computer simulation does predict the 180° phase lag between the combustion-chamber pressure and the exhaust-chamber pressure. The analytical model also has the capability to provide information about the mass flow of gas and air into the combustion chamber, the flow velocities in the flue tube, flame-front oscillations, and the position of the flame front inside the combustion chamber.

As mentioned earlier, an increase in the valve flow area resulted in a cessation of burner operation. This behavior was predicted by the simulation. For a 30% increase in valve area, the computer simulation showed that pressure oscillations develop but are not sustained. Experimental observations also revealed that if the valve size was too small, the unit would not operate without an auxiliary blower. This behavior was also predicted by the model.

Predicted operational behavior of the burner was found to be strongly a function of geometry. When the combustion-chamber volume was increased by 30%, the simulation predicted a decaying pulsation behavior. Also, when the flue-tube length was reduced by 50%, the prediction exhibited a resonant condition that was not sustained.

A model of the dual-combustion-chamber system was also developed. From the model results, it was observed that if both combustion chambers were exactly the same size, the system would operate in phase. However, if there were only a very small difference in their volumes, the unit would operate in the out-of-phase mode. This occurs because for different-size combustion chambers, the forcing functions acting on the gas plugs in the necks are of slightly different magnitudes. Since the two gas plugs are coupled by the spring element provided by the exhaust decoupling chamber, they tend to resonate out of phase with each other. (This mode of oscillation is at a specific energy level lower than that associated with the in-phase mode of operation.)

From predicted pressure oscillations, it can be seen that when the air-fuel mixtures in both combustion chambers are ignited at the same time, the pressure oscillations will go out of phase after a few operating cycles. This phenomenon was also observed experimentally, but it took a somewhat longer time to occur than predicted. The predicted pressure amplitude in each combustion chamber was 0.73 psi as compared to measured values of 0.83 psi. Predicted pressure pulsations in the exhaust decoupling chamber also agree with experimental results that show that the pressure amplitudes essentially cancel each other.

E.11 REMARKS

From the discussion of previous studies, it is obvious that the various combustors utilized do not permit a direct comparison or correlation of the experimental results. In fact, the studies confirm the inherently coupled nature of pulse combustors and the need for more detailed experimental data. Some of the studies are missing critical information (e.g., the data of Griffiths, Thompson, and Weber[21] would be more useful if the air/fuel ratio, the gas heating value, the combustion-chamber volume, and the actual inside diameters of the tailpipe and combustion chamber had been given). The data of Griffiths and Weber[23] also lack air/fuel ratios, the gas heating value, and the length/diameter ratios for the combustion-chamber volumes. Some data need additional explanation, such as the heat-transfer data of Reay[32], which show variations in the exhaust gas heat-transfer coefficient with cooling water flow. No supporting data for the Reynolds number used in heat-transfer correlations are given. Estimated Reynolds numbers give values that correspond to the laminar or transition flow regime, but turbulent-flow heat-transfer correlations are used by Hanby[41] and Reay.[32]

Francis et al.[31] list equations for the estimation of a valveless-combustor operating frequency that are based on the geometry of the combustion chamber and the air-inlet neck. There are many burners without an air-inlet neck, with "untuned" tailpipes, and with flapper valves. How does one estimate the frequencies of these combustors? Equations for frequency contain the gas velocity, which is temperature-dependent. Hanby[42] is the only investigator who has attempted to define what temperature to use. He concluded that the root-mean-square temperature should be used for a Schmidt burner. Unfortunately, this temperature cannot be predicted a priori.

The increase in heat transfer attributed to pulse combustion has been validated in a number of studies, but the magnitude of the reported increase varies. In the work of Reay,[32] the measured heat-transfer coefficients in part of the burner were less than predicted. No explanation for this occurrence was given.

There have been a number of investigations with the Schmidt burner, but the Helmholtz combustor appears to be preferred for heating applications. One reason for this choice may be that the only way a fixed-diameter Schmidt combustor can obtain added heat-transfer surface is by an increase in its length. However, increasing the burner length can lead to instabilities. Another reason may be that the Helmholtz burners can be built in a more compact form. Still, there is need for additional work to clarify the reasons for choosing one burner over another. The choice of an aerodynamic or flapper valve has somewhat been determined. The exhaust losses through an aerodynamic valve and the inability to muffle the inlet noise precludes the use of these valves for many applications.

Whereas theoretical considerations have not been covered (or have been treated only very slightly) in the previous studies, it is encouraging to note the reasonably good agreement between prediction and measurements obtained by Dhar et al.[30]

APPENDIX F

APPLICATIONS OF PULSE COMBUSTION

APPENDIX F: APPLICATIONS OF PULSE COMBUSTION

Proposed and actual applications of pulse combustion burners include: propulsion, steam raising, water heating, air heating, constant-volume pressure-rise combustion, portable heaters, drying and/or conveying of powders etc., fogging, ice melting, and others. A discussion of some applications is given by Putnam[2] and by Kentfield.[40] The following discussions are not intended to be exhaustive but only to summarize some of the applications and provide some references for further information.

F.1 PROPULSION

The best known application of pulse combustion for propulsion is the V-1 flying bomb used by the Germans in World War II. A history of this work is given by Schmidt[87] and Gosslau.[88] After the recovery of a V-1 engine by the U.S., considerable interest in and investigations of the pulse jet for aircraft propulsion arose. Additional information and references to these studies can be found in Appendix A of Ref. 21, and in Refs. 1, 2, 8, and 12-16. Interest in the pulse-jet aircraft engine faded because of its high noise level, its poor flight thermal efficiency, and the development of turbojet and ram-jet engines.

F.2 STEAM RAISING

The use of pulse combustors for steam raising was discussed in Chapter 1. Included were the coal-fired tests of Sommers,[6] Hanby and Brown,[18] and Severyanin.[19] Oil-fired units were described by Babkin.[7] The plentiful and cheap supplies of fuel oil, the advent of nuclear power, and the declining use of coal were probably the primary reasons for the lack of development of pulse combustion technology for steam raising. However, the renewed interest in coal combustion, along with the potential NO_x and soot reduction offered by pulse combustion, should provide an incentive for further investigations.

F.3 WATER HEATING

Even though Reynst[1] suggested a wide variety of water heaters, such as the one shown in Fig. 1.6, the high noise level of this combustor was probably the reason for its lack of development.

From 1956 to 1960, Kitchen[46,22] developed and tested several models of a small pulse-combustion hot-water-heating boiler at the Lucas-Rotax Ltd. plant in Toronto, Canada. The end result of these tests was a 107,000 Btu unit, called the "Pulsamatic,®*" that went into production in 1960. The next

---

*Pulsamatic® was a tradename used by Lucas-Rotax Ltd., Toronto, Ontario, Canada, for its pulse combustion units.

year Lucas-Rotax Ltd. licensed Greensteel Ltd. of Winnipeg to take over all manufacturing and distribution. Experimental work continued at Lucas-Rotax Ltd. until they ceased operation in 1962. Greensteel Ltd. continued production of the Pulsamatic® until 1966 and built a total of 645 units. Lucas-Rotax built about 150 units. No reason was given for the cessation of production, but it was probably due to high production cost (as compared to that for conventional boilers) in an era of cheap gas.

In 1976, Kitchen redesigned the Pulsamatic boiler, and it became the basis for the "Hydropulse" model manufactured by Hydrotherm, Inc., of Northvale, N.J.[89] Field-test results of Hydrotherm's units are given by Whitlock, Favors, and Renter.[90] Installations include a residence with radiant hot-water panels in the ceiling and a residence with a heat exchanger in a warm-air system and a domestic-hot-water heat loop. The tests were carried out in Minnesota and upstate Western New York, and both sites showed that natural gas consumption was reduced by 11-20%.

Francis, Hoggarth, and Reay[31] built a prototype immersion-tube water-heating unit. The Helmholtz burner had a mechanical flapper valve on the air inlet but no valve on the gas supply. The unit operated at a frequency of 64 Hz, with a 3/4-in. tailpipe and a 3-in. diameter combustion chamber. They also tested a 3-in. diameter Schmidt tube.

Woodworth[91] has reported on the program at Brookhaven National Laboratory on hardware development and energy analysis for gas- and oil-fired space-heating equipment. One unit undergoing laboratory testing is a condensing pulse combustion boiler being developed by Yankee Engineering. This combustor fires at about 36,000 Btu/h, and the entire combustion chamber plus resonator is surrounded by water. The unit has a sealed combustion system that uses the exhaust gases to preheat the incoming combustion air. Exit exhaust temperatures as low as 70°F are attainable. The boiler provides hydronic space heat as well as domestic hot water when coupled with a separate tank. The system can also be fitted with a fan-coil unit to provide an integrated furnace/domestic-hot-water system. This combustor was to be field-tested in 1980.

Brookhaven is also testing an oil-fired pulse combustion system being marketed by Turbopuls S.A., Geneva, Switzerland. The combustor has a unique oil-fired combustion head and air-inlet assembly that does not seem to foul the condensing section of the heat exchanger. Product literature from Turbopuls[92] shows that the combustion chamber and exhaust are surrounded by water. The unit used for domestic heating is 22.5 x 22.5 x 43-in. high and has an output rating of about 60,000 Btu/h. Its operating frequency is 87 Hz, with a pressure amplitude of +19.1 psi and - 11.8 psi. Heat transfer per unit area is reported to be three to five times greater than that of conventional combustors. The minimum average efficiency is 85-90% without condensation and up to 98% with condensation. The exhaust gas temperature ranges from about 2700°F in the combustion chamber to as low as 65°F at the exhaust. The content of the exhaust is 13.5-14.8% CO_2, less than 0.1% CO, and about 34 ppm NO_x. The noise level of the combustor is only 42 to 45 dBA in an undamped room. An air-intake and an exhaust silencer are used.

Lauton, Irwin, and Lauler[93] described a gas-fired pulse combustion water heater being developed jointly by the Shock Hydrodynamics Division of the Whittaker Corp. and American Appliance Manufacturing Corp., a subsidiary of Mor-Flor Industries. The heater has a gas input rate under 200,000 Btu/h and operates at a thermal efficiency based on flue-gas losses of 89-90% without the use of a secondary heat exchanger. The unit consists of a concentric air and gas flapper assembly at the top of the unit with a 10-in. diameter spherical combustion chamber and a 16-in. diameter spherical decoupler aligned below the valves. The gas and air enter from the top of the tank via their repective decouplers and the exhaust gases exit at the bottom. The resonator consists of four 1-in. diameter tubes 61-in. long, which are spiraled from the bottom of the combustion chamber to the top of the exhaust decoupler. The tank diameter is 18 in., and it has a 40-gal capacity. The orientation allows cold water to cool the combustion gases as it rises in the tank, and stratification of the hot water above the exhaust decoupler maintains a supply of hot water for instant availability. This also allows the condensate to drain downward.

The sound level is minimized by keeping the mean pressure low (consistent with adequate power to expel the combustion gases), minimizing the paths for sound flow, and using acoustic absorbers judiciously at key locations.

F.4 AIR HEATING

One of the first applications of pulse combustion for the direct heating of air was the unit developed by Huber[10] for buses and other vehicles. This is a gasoline-fired combustor whose operation is described by Putnam[2] (the original reference is in German).

Woodworth[91] states that Shock Hydrodynamics is working on a gas-fired pulse combustion furnace capable of firing at 40,000 to 90,000 Btu/h. A major consideration is to ensure minimization of the noise level, as harmonics and vibrational noise are very difficult to control in a furnace. After numerous permutations, a pre-production unit evolved that used a tuned spherical combustion chamber with a primary and a secondary heat exchanger. The system starts easily, operates stably, and has a total unmuffled-sound-power level of about 75 dBA. The sound level drops to the low 60s (in dBA) when the inlet and exhaust are decoupled. The final furnace was being constructed by American Appliance of California and was to undergo laboratory and field tests during the 1979-80 heating season.

Under the sponsorship of the Gas Research Institute, the American Gas Association Laboratories and Lennox Industries, Inc., for several years have been engaged in a program to commercialize a pulse combustion forced-air furnace. Drewry and Wright[94] report that in September 1980, Lennox Industries, Inc., announced its intention to begin production of the pulse combustion furnace sometime in the second half of 1981. The new furnace line

will involve eight models with outputs ranging from 38,000 to 124,000 Btu/h. The steady-state operating efficiency of the furnace exceeds 96%, with an overall seasonal efficiency expected to be at 92% or higher. Through an extensive R&D effort, the operating noise level of the furnace was reduced to approximately 60 decibels, which is comparable to the noise level of conventional forced-air heating systems. During the 1979-80 heating season, ten prototype furnaces were tested at various test sites across the U.S. and Canada. Adams[95] discusses these field tests. The furnaces were all natural-gas-fired, upflow units rated at 65,000 Btu/h input. In addition to having a low-pressure pulse combustion burner, they had a secondary heat exchanger that allowed them to operate in the condensing mode. Results of these tests verified the significant increase in efficiency achievable with the pulse combustion furnace relative to conventional heating systems. Expanded field testing of pulse combustion furnaces was to be continued by Lennox in the 1980-81 heating season, with an additional 14 test sites being included.

F.5 CONSTANT-VOLUME PRESSURE-RISE COMBUSTION FOR GAS TURBINES

The use of a pulse combustor with a gas-turbine cycle forms the basis for this application. Fuel is burned in a pulse combustor along with compressed air to give an increase in pressure instead of the pressure drop and loss of efficiency that occurs with conventional constant-pressure combustion systems. The exhaust gas from the combustor is then expanded through a turbine or a ram-jet nozzle. This idea dates back to the work of Holzwarth in 1905 and Karavodine in 1909. A brief discussion of their work is given by Reynst,[1] who was the best-known advocate of this idea, and by Putnam and Brown.[47] Additional information is given by Porter;[96] Marchal and Servanty;[13] Marchal;[15] Muller;[97] Swithenbank, Brown, and Saunders;[98,99] and Kentfield.[39,100]

F.6 PORTABLE HEATERS

The compact size of pulse combustors (arising from their high combustion intensity, their self-aspiration capability, and the lack of moving parts) makes them ideal portable heaters. However, noise emission is a problem, but it is solvable with mufflers. Kentfield[40] describes a vertical, propane-fueled, valveless, construction-site pulse combustion space heater with a maximum thermal output of approximately 270,000 Btu/h. The diameter of the heater is 28.3 in., and its height is 86.6 in. Air enters at the floor level, and the hot gases exhaust at the top. Rock-wool meshed between two layers of perforated sheet metal forms a passive muffler to inhibit the high-frequency components of the noise. The outer containment vessel is intended to serve as an active muffler. At a thermal output of 205,000 Btu/h, the noise level near the heater was 100 dBA. At 157,000 Btu/h output, the noise level was 95 dBA.

Kentfield also described a prototype, self-contained, gasoline-fueled, hand-held, high-intensity, warm-air blower or heater with an output of approximately 500,000 Btu/h. The unit is a carburetted version of the SNECMA/Lockwood configuration having a 2.875-in. diameter combustion chamber and a rectifier. A hand-operated air pump and a piezoelectric generator are used for starting. A Tillotson pressure-pulse-operated diaphragm fuel pump transfers gasoline from the tank to the carburetor. The heater is intended for uses such as warming diesel engines prior to start-up and other duties that might arise in very cold climates. Because of the requirements for portability, no attempts were made to silence the unit; it was assumed that the operator would wear ear-protectors for the 10 to 15-min anticipated operation time.

F.7 DRYING AND CONVEYING

Muller[35] reported on a 300,000 Btu/h pulse combustor for drying and conveying corn. Ellman, Belter, and Dockter[101] used a propane-fired, valveless, 8-ft long, 300,000 Btu/h pulse combustor as part of an entrained-lignite drying system. The combustor, with an operating frequency of 70 Hz, was enclosed by a secondary-air system, which also captured the backflow from the air-inlet valve. The exhaust gas from the combustor pumped secondary air from its containment, and this mixture (along with the fuel flow rate) was used to regulate the drying temperature from 700-1400°F. Lignite was entrained by the exhaust gases as it was fed by an auger into the bottom of an 8-in. diameter, 50-ft long, U-shaped vertical drying column, which terminated in a 24-in. diameter cyclone separator. The maximum throughput of lignite was 7000 lb/h. Lignite particles from 1/4 x 0-in. up to 3/4 x 1/2-in. in size were entrained, but drying of the finer material was more effective. The sound level of the pulse combustor enclosed in the secondary-air system was about 100 dB.

Belter[38] refers to the development of a grain-drying system similar to that described above, but with two openings for secondary air so that the drying temperature could be closely controlled. The unit was never used for grain drying, so no details are given. Belter also briefly mentions the design, construction, and operation of pulse combustors of 12, 20, and 35 ft in overall length. The last unit was described in Sec. 1.3.1 and was sufficient to dry 20 tons of lignite per hour. It operated on several fuel combinations including propane, pulverized lignite, dried lignite dust, and residual oil. The combustor was always started with propane. In addition, Belter speculates on the use of pulse combustion for conveying and presents some measured static pressures in the lignite-drying system.

Based on his development of high-performance pulsating jet pumps for aircraft and other military thrust-augmentation uses, Lockwood[102] now markets a system called "Jetsonic®*" for drying food and wastes with pulse combustion. The acoustic waves (noise) that result from pulse combustion provide the

*Jetsonic® is a tradename used by Jetsonic Processes, Palo Alto, Calif., for its drying systems.

mechanism of ultra-high heat and mass transfer. These broad-band sonic waves are composed of compression waves closely coupled with rarefaction waves. The net result is a very efficient and rapid removal of the moisture-laden boundary layer surrounding each particle, resulting in drying rates as much as ten times faster than with conventional drying systems. This high-speed drying continues down into the region where the rate of surface-moisture removal exceeds the rate at which moisture diffuses to the surface from the interior of a drying particle. It is postulated that the broad-band sonic-energy waves tend to vibrate the drying particles at their natural frequency. The faster flow of moisture to the surface is thought to be a mechanical response to the "push-pull" effect of the compression-vacuum waves. That is, a sort of "massaging" action accelerates the flow of moisture to the surface.

Valveless pulse-jets are ideal for these applications, when coupled with jet pumps. The resulting system converts the potential energy in fuels into heat for processing, broad-band sonics, and pumping of process gases with compact jet pumps. The extreme mechanical simplicity of resonant pulse combustion devices is a further economic advantage. No details of the pulse combustor are given.

Tamburello et al.[103] describe the development of a pulse combustor for incorporation into a fruit-and-vegetable dehydration unit.

F.8 FOGGING

The pulse combustor used by Persechino[104] for fogging had an air inlet that was shaped to promote a vortex action. Fog oil was evaporated on the outside surface of the combustion chamber and resonance tube and then aspirated into the hot-gas jet. The mixture aspirated cold air into the jet to condense the oil and produce a fog.

Putnam[4] refers to the U.S. Army M3A3 smoke generator,[105] but provides no details.

Mutchler[106] addresses the use of a pulse-jet engine as a smoke generator (also referred to as a multispectral obscurant generator) for use by the military.

F.9 ICE AND SNOW MELTING

Several single and double pulse-jet units were tested by Persechino.[11] These units were fired with either gasoline or diesel fuel that was vaporized by the heat of the combustion chamber. Although the units melted hard ice at a rapid rate, the exhaust pressure was insufficient to blow the ice and slush away. A final design, with dual-phased burners for quieter operation and a scraper blade attached to the exhaust end to knock ice away, was less than 5-ft long, weighed less than 15 lb, and could start at -95°F.

The development of a pulse combustion heater as the primary jet of a forced-convection heater for the protection of Canadian railroad track switches in remote areas under conditions of snow and ice is described by Ringer, Lane, and Slawinski.[37] The pulse combustor is a Helmholtz type that produces a thrust of 3.25 lb at its rating of 250,000 Btu/h when fired with propane. Standard stainless-steel pipe sections and fittings were used to fabricate the combustor. The combustion chamber is 2.5-in. sch 10 pipe, 6.5 in.-long, with a weld cap on one end and a 2.5 x 1.5-in. pipe reducer on the other. The resonance tube is 1.5-in. sch 10 pipe, 23.75 in.-long with a 6.5-in. long flare section (4° included angle) on the end. The fuel nozzle is simply a tube (0.125-in. inside diameter) mounted on the side of an Inconel® air-intake elbow (1-in. O.D. tube x 0.049-in. wall) discharging concentrically with the intake into the combustion chamber. The fuel flowing through the intake entrains additional air with it, thus promoting better breathing of the combustor and better mixing of the air and fuel. The nominal fuel supply pressure is 5 psig. Ignition is accomplished with a capacitor-discharge exciter system in conjunction with an automotive ignition coil and a spark plug, which is mounted in the weld-cap section of the combustion chamber.

The air inlet for the ejector pump is a tapered cone elbow so that any snow that enters the intake is accelerated into the pulse-jet efflux. The exhaust gas is mixed with the secondary-air supply in a venturi (4.25-in. diameter throat) and diffuser section attached to the end of the intake elbow. The combustion products and the secondary air are discharged from a conical diffuser into a distribution duct for the track switch.

Cold-chamber tests on the complete system, installed on a 22-ft switch, were conducted. The heater maintained the switch in satisfactory operating condition for five hours at a snowfall rate of 3 in./h with an ambient temperature of 0°F and a 15 mph wind. In addition, sound measurements of about 130 dB were made in a jet-engine test cell. Two prototypes were installed in a remote location on the Canadian Pacific Railway mainline in Northern Ontario for limited field trails.

F.10 OTHER USES OF PULSE COMBUSTION

Small-scale experimental work was conducted by Tracenckner[107] on gasification of gasoline, high-volatile bituminous coal, and lignite. The pulse combustor was 63-in. long with pear-shaped combustion chamber and a 1 3/8-in. diameter resonance tube. Lignite was gasified with an efficiency of 63% and a carbon conversion of 93%. With high-volatile bituminous coal, the once-through gasification efficiency was only 36% and the carbon conversion 62%. In both cases, only low-quality gas with a heating value of about 100 Btu/ft^3 was produced.

A pulse combustion system was developed by Pannier[108] to pulverize suitable materials by utilizing thermal shock and the abrasive action of particle collision. Material to be pulverized is fed into the combustion-air

inlet of a valveless pulsating-combustion chamber and then collected in a baffled chamber.

Belter[38] conducted laboratory tests at the Grand Forks Energy Research Laboratory on the use of dual pulse jets to produce continuing shock-tube reactions. Two valveless pulse jets were arranged with their tailpipes opposed and one diameter apart inside a reaction chamber. Lignite was injected into the two tailpipes and probably made numerous passages across the tailpipe gap, as several seconds passed before the product began to emerge from the system. The processed lignite was readily combustible and often would spontaneously burst into flame. Some product samples tested indicated that they were equal to a good commercial-grade active carbon. When steam was added to the reaction chamber, complete gasification of the lignite occurred. At a reaction chamber temperature of 1800°F, a gas consisting of 10% H_2, 11.9% CO_2, 0.4% O_2, and 6.4% CO was produced. Instead of an expected noise attenuation from internal wave reflection, a portion of the reinforced wave was expelled from each inlet and the noise level during operation was very high (estimated as 145 dB; the sound level exceeded the meter's range).

Putnam[2] reported on feasibility studies conducted at Battelle Memorial Institute in 1964 on using a hydrocarbon/air-fired, aerodynamically valved pulse combustor for magneto-fluid-dynamic power generation. A conclusion of the study was that such a unit could be built based on existing technology, but the available pressure rise limited the power-generation efficiency.

Preliminary studies were performed by Ibberson et al. with the aim of using a hydrocarbon/alcohol, KOH/oxygen-fired pulse combustor for magneto-hydrodynamic power generation.[109] Traveling-wave oscillations with a 1250 Hz frequency were obtained in a 1-m long rocket-like combustor. Electrical conductivity was found to be in phase with the pressure but less regular.

Other proposed applications include:

- Hot-gas recirculation in blast furnaces
- Movement of earth
- Replacement of fan or blower for supplying air to a conventional combustor
- Providing heat for hot-air balloons
- Inflation of emergency inflatable shelters
- Driving of piles
- Liquefaction of highly viscous materials
- Heating of bore-holes for oil extraction

F.11 REMARKS

In this appendix, a number of proposed or actual applications of pulse combustion have been briefly described. Undoubtedly, some applications have been overlooked, especially those investigated in the Soviet Union and those of Huber in Germany. In spite of all these studies, commercialization of the pulse combustor has lagged. The Pulsamatic® unit performed satisfactorily, but marketing ceased in 1966, probably because of the units' cost in comparison with conventional boilers in an era of cheap fuels. The awakening of industry to the scarcity of fuels and their rising prices in the early 1970s led to the marketing of the Hydrotherm pulse combustion boiler in 1979 and the Lennox furnace in 1981.

In addition to these domestic heating applications, pulse combustors are used by the military as smoke generators and are being promoted for food-drying. In spite of all the research into propulsion applications, the only apparent market is for propulsion engines for target drones or model airplanes. The reason for the lack of any industrial application is not clear; perhaps it is the noise-generation problem. Current studies at Battelle-Columbus by Corliss, Putnam, and Locklin[110] under contract with the Gas Research Institute may enhance the industrial application of pulse combustion, but it will take several years before this becomes apparent.

REFERENCES

1. *Pulsating Combustion: The Collected Works of F.H. Reynst,* M.W. Thring, Ed., Pergamon Press, New York, N.Y. (1961).

2. Putnam, A.A., *General Survey of Pulse Combustion,* Proc. of the First International Symposium on Pulsating Combustion, D.J. Brown, Ed., University of Sheffield, Sheffield, England (Sept. 20-23, 1971).

3. Reader, G.T., *Aspects of Pulsating Combustion,* Society of Automotive Engineers, pp. 543-557 (1978).

4. Putnam, A.A., *A Review of Pulse-Combustor Technology,* Proc. of the Symposium on Pulse Combustion Technology for Heating Applications, compiled by J.M. Clinch, Argonne National Laboratory Report ANL/EES-TM-87, pp. 1-21 (May 1980).

5. Reynst, F.H., *Pulsating Firing of Steam Boilers,* Engineers' Digest *14*:285-288; 328-330 (Aug.-Sept. 1953).

6. Sommers, H., *Experiences with Pulsating Tube Firing in an Experimental Installation,* Chapter 23 in *Pulsating Combustion: The Collected Works of F.H. Reynst,* M.W. Thring, Ed., Pergamon Press, New York, N.Y., pp. 262-274 (1961).

7. Babkin, Y.U., *Pulsating Combustion Chambers as Furnaces for Steam Boilers,* Teploenergetika *12*(9):23-27 (1965).

8. Bertin, J., F. Paris, and J. LeFoll, *The SNECMA Escopette Pulse Jets,* Interavia *8*(6):343 (1953).

9. *Gabriel's Heater,* Industrial and Engineering Chemistry *43*:17A (April 1951).

10. Huber, L., *Pulsator-Fired Heater for Service Vehicles,* Automobiltechnische Zeitschrift *66*(2):31-37 (1964).

11. Persechino, M.A., *Valveless Pulsejet De-Icer Application,* Naval Research Laboratory Report 5024 (Nov. 14, 1957).

12. Marchal, R., and P. Servanty, *Note sur le Developpement de Pulsoreacteurs sans Clapets,* Session Association Technique Maritime et Aeronautique, pp. 1-20 (1963).

13. Marchal, R., and P. Servanty, *Turbines a Gaz a Chambres de Combustion Pulsatoire,* Entropie *11*:37-40 (Sept.-Oct. 1966).

14. Servanty, P., *Reflexions sur la Combustion Pulsatoire,* Entropie *22*:49-63 (July-Aug. 1968).

15. Marchal, R., *Turbines a Gaz a Chambres de Combustion Pulsatoire,* Entropie *22*:15-19 (July-Aug. 1968).

16. Lockwood, R.M., *Pulse-Reactor Low Cost Lift-Propulsion Engines,* AIAA Paper No. 64-172, AIAA General Aviation Aircraft Design and Operations Meeting, Wichita, Kans. (May 25-27, 1964) [available from American Institute of Aeronautics and Astronautics].

17. Hanby, V.I., and T.D. Brown, *A Residual Fuel-Oil-Fired Pulsating Combustor,* J. Inst. Fuel, *48*:48-51 (March 1975).

18. Hanby, V.I., and D.J. Brown, *A 50 lb/h Pulsating Combustor for Pulverized Coal,* J. Inst. Fuel *41*:423-426 (Nov. 1968).

19. Severyanin, V.S., *The Combustion of Solid Fuel in a Pulsating Flow,* Teploenergetika *16*(1):6-8 (1968), Thermal Engineering *16*(1):9-13 (1969).

20. Ellman, R.C., J.W. Belter, and L. Dockter, *Operating Experience with Lignite-Fueled Pulse-Jet Engines,* Paper 69-WA-FU4, presented at the American Society of Mechanical Engineers Winter Annual Meeting, Los Angeles, Calif. (Nov. 10-20, 1969).

21. Griffiths, J.C., C.W. Thompson, and E.J. Weber, *New and Unusual Burners and Combustion Processes,* American Gas Association Laboratories Research Bulletin *96*:3-17 (Aug. 1963).

22. Kitchen, J.A., *Pulse Combustion Promises Cheaper Furnace Installations,* Product Design and Engineering *67*:50-53, 67 (May/June 1962).

23. Griffiths, J.C., and E.J. Weber, *The Design of Pulse Combustion Burners,* American Gas Association Laboratories Research Bulletin *107* (June 1969).

24. Kunsagi, L., *Silent Valveless Pulsating Combustor for Industrial Applications,* Proc. of the First International Symposium on Pulsating Combustion, D.J. Brown, Ed., University of Sheffield, Sheffield, England (Sept. 20-23, 1971).

25. Vogt, S.T., M.S. Yen, R.J. Schoenhals, and W. Soedel, *Performance Characteristics of a Pulse Combustion Water Heater,* Purdue University, West Lafayette, Indiana, Herrick Laboratories Report HL 78-30, Argonne National Laboratory Report ANL/EES-TM-19 (Aug. 1978).

26. Vogt, S.T., *Performance Characteristics of a Pulse Combustion Water Heater*, MSME Thesis, Purdue University, West Lafayette, Ind. (Dec. 1978).

27. Dhar, B., W. Soedel, and R.J. Schoenhals, *Experimental and Analytical Investigations of a Pulse Combustion Water Heater*, Purdue University, West Lafayette, Indiana, Herrick Laboratories Report HL 80-21, Argonne National Laboratory Contract No. 31-109-38-5449, Gas Research Institute Grant No. 5014-363-0247 (June 1980).

28. Vogt, S.T., M.S. Yen, R.J. Schoenhals, and W. Soedel, *Performance of a Pulse Combustion Gas-Fired Water Heater*, Paper No. 2563, ASHRAE Transactions *86*, Part 1, pp. 126-141 (1980).

29. Dhar, B., W. Soedel, and R.J. Schoenhals, *Measurements and Interpretation of Pressure and Sound Spectra of a Pulse Combustion Water Heater*, Proc. of the Symposium on Pulse Combustion Technology for Heating Applications, compiled by J.M. Clinch, Argonne National Laboratory Report ANL/EES-TM-87, pp. 105-128 (May 1980).

30. Dhar, B., H.C.G. Huang, J.H. Lee, W. Soedel, and R.J. Schoenhals, *Dynamic and Thermal Characteristics of A Pulse-Combustion Gas-Fired Water Heater*, Proc. of the Symposium on Pulse Combustion Applications, Atlanta, Ga. (March 2-3, 1982).

31. Francis, W.E., M.L. Hoggarth, and D. Reay, *A Study of Gas-Fired Pulsating Combustors for Industrial Applications*, Institution of Gas Engineers Journal *3*:301-323 (June 1963).

32. Reay, D., *The Thermal Efficiency, Silencing, and Practicability of Gas-Fired Industrial Pulsating Combustors*, J. Inst. Fuel *42*:135-142 (April 1969).

33. Briffa, F.E.J., and D.R. Romaine, *Experiments with Coupled Pulse Combustors*, Proc. of the 2nd Conference on Natural Gas Research and Technology, Institute of Gas Technology, Atlanta, Ga. (1972).

34. Katsnel'son, B.D., I.A. Marone, and A.A. Tarakanovskii, *An Experimental Study of Pulse Combustion*, Teploenergetika *16*(1):3-6 (1969).

35. Muller, J.L., *The Development of a Resonant Combustion Heater for Drying Applications*, The South African Mechanical Engineer *16*(7):137-146 (1967).

36. Beale, C.K., P.H. Clarke, and G. Everson, *A Comparison of the Dependence of the Pulsations in a Single-Orifice and a Double-Orifice Combustor on Heat Transfer or Acoustic Processes*, Proc. of the First International Symposium on Pulse Combustion, D.J. Brown, Ed., University of Sheffield, Sheffield, England (Sept. 20-23, 1971).

37. Ringer, T.R., J.F. Lane, and P.P. Slawinski, *A Pulsating Combustion System to Protect Railway Track Switches in Snow and Ice Conditions*, Proc. of the First International Symposium on Pulse Combustion, D.J. Brown, Ed., University of Sheffield, Sheffield, England (Sept. 20-23, 1971).

38. Belter, J.W., *A Review of the Use of Pulsating Combustors for Drying and Conveying*, Proc. of the First International Symposium on Pulse Combustion, D.J. Brown, Ed., University of Sheffield, Sheffield, England (Sept. 20-23, 1971).

39. Kentfield, J.A.C., *Progress Towards a Pressure-Generating Combustion Chamber for Gas Turbines*, Proc. of the First International Symposium on Pulse Combustion, D.J. Brown, Ed., University of Sheffield, Sheffield, England (Sept. 20-23, 1971).

40. Kentfield, J.A.C., *Pressure-Gain Combustion, A Review of Recent Progress*, Proc. of the Symposium on Pulse Combustion Technology for Heating Applications, compiled by J.M. Clinch, Argonne National Laboratory Report ANL/EES-TM-87, pp. 22-45 (May 1980).

41. Hanby, V.I., *Convective Heat Transfer in a Gas-Fired Pulsating Combustor*, Transactions of the American Society of Mechanical Engineers, J. Engineering Power *91*:48-52 (Jan. 1969).

42. Hanby, V.I., *Basic Considerations on the Operation of a Simple Pulse Combustor*, J. Inst. Fuel *44*:595-599 (Nov. 1971).

43. Hanby, V.I., and D.J. Brown, *Noise and Other Problems in the Operation of Pulsating Combustors*, Proc. of the First International Symposium on Pulsating Combustion, D.J. Brown, Ed., University of Sheffield, Sheffield, England (Sept. 20-23, 1971).

44. Noise Control in Industry, 2nd ed., J.D. Webb, Ed., Sound Research Laboratories Ltd., Holbrook Hall, Sudbury, Suffolk, England (1978).

45. Soedel, W., *Design Simple Low-Pass Filter Mufflers for Small Two-Cycle Engines*, Noise Control Engineering *10*(2):60-66 (1978).

46. Kitchen, J.A., *Canadian Development of Pulse Combustion Heating Equipment*, Proc. of the Symposium on Pulse Combustion for Heating Applications, compiled by J.M. Clinch, Argonne National Laboratory Report ANL/EES-TM-87, pp. 163-166 (May 1980).

47. Putnam, A.A., and D.J. Brown, *Combustion Noise: Problems and Potentials*, Chapter 5 in *Combustion Technology: Some Modern Developments*, A.B. Palmer and J.M. Beers, Eds., Academic Press, Inc., New York, N.Y., pp. 127-162 (1974).

48. Ahrens, F.W., and G.T. Kartsounes, *Pulse Combustion Technology for Heating Applications, Quarterly Progress Report, April-June 1978*, Argonne National Laboratory Report ANL/EES-TM-12 (July 1978).

49. Ahrens, F.W., J.M. Clinch, and G.T. Kartsounes, *Pulse Combustion Technology for Heating Applications, Quarterly Progress Report, July 1 to September 31, 1978 and October 1 to December 31, 1978*, Argonne National Laboratory Report ANL/EES-TM-36 (Feb. 1979).

50. Ahrens, F.W., C. Kim, and S.W. Tam, *An Analysis of the Pulse Combustion Burner*, ASHRAE Transactions *84*, Part 1, 488-507 (1978).

51. *Gas Engineers Handbook*, G.C. Segeler, Ed., Industrial Press, Inc., New York, N.Y. (1974).

52. Edwards, J.B., *Combustion Formation and Emission of Trace Species*, Ann Arbor Science Publishers, Inc., Ann Arbor, Mich. (1974).

53. Ahrens, F.W., and J.M. Clinch, *Pulse Combustion Technology for Heating Applications, Quarterly Progress Report, July 1 to September 30, 1979*, Argonne National Laboratory Report ANL/EES-TM-69 (Dec. 1979).

54. Ahrens, F.W., and J.M. Clinch, *Pulse Combustion Technology for Heating Applications, Quarterly Progress Report, October 1 to December 31, 1979*, Argonne National Laboratory Report ANL/EES-TM-78 (Jan. 1980)

55. Alhaddad, A.A., and G.A. Coulman, *Experimental and Theoretical Study of Heat Transfer in Pulse-Combustion Heaters*, Proc. of the Symposium on Pulse Combustion Applications, Atlanta, Ga. (March 2-3, 1981).

56. McAdams, W.H., *Heat Transmission*, 3rd ed., McGraw-Hill Book Co., New York, N.Y. (1954).

57. Ozisik, M.N., *Basic Heat Transfer*, McGraw-Hill Book Co., New York, N.Y. (1977).

58. Rohsenow, W.M., and J.P. Hartnett, Eds., *Handbook of Heat Transfer*, McGraw-Hill Book Co., New York, N.Y. (1973).

59. Kays, W.M., and M.E. Crawford, *Convective Heat and Mass Transfer*, 2nd ed., McGraw-Hill Book Co., New York, N.Y. (1980).

60. Severyanin, V.S., *Applications of Pulsating Combustion in Industrial Applications*, Proc. of the Symposium on Pulse Combustion Applications, Atlanta, Ga. (March 2-3, 1981).

61. Petukhov, B.S., *Heat Transfer and Friction in Turbulent Pipe Flow with Variable Physical Properties*, Advances in Heat Transfer, T.F. Irvine and J.P. Hartnett, Eds., *6*:503-564, Academic (1970).

62. Boelter, L.M.K., G. Young, and H.W. Iversen, NACA Technical Note No. 1451 (1948).

63. Dalle Donne, M., and F.H. Bowditch, *High Temperature Heat Transfer*, Nuclear Engineering *8*:20-29 (Jan. 1963).

64. McEligot, D.M., L.W. Ormand, and H.C. Perkins, Jr., *Internal Low Reynolds Number Turbulent and Transitional Gas Flow with Heat Transfer*, Transactions of the ASME, J. Heat Transfer *88*:239-245 (May 1966).

65. Martinelli, R.C., and L.M.K. Boelter, *The Analytical Prediction of Superposed Free and Forced Viscous Convection in a Vertical Pipe*, University of California (Berkeley) Publications in Engineering 5(2):23-58 (1942).

66. Eckert, E.R.G., and A.J. Diaguila, *Convective Heat Transfer for Mixed, Free, and Forced Flow through Tubes*, Transactions of the ASME *76*:497-504 (May 1954).

67. Axcell, B.P., and W.B. Hall, *Mixed Convection to Air in a Vertical Pipe*, Proc. of the Sixth National Heat Transfer Conf., Vol. 1, Mixed Convection, Pool Boiling, and Flow Boiling and Two-Phase Flow, pp. 37-42 (Aug. 7-11, 1978).

68. Fewster, J., and J.D. Jackson, *Enhancement of Turbulent Heat Transfer Due to Buoyancy for Downward Flow in Water in Vertical Tubes*, Proc. Seminar on Turbulent Buoyant Convection, I.C.H.M.T. Beograd (1976).

69. Hottel, H.C., *Radiant-Heat Transmission*, Chapter 4 in W.H. McAdams' Heat Transmission, 3rd ed., McGraw Hill Book Co., New York, N.Y. (1954).

70. Hottel, H.C., and A.F. Sarofim, *Radiative Transfer*, McGraw-Hill Book Co., New York, N.Y. (1967).

71. West, F.B., and A.T. Taylor, *The Effect of Pulsations on Heat Transfer, Turbulent Flow of Water Inside Tubes*, Chemical Engineering Progress *48*(1):39-43 (Jan. 1952).

72. Morrell, G., *An Empirical Method for Calculating Heat Transfer Rates in Resonating Gaseous Pipe Flow.* Jet Propulsion *28*:829-831 (Dec. 1958).

73. Jackson, T.W., W.B. Harrison, and W.C. Boteler, *Free Convection, Forced Convection, and Acoustic Vibrations in a Constant Temperature Vertical Tube,* Trarsactions of the ASME, J. Heat Transfer *81*:68-74 (Feb. 1959).

74. Lemlich, R., and C. Hwu, *The Effect of Acoustic Vibration on Forced Convective Heat Transfer,* J. of the American Institute of Chemical Engineers *7*(1):102-106 (March 1961).

75. Zartman, W.N., and S.W. Churchill, *Heat Transfer from Acoustically Resonating Gas Flames in a Cylindrical Burner,* J. of the American Institute of Chemical Engineers *7*(4):588-592 (Dec. 1961).

76. Baird, M.H.I., G.J. Duncan, J.I. Smith, and J. Taylor, *Heat Transfer in Pulsed Turbulent Flow,* Chemical Engineering Science *21*:197-199 (1966).

77. Mamayev, V.V., V.S. Nosov, and N.I. Syromyatnikov, *Investigation of Heat Transfer in Pulsed Flow of Air in Pipes,* Heat Transfer, Soviet Research *8*(3):111-116 (May-June 1976).

78. Ahrens, F.W., *Prediction of Heat Transfer in Pulse-Combustion Burners,* Proc. of the Symposium on Pulse Combustion for Heating Applications, compiled by J.M. Clinch, Argonne National Laboratory Report ANL/EES-TM-87, pp. 46-66 (May 1980).

79. Brown, D.J., *Noise Emission and Acoustic Efficiency in Pulsating Combustion,* Combustion Science and Technology *3*:51-52 (1971).

80. Belles, F.E., P.S. Vishwanath, and J.E. Ives, *Sound Characteristics of a Family of Pulse Burners at Various Heat-Release Rates,* Proc. of the Symposium on Pulse Combustion Applications, Atlanta, Ga. (March 2-3, 1982).

81. Chiu, H.H., J.M. Clinch, C.A. Blomquist, and E.J. Croke, *Pulse Combustion Noise: Problems and Solutions,* Proc. of the 1981 International Gas Research Conf., Los Angeles, Calif. (Sept. 28-Oct. 1, 1981).

82. Winiarski, L., *A Logically Simple Method for Solving the Gas Dynamics of a Pulsating Combustor,* Proc. of the First International Symposium on Pulsating Combustion, D.J. Brown, Ed., University of Sheffield, Sheffield, England (Sept. 20-23, 1971).

83. Winiarksi, L., *Pulsating Combustors: Modeling and Applications,* Proc. of the Symposium on Pulse Combustion Technology for Heating Applications, compiled by J.M. Clinch, Argonne National Laboratory Report ANL/EES-TM-87, pp. 67-70 (May 1980).

84. Edelman, R.B., A. Turan, and D.H. France, *Modeling of the Pulse-Combustion Process*, Proc. of the Symposium on Pulse Combustion Technology for Heating Applications, compiled by J.M. Clinch, Argonne National Laboratory Report ANL/EES-TM-87, pp. 71-94 (May 1980).

85. Chiu, H.H., *Combustion Performance and Noise Emission Characteristics of Pulse Combustion*, Proc. of the Symposium on Pulse Combustion Technology for Heating Applications, compiled by J.M. Clinch, Argonne National Laboratory Report ANL/EES-TM-87, pp. 129-143 (May 1980).

86. Kitchen, J.A., *Pulsating Combustion Chambers for Heat Equipment*, Proc. of the Symposium on Pulse Combustion Applications, Atlanta, Ga. (March 2-3, 1982).

87. Schmidt, P., *On the History of the Development of the Schmidt Tube*, AGARDograph No. 20:375-399 (1957).

88. Gosslau, F., *Development of the V-1 Pulse Jet*, AGARDOgraph No. 20:400-418 (1957).

89. Hydropulse Literature, Hydrotherm, Inc., Northvale, N.J. (undated).

90. Whitlock, D.J., S.F. Favors, and G. Reuter, *Field Tests on Pulse-Combustion Boilers for Space Heating and Domestic Water Heating*, Proc. of the Symposium on Pulse Combustion Applications, Atlanta, Ga. (March 2-4, 1982).

91. Woodworth, L.M., *R&D Activities in Pulse-Combustion at BNL*, Proc. of the Syposium on Pulse Combustion for Heating Applications, compiled by J.M. Clinch, Argonne National Laboratory Report ANL/EES-TM-87, pp. 181-189 (May 1980).

92. Turbopuls Literature, TURBOPULS, S.A., Geneva, Switzerland (undated).

93. Lauten, E.A., L. Irwin, and A. Lauler, *Development of a Gas-Fired Pulse-Combustion Commercial Water Heater*, Proc. of the Symposium on Pulse Combustion Applications, Atlanta, Ga. (March 2-3, 1982).

94. Drewry, J.E., and L.R. Wright, *Lennox Announces Plans for Pulse Combustion Furnace*, Gas Research Institute Digest 3(4):10-12 (Nov. 1980).

95. Adams, C.W., *Performance Results of the Lennox Pulse-Combustion Furnace Field Trials*, Proc. of the Symposium on Pulse Combustion Applications, Atlanta, Ga. (March 2-3, 1982).

96. Porter, C.D., *Valveless-Gas-Turbine Combustors with Pressure Gain*, Paper No. 58-GTP-11, presented at the ASME Gas Turbine Power Conf. and Exhibit, Washington, D.C. (March 2-6, 1958).

97. Muller, J.L., *Theoretical and Practical Aspects of the Application of Resonant Combustion Chambers in the Gas Turbine,* Council for Scientific and Industrial Research (CSIR) Report No. MEG83, Pretoria, South Africa (1969).

98. Swithenbank, J., D.J. Brown, and R.J. Saunders, *The Application of Pulsating Combustion to Power Generation Using Gas Turbines,* Proc. of The First International Symposium on Pulsating Combustion, D.J. Brown, Ed., University of Sheffield, Sheffield, England (Sept. 20-23, 1971).

99. Swithenbank, J., D.J. Brown, and R.J. Saunders, *Some Implications of the Use of Pulsating Combustion for Power Generation Using Gas Turbines,* J. Inst. Fuel *47*:181-189 (Sept. 1974).

100. Kentfield, J.A.C., M. Rehman, and E.S. Marzouk, *A Simple Pressure Gain Combustor for Gas Turbines,* Transactions of the ASME, J. Engineering Power *99*(2):153-158 (April 1977).

101. Ellman, R.C., J.W. Belter, and L. Dockter, *Adapting a Pulse-Jet Combustion System to Entrained Drying of Lignite,* Proc. of the 5th International Coal Preparation Congress, Pittsburgh, Penn., pp. 463-476 (Oct. 1966).

102. Lockwood, R.M., *Drying Food and Wastes with Pulsating Combustion,* Proc. of the Symposium on Pulse Combustion for Heating Applications, compiled by J.M. Clinch, Argonne National Laboratory Report ANL/EES-TM-87, pp. 224-238 (May 1980).

103. Tamburello, N., G.A. Hill, J. Goldman, A. Seginer, M. Salomon, and Y. Timnat, *The Development of A Vegetable and Fruit Dehydration Unit with a Pulse-Combustion Chamber,* Proc. of the Symposium on Pulse Combustion Applications, Atlanta, Ga. (March 2-3, 1982).

104. Persechino, M.A., *Experimental Valveless Pulse-Jet Diesel-Fueled Fog Generator,* Naval Research Laboratory Report 5414 (Dec. 1959).

105. *Generator, Smoke, Mechanical, Pulse Jet, M3A3,* Operator's and Organizational Maintenance Manual TM3-1040-202-12, Headquarters, Department of the Army (Dec. 1975).

106. Mutchler, P.A., *A Pulse-Combustor Fog Generator and Potential Applications to Industrial/Commercial Heating,* Proc. of the Symposium on Pulse Combustion Applications, Atlanta, Ga. (March 2-3, 1982).

107. Tracenckner, K., *Pulverized-Coal Gasification Ruhrgas Process,* Transactions of the ASME *75*:1095-1101 (Aug. 1953).

108. Pannier, G., *The Pyro-Jet Grinder,* Minerals Processing *8*(6):16-18 (June 1967).

109. Ibberson, V.J., J.M. Beer, J. Swithenbank, D.S. Taylor, and M.W. Thring, *A Combustion Oscillator for M.H.D. Energy Conversion,* Thirteenth Symposium (International) on Combustion, Salt Lake City, Utah (Aug. 1970); The Combustion Institute, Pittsburgh, Penn., pp. 565-572 (1971).

110. Corliss, J.M., A.A. Putnam, and D.W. Locklin, *Status of A Gas-Fired Aerovalved Pulse-Combustion System for Steam Raising,* Proc. of the Symposium on Pulse Combustion Applications, Atlanta, Ga. (March 2-3, 1982).

MEMBERS OF ARGONNE UNIVERSITIES ASSOCIATION

The University of Arizona
Carnegie-Mellon University
Case Western Reserve University
The University of Chicago
University of Cincinnati
Illinois Institute of Technology
University of Illinois
Indiana University
The University of Iowa
Iowa State University
The University of Kansas
Kansas State University
Loyola University of Chicago
Marquette University
The University of Michigan
Michigan State University
University of Minnesota
University of Missouri
Northwestern University
University of Notre Dame
The Ohio State University
Ohio University
The Pennsylvania State University
Purdue University
Saint Louis University
Southern Illinois University
The University of Texas at Austin
Washington University
Wayne State University
The University of Wisconsin-Madison

This informal report presents preliminary results of ongoing work or work that is more limited in scope and depth than that described in formal reports issued by the Energy and Environmental Systems Division.

Printed in the United States of America. Available from National Technical Information Service,
U. S. Department of Commerce, 5285 Port Royal Road, Springfield, Virginia 22161.